Assessing right ventricular function and the pulmonary circulation in pulmonary hypertension

Onno Anthonius Spruijt

Het verschijnen van dit proefschrift werd mede mogelijk gemaakt door de steun van

Financial support for printing of this thesis was kindly provided by:

Layout and design:

Onno A. Spruijt, illustratie en vormgeving

Printed by:

GVO drukkers & vormgevers b.v. | Ede

ISBN: 978-94-6332-237-9

VRIJE UNIVERSITEIT

Assessing right ventricular function and the pulmonary circulation in pulmonary hypertension

ACADEMISCH PROEFSCHRIFT

ter verkrijging van de graad Doctor aan
de Vrije Universiteit Amsterdam,
op gezag van de rector magnificus
prof.dr. V. Subramaniam,
in het openbaar te verdedigen
ten overstaan van de promotiecommissie
van de Faculteit der Geneeskunde
op donderdag 2 november 2017 om 11.45 uur
in de aula van de universiteit,
De Boelelaan 1105

door

Onno Anthonius Spruijt

geboren te Amsterdam

promotor: prof.dr. A. Vonk Noordegraaf

copromotoren: dr. H.J. Bogaard
dr. J.T. Marcus

The work presented in this thesis was performed at the department of Pulmonary Medicine of the VU University Medical Center / Institute for Cardiovascular Research, Amsterdam, The Netherlands.

CONTENTS

CHAPTER 1

General introduction and thesis outline

Adapted from book chapter: The right ventricle in health and disease, Springer 2014

OA Spruijt[1], A Vonk Noordegraaf[1], HJ Bogaard[1]

[1]Department of Pulmonary Medicine, VU University Medical Center, Amsterdam, The Netherlands

Pulmonary hypertension:

After successfully and safely using the cardiac catheter technique in animals, Dr. Werner Forssmann performed in 1929 the first recorded human cardiac catheterization of his own right heart. Andre Cournand and Dickinson Richards did further development of this technique for clinical purposes in 1944 and demonstrated the safety and feasibility of this technique in a large cohort of patients. For their contributions to the understanding of cardiac physiology, Forssmann, Cournand and Richards received the Nobel Prize in Physiology in 1956 (Figure 1) [1].

Figure 1: Forssmann, Richards and Cournand receiving the Nobel Prize in Physiology.

Today, the right heart catheterization (RHC) is still the gold standard for the hemodynamic evaluation of the right ventricle (RV) and pulmonary circulation. During a RHC, the pressure is measured and recorded in the right atrium (RA), right ventricle (RV) and pulmonary artery (PA).

Shortly after the clinical introduction of the RHC technique, it became clear that elevated pulmonary vascular pressures were related to symptoms of dyspnea and fatigue. Paul Wood defined in 1958 a mean pulmonary artery pressure (mPAP) of 25 mmHg as the upper limit of normal on the basis of measurements performed in 60 healthy subjects [2]. The same definition of pulmonary hypertension (PH) is still used today and the RHC remains the gold standard for the diagnosis of PH [3].

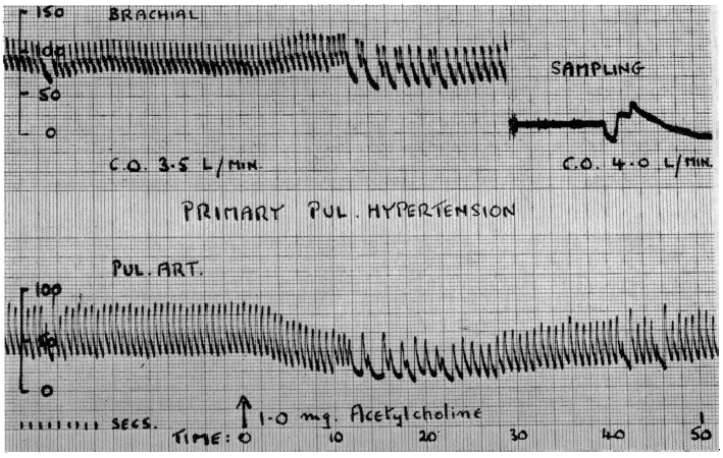

Figure 2: Using acetylcholine as a pulmonary vasodilator, Paul Wood showed in patients with 'Primary PH that the administration of acetylcholine leaded to a decrease in pulmonary artery pressure in combination with an increase in cardiac output proving the increased vasoconstriction in this disease.

Wood's studies using acetylcholine in PH patients also contributed to the classification of PH (Figure 2), which has been modified several times in the last five decades. Approximately 40 causes of PH are now recognized, which are categorized in 5 main groups (Table 1). Left sided heart failure (group 2) is the most common cause of PH [3].

Since the cardiovascular system is a closed loop system, different (patho)physiological hemodynamic changes can initiate an increase in mPAP. The hemodynamic mechanisms resulting in an increase in mPAP are, an increase in pulmonary vascular resistance (PVR), an increase in pulmonary arterial wedge pressure (PAWP) and an increase in cardiac output (CO).

Table 1: Clinical classification of pulmonary hypertension according to guideline (Galie ERJ 2015)

1. Pulmonary arterial hypertension
1.1 Idiopathic
1.2 Heritable
1.2.1 BMPR2 mutation
1.2.2 Other mutations
1.3 Drugs and toxins induced
1.4 Associated with:
1.4.1 Connective tissue disease
1.4.2 Human immunodeficiency virus (HIV) infection
1.4.3 Portal hypertension
1.4.4 Congenital heart disease
1.4.5 Schistosomiasis
1'. Pulmonary veno-occlusive disease and/or pulmonary capillary haemangiomatosis
2. Pulmonary hypertension due to left heart disease
3. Pulmonary hypertension due to lung diseases and/or hypoxia
4. Chronic thromboembolic pulmonary hypertension and other pulmonary artery obstructions
5. Pulmonary hypertension with unclear and/or multifactorial mechanisms

An increase in the afterload of the RV leads to an increase in mPAP since the RV needs to build up more pressure to maintain an adequate CO. The load on the outflow of the RV can be divided into the resistance to steady state flow and the resistance to pulsatile flow from vascular impedance [4]. The resistance to steady state flow is known as the pulmonary vascular resistance (PVR) and is defined as PVR = (mPAP – PAWP) / CO. An increase in PVR can be due to a decrease in the pulmonary vessel radius or due to the loss of arterial surface [4]. A decrease in pulmonary arterial vessel radius is seen in group 1 and 4 PH patients and is due to thickening of the vascular wall, intravascular occlusions (either by exuberantly proliferating endothelial and smooth muscle cells or thrombosis and emboli) and loss of vessel number (rarefaction). Hypoxic vasoconstriction, also seen in group 3 PH patients can contribute to a decrease in the pulmonary arterial diameter. A decrease in arterial surface area is often observed in emphysema. Vascular rarefaction as the sole cause of an increased PVR is still a matter of debate, since even in severe emphysema, PH is rare. PVR can also be increased in conditions associated with an increased blood viscosity.

Resistance to pulsatile flow is mostly described by an inverse measure, the pulmonary arterial compliance. Pulmonary arterial compliance is assessed by stroke volume (SV) divided by the pulse pressure (PP) (SV/PP). It has been shown that in the pulmonary circulation PVR and compliance are inversely related [5]. The product of PVR and compliance, known as the RC time (T), can be calculated as T = PVR x compliance = ((mPAP – PAWP) / (SV x HR)) x (SV/PP) = T x ((mPAP – PAWP) / PP). Over a wide range of PVR, T remains relatively stable in healthy people and patients with precapillary PH [5-7].

mPAP can also be increased due to an increased PAWP. During RHC a balloon can be inflated to temporarily close a small pulmonary artery branch. The pressure proximal from the inflated balloon is the PAWP and is a surrogate measure of the pressure in the post-capillary system including the left atrial pressure. Left heart failure or left sided valvular disease results in an increase in PAWP, which can subsequently increase mPAP. A PAWP > 15mmHg is defined as abnormal and is due to left heart disease. Therefore, PH can be classified in pre- and postcapillary PH based on the PAWP [3]. The significance of a PAWP between 12 and 15mmHg is still unclear.

The degree to which an increase in CO could lead to an increase in mPAP depends on the degree to which lung vessels can distend and be recruited. The magnitude of vascular distention and lung vascular recruitment during exercise is still hotly debated. During exercise an increased demand for oxygen will increase CO, which is usually followed by at least some increase in the mPAP [8].

Conditions like congenital heart disease, hyperthyroidism, portal hypertension and congenital portosystemic venous shunts can also increase CO and increase mPAP [9-11]. Nevertheless, overwhelmingly patients with PH have a decreased CO as a result of the increase in PVR and RV failure.

The right ventricle in pulmonary hypertension

The increased resistance of the pulmonary vascular bed in PH patients increases the load on the RV. In order to maintain an adequate CO, the RV needs to adapt. RV adaption is a complex interplay of RV remodeling, neuro-hormonal activation, changes in myocardial metabolism and changes in coronary artery perfusion. In order to maintain cardiac output, the RV needs to generate higher pressures to overcome the increased resistance of the pulmonary vascular bed. According to Laplace law (wall stress = (pressure x radius) / (2 x wall thickness)) this increase in pressures will increase wall stress subsequently changing myocardial metabolism and activating the neurohormonal system [12]. The subsequent effects on RV remodeling are not clear-cut since also other aspects as time of onset of PH, the underlying etiology of PH and possibly genetics play a role in the process of RV adaption. Simplified, the first step in the process of remodeling is RV hypertrophy and an increase in contractility. RV hypertrophy decreases wall stress, however can increase RV diastolic stiffness [13, 14]. If, despite these adaptive changes, cardiac output cannot be maintained, the RV will dilate further increasing wall stress. Ultimately, this will lead to RV failure. Maintenance of RV systolic function is important since RV systolic function is the main predictor of survival [15-19].

Exercise intolerance in patients with pulmonary hypertension

During exercise the cardiopulmonary system is pushed to its upper limits. The increased demand for oxygen delivery to the tissues is met by an almost 4 fold increase in CO. The entire CO passes through the pulmonary circulation and the pulmonary circulation prevents a proportional increase in mPAP by vasodilatation and vessel recruitment [20].

PH patients often complain of exercise induced dyspnea and this impaired exercise tolerance is mainly due to circulatory limitations. Exercise induced dyspnea in PH patients is primarily due to the inability to increase pulmonary blood flow during exercise. This limited increase in CO is caused by an inability to increase SV and due to an abnormal chronotropic response [21, 22]. The inability to increase SV is the result of the increase in PVR and RV dysfunction [21, 23-25]. An abnormal chronotropic response is demonstrated as a decreased maximal heart rate (HR) in PH and is believed

to be the result of an imbalance of the autonomic nervous system [22, 26-28]. The decrease in CO for a given workload results in insufficient oxygen delivery to peripheral tissues, anaerobic metabolism of glucose and muscle weakness due to acidosis [29]. Together these changes limit the maximal uptake of oxygen (VO_2max) and result in early exercise termination. In PH, a reduced VO_2max, O_2 pulse and a reduced VO_2 at the anaerobic threshold (VO_2AT) result from a decreased blood flow and reflect RV dysfunction[30].

A second problem in PH is an increased ventilatory requirement, which is still poorly understood, but likely contributes to the patients' sensation of dyspnea. In precapillary PH, dead space ventilation occurs because of hypoperfusion of normally ventilated alveoli due to loss of the pulmonary capillary bed. Dead space ventilation could lead to problems eliminating carbon dioxide, increasing minute ventilation (VE).

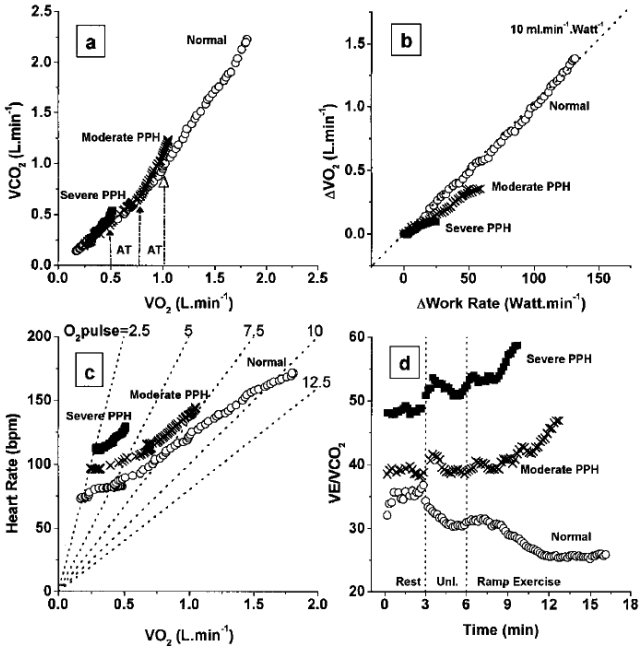

Figure 3: Comparison of VO_2max, O_2 pulse and VE/VCO_2 between PAH patients and healthy controls. A: Decrease in AT- , B: decrease in VO_2max- , C: decrease in O_2 pulse- , D: increase in VE/CO_2 slope- in PAH patients compared to healthy controls.

However, because PH patients are often hypocapnic at rest and during exercise, it is assumed that in addition to dead space ventilation, alveolar hyperventilation further contributes to the increased ventilatory requirement [31]. It is believed that exercise induced alveolar hyperventilation in PH is due to the summation of lactate acidosis, a hypoxemic ventilatory drive and a sympathetic nerve

overdrive. This ventilatory inefficiency (increased VE/VCO_2 slope) is a hallmark of PH and may contribute to the sensation of dyspnea [23, 26, 29, 32] (Figure 3). Finally, diaphragm weakness can lead to a further increase of breathlessness during exercise [33].

Recently, invasive assessment of hemodynamics during exercise has received interest in PH studies. Such exercise protocols are completed with pulmonary artery and radial artery catheters *in situ*, giving a more complete hemodynamic and ventilatory evaluation during exercise [34] (figure 4).

Figure 4: Invasive cardiopulmonary exercise test.

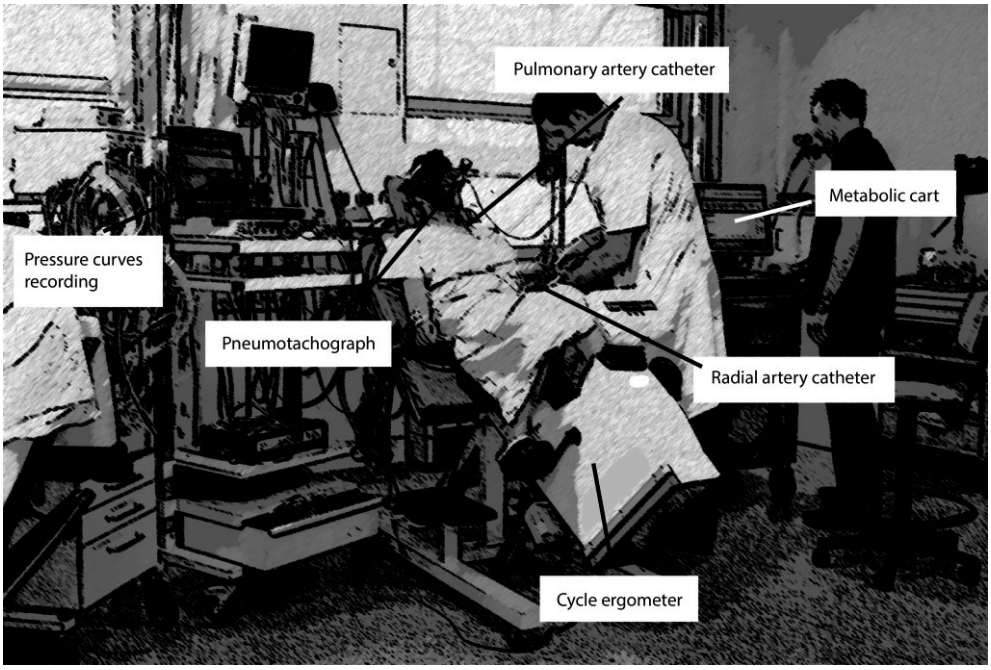

The ability to increase CO during exercise depends on the fitness of an individual and the slope of the mPAP-CO relationship which is steeper in older subjects [35]. It has been suggested that a mPAP of 30mmHg at a CO <10L/min and a mPAP-CO slope >3mmHg per L/min represent the upper limits of normal. A slope of >2,5mmHg per L/min is probably abnormal in younger individuals [8, 35-38]. Such criteria for the upper limits of normal for the mPAP-CO relation are not yet officially endorsed in the PH guidelines because they require external validation.

A study by Gruenig et al [39] used the rise in systolic pulmonary artery pressure (sPAP) during exercise, assessed with echocardiography, as a measure of the contractile reserve of the RV. They showed in PAH and CTEPH patients that the increase of sPAP during exercise was an independent predictor of survival with a better survival in the patients with a bigger contractile reserve [39].

Likewise, changes in PVR and PCWP from rest to exercise are poorly characterized. A recent meta-analysis showed that changes in PVR and PAWP during exercise dependent on age [40].

Despite the suggestion that evaluation of the hemodynamic response to exercise aids the early detection of pathological cardiopulmonary changes and the distinction between exercise-induced PH and left-sided diastolic dysfunction [34, 38], more and more widely disseminated experience with invasive CPET is necessary to determine its value.

Outline of this thesis

In this thesis, a number of techniques and methods were evaluated that may contribute to earlier recognition of PAH and improved monitoring and prognostication.

Early recognition and prognostication in pulmonary hypertension

Due to the non-specific nature of symptoms at presentation, most patients with pulmonary arterial hypertension are diagnosed by the time their disease is already in an advanced stage. Early detection of PH and a timely initiation of treatment can significantly improve clinical outcome. Computed tomography pulmonary angiography (CTPA) is a diagnostic tool often used in the diagnostic process of patients that present with unexplained dyspnea, for example to exclude pulmonary emboli. A well-known clue for the presence of pulmonary hypertension on CTPA is an increased ratio between the diameter of the pulmonary artery and the diameter of the ascending aorta. In **chapter 2**, we investigated whether a combination of dimensional measurements of the pulmonary artery and the heart would increase the predictive value of computed tomography pulmonary angiography for the presence of pulmonary hypertension. The prognostic value of right ventricular parameters in pulmonary hypertension is well-established. Whether a combination of parameters of the right heart merged into a simple risk score predict outcome in precapillary pulmonary hypertension was investigated in **chapter 3**.

Treatment response in pulmonary hypertension

Since the prognosis of patients with pulmonary hypertension is determined by right ventricular function, monitoring of right ventricular function is of utmost importance. In **chapter 4** we summarized available methods for measuring the right ventricular response to therapy. Cardiac magnetic resonance imaging is the gold standard for monitoring right ventricular function. Since this technique is expensive, not widely available and analyses are time-consuming, monitoring right ventricular function using simple echocardiographic measurements would be ideal in daily practice. Therefore, in **chapter 5**, we investigated the usage of simple echocardiographic parameters for the serial assessment of RV function. In **chapter 6** we investigated whether the hemodynamic and cardiac responses to PH specific therapy are different between patients with idiopathic pulmonary arterial hypertension and a severely reduced diffusion capacity of the lung for carbon monoxide compared to patients with idiopathic pulmonary arterial hypertension with a more preserved diffusion capacity of the lung for carbon monoxide.

Emerging modalities in pulmonary hypertension

Chapter 7 summarizes emerging imaging techniques in the setting of pulmonary hypertension. As depicted in the introduction the diagnosis of PH is made during RHC. Subsequently, assessing disease severity and monitoring of patients is done by assessing hemodynamics, indices of right ventricular function as well as exercise tests. However, currently there is no possibility to clinically assess the primary disease process in the pulmonary arteries of patients with precapillary pulmonary hypertension. Since preclinical studies are increasingly focusing on therapies directly targeting the pulmonary vascular remodeling, there is an urgent need for an imaging method that allows quantification of this remodeling. Such a technique would not only provide insight into the underlying disease process, but would also enable assessment of responses to targeted therapies. Therefore, in **chapter 8**, we investigated whether 3'-[18F]fluoro-3'-deoxythymidine ([18F]-FLT) positron emission tomography (PET/CT) could be used to quantitatively assess proliferation in the pulmonary vasculature of PAH patients. Furthermore, we tested whether [18F]-FLT was able to track the pulmonary vascular remodeling and reverse remodeling after administration of targeted therapies in a monocrotaline PH rat model.

An emerging technique to characterize the myocardium by cardiac magnetic resonance imaging is native T1-mapping. In **chapter 9** we investigated this technique in precapillary pulmonary hypertension patients.

As summarized in the general introduction, patients with pulmonary hypertension have a decreased exercise tolerance and this exercise intolerance in mainly determined by circulatory limitations. Whether this exercise intolerance coincides with an inability to increase right ventricular contractility was investigated in **chapter 10** during an invasive cardiopulmonary exercise test.

References:

[1] Nossaman BD, Scruggs BA, Nossaman VE, Murthy SN, Kadowitz PJ. History of right heart catheterization: 100 years of experimentation and methodology development. Cardiology in review. 2010; 18:94-101
[2] Wood P. Pulmonary hypertension with special reference to the vasoconstrictive factor. British heart journal. 1958; 20:557-70
[3] Galie N, Hoeper MM, Humbert M, Torbicki A, Vachiery JL, Barbera JA, et al. Guidelines for the diagnosis and treatment of pulmonary hypertension. The European respiratory journal. 2009; 34:1219-63
[4] Champion HC, Michelakis ED, Hassoun PM. Comprehensive invasive and noninvasive approach to the right ventricle-pulmonary circulation unit: state of the art and clinical and research implications. Circulation. 2009; 120:992-1007
[5] Lankhaar JW, Westerhof N, Faes TJ, Gan CT, Marques KM, Boonstra A, et al. Pulmonary vascular resistance and compliance stay inversely related during treatment of pulmonary hypertension. European heart journal. 2008; 29:1688-95
[6] Lankhaar JW, Westerhof N, Faes TJ, Marques KM, Marcus JT, Postmus PE, et al. Quantification of right ventricular afterload in patients with and without pulmonary hypertension. American journal of physiology. 2006; 291:H1731-7
[7] Tedford RJ, Hassoun PM, Mathai SC, Girgis RE, Russell SD, Thiemann DR, et al. Pulmonary capillary wedge pressure augments right ventricular pulsatile loading. Circulation. 2012; 125:289-97
[8] Argiento P, Vanderpool RR, Mule M, Russo MG, D'Alto M, Bossone E, et al. Exercise stress echocardiography of the pulmonary circulation: limits of normal and sex differences. Chest. 2012; 142:1158-65
[9] Mehta PA, Dubrey SW. High output heart failure. Qjm. 2009; 102:235-41
[10] Hoeper MM, Krowka MJ, Strassburg CP. Portopulmonary hypertension and hepatopulmonary syndrome. Lancet. 2004; 363:1461-8
[11] Spruijt OA, Bogaard HJ, Vonk-Noordegraaf A. Pulmonary arterial hypertension combined with a high cardiac output state: Three remarkable cases. Pulmonary circulation. 2013; 3:440-3
[12] Vonk-Noordegraaf A, Haddad F, Chin KM, Forfia PR, Kawut SM, Lumens J, et al. Right heart adaptation to pulmonary arterial hypertension: physiology and pathobiology. Journal of the American College of Cardiology. 2013; 62:D22-33
[13] Rain S, Handoko ML, Trip P, Gan CT, Westerhof N, Stienen GJ, et al. Right ventricular diastolic impairment in patients with pulmonary arterial hypertension. Circulation. 2013; 128:2016-25, 1-10
[14] Trip P, Rain S, Handoko ML, van der Bruggen C, Bogaard HJ, Marcus JT, et al. Clinical relevance of right ventricular diastolic stiffness in pulmonary hypertension. The European respiratory journal. 2015; 45:1603-12
[15] Benza RL, Miller DP, Gomberg-Maitland M, Frantz RP, Foreman AJ, Coffey CS, et al. Predicting survival in pulmonary arterial hypertension: insights from the Registry to Evaluate Early and Long-Term Pulmonary Arterial Hypertension Disease Management (REVEAL). Circulation. 2010; 122:164-72
[16] Humbert M, Sitbon O, Chaouat A, Bertocchi M, Habib G, Gressin V, et al. Survival in patients with idiopathic, familial, and anorexigen-associated pulmonary arterial hypertension in the modern management era. Circulation. 2010; 122:156-63
[17] van de Veerdonk MC, Kind T, Marcus JT, Mauritz GJ, Heymans MW, Bogaard HJ, et al. Progressive right ventricular dysfunction in patients with pulmonary arterial hypertension responding to therapy. Journal of the American College of Cardiology. 2011; 58:2511-9
[18] van de Veerdonk MC, Marcus JT, Westerhof N, de Man FS, Boonstra A, Heymans MW, et al. Signs of right ventricular deterioration in clinically stable patients with pulmonary arterial hypertension. Chest. 2015; 147:1063-71
[19] van Wolferen SA, Marcus JT, Boonstra A, Marques KM, Bronzwaer JG, Spreeuwenberg MD, et al. Prognostic value of right ventricular mass, volume, and function in idiopathic pulmonary arterial hypertension. European heart journal. 2007; 28:1250-7
[20] Waxman AB. Exercise physiology and pulmonary arterial hypertension. Progress in cardiovascular diseases. 2012; 55:172-9
[21] Holverda S, Gan CT, Marcus JT, Postmus PE, Boonstra A, Vonk-Noordegraaf A. Impaired stroke volume response to exercise in pulmonary arterial hypertension. Journal of the American College of Cardiology. 2006; 47:1732-3
[22] Ramos RP, Arakaki JS, Barbosa P, Treptow E, Valois FM, Ferreira EV, et al. Heart rate recovery in pulmonary arterial hypertension: relationship with exercise capacity and prognosis. American heart journal. 2012; 163:580-8
[23] Fowler RM, Gain KR, Gabbay E. Exercise intolerance in pulmonary arterial hypertension. Pulmonary medicine. 2012; 2012:359204
[24] Claessen G, La Gerche A, Dymarkowski S, Claus P, Delcroix M, Heidbuchel H. Pulmonary vascular and right ventricular reserve in patients with normalized resting hemodynamics after pulmonary endarterectomy. Journal of the American Heart Association. 2015; 4:e001602
[25] Claessen G, La Gerche A, Wielandts JY, Bogaert J, Van Cleemput J, Wuyts W, et al. Exercise pathophysiology and sildenafil effects in chronic thromboembolic pulmonary hypertension. Heart (British Cardiac Society). 2015; 101:637-44
[26] Velez-Roa S, Ciarka A, Najem B, Vachiery JL, Naeije R, van de Borne P. Increased sympathetic nerve activity in pulmonary artery hypertension. Circulation. 2004; 110:1308-12
[27] Provencher S, Chemla D, Herve P, Sitbon O, Humbert M, Simonneau G. Heart rate responses during the 6-minute walk test in pulmonary arterial hypertension. The European respiratory journal. 2006; 27:114-20
[28] Minai OA, Gudavalli R, Mummadi S, Liu X, McCarthy K, Dweik RA. Heart rate recovery predicts clinical worsening in patients with pulmonary arterial hypertension. American journal of respiratory and critical care medicine. 2012; 185:400-8

[29] Sun XG, Hansen JE, Oudiz RJ, Wasserman K. Exercise pathophysiology in patients with primary pulmonary hypertension. Circulation. 2001; 104:429-35
[30] Wasserman K. Principles of Exercise Testing and Interpretation. Philadelphia: Lippincott Williams & Wilkins 1999.
[31] Hoeper MM, Pletz MW, Golpon H, Welte T. Prognostic value of blood gas analyses in patients with idiopathic pulmonary arterial hypertension. The European respiratory journal. 2007; 29:944-50
[32] Guazzi M, Cahalin LP, Arena R. Cardiopulmonary exercise testing as a diagnostic tool for the detection of left-sided pulmonary hypertension in heart failure. Journal of cardiac failure. 2013; 19:461-7
[33] de Man FS, van Hees HW, Handoko ML, Niessen HW, Schalij I, Humbert M, et al. Diaphragm muscle fiber weakness in pulmonary hypertension. American journal of respiratory and critical care medicine. 2011; 183:1411-8
[34] Maron BA, Cockrill BA, Waxman AB, Systrom DM. The invasive cardiopulmonary exercise test. Circulation. 2013; 127:1157-64
[35] Kovacs G, Berghold A, Scheidl S, Olschewski H. Pulmonary arterial pressure during rest and exercise in healthy subjects: a systematic review. The European respiratory journal. 2009; 34:888-94
[36] D'Alto M, Ghio S, D'Andrea A, Pazzano AS, Argiento P, Camporotondo R, et al. Inappropriate exercise-induced increase in pulmonary artery pressure in patients with systemic sclerosis. Heart (British Cardiac Society). 2011; 97:112-7
[37] Naeije R. In defence of exercise stress tests for the diagnosis of pulmonary hypertension. Heart (British Cardiac Society). 2011; 97:94-5
[38] Tolle JJ, Waxman AB, Van Horn TL, Pappagianopoulos PP, Systrom DM. Exercise-induced pulmonary arterial hypertension. Circulation. 2008; 118:2183-9
[39] Grunig E, Tiede H, Enyimayew EO, Ehlken N, Seyfarth HJ, Bossone E, et al. Assessment and Prognostic Relevance of Right Ventricular Contractile Reserve in Patients with Severe Pulmonary Hypertension. Circulation. 2013;
[40] Kovacs G, Olschewski A, Berghold A, Olschewski H. Pulmonary vascular resistances during exercise in normal subjects: a systematic review. The European respiratory journal. 2012; 39:319-28
[41] Nickel N, Golpon H, Greer M, Knudsen L, Olsson K, Westerkamp V, et al. The prognostic impact of follow-up assessments in patients with idiopathic pulmonary arterial hypertension. The European respiratory journal. 2012; 39:589-96

1

CHAPTER 2

Predicting Pulmonary Hypertension with Standard Computed Tomography Pulmonary Angiography

International Journal of Cardiovascular Imaging 2015

OA Spruijt[1], HJ Bogaard[1], MW Heijmans[2], RJ Lely[3], MC van de Veerdonk[1], FS de Man[1,4], N Westerhof[1,4], A Vonk Noordegraaf[1]

[1]Department of Pulmonary Medicine, VU University Medical Center, Amsterdam
[2]Department of Epidemiology and Biostatistics, VU University Medical Center, Amsterdam
[3]Department of Radiology, VU University Medical Center, Amsterdam
[4]Department of Physiology, VU University Medical Center, Amsterdam

Abstract

Introduction: The most common feature of pulmonary hypertension (PH) on computed tomography pulmonary angiography (CTPA) is an increased diameter-ratio of the pulmonary artery to the ascending aorta (PA/AA_{AX}). The aim of this study was to investigate whether combining PA/AA_{AX} measurements with ventricular measurements improves the predictive value of CTPA for precapillary PH.

Methods: Three predicting models were analyzed using baseline CTPA scans of 51 treatment naïve precapillary PH patients and 25 non-PH controls: model 1: PA/AA_{AX} only; model 2: PA/AA_{AX} combined with the ratio of the right ventricular and left ventricular diameter measured on the axial view (RV/LV_{AX}); model 3: PA/AA_{AX} combined with the RV/LV-ratio measured on a four chamber view (RV/LV_{4CH}). Prediction models were compared using multivariable binary logistic regression, ROC analyses and decision curve analyses (DCA).

Results: Multivariable binary logistic regression showed an improvement of the predictive value of model 2 (-2LL=26.48) and 3 (-2LL=21.03) compared to model 1 (-2LL=21.03). ROC analyses showed significantly higher AUCs of model 2 and 3 compared to model 1 ($p=0.011$ and $p=0.007$, respectively). DCA showed an increased clinical benefit of model 2 and 3 compared to model 1. The predictive value of model 2 and 3 was almost equal. We found an optimal cut-off value for the RV/LV-ratio for predicting precapillary PH of $RV/LV \geq 1.20$.

Conclusions: The predictive value of CTPA for precapillary PH improves when ventricular and pulmonary artery measurements are combined. A $PA/AA_{AX} \geq 1$ or a $RV/LV_{AX} \geq 1.20$ needs further diagnostic evaluation to rule out or confirm the diagnosis.

Introduction

Pulmonary hypertension (PH) is defined as an increase in mean pulmonary artery pressure (mPAP) above 25 mmHg [1]. Irrespective of the exact cause, the condition leads to right heart failure and finally death [2].

Most PH patients are diagnosed by the time their disease is in an advanced stage [3, 4]. The non-specific nature of symptoms at presentation (exercise-induced dyspnea, fatigue) leads to failure of physicians to recognize the disease and an undesirable late diagnosis. [4-7]. Early detection of PH and a timely initiation of treatment can significantly improve the clinical outcome [8-10]. A unique opportunity for an earlier diagnosis of PH is provided when a standard non-ECG gated computed tomography pulmonary angiography (CTPA) is performed to evaluate a patient presenting with shortness of breath. To the attentive radiologist, CTPA may provide important clues towards a diagnosis of PH.

An intensively studied feature to predict PH on CTPA is an increased diameter ratio of the pulmonary artery (PA) to ascending aorta (AA) [11-17]. Studies showed that this parameter has a sensitivity of 58-87% for the diagnosis of PH. A way to improve the diagnostic sensitivity is to add information on the structure of the heart.

The clinical value of the ratio of the transverse diameter of the right ventricle (RV) and the left ventricle (LV) measured on the axial (AX) view and on a manually reconstructed four chamber (4CH) view is known as a typical sign of RV failure in acute pulmonary embolism [18, 19]. One study measured the RV/LV diameter ratio on the axial view in mainly post-capillary PH patients and found a sensitivity of 86% [16]. It is unknown whether adding ventricular measurements to the PA/AA-ratio improves the diagnostic model of CTPA for precapillary PH.

Therefore, the aim of our study is to investigate whether combining PA measurements with ventricular measurements improves the predictive value of CTPA for precapillary PH.

Methods

Study subjects

The PH center in the VU University Medical Center is a tertiary referral center for pulmonary hypertension patients in the Netherlands. From a large database of subjects who had been referred to the VU University Medical Center from 2002 through 2012 for the evaluation of pulmonary hypertension, we retrospectively, randomly selected treatment naïve precapillary PH patients. Only

subjects in whom both a baseline right heart catheterization and baseline CTPA were performed, were included in this study. In total, 51 precapillary PH patients were randomly selected. Precapillary PH was diagnosed according to the World Health Organization guidelines (mean pulmonary artery pressure > 25 mmHg and a pulmonary arterial wedge pressure ≤15 mmHg) [1].

25 subjects who were referred to our center for suspected pulmonary hypertension and who appeared to have normal pulmonary artery pressures during right heart catheterization and without a history of left heart disease, were randomly chosen and used as controls.

The study was approved by The Medical Ethics Review Committee of the VU University Medical Center. The study does not fall within the scope of the Medical Research Involving Human Subjects Act (WMO). Therefore, the study was approved without requirement of a consent statement.

CTPA image acquisition

CTPA studies of the entire chest were performed on either a 4-slice multi-detector CT system (Somatom Volume Zoom, Siemens, Erlangen, Germany) or a 64-slice multi-detector CT system (Somatom Sensation, Siemens, Erlangen, Germany). 18 CTPA studies were performed on the 4-slice CT system and 58 CTPA studies were performed on the 64-slice CT system. The Dose Length Product (DLP) was 266 ± 118 mGy.cm.

For the 4-slice multi-detector CT scanning parameters were 140kV and 100mAs with dose modulation at a slice collimation of 4x1,0mm, a rotation time of 0,5 seconds and a pitch of 1,25 out of which 1,5mm axial slices with 1mm reconstruction increment were reconstructed. The series were acquired using bolus tracking within the PA at maximum inspiration after intravenous injection (4ml/s) of 100ml of a low-osmolar, non-ionic contrast agent with iodine concentration of 300mg/ml (Ultravist-300 Iopromide; Bayer Pharma AG, Berlin, Germany), using an injection pump through an 18g cannula preferably in the right antecubital vein.

For the 64-slice multidetector CT, a slice collimation of 32x0,6mm, a rotation time of 0,33 seconds and a pitch of 0,75 was used. The series were acquired using a test bolus (30ml at 6ml/s) with tracking in the PA and a scan bolus with calculated delay at maximum inspiration after intravenous injection (≤60ml at 6ml/s) of a low-osmolar, non-ionic contrast agent with a iodine concentration of 300mg/ml (Ultravist-300 Iopromide; Bayer Pharma AG, Berlin, Germany), using an injection pump through an 18g cannula mostly in the right antecubital vein.

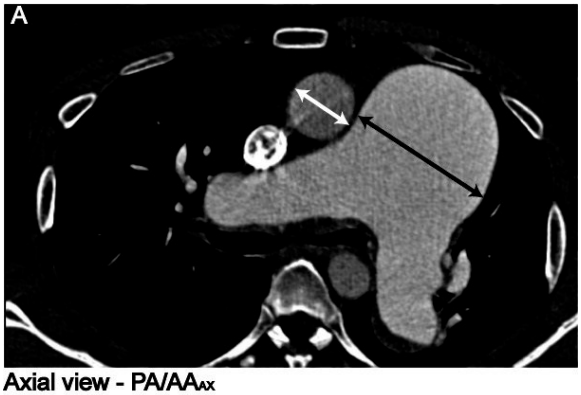

Axial view - PA/AA_{AX}

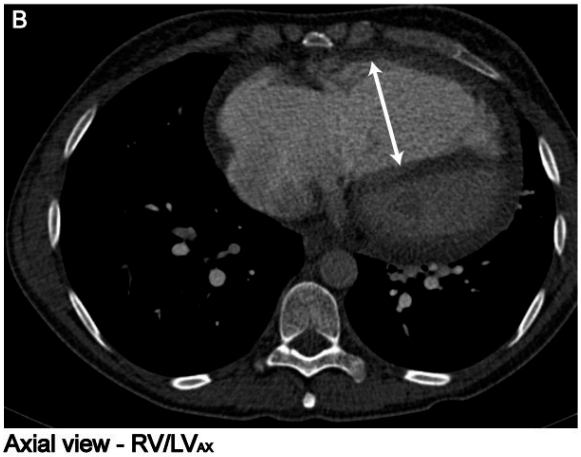

Axial view - RV/LV_{AX}

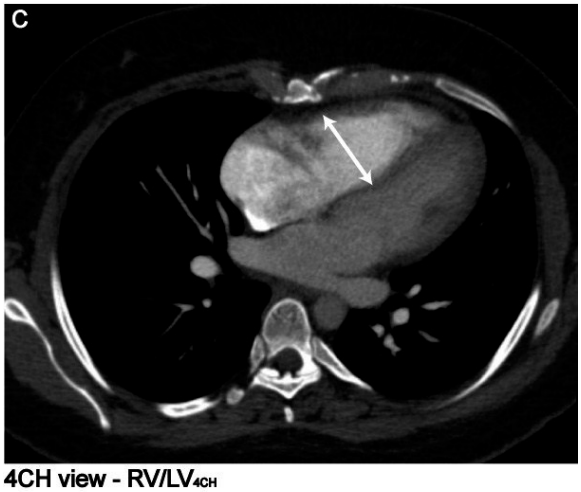

4CH view - RV/LV_{4CH}

Figure 1: CTPA parameters. A: Pulmonary artery (PA) and ascending aorta (AA) ratio (PA/AA_{AX}) on an axial view at the level of the bifurcation of the pulmonary trunk. B: Right ventricle (RV) and left ventricle (LV) ratio (RV/LV_{AX}) on an axial view. The RV diameter is measured perpendicular to the long axis of the heart. The LV diameter is not measured in this image, since the maximum diameter of the LV is not necessarily on the same image. C: RV/LV_{4CH} on a four chamber (4CH) view.

CTPA image analyses

CTPA studies were analyzed using a Sectra PACS IDS7 workstation. Measurements were performed by an investigator from the department of pulmonary diseases under supervision of a radiologist with special interest in thorax imaging. Intraobserver variability was tested by repeated measurements in 10 CT studies. To test interobserver variability, measurements were repeated in 20 CT studies by another investigator from the same department. Both observers were blinded to patients' medical history, hemodynamic data and diagnosis.

CTPA parameters

PA/AA_{AX} - Maximum diameters of the main pulmonary artery (PA) and ascending aorta (AA) were obtained at the level of the bifurcation of the pulmonary trunk according to previous studies [11, 12]. PA and AA measurements were done on the same image in the axial view (figure 1A). Afterwards the PA/AA ratio was calculated.

RV/LV_{AX} - Maximum transverse diameters of the RV and LV, defined as the widest distance of the endocardium between the interventricular septum and the free wall, were measured in the axial plane perpendicular to the long axis of the heart. Maximum diameters of the RV and LV were not necessarily obtained from the same image. Subsequently the RV/LV ratio was calculated (figure 1B).

RV/LV_{4CH} - Multiplanar reconstruction (MPR) was used to manually reconstruct a 4CH view in the same manner as described earlier [18, 20]. Similar to the ventricular measurements in the axial view, the maximum transverse diameters of the RV and LV were obtained from the 4CH view and the RV/LV ratio was calculated. Again maximum diameters of the RV and LV were not necessarily acquired from the same image (figure 1C).

Statistical analysis

Continuous data are presented as mean ± standard deviation (SD) and absolute numbers for categorical variables. Differences between mean values from precapillary pulmonary hypertension patients and control subjects were analyzed using the unpaired Student t test (variables with a normal distribution) or Mann-Whitney U tests (variables not normally distributed). Intra and-interobserver variability of the three CTPA parameters were analyzed using simple linear regression analysis. Univariable binary logistic regression analysis was used to test the predictive value of the three different CTPA parameters separately for precapillary pulmonary hypertension.

To test whether adding ventricular measurements to the PA/AA_{AX}-ratio would improve the diagnostic model of CTPA for precapillary pulmonary hypertension, we compared three different diagnostic models: Model 1: PA/AA_{AX} (standard); Model 2: PA/AA_{AX} + RV/LV_{AX}; and Model 3: PA/AA_{AX} + RV/LV_{4CH} (table 1).

Prediction models	
Model 1	PA/AA_{AX}
Model 2	PA/AA_{AX} + RV/LV_{AX}
Model 3	PA/AA_{AX} + RV/LV_{4CH}

Table 1: Prediction models. PA/AA_{AX} = ratio between pulmonary artery and ascending aorta. RV/LV_{AX} = ratio between RV and LV in the axial plane. RV/LV_{4CH} = ratio between RV and LV in the 4CH view.

The statistical approach to test the predictive value for precapillary PH of the three diagnostic models contained three different steps.

First we tested the predictive value of the three different models using multivariable binary logistic regression analysis. Second, the predictive value of the three different diagnostic models were tested using the area under the curve (AUC) derived from the Receiver Operating Characteristic curves. The AUC from the different models were compared using the DeLong method.

Third, to test the predictive value of the different diagnostic models within the clinical context of this study, we used decision curve analysis. With decision curve analysis it is possible to evaluate the clinical net benefit of the different prediction models [21, 22]. The net benefit is defined as the sum of benefits (true positives) minus the harms (false positives). Importantly, the threshold probability of the outcome determines the weights given to the true positives and false positives. The threshold probability is defined as the minimum probability of precapillary PH where a physician would decide to act. In this study it means that on the basis of the CTPA scan, it is decided to do further diagnostic tests to confirm the diagnosis. Since the exact threshold probability is unknown and will vary among physicians, we calculated the net benefit over a variety of probabilities. These net benefits can be calculated from the net benefit when nobody has precapillary PH (no positives) or from the net benefit when everybody has precapillary PH (no negatives). In this study, we focused on a range of low threshold probabilities (1-20%) since the weight assigned to false negatives (missing the diagnosis) is considerably larger than to false positives (further diagnostic evaluation).

For clinical purposes of the diagnostic models, a cut-off value to define precapillary PH is demanded. An established cut-off value to define PH is $PA/AA_{AX} > 1$ [12]. A well-recognized cut-off value for the

RV/LV-ratio is lacking. A frequently applied method for determining a cut-off value is calculation of the Youden Index, which is the cut-off value belonging to the highest sum of the combination of sensitivity and specificity, derived from the ROC-analysis. Since this cut-off value is not necessarily the optimal cut-off value within the clinical context, we chose a range of cut-off values to determine an optimal cut-off value.

Statistical analyses were performed using SPSS (version 20.0, SPSS, inc, Chicago, Illinois) and R (R Foundation for Statistical Computing, Vienna, Austria, 2013) . P-values <0.05 were considered statistically significant.

Results

Baseline characteristics of both groups are summarized in table 2. Between groups there were expected differences in mean pulmonary artery pressure (mPAP), pulmonary vascular resistance (PVR), right atrial pressure (RAP) and cardiac output (CO). The average interval time between the baseline right heart catheterization and CTPA in the precapillary PH group was 16 ± 7 days and 15 ± 5 days in the control group. Mean values of all three CTPA parameters were significantly different between precapillary PH patients and controls (table 3).

	PH (n=51)	**Controls (n=25)**
Gender	71% female	76% female
Age (years)	56 ± 16	55 ± 15
Precapillary PH		
IPAH	41	
CTEPH	10	
mPAP (mmHg)	48 ± 16	16 ± 4*
PAWP (mmHg)	7 ± 3	6 ± 3
PVR (Dyne.s/cm^5)	774 ± 452	126 ± 70*
RAP (mmHg)	8 ± 5	3 ± 2*
CO (L/min)	5.1 ± 0.3	6.9 ± 0.4*

Table 2: Baseline characteristics. IPAH = idiopathic pulmonary arterial hypertension; CTEPH = chronic trombo-embolic pulmonary hypertension; mPAP = mean pulmonary artery pressure; PAWP = pulmonary artery wedge pressure; PVR = pulmonary vascular resistance; RAP = right atrial pressure; CO = cardiac output. *p<0.05 compared with the PH group.

CTPA parameters	PH	Controls
PA/AA_{AX}	1.20 ± 0.30	0.85 ± 0.13*
RV/LV_{AX}	1.62 ± 0.42	1.00 ± 0.20*
RV/LV_{4CH}	1.65 ± 0.42	1.00 ± 0.18*

Table 3: CTPA parameters. Mean values ± SD. PA/AA_{AX} = ratio between pulmonary artery and ascending aorta. RV/LV_{AX} = ratio between RV and LV in the axial plane. RV/LV_{4CH} = ratio between RV and LV in the 4CH view. *p<0.05 compared with the PH group.

Intra- and interobserver variability

Intra- and interobserver variability was tested with simple linear regression and showed good agreement for all three parameters (Intra: PA/AA_{AX}: β=0.974 p<0.001; RV/LV_{AX}: β=0.958 p<0.001; RV/LV_{4CH}: β=0.896 p=0.001. Inter: PA/AA_{AX}: β=0.971 p<0.001; RV/LV_{AX}: β=0.965 p<0.001; RV/LV_{4CH}: β=0.930 p<0.001).

Univariable and multivariable binary logistic regression analysis

Univariable binary logistic regression analysis showed that all three CTPA parameters were predictors of precapillary PH (Table 4). Multivariable binary logistic regression analysis showed an improvement of the predictive value for precapillary PH of model 2 (-2LL=26.48) and 3 (-2LL=21.03) compared with model 1 (-2LL=56.56) and showed a slightly better predictive value of model 3(-2LL=21.03) compared to model 2(-2LL=26.48) (table 5). A multivariate model with all three CTPA parameters was not possible because the correlation between RV/LVAX and RV/LV4CH was too strong (multicollinearity, VIF=6.5).

CTPA parameters	-2LL	B	OR	95% C.I.	p-value
PA/AA_{AX}	56.56	1.19	3.27	1.78 – 6.03	p<0.001
RV/LV_{AX}	47.22	0.82	2.26	1.51 – 3.39	p<0.001
RV/LV_{4CH}	44.77	0.86	2.37	1.51 – 3.71	p<0.001

Table 4: Univariable binary logistic regression analysis. B = beta; OR = odds ratio; 95% C.I. = 95% confidence interval.

ROC analysis

The AUC of the three different models are shown in figure 2. The AUC of model 2 and 3 were significantly higher than the AUC of model 1 (p=0.011 and p=0.007, respectively). There was no significant difference in the AUC between model 2 and 3 (p=0.266).

Prediction models		-2LL	B	OR	95% C.I.	p-value
Model 1	PA/AA_{AX}	56.56	1.19	3.27	1.78 – 6.03	P<0.001
Model 2	PA/AA_{AX}	26.48	1.79	5.99	1.67 – 21.45	P=0.006
	RV/LV_{AX}		0.82	2.28	1.37 – 3.78	P=0.001
Model 3	PA/AA_{AX}	21.03	2.40	10.98	1,73 – 69.52	P=0.011
	RV/LV_{4CH}		1.12	3.07	1.46 – 6.46	P=0.003

Table 5: Multivariate binary logistic regression analysis. -2LL=log-likelihood statistic; B= beta; OR = odds ratio; 95% C.I. = 95% confidence interval.

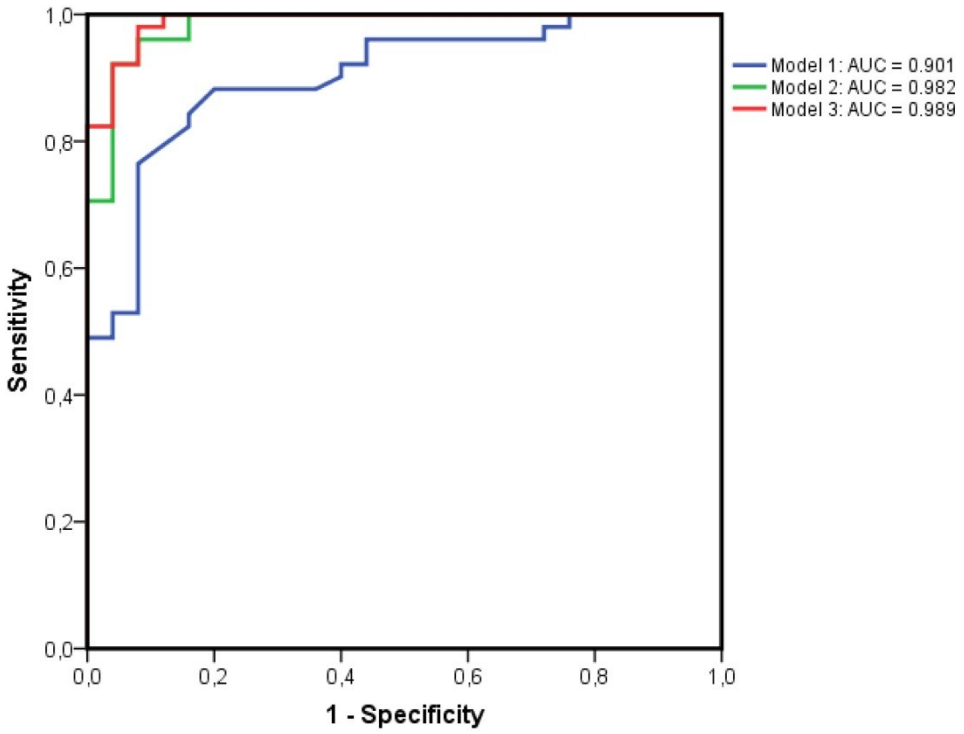

Figure 2: Area Under the Curve (AUC) of the three different models. Blue line = model 1; Green line = model 2; Red line = model 3.

Decision curve analysis

The DCA curves of the three models are illustrated in figure 3. The black line represents the net benefit at different threshold probabilities if we would not use any model and decide that nobody has precapillary PH (no positives). Since the net benefit is defined as the sum of the true positives minus the false positives, the net benefit is zero at the entire range of threshold probabilities. The grey line represent the net benefit if we decide that everybody has precapillary PH (no negatives) and any of the models would not be used. We determined, at a range of low threshold probabilities (0-20%), the net benefit of the three diagnostic models with respect to calling everybody a precapillary PH patient (grey line).

Results are summarized in table 6. The net benefit of model 2 and 3 was, over the entire range of low threshold probabilities, better than the net benefit of model 1, with a decrease of up to 25 false positive patients without an increase in false negative patients. The net benefit of model 3 was also slightly better than model 2.

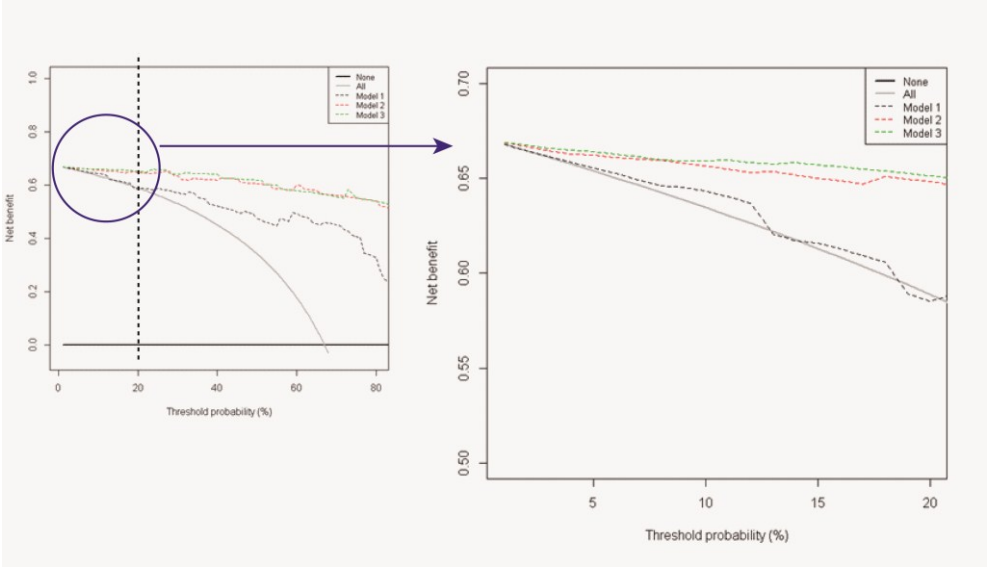

Figure 3: Decision curve analysis. Decision curve analysis of the three models to predict the presence of precapillary PH. On the right an expended view of the curves at low threshold probabilities, ranging from 0 to 20%

Threshold probability %	False Positives	NB PH all	NB Model 1: PA/AA_{AX}	Delta NB	Decrease in false positives (per 100 patients) without an increase in false negatives
1	25	0.6677299	0.6677299	0.0000000	0
2	24	0.6643394	0.6646079	0.0002685	1
5	22	0.6537396	0.6558172	0.0020776	4
10	19	0.6345029	0.6432749	0.0087720	8
15	18	0.6130031	0.6160991	0.0030960	2
20	18	0.5888158	0.5855263	-0.0032895	-1
Threshold probability %		**NB PH all**	**NB Model 2: PA/AA_{AX} + RV/LV_{AX}**	**Delta NB**	**Decrease in false positives (per 100 patients) without an increase in false negatives**
1	18	0.6677299	0.6686603	0.0009304	9
2	17	0.6643394	0.6664877	0.0021482	11
5	13	0.6537396	0.6620499	0.0083102	16
10	10	0.6345029	0.6564328	0.0219298	20
15	9	0.6130031	0.6501548	0.0371517	21
20	7	0.5888158	0.6480263	0.0592105	24
Threshold probability %		**NB PH all**	**NB Model 3: PA/AA_{AX} + RV/LV_{4CH}**	**Delta NB**	**Decrease in false positives (per 100 patients) without an increase in false negatives**
1	16	0.6677299	0.6689261	0.0011962	12
2	14	0.6643394	0.6672932	0.0029538	14
5	10	0.6537396	0.6641274	0.0103878	20
10	8	0.6345029	0.6593567	0.0248538	22
15	6	0.6130031	0.6571207	0.0441176	25
20	6	0.5888158	0.6513158	0.0625000	25

Table 6: Net benefits(NB) of model 1, 2 and 3. The net benefit (NB) is calculated as: NB = (true positives / n) – ((false positives / n) x (Pt / (1-Pt)). Subsequently, the decrease in false positives per 100 patients without an increase in false negatives is calculated as: (NB_{model} – NB_{all}) x 100(Pt / 1-Pt). Pt = Threshold probability [21, 22].

Cut-off value

To find an optimal cut-off value for defining precapillary PH, we analyzed a range of cut-off values which are summarized in table 7. Since the weight assigned to false-negatives is larger than to false-positives, we looked for a cut-off value with a high sensitivity and negative predictive value, in combination with a relatively high specificity. Therefore, we chose as an optimal cut-off value for the RV/LV- ratio: RV/LV ≥ 1.20.

Prediction models	Sensitivity(%)	Specificity(%)	PPV(%)	NPV(%)
Model 1:				
$PA/AA_{AX} \geq 1$	75	92	95	64
Model 2:				
$PA/AA_{AX} \geq 1$ or $RV/LV_{AX} \geq 1$	100	48	80	100
$PA/AA_{AX} \geq 1$ or $RV/LV_{AX} \geq 1.10$	100	68	86	100
$PA/AA_{AX} \geq 1$ or $RV/LV_{AX} \geq 1.15$	98	76	89	95
$PA/AA_{AX} \geq 1$ or $RV/LV_{AX} \geq 1.20$	94	80	91	87
$PA/AA_{AX} \geq 1$ or $RV/LV_{AX} \geq 1.30$	94	84	92	88
Model 3:				
$PA/AA_{AX} \geq 1$ or $RV/LV_{4CH} \geq 1$	100	40	77	100
$PA/AA_{AX} \geq 1$ or $RV/LV_{4CH} \geq 1.10$	100	68	86	100
$PA/AA_{AX} \geq 1$ or $RV/LV_{4CH} \geq 1.15$	98	76	89	95
$PA/AA_{AX} \geq 1$ or $RV/LV_{4CH} \geq 1.20$	96	80	91	91
$PA/AA_{AX} \geq 1$ or $RV/LV_{4CH} \geq 1.30$	94	84	92	88

Table 7: Sensitivity, specificity, positive predictive values and negative predictive values. PPV=positive predictive value; NPV=negative predictive value.

Discussion

In this study we tested different prediction models for precapillary PH using CTPA. Using an extensive statistical approach to obtain the best prediction model, we were able to show that combining ventricular and pulmonary artery measurements (model 2 and 3) improved the predictive value of CTPA for precapillary PH.

Earlier studies mainly focused on PA/AA_{AX} to predict PH and showed that a $PA/AA_{AX}>1$ has a sensitivity and specificity ranging from 58 to 87% and 73 to 95%, respectively [14, 15, 18-20]. This is in line with our results ($PA/AA_{AX}>1$: sensitivity 75% and specificity 92%).

Multivariable binary logistic regression analyses and the significantly higher AUCs of model 2 and 3 compared to model 1, showed that there is a statistically significant improvement of the prediction model when ventricular and pulmonary artery measurements are combined. DCA confirmed the clinical relevance of this approach. Arguing that, missing the diagnosis is worse than performing unnecessary diagnostic tests, we assigned a higher weight to false negatives than to false positives and focused on a range of low threshold probabilities. We showed that, even at this range of low threshold probabilities, in comparison to model 1, models 2 and 3 allowed a decrease in number of false positives without an increase in the number of false negatives. As such, adding ventricular measurements to pulmonary artery measurements statistically improves the prediction model with clinical relevance.

We are aware of only one other study investigating ventricular measurements on CTPA to predict PH. Chan et al measured the RV/LV ratio in the axial view and found that a RV/LV>1.28 predicted PH with a sensitivity of 85.7% and 86.1% [16]. There are no studies that used a combination of ventricular and pulmonary measurements to improve the predictive value of CTPA.

Manual reconstructed 4CH-views for determining ventricular diameters on standard CTPA have not been previously used in radiological studies of PH. In studies of patients of acute PE, some investigators indicated that the RV/LV determined in the 4 chamber view provided superior prediction of subsequent adverse events than the same ratio measured in the axial view, although other studies didn't find any differences [18, 19, 23].

In this study, ROC analyses showed no significant difference between model 2 and 3 ($p=0.266$) and also the net benefits determined with DCA were almost equal in both models. Therefore, determination of the RV/LV ratio in the axial view seems preferable as it does not require a manual reconstruction of the image.

We analyzed a range of cut-off values for the RV/LV ratio and did not use ROC analysis, as this method may not necessarily yield a clinically relevant cut-off value. To avoid missed diagnosis, the most suitable cut-off value for defining precapillary PH in this study was $RV/LV \geq 1.20$ (model 2: sensitivity 94%, specificity 80%, PPV 91%, NPV 87%; model 3: sensitivity 96%, specificity 80%, PPV 91%, NPV 91%).

Recognizing the signs of pulmonary hypertension on CTPA provides the radiologist with a tool to identify the disease timely. CTPA is often performed early in the diagnostic process of patients with unexplained dyspnea. Combining ventricular and pulmonary artery measurements decreases the chance that the diagnosis of precapillary PH is missed. When there is suspicion of precapillary PH, and a CTPA is made, we recommend radiologists to assess not only the diameters of the great vessels, but also of both ventricles. When the PA/AA-ratio is greater or equal to 1 or when the RV/LV is greater or equal to 1.20, further diagnostic tests, to confirm or rule out PH are required. As a next diagnostic step, we would recommend to perform an echocardiography.

We want to emphasize, that CTPA measurements should not be used as a primary screening tool for precapillary PH. In isolation, CTPA measurements are not suitable to rule out or confirm the diagnosis of precapillary PH.

The reason for including patients with idiopathic pulmonary arterial hypertension and chronic thromboembolic pulmonary hypertension in this analysis is that a timely diagnosis in these conditions can be lifesaving. Whether or not our results can be extrapolated to other forms of precapillary PH for which no treatment is currently available requires further investigations. In addition, we excluded patients with PH due to left sided systolic or diastolic heart failure (WHO group 2). That this may not be a major problem is suggested by the study of Chan et al. [16], in which mostly WHO group 2 PH patients were included and PA/AA_{AX} and RV/LV_{AX}, measured separately, were good predictors of PH.

Study limitations

First of all, baseline hemodynamic results suggested that all our PH patients were diagnosed in an advanced stage of their disease. We do not know whether our findings can be extrapolated to the earliest stages of the disease. Another limitation is that we performed a retrospective analysis. Preferably, a prospective analysis would be performed in a general population undergoing a CTPA for the evaluation of dyspnea. However, performing such a study would be very difficult regarding the low prevalence of precapillary PH.

18 CTPA studies were performed on a 4-slice CT system. Theoretically, on a 4-slice CT system, not all slices depicting the heart are in the same phase of the cardiac cycle. However, since the slices depicting the maximum diameter of the RV and LV were mostly adjacent or very close to each other, we did no experienced this problem.

Conclusions

The predictive value of CTPA for precapillary PH improves when ventricular and pulmonary artery measurements are combined. A $PA/AA_{AX} \geq 1$ or a $RV/LV_{AX} \geq 1.20$ needs further diagnostic evaluation to rule out or confirm the diagnosis.

References

[1] Galie N, Hoeper MM, Humbert M, Torbicki A, Vachiery JL, Barbera JA, et al. Guidelines for the diagnosis and treatment of pulmonary hypertension. The European respiratory journal. 2009; 34:1219-63
[2] Vonk Noordegraaf A, Galie N. The role of the right ventricle in pulmonary arterial hypertension. Eur Respir Rev. 2011; 20:243-53
[3] Ling Y, Johnson MK, Kiely DG, Condliffe R, Elliot CA, Gibbs JS, et al. Changing demographics, epidemiology, and survival of incident pulmonary arterial hypertension: results from the pulmonary hypertension registry of the United Kingdom and Ireland. Am J Respir Crit Care Med. 2012; 186:790-6
[4] Badesch DB, Raskob GE, Elliott CG, Krichman AM, Farber HW, Frost AE, et al. Pulmonary arterial hypertension: baseline characteristics from the REVEAL Registry. Chest. 2010; 137:376-87
[5] Strange G, Gabbay E, Kermeen F, Williams T, Carrington M, Stewart S, et al. Time from symptoms to definitive diagnosis of idiopathic pulmonary arterial hypertension: The delay study. Pulmonary circulation. 2013; 3:89-94
[6] Wilkens H, Grimminger F, Hoeper M, Stahler G, Ehlken B, Plesnila-Frank C, et al. Burden of pulmonary arterial hypertension in Germany. Respiratory medicine. 2010; 104:902-10
[7] Brown LM, Chen H, Halpern S, Taichman D, McGoon MD, Farber HW, et al. Delay in recognition of pulmonary arterial hypertension: factors identified from the REVEAL Registry. Chest. 2011; 140:19-26
[8] Humbert M, Gerry Coghlan J, Khanna D. Early detection and management of pulmonary arterial hypertension. Eur Respir Rev. 2012; 21:306-12
[9] Humbert M, Sitbon O, Chaouat A, Bertocchi M, Habib G, Gressin V, et al. Survival in patients with idiopathic, familial, and anorexigen-associated pulmonary arterial hypertension in the modern management era. Circulation. 2010; 122:156-63
[10] Galie N, Rubin L, Hoeper M, Jansa P, Al-Hiti H, Meyer G, et al. Treatment of patients with mildly symptomatic pulmonary arterial hypertension with bosentan (EARLY study): a double-blind, randomised controlled trial. Lancet. 2008; 371:2093-100
[11] Tan RT, Kuzo R, Goodman LR, Siegel R, Haasler GB, Presberg KW. Utility of CT scan evaluation for predicting pulmonary hypertension in patients with parenchymal lung disease. Medical College of Wisconsin Lung Transplant Group. Chest. 1998; 113:1250-6
[12] Ng CS, Wells AU, Padley SP. A CT sign of chronic pulmonary arterial hypertension: the ratio of main pulmonary artery to aortic diameter. J Thorac Imaging. 1999; 14:270-8
[13] Sanal S, Aronow WS, Ravipati G, Maguire GP, Belkin RN, Lehrman SG. Prediction of moderate or severe pulmonary hypertension by main pulmonary artery diameter and main pulmonary artery diameter/ascending aorta diameter in pulmonary embolism. Cardiol Rev. 2006; 14:213-4
[14] Rajaram S, Swift AJ, Capener D, Elliot CA, Condliffe R, Davies C, et al. Comparison of the diagnostic utility of cardiac magnetic resonance imaging, computed tomography, and echocardiography in assessment of suspected pulmonary arterial hypertension in patients with connective tissue disease. J Rheumatol. 2012; 39:1265-74
[15] Edwards PD, Bull RK, Coulden R. CT measurement of main pulmonary artery diameter. Br J Radiol. 1998; 71:1018-20
[16] Chan AL, Juarez MM, Shelton DK, MacDonald T, Li CS, Lin TC, et al. Novel computed tomographic chest metrics to detect pulmonary hypertension. BMC Med Imaging. 2011; 11:7
[17] Corson N, Armato SG, 3rd, Labby ZE, Straus C, Starkey A, Gomberg-Maitland M. CT-Based Pulmonary Artery Measurements for the Assessment of Pulmonary Hypertension. Academic radiology. 2014; 21:523-30
[18] Quiroz R, Kucher N, Schoepf UJ, Kipfmueller F, Solomon SD, Costello P, et al. Right ventricular enlargement on chest computed tomography: prognostic role in acute pulmonary embolism. Circulation. 2004; 109:2401-4
[19] Dogan H, Kroft LJ, Huisman MV, van der Geest RJ, de Roos A. Right ventricular function in patients with acute pulmonary embolism: analysis with electrocardiography-synchronized multi-detector row CT. Radiology. 2007; 242:78-84
[20] Schoepf UJ, Kucher N, Kipfmueller F, Quiroz R, Costello P, Goldhaber SZ. Right ventricular enlargement on chest computed tomography: a predictor of early death in acute pulmonary embolism. Circulation. 2004; 110:3276-80
[21] Vickers AJ, Elkin EB. Decision curve analysis: a novel method for evaluating prediction models. Med Decis Making. 2006; 26:565-74
[22] Steyerberg EW, Vickers AJ, Cook NR, Gerds T, Gonen M, Obuchowski N, et al. Assessing the performance of prediction models: a framework for traditional and novel measures. Epidemiology (Cambridge, Mass. 2010; 21:128-38
[23] Stein PD, Matta F, Yaekoub AY, Goodman LR, Sostman HD, Weg JG, et al. Reconstructed 4-chamber views compared with axial imaging for assessment of right ventricular enlargement on CT pulmonary angiograms. J Thromb Thrombolysis. 2009; 28:342-7

CHAPTER 3

Right Heart Score for Predicting Outcome in Idiopathic, Familial or Drug- and Toxin-associated Pulmonary Arterial Hypertension

Journal of the American College of Cardiology: Cardiovascular Imaging 2015

F Haddad[1], OA Spruijt[2], AY Denault[3], O Mercier[4], N Bruner[5], D Furman[1], E Fadel[4], HJ Bogaard[2], I Schnittger[1], B Vrtovec[1], J Wu[1], V de Jesus Perez[5], A Vonk Noordegraaf[2], RT Zamanian[5]

[1]Department of Cardiovascular Medicine, Stanford University and Stanford Cardiovascular Institute, Palo Alto, CA
[2]Department of Pulmonary Medicine, VU University Medical Center, Amsterdam
[3]Department of Anesthesia and Critical Care, Montreal Heart Institute, Montreal University
[4]Cardiovascular and Thoracic Research Center, Marie-Lannelongue Surgical Center, Université Paris-sud
[5]Department of Pulmonary and Critical Care Medicine, Stanford University and the Vera Moulton Wall Center for Pulmonary Vascular Disease

Abstract

Introduction: This study sought to determine whether a simple score combining indexes of right ventricular (RV) function and right atrial (RA) size would offer good discrimination of outcome in patients with pulmonary arterial hypertension (PAH). Identifying a simple score of outcome could simplify risk stratification of patients with PAH and potentially lead to improved tailored monitoring or therapy.

Methods: We recruited patients from both Stanford University (derivation cohort) and VU University Medical Center (validation cohort). The composite endpoint for the study was death or lung transplantation. A Cox proportional hazard with bootstrap CI adjustment model was used to determine independent correlates of death or transplantation. A predictive score was developed using the beta coefficients of the multivariable models.

Results: For the derivation cohort (n=95), the majority of patients were female (79%), average age was 43±11 years, mean pulmonary arterial pressure was 54±14 mmHg, and pulmonary vascular resistance index was 25±12 WUxm2. Over an average follow-up of 5 years, the composite endpoint occurred in 34 patients, including 26 deaths and 8 patients requiring lung transplant. On multivariable analysis, RV systolic dysfunction grade (HR: 3.4 per grade; 95%CI: 2.0-7.8 p<0.001), severe RA enlargement (HR: 3.0 95%CI: 1.3-8.1 p=0.009), and systemic blood pressure <110 mmHg (HR: 3.3; 95% CI: 1.5 to 9.4; p < 0.001) were independently associated with outcome. A right heart (RH) score constructed on the basis of these 3 parameters compared favorably with the National Institutes of Health survival equation (AUC=0.88; 95%CI: 0.79-0.94 vs. AUC=0.60; 95%CI: 0.49-0.71 p<0.001) but was not statistically different than the REVEAL (Registry to Evaluate Early and Long-Term PAH Disease Management) score c-statistic of 0.80 (95%CI: 0.69-0.88) with p=0.097. In the validation cohort (n=87), the RH score remained the strongest independent correlate of outcome.

Conclusions: In patients with prevalent PAH, a simple RH score may offer good discrimination of long-term outcome.

Introduction

Pulmonary arterial hypertension (PAH) is a rare condition caused by the progressive narrowing of the small pulmonary arteries, leading to increased pulmonary vascular resistance and right-sided heart failure [1]. Despite advances in therapy, the mortality remains high, approaching 30% to 50% at 5 years in symptomatic patients [1, 2]. In recent years, right ventricular (RV) function has emerged as one of the strongest predictors of outcome in PAH [3]. Hemodynamic studies have highlighted the prognostic importance of elevated right atrial (RA) pressure and decreased cardiac output, whereas imaging studies have highlighted the importance of RV remodeling and systolic function [2, 4-6]. Moreover, recent scores, such as the REVEAL (Registry to Evaluate Early and Long-Term PAH Disease Management) score, have integrated several of the clinical and functional parameters [2].

To date, only a few studies have investigated whether RA size or function has incremental value to RV function in predicting outcome in PAH. The importance of RA size in PAH was first suggested by Bustamente-Labarta et al. [7] in their series of 25 patients. In a larger study in patients with PAH (n=81), Raymond et al. [8] found that there was a trend for an independent association between RA area index (p=0.106) and the composite endpoint of death or transplantation. To our knowledge, no study has of yet also investigated the prognostic value of RA function measured by active and passive emptying fractions (RAEF) in PAH.

For our study, we first hypothesized that measures of RA size or function would be independently associated with event-free survival in PAH. We further hypothesized that a simple score combining quantitative measures of right heart size or function would provide good discrimination of outcome in PAH.

Methods

Study design

Our study included a derivation cohort at Stanford University, followed by a validation cohort at the VU University Medical Center. After ethics committee approval, consecutive adult patients followed at Stanford University between January 1999 and January 2009 with a confirmed diagnosis of idiopathic or drug and toxin PAH were considered for inclusion in the study. The diagnosis of PAH was on the basis of the standard definition of mean pulmonary arterial pressure ≥25mmHg and pulmonary artery wedge pressure ≤15mmHg [9]. We excluded patients for whom an echocardiogram was not available and patients with evidence of atrial fibrillation at baseline, left

heart failure, and significant parenchymal lung disease. Patients recruited at the VU University Medical Center had a diagnosis of idiopathic or familial PAH and underwent cardiac magnetic resonance (CMR) as part of a prospective study to evaluate the role of CMR in the management of PAH, for which medical ethical consent approval was obtained.

The composite endpoint of the study was death or lung transplantation. Death was verified through the national Social Security Death Index and transplantation through chart review. Data collection included demographics, 6-min walking distance (6MWD), estimated glomerular filtration rate, N-terminal pro–B-type natriuretic peptide (NTproBNP) levels, diffusion capacity of carbon monoxide, and hemodynamics. Renal function was estimated using the modified diet and renal equation [10]. For purposes of standardization, data were collected on the first outpatient visit after stabilization on disease-modifying medications (prostanoids, endothelin receptor blockers, or phosphodiesterase inhibitors). We chose this time point for 2 reasons. First, this time point corresponded to the same day patients completed echocardiography, 6MWD, and laboratory testing (metabolic panel and NT-proBNP). In addition, the baseline right heart catheterization was often obtained within a 3- to 6-month time frame of this visit.

Echocardiography

Digitized echocardiographic studies were analyzed by the Stanford Cardiovascular Institute biomarker and phenotypic core laboratory in accordance with published guidelines of the American Society of Echocardiography (ASE) [11]. All measures were averaged over 3 cycles, and RV or RA size measures were indexed to body surface area. RV end-diastolic and end-systolic areas, as well as RA size, were measured from the apical 4-chamber view (Figure 1). RV function was quantified using right ventricular fractional area change (RVFAC), tricuspid annular systolic excursion (TAPSE), and right ventricular myocardial performance index (RVMPI), as previously described [11-13]. RA size was measured at end-systole (RAmax), pre-atrial contraction (RApre-A), and end-diastole (RAmin) (Figure 2), and total, passive, and active RAEF were calculated as follows:

$$RAEF_{total} = (RA_{max} - RA_{min}) / RA_{max}$$

$$RAEF_{passive} = (RA_{max} - RA_{pre\text{-}A}) / RA_{max}$$

$$RAEF_{active} = (RA_{pre\text{-}A} - RA_{min}) / RA_{pre\text{-}A}$$

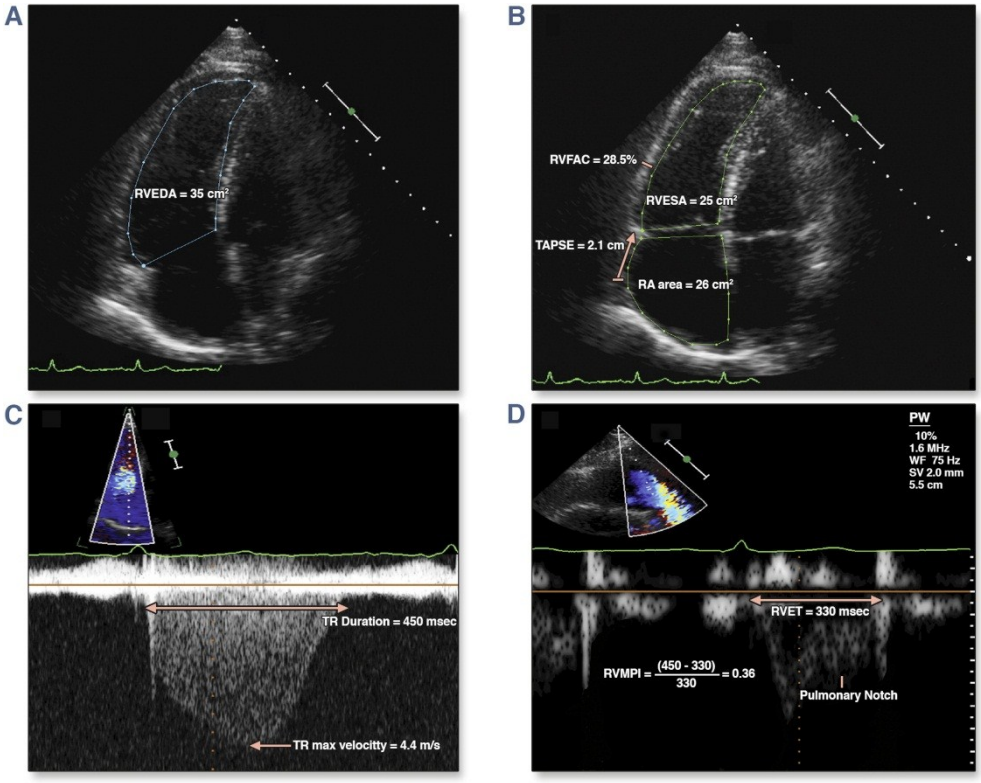

Figure 1: Representative Measures of Right Heart Size and Functional Parameters. A: Measures of right ventricular end-diastolic area (RVEDA). B: Measures of right ventricular end-systolic area (RVESA) and 2-dimensional tricuspid annular systolic excursion (TAPSE). C: Measures of tricuspid regurgitation (TR) duration. D: Measures of RV ejection time. RA = right atrial; RVET = right ventricular ejection time; RVFAC = right ventricular fractional area change; RVMPI = right ventricular myocardial performance index.

Reference values for right heart remodeling and function

RV systolic dysfunction was classified based on RVFAC as mild (25-35%), moderate (18-24%), or severe (≤17%) [11]. For indexed values of RA size and function, because no values are referenced in the ASE guidelines, we used 95% of the upper limit of 95 prospectively recruited age- and sex-matched healthy controls on the basis of a 50-point questionnaire. Dimensions were categorized using similar thresholds as the left atrial volumes: mild increase (increase <18% of reference value) and severe increase (increase >40% of reference value). For indexed RA area and right ventricular end-diastolic area (RVEDA), the upper limit of normal was 11 cm^2/m^2 and for indexed right ventricular end-systolic area (RVESA), the upper limit was 7.5 cm^2/m^2.

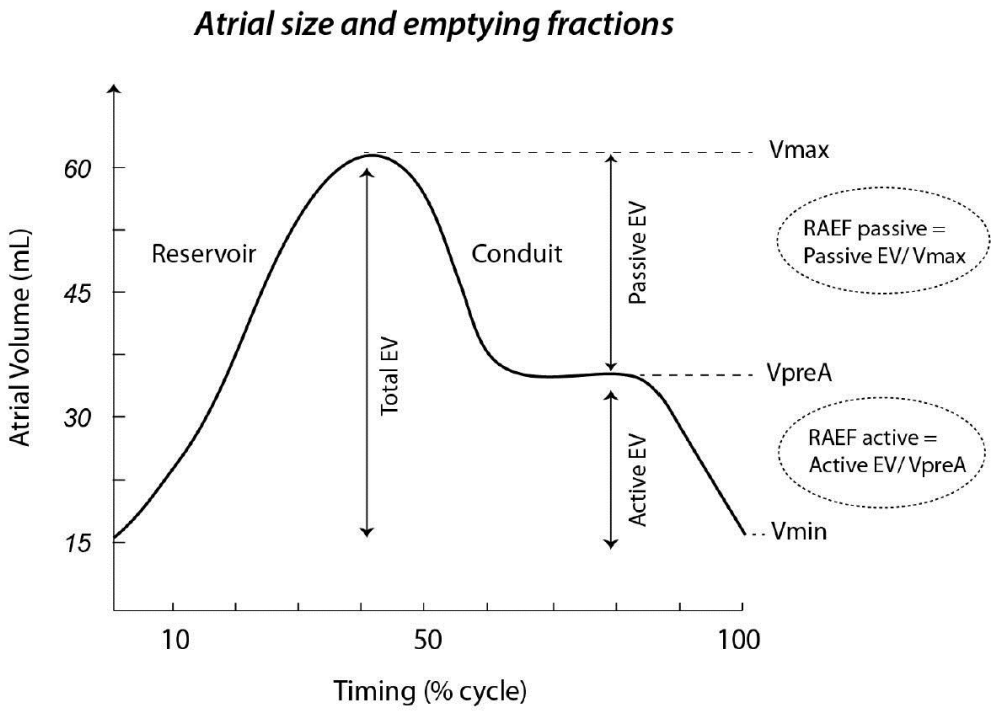

Figure 2: Atrial Size and Emptying Fractions. The figure depicts the different concepts related to RA volumes and the related concepts of total, passive, and RA emptying fractions. EV = emptying volume; RAEF = right atrial emptying fractions; Vmax = maximal volume; Vmin = minimal volume; VpreA = pre-atrial contraction volume.

CMR protocol in the validation cohort

CMR was performed on a 1.5T Sonato scanner (Siemens Medical Solutions, Erlangen, Germany), equipped with a 6-element phased-array receiver coil. Short-axis images from base to apex of the ventricles were obtained with a typical slice thickness of 5mm, and an interslice gap of 5mm was used for estimation of ventricular volumes using the Simpson method, as previously described [14]. The thresholds chosen for the CMR categorical classification were pre-defined at the beginning of the study. We chose the threshold of 35% for moderate RVEF dysfunction similar to the previously established cutoff in the study of van de Veerdonk et al. [14].

In addition, on the basis of a prior study from our group, we found that RVFAC of 25% corresponded best to an RVEF of 35% [15]. We used the same threshold for RA area for the echocardiographic and CMR studies.

Statistical analysis

Continuous data are presented as mean ± SD if the Kolmogorov-Smirnov test showed a normal distribution; otherwise, data are presented as median ± interquartile range (IQR). Categorical variables are expressed as frequency and percentage. Comparisons between groups were performed using 2-sided Student t tests with adjustment for unequal variance as needed. For non-normally distributed variables such as NT-pro-BNP level, transformation to the common logarithm was performed before analysis. Linear regression analysis was used to determine independent associations between hemodynamic and structural or functional right heart parameters. The association between clinical and echocardiographic parameters and outcome was analyzed using Cox proportional hazards models. The assumption of proportional hazards was assessed by plotting the scaled Schoenfeld residuals for each independent variable against time; these correlations were found to be nonsignificant for all variables included in the multivariable model. We used hierarchical modeling to determine factors independently associated with outcome and chose to include at maximum 1 covariate per 10 events to minimize overfitting of the model. We avoided including in the model variables that were collinearly related to each other. We used bootstrapping with 5000 iterations to estimate hazard ratios and bias-corrected 95% confidence interval (CI) for the multivariable models. For building the predictive score, the smallest absolute beta coefficient was assigned a value of 0 and values for subsequent variables were assigned on the basis of multiples of their respective beta coefficients to the nearest 0.5 approximation for categories with significantly different beta coefficients [16]. The survival c-statistic was calculated to show the discriminatory ability of the models and was used to compare the predictive score with the validated REVEAL score and National Institutes of Health (NIH) survival equation. Intraobserver variability was assessed using the average difference in absolute measurement and the intraclass correlation coefficient (ICC). Statistical analysis was done using PASW statistical program (version 18.0, SPSS Inc., Chicago, Illinois).

Results

Study population

Of 128 patients with idiopathic and drug- and toxin-associated PAH who were seen during the study period, 106 were enrolled in the prospective registry. Eleven patients were excluded from the study for the following reasons: unavailable echocardiogram (n=2), atrial fibrillation (n=1), lost to follow-up (n=5), left heart failure (n=2), and restrictive lung disease (n=1).

Characteristics	n=95
Age (years)	43±11
Women	75 (79%)
White	84 (88%)
Etiology of PAH	
Idiopathic or familial	44 (46%)
Drugs and toxin (history of use)	51 (55%)
Body mass index (kg/m^2)	30±6
Right heart catheterization	
HR (BPM)	82±14
SBP (mmHg)	120±17
RAP (mmHg)	10±6
mPAP (mmHg)	54±14
PAWP (mmHg)	10±4
CI (L/min/m^2)	2.0±0.6
PVRI (WUxm^2)	25±12
6MWD (m)	432±117
DLCO (%)	75±23
Comorbid conditions	
CKD (eGFR <60ml/min/1.73m^2)	22 (23%)
Hyponatremia (<136 mEq/l)	9 (9.5%)
Diabetes mellitus	3 (3%)
Systemic hypertension	4 (4%)
Medication	
Diuretics	48 (51%)
Prostanoid therapy	43 (45%)
PDE5I	31 (33%)
ERA	39 (41%)
Warfarin	59 (63%)

Table 1: Values are mean ± SD or n (%). CI = cardiac index; CKD = chronic kidney disease; DLCO = diffusion of carbon monoxide; eGFR = estimated glomerular filtration rate; HR = heart rate, mPAP = mean pulmonary arterial pressure; PAH = pulmonary arterial hypertension; PAWP = pulmonary capillary wedge pressure; PVRI = pulmonary vascular resistance index; RAP = right atrial pressure; SBP = systolic blood pressure.

Table 1 summarizes the characteristics of the study population. The average follow-up time for our study was 5.0±2.4 years. The mean pulmonary arterial pressure was 54±14mmHg, and the

pulmonary vascular resistance index (PVRI) score was 25±12 WUxm^2. Forty-five percent of patients (n=43) were on prostanoid therapy, and 19% of patients (n=18) were on combination therapy. Figure 3 summarizes the relationship between RA size, RAEF, and RV function as assessed by RVFAC. Compared with healthy controls, patients with PAH had a greater degree of RA and RV enlargement and lower RAEF. In general, RA enlargement and impaired active RAEF were more common among patients with severe RV dysfunction (Figures 3B and 3D).

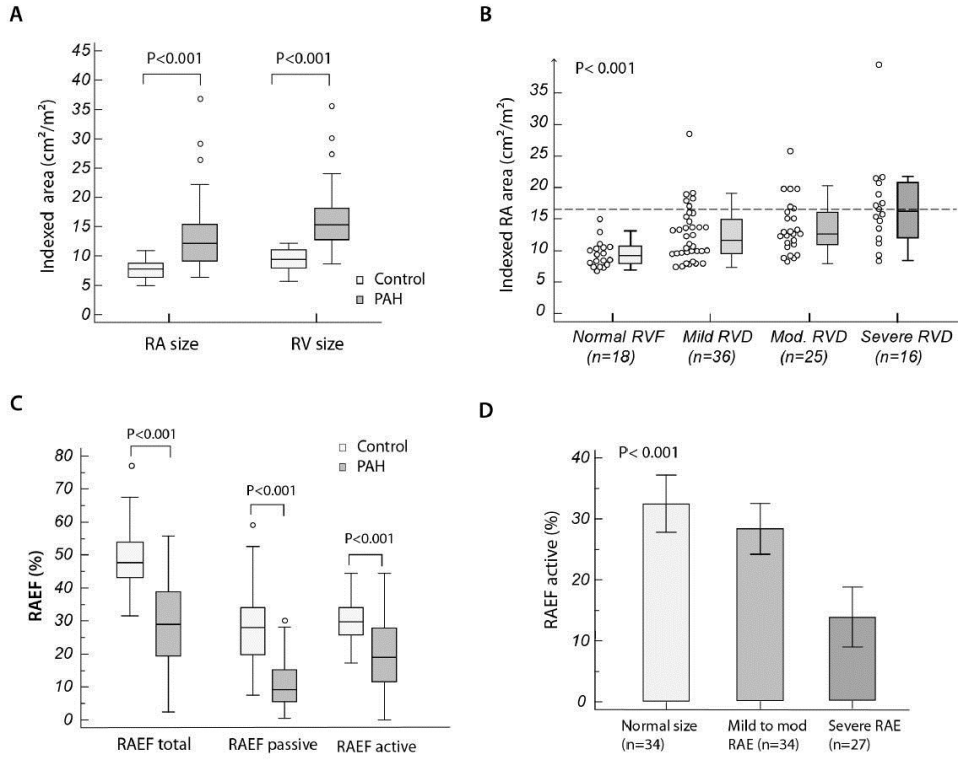

Figure 3: Ventricular and Atrial Remodeling and Function in the Study Population. A: Box-and-whisker plot of indexed RA and RV areas of patients with pulmonary arterial hypertension (PAH) and healthy controls. B: Box-and-whisker plot of indexed RA area according to the pre-defined categories of right ventricular dysfunction (RVD). C: Box-and-whisker plot of total, active, and passive RAEF of patients with PAH and healthy controls. D: Bar graph with 95% confidence interval for mean value for active RAEF, stratified according to the pre-defined categories of RA size. In the box-and-whisker plots, the central box represents the values from the lower to upper quartile (25th to 75th percentile); the middle line represents the median; and the line extends from the minimum to the maximum value, excluding outlier values. RAE = right atrial enlargement; RVF = right ventricular function; other abbreviations as in Figures 1 and 2.

Relationship between metrics of right heart function and hemodynamics

The different parameters of right heart size and function are not independent of each other; their inter-relationship is important to consider before outcome models are built. As expected, there was also strong collinearity between parameters of RV function (R^2=0.61 between RVFAC and TAPSE [p<0.001] and R^2=0.51 between RVFAC and RVMPI [p<0.001]), as well as between RVEDA and RA area (R^2=0.51; p<0.001). Table 2 summarizes factors independently associated with RVFAC, RA area index, active and passive RAEF, and log NT-proBNP levels. We favored including in the model factors that were not only correlates but also potential determinants. As covariates, factors considered included demographic factors (age and sex), load parameters (PVRI and right atrial pressure [RAP]), functional indexes (tricuspid regurgitation and TAPSE), or renal function for NT-proBNP. Among other associations, we found that pericardial effusion, which was present in 17 patients, was strongly related to both RAP and RA size (chi-square=22; p=0.01). Systolic blood pressure (SBP) was significantly correlated with cardiac output, as well as the use of intravenous prostanoids (R^2=0.28; p<0.011; r=0.40 with cardiac output and r=-0.28 with prostanoids).

	RVFAC	**RAI**	**$RAEF_{active}$**	**$RAEF_{passive}$**	**Log NT-proBNP**
R^2	0.32	0.61	0.41	0.27	0.59
Correlates	PVRI (r=-0.44)	RAP (r=0.44)	RAP (r=-0.27)	Age (r=-0.35)	RVFAC (r=-0.48)
	Male (r=-0.30)	TR (r=0.45)	TAPSE (r=0.33)	TAPSE (r=0.47)	RAI (r=0.40)
			Male (r=-0.27)		eGFR (r=-0.31)
					Male (r=-0.24)

Table 2: The multivariate models presented are all p < 0.001. PVRI is based on the most recent right heart catheterization. r corresponds to partial correlation coefficients. NT-proBNP = N-terminal pro–B-type natriuretic peptide; RAEF = right atrial emptying fractions; RAI = right atrial area index; RVFAC = right ventricular fractional area change; TAPSE = tricuspid annular systolic excursion; TR = tricuspid regurgitation; other abbreviations as in Table 1.

Outcome analysis in the derivation cohort

The composite endpoint occurred in 34 patients (36%), including 26 deaths and 8 lung transplants. Event-free survival at 1, 3, and 5 years was 95%, 89%, and 81%, respectively. The predicted NIH survival equation 1-, 3-, and 5-year survival estimates were 66%, 44%, and 33%, respectively, and the revised NIH prediction scores were 91%, 71%, and 63% [17]. Several parameters of right heart structure and function were strongly related to outcome on univariate analysis (Table 3).

	HR	95%CI	P-value
Clinical			
Age, per 10 years	0.75	0.54-1.03	0.082
Male	1.90	0.90-4.03	0.094
DT vs. Idiopathic	0.94	0.47-1.85	0.84
NYHA functional class, III+IV vs I+II	2.67	1.34-5.32	0.005*
Walking distance, per 100m	0.73	0.55-0.96	0.026*
SBP, per 10mmHg	0.73	0.58-0.92	0.009*
HR, per 10 bpm	1.17	0.89-1.54	0.26
DLCO, per 10%	0.97	0.88-1.09	0.61
Comorbidities			
CKD	2.18	1.07-4.46	0.033*
Hyponatremia	1.80	0.69-4.68	0.23
Log NT-proBNP	4.81	2.13-10.86	<0.001*
RV parameters			
RVEDAI, per 3cm2/m2	1.60	1.29-2.04	<0.001*
RVESAI, per 3cm2/m2	1.82	1.49-2.22	<0.001*
RVFAC, per 5%	0.52	0.41-0.67	<0.001*
TAPSE, per 0.3cm	0.61	0.46-0.82	0.001*
RVMPI, per 0.3U	2.06	1.16-3.69	0.015*
Right atrial parameters			
RAI, per 5 cm2/m^2	1.81	1.44-2.28	<0.001*
RAEF active, per 5%	0.69	0.57-0.83	<0.001*
RAEF passive, per 5%	1.27	1.02-1.58	0.029
Septal curvature			
Diastolic EI, per 0.5U	1.84	1.19-2.87	0.007*
Systolic EI, per 0.5U	1.33	1.11-1.57	0.001*
Tricuspid regurgitation	1.95	1.30-2.90	0.002*
Hemodynamics			
RAP, per 5mmHg	2.12	1.51-3.01	<0.001*
RVSP, per 10mmHg	1.14	0.91-1.43	0.25
RVSP/SBP, per 0.25	2.77	1.61-4.75	<0.001*
SVI, per 5ml/m^2	0.82	0.70-0.97	0.019*
Cardiac index <1.8l/min/m^2	2.22	1.09-4.50	0.025*
PVRI, per 10 WU x m^2	1.41	1.02-1.96	0.039*

LV parameters			
LVID, per 0.5cm	0.79	0.54-0.99	0.049*
LVEF, per 5%	0.72	0.60-0.88	0.001*

Table 3: Univariable analysis of factors associated with the composite endpoint. *Statistically significant. DT = drug and toxin; EI = eccentricity index; LVID = left ventricular internal dimension; LVEF = left ventricular ejection fraction; NYHA = New York Heart Association; RVEDAI = right ventricular end-diastolic area index; RVESAI = right ventricular end-systolic area index; RVMPI = right ventricular myocardial performance index; RVSP = right ventricular systolic pressure; SVI = stroke volume index; other abbreviations as in Tables 1 and 2.

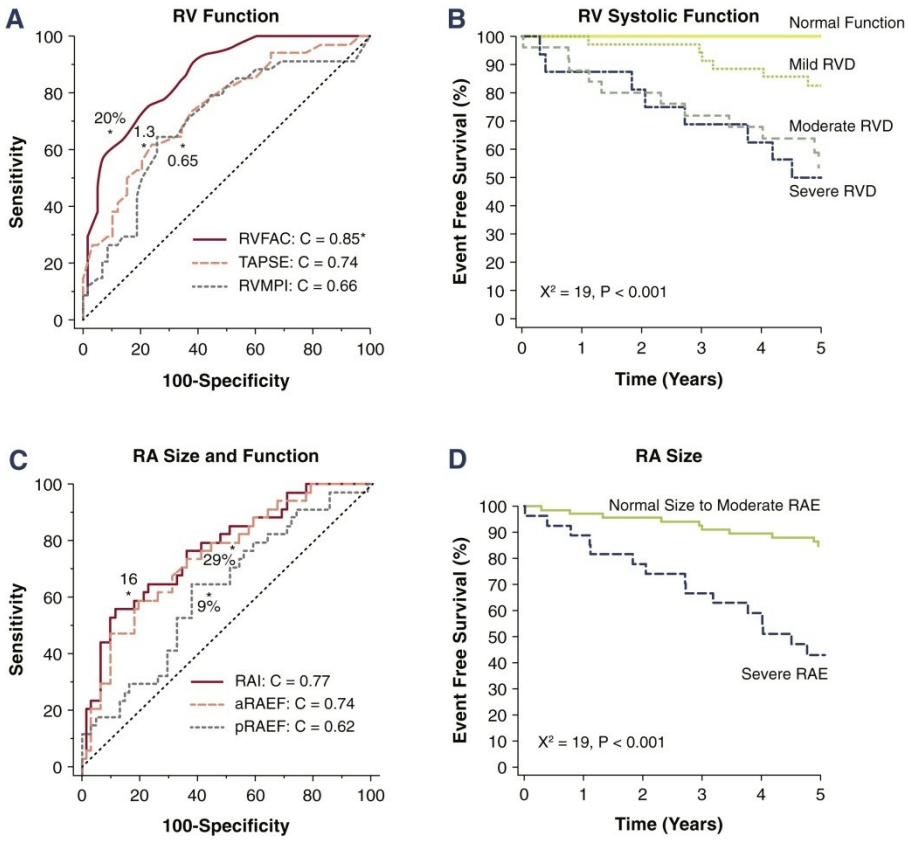

Figure 4: C-statistics and Kaplan-Meier Curves for Selected Parameters of RV and RA Function. A: C-statistic between indexes of RV function. B: Five-year Kaplan-Meier curve of RV systolic dysfunction on the basis of RVFAC. C: C-statistic between RA indexes. (D) Five-year Kaplan-Meier curve and severe RA enlargement. *In A and C, the criterion value noted on the graph is the optimal criterion value corresponding with the Youden index J with equal weight given to sensitivity and specificity. aRAEF = active right atrial emptying fractions; pRAEF = passive right atrial emptying fractions; RAI = right atrial area index; other abbreviations as in figures 1, 2, and 3.

The strongest relationships were found with RVEDA index, RVESA index, RVFAC, TAPSE, RA size, active RAEF, and log NT-proBNP levels. In addition, New York Heart Association (NYHA) functional class, resting SBP, kidney function, low cardiac index on right heart catheterization, and PVRI were associated with outcome. Figure 4 presents the c-statistic of the RV and RA parameters, as well as their Kaplan-Meier survival curves from RVFAC and RA index categories. With the area-length method, volumetric measures of RA size or RAEF were not associated with significantly different c-statistics (p=0.79 and p=0.87, respectively). To minimize overfitting the multivariable Cox proportional hazards model, we only included 4 variables in the initial analysis (i.e., RVFAC, RA index, resting SBP, and NYHA functional class III and IV vs. I and II). The choice of variables was based on the following rationale: 1) RVFAC was more strongly associated with outcome than other RV functional parameters and was not collinearly related to RA size in contrast to RVEDA or RVESA; 2) RA size was more reproducible than active RAEF in our study population; 3) SBP was not collinearly related to RVFAC—in contrast, there was a moderate relationship between RV systolic pressure or relative RV systolic pressure and RVFAC (r=0.45; p < 0.001 and r=0.48; p<0.001); and 4) NYHA functional class was related to outcome in many previous studies. On multivariable analysis, RVFAC, RA size, and SBP were strongly and independently associated with outcome, as shown in Table 4 (both in continuous and categorical analyses). In the subgroup of patients for whom NT-proBNP level was available (n=79), NT-proBNP level was not retained in the multivariable model.

	HR	**95%CI**	**p-value**
Multivariable model – continuous			
RVFAC, per 5%	0.6	0.4-0.7	<0.001
RAI, per 5cm2/m2	1.4	1.1-2.8	0.021
SBP, per 10mmHg	0.7	0.5-0.9	0.007
Multivariable model – categorical			
RV systolic dysfuncti on per grade*	3.4	2.0-7.75	<0.001
Severe RAE, >16cm2/m2	3.0	1.3-8.1	0.009
SBP <110mmHg	3.3	1.5-9.4	0.002
RH score (categorial)			
RH score, per grade	3.2	2.3-5.4	<0.001

Table 4: Independent Correlates of the Composite Endpoint in the Derivation Cohort. *RV dysfunction was classified into normal (no dysfunction), mild, or moderate to severe according to the American Society of Echocardiography criteria. Model was adjusted for age and sex. RAE = right atrial enlargement; RH = right heart; other abbreviations as in Tables 1 and 2.

Right heart score and other validated scores

A right heart score was built on the basis of the beta coefficients of the multivariable model, assigning a baseline value of 1 and additional points for each category of risk (Table 5). The right heart score had a c-statistic of 0.88 (95%CI: 0.79-0.94), the REVEAL score had a c-statistic of 0.80 (95%CI: 0.69-0.88), and the NIH survival equation had a c-statistic of 0.60 (95%CI: 0.49-0.71). With the DeLong method, both the right heart score and the REVEAL score had significantly higher c-statistics than the NIH survival equation ($p<0.001$ and $p=0.013$, respectively). There was no statistical difference between the right heart score and the REVEAL score in the cohort ($p=0.097$). Figure 5 illustrates the Kaplan-Meier survival curves associated with the right heart score, as well as its relationship with other scores.

Baseline value	1
RV function	
Normal	0
Mild	1
Moderate to severe	2
RA size	
Less than severe RAE	0
Severe RAE	1
SBP	
SBP >110mmHg	0
SBP <110mmHg	1
RH score	1-5

Table 5: Example of RH Score and Point Allocation. RV dysfunction was classified into normal (no dysfunction), mild, or moderate to severe according to the American Society of Echocardiography criteria.

Validation cohort

The validation cohort included 87 patients with idiopathic or familial PAH followed at VU Medical Center between 2001 and 2012. The average age was 47.8±16.0 years, the majority of patients were female (75%), baseline PVR was 11.2±5 Wood units, and baseline 6MWD was 407±127 m. All patients were on disease-modifying therapy, the average time between CMR and diagnosis was 1.5±1.5 years, and the average follow-up time was 4.2±3.2 years. The composite endpoint occurred in 29 patients, including 23 deaths and 6 lung transplants. On univariate analysis, the strongest

correlates of outcome included right ventricular ejection fraction (RVEF) (chi-square=12; p<0.001), RA index (chi-square=11; p<0.001), RV end-systolic volume index (chi-square=9; p<0.001), right heart score (chi-square=14; p<0.001), and more weakly 6MWD (chi-square=5; p=0.03). On multivariable analysis, right heart score (HR: 1.9 per grade; 95%CI: 1.4-2.6) and age (HR: 1.3 per grade; 95%CI: 0.98-1.69) were the only 2 variables independently associated with outcome, with chi-square=19 (p<0.001).

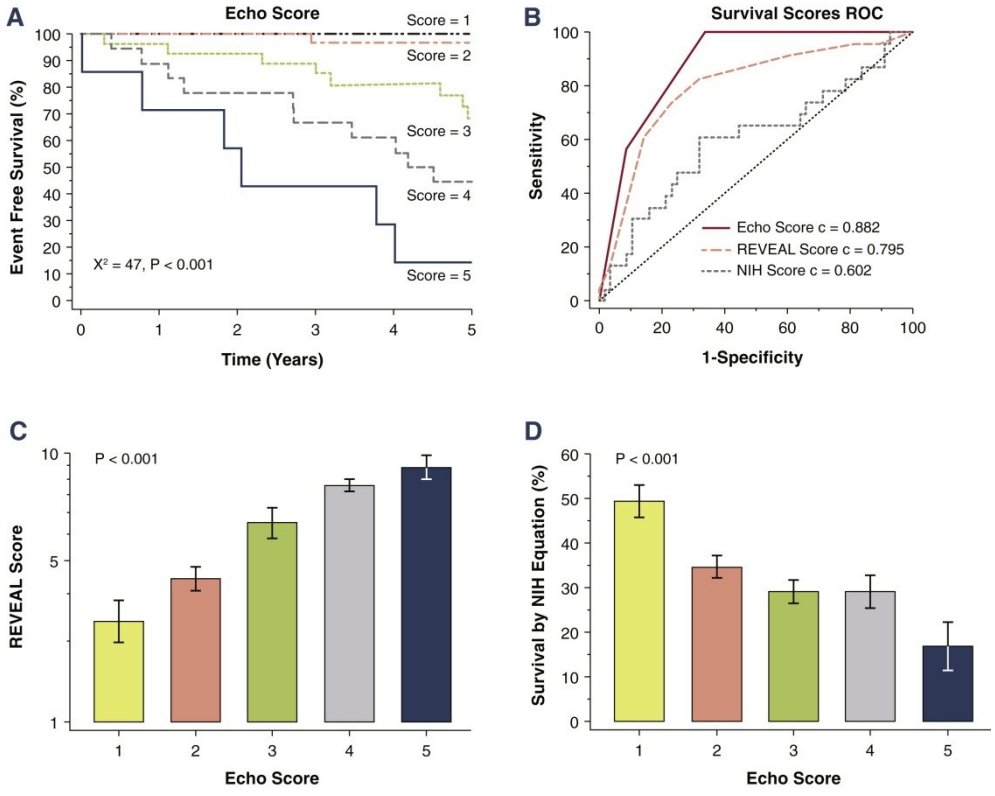

Figure 5: Right Heart Score in Relation to the REVEAL and NIH Scores. A: Five-year Kaplan-Meier curve on the basis of the right heart score. B: C-statistic between the right heart score and the REVEAL (Registry to Evaluate Early and Long-Term PAH Disease Management) score and 5-year predicted National Institutes of Health (NIH) survival. C: Strong relationship between the right heart score and the REVEAL score, with 95% CI for the mean value. (D) Strong relationship between the right heart score and the NIH score, with 95% confidence interval for the mean value.

The c-statistic for the right heart score in the validation cohort (0.76; IQR: 0.66-0.84) was significantly different from the c-statistic for the NIH survival equation (0.59; IQR: 0.48-0.70;

p=0.030). Because NT-proBNP levels and the percentage-predicted diffusion capacity of carbon monoxide were not systematically available, the derived REVEAL score could not be calculated in the majority of patients at the time of follow-up.

Intervariability of echocardiographic measures

For RVFAC, the average difference in absolute measurement was 2.1±1.6%, with an ICC of 0.84; for TAPSE, the average difference in absolute measurement was 0.1±0.1cm, with an ICC of 0.93; and for RVMPI, the average difference in absolute measurement was 0.09±0.11, with an ICC of 0.85. The ICCs for maximal, minimal, and pre-atrial systole RA volumes were 0.95, 0.97, and 0.87, respectively. The ICC was 0.89 for total RAEF, 0.72 for active RAEF, and 0.84 for passive RAEF.

Discussion

Our study is the first to demonstrate that a simple score combining measures of RV systolic function, RA size, and SBP offered a good discrimination of outcome in patients with established PAH. Consistent with other studies, the results of our study highlighted that the quantitative metrics of right heart remodeling or function may simplify the risk stratification of patients with PAH [3, 18]. The REVEAL score and the NIH survival equation represent the 2 most validated survival scores in PAH [2, 5]. The NIH registry score relies on hemodynamic parameters, whereas the REVEAL registry score incorporates clinical, functional, and imaging parameters. Although our sample size was small, confidence in our results is provided by the fact that the right heart score correlated well with established outcome scores, the findings were validated in an independent cohort, and the results were consistent using different imaging modalities. In a recent publication, in a large series of patients with PAH, Fine et al. [18] showed that RV global longitudinal strain (RVGLS), log NT-proBNP levels, and NYHA functional class were independent correlates of clinical deterioration in patients with PAH. Consistent with the study of Fine et al. [18], our study also highlighted the importance of right heart function. In contrast, NYHA functional class and log NT-proBNP levels did not emerge as independent correlates of outcome due to their strong relationship with RV function and RA size; alternatively, our study may have been underpowered to assess their incremental value. In the REVEAL registry score, qualitative assessment of RV function was considered but did not emerge in the multivariate model; one can theorize, although not yet proven, that this may reflect the inter-laboratory variability in assessing RV function and the multiple grades of dysfunction considered (5 classes). With echocardiography, different metrics of RV systolic function have been considered,

including RVFAC, TAPSE, RVMPI, and more recently RVGLS [3, 12, 13, 18]. In our study, RVFAC emerged as a stronger correlate of outcome than either TAPSE or RVMPI. In a recent study, we showed that RVFAC was more closely related to RVEF than TAPSE [19]. Moreover, we showed that an RVFAC of 25%corresponded best to an RVEF of 35%, a commonly chosen threshold for moderate RV dysfunction in CMR imaging studies of patients with PAH [14, 15]. In comparison to RVFAC, TAPSE has the advantage of reproducibility but does not take into account the radial component of RV contraction [20]. Although RVMPI combines information of both systolic and diastolic function, in different studies it has not appeared to carry stronger prognostic value than RVFAC, TAPSE, or RVGLS [18, 21]. Although not yet proven, this may be in part due to pseudo-normalization of RVMPI values, which can occur in patients with severe dysfunction. As shown in the recent study of Fine et al. [18], RVGLS emerged as the best metric of RV function compared with RVFAC and TAPSE in PAH; ongoing studies are currently validating the findings in independent cohorts. One of the most important contributions of our study was to prove the independent contribution to RA size [22]. In fact, in contrast to studies on atrial remodeling in left heart failure, there have been a limited number of studies addressing atrial remodeling or atrial function in PAH [7, 8, 23]. Bustamante-Labarta et al. [7] were the first to suggest an association between RA size and outcome in 25 patients with PAH. In the study of Raymond et al. [8], in 81 patients with NYHA functional class III or IV PAH, there was a trend for an independent association between RA area indexed to height and the composite endpoint of death or transplantation (p=0.106). In the recent study of Kane et al. [23], severe RA enlargement assessed qualitatively were also predictive of survival when corrected for age, sex, and functional class. Mechanistically, RA size is strongly associated with RAP, and tricuspid regurgitation severity can therefore provide important information on adverse ventricular remodeling. However, further studies are needed to provide better normative indexed thresholds of RA size. In addition to changes in RA remodeling, we showed that RA function was significantly impaired in patients with PAH. Although the change affected both passive and atrial components of atrial function, better prognostic information was provided by active atrial emptying. The association between active RAEF and RAP, as well as TAPSE, is not surprising because RAP may be an indirect metric of RA afterload and TAPSE may limit the extent of active RAEF as the atria cannot contract if the ventricle has a limited annular excursion. As a marker of outcome, active RAEF has the potential disadvantage of lower reproducibility compared with maximal RA size; in addition it is more collinearly related with metrics of RV systolic function, which may limit its incremental value in multivariate models. Conversely, RA size was more related to RV end-systolic dimensions, which

may limit their incremental values if considered together as covariates. The sex differences related to active RAEF will require further study and validation. The association that we found between SBP and outcome was consistent with the findings of the REVEAL registry and may reflect lower cardiac output or the use of prostanoid therapy. Our study has 3 main clinical implications. First, a simple right heart score can be useful for stratified randomization strategies in phase II clinical trials because matching based only on NYHA functional class may not capture the complexity of the disease process and all variables from the REVEAL registry may not be available. Second, a simple right heart score can serve as a "benchmark" against which the incremental value of novel biomarkers can be assessed. Third, empirically patients with higher scores could be monitored more closely clinically because they are at higher risk of clinical deterioration. However, it is important to mention that our study was not designed to provide a comparison with well-validated scores, such as the REVEAL registry score, and should by no means be considered interchangeable. Our study does however suggest, as did the study of Fine et al. [18], that quantitative assessment of right heart function and remodeling may simplify risk assessment in patients with PAH.

Study limitations

The small sample size limited the number of variables that we could consider in the multivariable model. The strong relationship with the REVEAL registry and NIH survival equation, however, brought indirect external validation to our findings, as did the validation cohort. Second, we did not include more complex imaging modalities, such as strain imaging, in our study. Finally, it is important to emphasize that our study focused on prevalent cases of patients with PAH, rather than incident treatmentnaive patients.

Conclusions

In this study, we showed that in patients with idiopathic, familial, or drug- and toxin-associated PAH, a simple right heart score combining indexes of right heart remodeling and function could predict longterm outcome. If further validated, this simple score may significantly improve the evaluation of novel biomarkers and help guide stratified randomization in clinical trials.

Acknowledgments

The authors thank the Vera Moulton Wall Center, Stanford Cardiovascular Institute, and Pai Chan Lee Research Fund at Stanford University for their support.

References

[1] Humbert M, Sitbon O, Chaouat A, Bertocchi M, Habib G, Gressin V, et al. Survival in patients with idiopathic, familial, and anorexigen-associated pulmonary arterial hypertension in the modern management era. Circulation. 2010; 122:156-63

[2] Benza RL, Miller DP, Gomberg-Maitland M, Frantz RP, Foreman AJ, Coffey CS, et al. Predicting survival in pulmonary arterial hypertension: insights from the Registry to Evaluate Early and Long-Term Pulmonary Arterial Hypertension Disease Management (REVEAL). Circulation. 2010; 122:164-72

[3] Vonk-Noordegraaf A, Haddad F, Chin KM, Forfia PR, Kawut SM, Lumens J, et al. Right heart adaptation to pulmonary arterial hypertension: physiology and pathobiology. Journal of the American College of Cardiology. 2013; 62:D22-33

[4] Bossone E, D'Andrea A, D'Alto M, Citro R, Argiento P, Ferrara F, et al. Echocardiography in pulmonary arterial hypertension: from diagnosis to prognosis. J Am Soc Echocardiogr. 2011; 26:1-14

[5] D'Alonzo GE, Barst RJ, Ayres SM, Bergofsky EH, Brundage BH, Detre KM, et al. Survival in patients with primary pulmonary hypertension. Results from a national prospective registry. Annals of internal medicine. 1991; 115:343-9

[6] van Wolferen SA, van de Veerdonk MC, Mauritz GJ, Jacobs W, Marcus JT, Marques KM, et al. Clinically significant change in stroke volume in pulmonary hypertension. Chest. 2011; 139:1003-9

[7] Bustamante-Labarta M, Perrone S, De La Fuente RL, Stutzbach P, De La Hoz RP, Torino A, et al. Right atrial size and tricuspid regurgitation severity predict mortality or transplantation in primary pulmonary hypertension. J Am Soc Echocardiogr. 2002; 15:1160-4

[8] Raymond RJ, Hinderliter AL, Willis PW, Ralph D, Caldwell EJ, Williams W, et al. Echocardiographic predictors of adverse outcomes in primary pulmonary hypertension. Journal of the American College of Cardiology. 2002; 39:1214-9

[9] Simonneau G, Robbins IM, Beghetti M, Channick RN, Delcroix M, Denton CP, et al. Updated clinical classification of pulmonary hypertension. Journal of the American College of Cardiology. 2009; 54:S43-54

[10] Poggio ED, Wang X, Greene T, Van Lente F, Hall PM. Performance of the modification of diet in renal disease and Cockcroft-Gault equations in the estimation of GFR in health and in chronic kidney disease. J Am Soc Nephrol. 2005; 16:459-66

[11] Rudski LG, Lai WW, Afilalo J, Hua L, Handschumacher MD, Chandrasekaran K, et al. Guidelines for the echocardiographic assessment of the right heart in adults: a report from the American Society of Echocardiography endorsed by the European Association of Echocardiography, a registered branch of the European Society of Cardiology, and the Canadian Society of Echocardiography. J Am Soc Echocardiogr. 2010; 23:685-713; quiz 86-8

[12] Forfia PR, Fisher MR, Mathai SC, Housten-Harris T, Hemnes AR, Borlaug BA, et al. Tricuspid annular displacement predicts survival in pulmonary hypertension. American journal of respiratory and critical care medicine. 2006; 174:1034-41

[13] Yeo TC, Dujardin KS, Tei C, Mahoney DW, McGoon MD, Seward JB. Value of a Doppler-derived index combining systolic and diastolic time intervals in predicting outcome in primary pulmonary hypertension. The American journal of cardiology. 1998; 81:1157-61

[14] van de Veerdonk MC, Kind T, Marcus JT, Mauritz GJ, Heymans MW, Bogaard HJ, et al. Progressive right ventricular dysfunction in patients with pulmonary arterial hypertension responding to therapy. Journal of the American College of Cardiology. 2011; 58:2511-9

[15] Shiran H, Zamanian RT, McConnell MV, Liang DH, Dash R, Heidary S, et al. Relationship between echocardiographic and magnetic resonance derived measures of right ventricular size and function in patients with pulmonary hypertension. J Am Soc Echocardiogr. 2014; 27:405-12

[16] Laupacis A, Sekar N, Stiell IG. Clinical prediction rules. A review and suggested modifications of methodological standards. Jama. 1997; 277:488-94

[17] Thenappan T, Shah SJ, Rich S, Tian L, Archer SL, Gomberg-Maitland M. Survival in pulmonary arterial hypertension: a reappraisal of the NIH risk stratification equation. The European respiratory journal. 2010; 35:1079-87

[18] Fine NM, Chen L, Bastiansen PM, Frantz RP, Pellikka PA, Oh JK, et al. Outcome prediction by quantitative right ventricular function assessment in 575 subjects evaluated for pulmonary hypertension. Circ Cardiovasc Imaging. 2013; 6:711-21

[19] Shiran H, Haddad F, Miller DC, Liang D. Comparison of aortic root diameter to left ventricular outflow diameter versus body surface area in patients with marfan syndrome. The American journal of cardiology. 2012; 110:1518-22

[20] Kind T, Mauritz GJ, Marcus JT, van de Veerdonk M, Westerhof N, Vonk-Noordegraaf A. Right ventricular ejection fraction is better reflected by transverse rather than longitudinal wall motion in pulmonary hypertension. J Cardiovasc Magn Reson. 2010; 12:35

[21] Ghio S, Klersy C, Magrini G, D'Armini AM, Scelsi L, Raineri C, et al. Prognostic relevance of the echocardiographic assessment of right ventricular function in patients with idiopathic pulmonary arterial hypertension. International journal of cardiology. 2010; 140:272-8

[22] Grunig E, Henn P, D'Andrea A, Claussen M, Ehlken N, Maier F, et al. Reference values for and determinants of right atrial area in healthy adults by 2-dimensional echocardiography. Circ Cardiovasc Imaging. 2013; 6:117-24

[23] Kane GC, Maradit-Kremers H, Slusser JP, Scott CG, Frantz RP, McGoon MD. Integration of clinical and hemodynamic parameters in the prediction of long-term survival in patients with pulmonary arterial hypertension. Chest. 2011; 139:1285-93

CHAPTER 4

Assessment of right ventricular responses to therapy in pulmonary hypertension

Drug Discovery Today 2014

OA Spruijt[1], HJ Bogaard[1], A Vonk Noordegraaf[1]

[1]Department of Pulmonary Medicine, VU University Medical Center, Amsterdam, The Netherlands

Abstract

Irrespective of its cause, pulmonary hypertension (PH) leads to an increase in pulmonary vascular resistance. Failing adaption of the right ventricle (RV) to the increased afterload is the main cause of death in PH patients and therefore monitoring RV function during treatment is essential. However, consensus on the optimal method for serial assessment of RV function is lacking and therefore the major clinical trials on PH specific therapies have not provided clear answers with respect to the response of the RV to treatment. This short review will give an overview of the most important load-dependent and load-independent parameters to assess RV response to therapy in PH patients.

Introduction

Pulmonary hypertension (PH) is a hemodynamic condition caused by a variety of underlying etiologies leading to a progressive increase in pulmonary vascular resistance (PVR) and pulmonary artery pressure (PAP). The diagnosis of PH is based on a right heart catheterization (RHC) showing a mean PAP (mPAP) > 25 mmHg. Coping of the RV to increases in afterload is through mechanisms of hypertrophy and dilatation and is essential in determining patient outcome: RV failure is the main cause of death in PH [1]. Established predictors of long-term outcome in PAH all represent RV function in one way or another: cardiac output (CO), mixed venous oxygen saturation, right atrial pressure, NT-proBNP, NYHA functional class and exercise capacity [2]. When performed at baseline or after initiation of treatment, cardiac imaging by means of echocardiography (ECHO) and cardiac magnetic resonance imaging (cMRI) provides additional prognostic information [3]. The mechanisms of RV adaptation to increases in load are not fully understood and have only recently become an important research topic. The importance of the RV, 'the forgotten chamber' in PH, was long unrecognized and very few investigators studied RV responses to PH therapy [4]. The possibility to treat the RV directly – i.e. not by decreasing afterload- was addressed in a few preclinical studies [5, 6], but never in PH patients. While there is an urgent need to study the RV response to PH therapy, there is no universally accepted consensus on the optimal method of assessing RV function and structure [2]. This short review will give an overview of, in our opinion, the most suitable functional parameters to assess the RV response to therapy in PH patients.

RV function and structure after initiation of treatment

While treatment of PH with specific therapy leads to a reduction in PVR in the majority of patients, this is not necessarily accompanied by an improvement in RV function [7]. The poor correlation between treatment associated changes in PVR and changes in RV function may be explained by a persistently elevated PVR (in most patients, drug treatment partially normalizes afterload at best), or by a load-independent deterioration of RV function over time. In addition, vasodilators may have direct pharmacological effects on the heart. Such direct effects have been suggested of all classes of PH treatment in preclinical studies [8-10], but were never evaluated in humans. Accurate assessment of cardio-specific effects of treatment requires a load-independent description of the function of the RV, which is not routinely provided by RHC or cardiac imaging (see table 1). Commonly studied load-dependent RV functional parameters are stroke volume (SV) and CO (calculated as SV times heart rate). SV and CO can be assessed during RHC using the thermodilution

or (in)direct Fick method, and also using (Doppler) ECHO or cMRI. It has been shown that changes in SV track RV responses to therapy [11, 12]. In PAH patients, an increased SV is achieved with intravenous infusion of epoprostenol [13, 14] and with oral treatment with Bosentan [15]. Not only is SV a sensitive parameter to measure RV responses, it has been shown that a change in SV of 10ml during follow-up should be considered clinically relevant [16]. An increase in CO in PAH patients has been shown with Ambrisentan, Bosentan, Sildenafil and Epoprostenol [14, 17-20]. In all these studies, improvements in SV and CO may have come about due to a reduction in afterload, an improvement in intrinsic RV function, or both.

RV parameters	Modalities
Load-dependent	
Stroke volume	RHC, cMRI, Doppler-ECHO
Right ventricular ejection fraction	cMRI, 3D-ECHO
Cardiac output	RHC, cMRI, 3D-ECHO
Longitudinal shortening	2D-ECHO, cMRI
Transverse shortening	2D-ECHO, cMRI
Eccentricity index	2D-ECHO, cMRI
Right ventricular mass	cMRI
Tei	Doppler-ECHO
Strain	2D-ECHO, cMRI
Load-independent	
Ees	RHC (favorably combined with cMRI or 3D-ECHO for assessment of EDV and ESV)
Ea	RHC (favorably combined with cMRI or 3D-ECHO for assessment of EDV and ESV)
Ees/Ea	RHC

Table 1: Overview of modalities to assess different RV parameters. RHC = right heart catheterization; cMRI = cardiac magnetic resonance imaging; ECHO = echocardiography; EDV = end-diastolic volume; ESV = end-systolic volume

Cardiac Imaging by magnetic resonance and echocardiography

Imaging by means of cMRI or ECHO has the major advantage of being non-invasive. The disadvantage of imaging, however, is that the obtained functional information is load-dependent

while the load itself is not assessed. Despite the prognostic value of baseline imaging, cMRI and ECHO parameters were never used as end-points in the major clinical trials evaluating the effects of PH specific treatment. Imaging-related evaluation of the RV response to therapy has rather been part of descriptive cohort studies [1]. Right ventricular ejection fraction (RVEF) is considered as one of the most important load-dependent measures of RV function. Improvement of the RVEF to PH therapy was described with Ambrisentan treatment [19] and with the combination of Bosentan and Sildenafil [21]. A change in RVEF during treatment predicts long-term outcome in PAH patients [7, 12].

RVEF is calculated as 100% x the difference between end-diastolic volume (EDV) and end-systolic volume (ESV), divided by EDV, or 100% x (EDV-ESV)/EDV. cMRI is considered as the golden standard for assessment of RV volumes, which has led to growing interest in its use in the evaluation of PH patients. With cMRI high resolution 3D images allow accurate assessment of RV volumes despite the complex anatomy of the RV. The most essential drawbacks of cMRI are the relative expensiveness, limited availability, incompatibility with metallic devices like cardiac pacemakers and defibrillators and it is not suitable for bedside analysis. 3D-ECHO is a promising technique for the measurement of cardiac volumes. With 3D-ECHO there is no need to make the mathematical assumptions which are necessary with 2D-ECHO. ECHO is widely available, is relatively inexpensive and can be used for bedside analysis. In a recent meta-analysis, 23 comparative studies on RV volume assessment using 3D-ECHO and cMRI were analyzed and it was concluded that 3D-ECHO underestimates RV volumes. Important for application in PH patients, underestimation of RV volumes and RVEF was greater in dilated RV's [22-24]. The most important reason for underestimation of RV volumes by ECHO is blurring of the images due to the distance between the transducer and the RV border. The blurred area can become incorporated into the measurement of the RV wall, which leads to an underestimation of RV volumes. Furthermore, suboptimal coverage of the RV outflow tract and a low temporal resolution may contribute to underestimation of the EDV and overestimation of the ESV by 3D-ECHO [22-27]. Inter-observer variability is also higher for 3D-ECHO in comparison to cMRI [25-27]. However, with improvements in temporal and spatial resolution, 3D-ECHO may become an accurate and readily available substitute for cMRI.

The complex anatomy of the RV complicates the assessment of RV volumes and, hence, RVEF. Because automatic contour detection is very difficult, assessing volumes is time-consuming. In an attempt to save analysis time, RV function has been described using one-dimensional measurements. Longitudinal shortening of the RV can be assessed by M-Mode ECHO determining

the Tricuspid Annular Plane Systolic Excursion (TAPSE). TAPSE describes the absolute longitudinal movement of the lateral tricuspid annulus towards the apex and is a widely applied measure of RV function. TAPSE can also be measured with cMRI. Although the complex geometry of the RV makes measurements of RV function using uni-dimensional measurements difficult, TAPSE shows a reasonably good correlation with RVEF [28, 29]. When measured at baseline, TAPSE has important prognostic value and the measurement is also sensitive to changes in RV function during follow-up [30, 31]. However, because longitudinal shortening reaches a floor level during progressive RV failure, a determination of transverse shortening is preferred when RV function is monitored in end-stage PH [32].

Flattening or even shifting of the inter ventricular septum from right to left is frequently seen in PH and is due to a delay in the time to peak shortening of the RV compared to the LV [33]. A frequently applied method to quantify bowing of the inter ventricular septum is the eccentricity index (EI), which can be obtained with ECHO and cMRI. EI is measured in a short-axis view of the LV cavity at end-systole or end-diastole and is defined as the ratio of the LV diameter parallel to the inter ventricular septum and the LV diameter perpendicular to the inter ventricular septum. Normally the EI is around 1 and EI increases with bowing of the inter ventricular septum. It has been shown that Bosentan treatment decreased the end-systolic EI in PAH patients [17, 18, 20]. Improvement of diastolic EI was seen in PAH patients who received Sildenafil in addition to prostanoids [34].

An important aspect in the pathogenesis of PH is hypertrophy of the RV wall. With cMRI it is possible to obtain RV mass as well as LV mass including trabeculae. The increase in RV mass due to the increase in afterload is believed to have a protective effect on the RV since it reduces wall stress following the law of Laplace. Wilkins et al compared the adding of Sildenafil or Bosentan to first line monotherapy and found a reduction of RV mass when Sildenafil was added, but not Bosentan [20]. A reduction of RV mass with Sildenafil has also been described in other studies [21, 35] and has been suggested to be related to intrinsic effects on the heart, in addition to vasodilating effects [9]. No change in RV mass was decribed with Ambrisentan [19].

The myocardial performance index, also known as the Tei index, describes global RV function and integrates systolic and diastolic function. The Tei index is measured by the ratio of isovolumic time intervals (isovolumic relaxation time plus isovolumic contraction time) and the ejection time, so that a deterioration of RV function results in an increase in Tei index. Tei index can be assessed with Doppler-ECHO without the need of making geometric assumptions. It has been shown that in PAH patients, Tei index decreases with Bosentan [17, 18, 36, 37] and with intravenous epoprostenol

treatment [38]. A final emerging technique to describe RV function is the measurement of myocardial deformation or strain. This method allows a global and regional assessment of RV function and can be assessed with 2D Speckle-tracking ECHO and tagged cMRI. Strain measurements were only applied in a few studies in PH [39]. Using 2D speckle tracking ECHO it was shown that in PH, RV free wall longitudinal peak systolic strain is decreased, correlates with RVEF and contains prognostic value [40, 41]. In addition, strain and strain rates can improve after initiation of PH therapy or after pulmonary endarterectomy in chronic thromboembolic pulmonary hypertension [42, 43].

In our opinion, volumetric RV measurements are the most suitable load-dependent parameters to measure RV responses to therapy. Baseline SV and RVEF and the change of SV and RVEF during treatment are strong predictors of mortality and can track RV response to treatment [7, 11].

Load-independent parameters

When load-dependent parameters are used, one cannot distinguish cardiac-specific effects of treatment from indirect effects on RV function. Several methods are available to describe load-independent RV function and the pressure-volume relationship is most commonly used and is readily available. It is well established that combined volume and pressure measurements provide a load-independent assessment of RV function. A load-independent measure of RV contractility is the end-sytolic elastance (Ees) described by the slope of the line connecting multiple end-systolic points, the end systolic pressure volume relation (ESPVR) [44]. In order to derive the ESPVR and to calculate Ees, multiple end-systolic points are required. To obtain multiple pressure-volume loops, it is necessary to briefly change preload conditions, for example by partial occlusion of the caval vein. Because this is considered dangerous in PH patients, attempts have been made to simplify the measurement of the Ees. A sufficient way to obtain a second point, in order to calculate the slope of the ESPVR, is the single beat method. This method uses a RV pressure curve of an ejecting beat to extrapolate the pressure curve of an isovolumic beat in order to obtain the maximum isovolumic pressure (Pmax). Pmax can be used as a second point to measure the ESPVR and subsequently Ees [45]. Since the end-systolic ventricular pressure almost equals the mPAP [46], Ees can be derived from the equation Ees = (mPAP-Pmax) / SV (Figure 1).

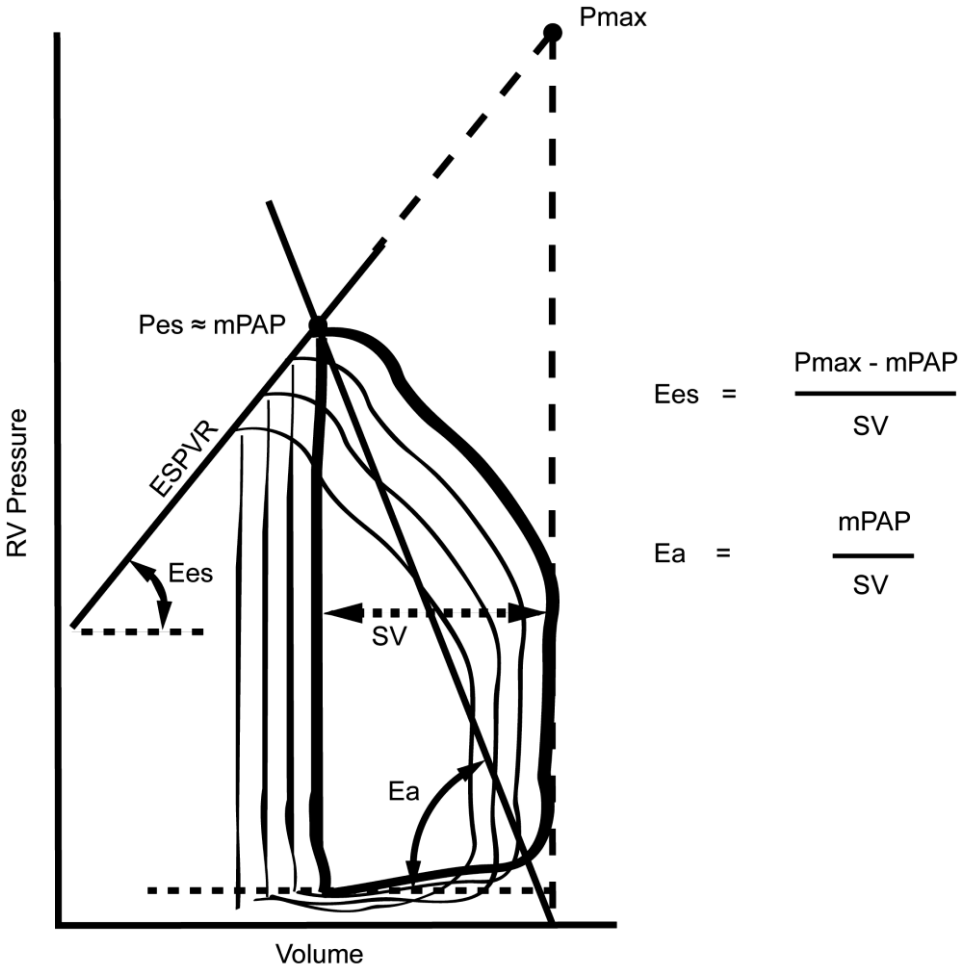

Figure 1: Pressure-volume loop. Pes = end-systolic pressure; mPAP = mean pulmonary artery pressure; Pmax = maximal isovolumic pressure; ESPVR = end-systolic pressure volume relationship; Ees = RV contractility; Ea = pulmonary vascular resistance; SV = stroke volume. Adapted from [6].

From the pressure-volume relationship it is also possible to derive the resistance of the pulmonary vascular system. The slope of the line connecting the end-systolic and end-diastolic point, the Ea (mPAP/SV), is a measure of pulmonary vascular resistance and therefore a measure of afterload on the RV (figure 1). Coupling of the RV to its load (RV-A coupling) is calculated as Ees/Ea (Figure 1), and this ratio is believed to reflect cardiac efficiency [44].

Pre-clinical studies have shown that in PH as compared to controls RV contractility, or Ees, is increased and that RV-A coupling is decreased [6, 47, 48]. β-Adrenergic receptor blockade increases contractility and partially restores Ees/Ea in rats with PH induced by monocrotaline (MCT) [6]. Sildenafil improved RV contractility in rats with mechanical RV pressure overload due to pulmonary artery banding [49]. Similar contractility improving effects of Sildenafil were also suggested in another study on MCT rats using a Langendorf preparation [9]. With the same experimental set-up, this group also showed a decrease in RV contractility in MCT rats after Bosentan treatment [8].
Despite the preclinical evidence of direct cardiac effects of pulmonary vasodilators, RV contractility and RV-A coupling were never assessed in clinical trials in PAH patients. In contrast to the cited experimental studies, a recent meta-analysis using pump-function graph analyses, suggested that PAH therapies have little or no cardiac specific effects on top of their vasodilating effects [4]. This may not be true for some of the newer drugs, including growth factor receptor inhibitors.

RV function during exercise

During exercise the cardiovascular system is pushed to its upper limits. Holverda et al [50] showed that exercising iPAH patients show no increase in SV and even a decrease in RVEF. This implies that RV failure becomes more manifest during exercise. Although assessing load-dependent parameters of RV function during exercise is challenging, its interest is rising [51]. Load-independent measurements of RV function can also be assessed during exercise using an exercise protocol during RHC [52]. Future studies will have to reveal if RV functional parameters obtained during exercise could be more sensitive to assess RV responses to therapy.

Conclusions

Today, after two decades of treating PH patients with pulmonary vasodilators, a thorough understanding of RV responses to therapy is still lacking. Given the importance of RV function in patient outcome, future studies on new PH therapies should include a comprehensive determination of load-dependent and load-independent effects of treatment on the RV. Serial assessment of RV structure and function should include a combination of RV parameters and should at least include volumetric parameters. PH therapies specifically targeting the RV, e.g. treatment with β-adrenergic receptor blockers, should use load-independent parameters to determine cardiac-specific effects of therapy.

References:

[1] Vonk Noordegraaf A, Galie N. The role of the right ventricle in pulmonary arterial hypertension. Eur Respir Rev. 2011; 20:243-53

[2] Galie N, Hoeper MM, Humbert M, Torbicki A, Vachiery JL, Barbera JA, et al. Guidelines for the diagnosis and treatment of pulmonary hypertension. The European respiratory journal. 2009; 34:1219-63

[3] Vonk-Noordegraaf A, Souza R. Cardiac magnetic resonance imaging: what can it add to our knowledge of the right ventricle in pulmonary arterial hypertension? The American journal of cardiology. 2012; 110:25S-31S

[4] Handoko ML, de Man FS, Allaart CP, Paulus WJ, Westerhof N, Vonk-Noordegraaf A. Perspectives on novel therapeutic strategies for right heart failure in pulmonary arterial hypertension: lessons from the left heart. Eur Respir Rev. 2010; 19:72-82

[5] Bogaard HJ, Natarajan R, Mizuno S, Abbate A, Chang PJ, Chau VQ, et al. Adrenergic receptor blockade reverses right heart remodeling and dysfunction in pulmonary hypertensive rats. American journal of respiratory and critical care medicine. 2010; 182:652-60

[6] de Man FS, Handoko ML, van Ballegoij JJ, Schalij I, Bogaards SJ, Postmus PE, et al. Bisoprolol delays progression towards right heart failure in experimental pulmonary hypertension. Circ Heart Fail. 2012; 5:97-105

[7] van de Veerdonk MC, Kind T, Marcus JT, Mauritz GJ, Heymans MW, Bogaard HJ, et al. Progressive right ventricular dysfunction in patients with pulmonary arterial hypertension responding to therapy. Journal of the American College of Cardiology. 2011; 58:2511-9

[8] Nagendran J, Sutendra G, Paterson I, Champion HC, Webster L, Chiu B, et al. Endothelin axis is upregulated in human and rat right ventricular hypertrophy. Circulation research. 2013; 112:347-54

[9] Nagendran J, Archer SL, Soliman D, Gurtu V, Moudgil R, Haromy A, et al. Phosphodiesterase type 5 is highly expressed in the hypertrophied human right ventricle, and acute inhibition of phosphodiesterase type 5 improves contractility. Circulation. 2007; 116:238-48

[10] van Albada ME, Berger RM, Niggebrugge M, van Veghel R, Cromme-Dijkhuis AH, Schoemaker RG. Prostacyclin therapy increases right ventricular capillarisation in a model for flow-associated pulmonary hypertension. European journal of pharmacology. 2006; 549:107-16

[11] van Wolferen SA, Marcus JT, Boonstra A, Marques KM, Bronzwaer JG, Spreeuwenberg MD, et al. Prognostic value of right ventricular mass, volume, and function in idiopathic pulmonary arterial hypertension. European heart journal. 2007; 28:1250-7

[12] Chin KM, Kingman M, de Lemos JA, Warner JJ, Reimold S, Peshock R, et al. Changes in right ventricular structure and function assessed using cardiac magnetic resonance imaging in bosentan-treated patients with pulmonary arterial hypertension. The American journal of cardiology. 2008; 101:1669-72

[13] Barst RJ, Rubin LJ, Long WA, McGoon MD, Rich S, Badesch DB, et al. A comparison of continuous intravenous epoprostenol (prostacyclin) with conventional therapy for primary pulmonary hypertension. The New England journal of medicine. 1996; 334:296-301

[14] Roeleveld RJ, Vonk-Noordegraaf A, Marcus JT, Bronzwaer JG, Marques KM, Postmus PE, et al. Effects of epoprostenol on right ventricular hypertrophy and dilatation in pulmonary hypertension. Chest. 2004; 125:572-9

[15] Kopec G, Tyrka A, Miszalski-Jamka T, Mikolajczyk T, Waligora M, Guzik T, et al. Changes in exercise capacity and cardiac performance in a series of patients with Eisenmenger's syndrome transitioned from selective to dual endothelin receptor antagonist. Heart, lung & circulation. 2012; 21:671-8

[16] van Wolferen SA, van de Veerdonk MC, Mauritz GJ, Jacobs W, Marcus JT, Marques KM, et al. Clinically significant change in stroke volume in pulmonary hypertension. Chest. 2011; 139:1003-9

[17] Sitbon O, Gressin V, Speich R, Macdonald PS, Opravil M, Cooper DA, et al. Bosentan for the treatment of human immunodeficiency virus-associated pulmonary arterial hypertension. American journal of respiratory and critical care medicine. 2004; 170:1212-7

[18] Galie N, Hinderliter AL, Torbicki A, Fourme T, Simonneau G, Pulido T, et al. Effects of the oral endothelin-receptor antagonist bosentan on echocardiographic and doppler measures in patients with pulmonary arterial hypertension. Journal of the American College of Cardiology. 2003; 41:1380-6

[19] Blalock SE, Matulevicius S, Mitchell LC, Reimold S, Warner J, Peshock R, et al. Long-term outcomes with ambrisentan monotherapy in pulmonary arterial hypertension. Journal of cardiac failure. 2010; 16:121-7

[20] Wilkins MR, Paul GA, Strange JW, Tunariu N, Gin-Sing W, Banya WA, et al. Sildenafil versus Endothelin Receptor Antagonist for Pulmonary Hypertension (SERAPH) study. American journal of respiratory and critical care medicine. 2005; 171:1292-7

[21] van Wolferen SA, Boonstra A, Marcus JT, Marques KM, Bronzwaer JG, Postmus PE, et al. Right ventricular reverse remodelling after sildenafil in pulmonary arterial hypertension. Heart (British Cardiac Society). 2006; 92:1860-1

[22] Shimada YJ, Shiota M, Siegel RJ, Shiota T. Accuracy of right ventricular volumes and function determined by three-dimensional echocardiography in comparison with magnetic resonance imaging: a meta-analysis study. J Am Soc Echocardiogr. 2010; 23:943-53

[23] Ostenfeld E, Carlsson M, Shahgaldi K, Roijer A, Holm J. Manual correction of semi-automatic three-dimensional echocardiography is needed for right ventricular assessment in adults; validation with cardiac magnetic resonance. Cardiovascular ultrasound. 2012; 10:1
[24] van der Zwaan HB, Geleijnse ML, McGhie JS, Boersma E, Helbing WA, Meijboom FJ, et al. Right ventricular quantification in clinical practice: two-dimensional vs. three-dimensional echocardiography compared with cardiac magnetic resonance imaging. Eur J Echocardiogr. 2011; 12:656-64
[25] Grapsa J, O'Regan DP, Pavlopoulos H, Durighel G, Dawson D, Nihoyannopoulos P. Right ventricular remodelling in pulmonary arterial hypertension with three-dimensional echocardiography: comparison with cardiac magnetic resonance imaging. Eur J Echocardiogr. 2010; 11:64-73
[26] Nesser HJ, Tkalec W, Patel AR, Masani ND, Niel J, Markt B, et al. Quantitation of right ventricular volumes and ejection fraction by three-dimensional echocardiography in patients: comparison with magnetic resonance imaging and radionuclide ventriculography. Echocardiography (Mount Kisco, NY. 2006; 23:666-80
[27] Niemann PS, Pinho L, Balbach T, Galuschky C, Blankenhagen M, Silberbach M, et al. Anatomically oriented right ventricular volume measurements with dynamic three-dimensional echocardiography validated by 3-Tesla magnetic resonance imaging. Journal of the American College of Cardiology. 2007; 50:1668-76
[28] Sato T, Tsujino I, Ohira H, Oyama-Manabe N, Yamada A, Ito YM, et al. Validation study on the accuracy of echocardiographic measurements of right ventricular systolic function in pulmonary hypertension. J Am Soc Echocardiogr. 2012; 25:280-6
[29] Nijveldt R, Germans T, McCann GP, Beek AM, van Rossum AC. Semi-quantitative assessment of right ventricular function in comparison to a 3D volumetric approach: a cardiovascular magnetic resonance study. European radiology. 2008; 18:2399-405
[30] Forfia PR, Fisher MR, Mathai SC, Housten-Harris T, Hemnes AR, Borlaug BA, et al. Tricuspid annular displacement predicts survival in pulmonary hypertension. American journal of respiratory and critical care medicine. 2006; 174:1034-41
[31] Brown SB, Raina A, Katz D, Szerlip M, Wiegers SE, Forfia PR. Longitudinal shortening accounts for the majority of right ventricular contraction and improves after pulmonary vasodilator therapy in normal subjects and patients with pulmonary arterial hypertension. Chest. 2011; 140:27-33
[32] Mauritz GJ, Kind T, Marcus JT, Bogaard HJ, van de Veerdonk M, Postmus PE, et al. Progressive changes in right ventricular geometric shortening and long-term survival in pulmonary arterial hypertension. Chest. 2012; 141:935-43
[33] Marcus JT, Gan CT, Zwanenburg JJ, Boonstra A, Allaart CP, Gotte MJ, et al. Interventricular mechanical asynchrony in pulmonary arterial hypertension: left-to-right delay in peak shortening is related to right ventricular overload and left ventricular underfilling. Journal of the American College of Cardiology. 2008; 51:750-7
[34] Ruiz MJ, Escribano P, Delgado JF, Jimenez C, Tello R, Gomez MA, et al. Efficacy of sildenafil as a rescue therapy for patients with severe pulmonary arterial hypertension and given long-term treatment with prostanoids: 2-year experience. J Heart Lung Transplant. 2006; 25:1353-7
[35] Michelakis ED, Tymchak W, Noga M, Webster L, Wu XC, Lien D, et al. Long-term treatment with oral sildenafil is safe and improves functional capacity and hemodynamics in patients with pulmonary arterial hypertension. Circulation. 2003; 108:2066-9
[36] Dyer KL, Pauliks LB, Das B, Shandas R, Ivy D, Shaffer EM, et al. Use of myocardial performance index in pediatric patients with idiopathic pulmonary arterial hypertension. J Am Soc Echocardiogr. 2006; 19:21-7
[37] Kaya MG, Lam YY, Erer B, Ayhan S, Vatankulu MA, Nurkalem Z, et al. Long-term effect of bosentan therapy on cardiac function and symptomatic benefits in adult patients with Eisenmenger syndrome. Journal of cardiac failure. 2012; 18:379-84
[38] Sebbag I, Rudski LG, Therrien J, Hirsch A, Langleben D. Effect of chronic infusion of epoprostenol on echocardiographic right ventricular myocardial performance index and its relation to clinical outcome in patients with primary pulmonary hypertension. The American journal of cardiology. 2001; 88:1060-3
[39] Giusca S, Jurcut R, Coman IM, Ghiorghiu I, Catrina D, Popescu BA, et al. Right ventricular function predicts clinical response to specific vasodilator therapy in patients with pulmonary hypertension. Echocardiography (Mount Kisco, NY. 2013; 30:17-26
[40] Haeck ML, Scherptong RW, Marsan NA, Holman ER, Schalij MJ, Bax JJ, et al. Prognostic value of right ventricular longitudinal peak systolic strain in patients with pulmonary hypertension. Circ Cardiovasc Imaging. 2012; 5:628-36
[41] Li Y, Xie M, Wang X, Lu Q, Fu M. Right ventricular regional and global systolic function is diminished in patients with pulmonary arterial hypertension: a 2-dimensional ultrasound speckle tracking echocardiography study. The international journal of cardiovascular imaging. 2013; 29:545-51
[42] Hardegree EL, Sachdev A, Villarraga HR, Frantz RP, McGoon MD, Kushwaha SS, et al. Role of serial quantitative assessment of right ventricular function by strain in pulmonary arterial hypertension. The American journal of cardiology. 2013; 111:143-8
[43] Mauritz GJ, Vonk-Noordegraaf A, Kind T, Surie S, Kloek JJ, Bresser P, et al. Pulmonary endarterectomy normalizes interventricular dyssynchrony and right ventricular systolic wall stress. J Cardiovasc Magn Reson. 2012; 14:5
[44] Westerhof N. Snapshots of Hemodynamics: An Aid for Clinical Research and Graduate Education. 2nd ed. New York: Springer 2010.
[45] Brimioulle S, Wauthy P, Ewalenko P, Rondelet B, Vermeulen F, Kerbaul F, et al. Single-beat estimation of right ventricular end-systolic pressure-volume relationship. American journal of physiology. 2003; 284:H1625-30

[46] Chemla D, Hebert JL, Coirault C, Salmeron S, Zamani K, Lecarpentier Y. Matching dicrotic notch and mean pulmonary artery pressures: implications for effective arterial elastance. The American journal of physiology. 1996; 271:H1287-95
[47] Pagnamenta A, Dewachter C, McEntee K, Fesler P, Brimioulle S, Naeije R. Early right ventriculo-arterial uncoupling in borderline pulmonary hypertension on experimental heart failure. J Appl Physiol. 2010; 109:1080-5
[48] Ghuysen A, Lambermont B, Kolh P, Tchana-Sato V, Magis D, Gerard P, et al. Alteration of right ventricular-pulmonary vascular coupling in a porcine model of progressive pressure overloading. Shock (Augusta, Ga. 2008; 29:197-204
[49] Borgdorff MA, Bartelds B, Dickinson MG, Boersma B, Weij M, Zandvoort A, et al. Sildenafil enhances systolic adaptation, but does not prevent diastolic dysfunction, in the pressure-loaded right ventricle. European journal of heart failure. 2012; 14:1067-74
[50] Holverda S, Gan CT, Marcus JT, Postmus PE, Boonstra A, Vonk-Noordegraaf A. Impaired stroke volume response to exercise in pulmonary arterial hypertension. Journal of the American College of Cardiology. 2006; 47:1732-3
[51] La Gerche A, Claessen G, Van de Bruaene A, Pattyn N, Van Cleemput J, Gewillig M, et al. Cardiac MRI: a new gold standard for ventricular volume quantification during high-intensity exercise. Circ Cardiovasc Imaging. 2012; 6:329-38
[52] Maron BA, Cockrill BA, Waxman AB, Systrom DM. The invasive cardiopulmonary exercise test. Circulation. 2013; 127:1157-64

4

CHAPTER 5

Serial assessment of RV systolic function in patients with precapillary pulmonary hypertension using simple echocardiographic parameters: a comparison with CMRI

Journal of Cardiology 2016

OA Spruijt[1], MC Di Pasqua[2], HJ Bogaard[1], CEE van der Bruggen[1], F Oosterveer[1], JT Marcus[3], A Vonk Noordegraaf[1], ML Handoko[4]

[1]Department of Pulmonary Medicine, VU University Medical Center, Amsterdam
[2]Department of Cardiology, Ferrarotto hospital, University of Catania, Italy
[3]Department of Physics and Medical Technology, VU University Medical Center, Amsterdam
[4]Department of Cardiology, VU University Medical Center, Amsterdam

Abstract

Introduction: Although cardiac magnetic resonance imaging (CMRI) is the gold standard for the (serial) assessment of right ventricular (RV) function, the technique has several drawbacks: CMRI is relatively expensive, has limited availability and the analyses are time consuming. Echocardiography (echo) can overcome several of these issues. The aim of this study was to compare simple echo-derived parameters of RV systolic function with CMRI-derived RV ejection fraction (RVEF) in patients with precapillary pulmonary hypertension (PH) and to determine which echo parameters best followed the change in CMRI-derived-RVEF during follow-up.

Methods: CMRI and echo were performed in 96 precapillary PH patients. In 38 patients a second set of a CMRI and echo were available. Retrospectively, echo-derived right ventricular fractional area change (RVFAC), tricuspid annulus plane systolic excursion (TAPSE), fractional transversal (FTWM) and longitudinal wall motion (FLWM) were assessed and compared with CMRI-derived-RVEF. Furthermore, the changes in RVFAC, TAPSE, FTWM and FLWM during follow-up were compared with the change in CMRI-derived-RVEF.

Results: All four echo parameters were significantly correlated to CMRI-derived-RVEF. The strongest relationship was seen between CMRI-derived-RVEF and RVFAC (r^2=0.567). However, sensitivity for predicting a deterioration in CMRI-derived RVEF was poor for all four echo-derived parameters (ranging from 33-56%).

Conclusions: Although RVFAC, TAPSE, FTWM and FLWN were significantly correlated to CMRI-derived-RVEF, all four echo parameters showed a low sensitivity for predicting a deterioration in CMRI-derived RVEF during follow-up. Therefore, RVFAC, TAPSE, FTWM and FLWN are not suitable parameters for the serial assessment of RV systolic function in patients with precapillary PH.

Introduction

Precapillary pulmonary hypertension (PH) is a progressive condition affecting the small pulmonary arteries, that increases the load on the right ventricle (RV). Survival in patients with precapillary PH is strongly related to RV systolic function [1-5] and several studies have shown the strong prognostic value of RV ejection fraction (RVEF) [3, 5]. Therefore, it is of utmost importance to monitor RV systolic function during the follow-up of patients with precapillary PH [3, 4, 6].

Although CMRI-derived-RVEF is the gold standard for the (serial) assessment of RV systolic function, it has several drawbacks: CMRI is relatively expensive, has limited availability and is incompatible with metallic devices [7]. Furthermore, for assessing RVEF it is necessary to manually trace the endocardial border on the complete stack of short-axis slices making determination of RVEF time-consuming. Therefore, using CMRI-derived-RVEF for the assessment of RV systolic function is not always the most practical option during daily practice.

In contrast to CMRI, echocardiography (echo) is inexpensive, readily available and can be applied at the bedside. Several simple and rapidly quantifiable echo-derived parameters of RV systolic function are available [8] and provide important prognostic information in precapillary PH [9, 10]. Two recent studies compared two echo-derived parameters of RV systolic function, RVFAC and tricuspid annulus plane systolic excursion (TAPSE) in precapillary PH patients with CMRI-derived-RVEF [11, 12]. However, these studies were performed in small cohorts and showed conflicting results. More importantly, it is unknown whether simple echo-derived parameter of RV systolic function can follow the change in CMRI-derived-RVEF during follow-up and hence can be used for the serial assessment of RV function in patients with precapillary PH.

The aim of this study was to compare simple echo-derived parameters of RV systolic function with CMRI-derived-RVEF in a large cohort of precapillary PH patients and to investigate whether echo-derived parameters of RV systolic function were able to follow the changes in CMRI-derived-RVEF during follow-up.

Methods

Study population

Retrospectively, precapillary PH patients that underwent an echo and CMRI in the VU University Medical Center between April 2010 and August 2014 were included. Available data was prospectively completed with precapillary patients that underwent an echo and CMRI within one

day between September 2014 and March 2015. In total 96 precapillary PH patients could be included, 31 treatment naïve and 65 patients under specific PH treatment (table 1). Precapillary PH was defined as a mean pulmonary arterial pressure (mPAP) ≥ 25 mmHg and pulmonary arterial wedge pressure (PAWP) ≤ 15 mmHg at rest assessed during a right heart catheterization (RHC) performed according to current ERS/ESC guidelines [13].

Of the 96 patients with precapillary PH, 38 patients had a second complete set at of an echo and CMRI at follow-up. These data were used to compare the change in echo-derived parameters of RV function with the change in CMRI-derived-RVEF.

This study was approved by The Medical Ethics Review Committee of the VU University Medical Center. Since the study did not fall within the scope of the Medical Research Involving Human Subjects Act (WMO), the study was permitted without requirement of an informed consent statement.

Echocardiography

Echocardiography was performed on a PHILIPS Sparq Ultrasound System with a S4-2 Ultrasound Probe. Measurements were done according to current guidelines [14]. Echo's were performed by echo technicians of the echocardiography laboratory of the department of Cardiology of the VU University Medical Center. Post-processing analyses were retrospectively performed of all echo-data by one observer (MCDP). A second observer (OAS) analysed 15 echo-studies to determine interobserver variability.

Right ventricular fractional area change (RVFAC)

RVFAC was obtained from an apical four-chamber view by tracing the right ventricular endocardial border at end-diastole and end-systole. End-systole was defined as the smallest RV area. RVFAC was calculated as:

$$\mathrm{RVFAC} = \frac{(end\ diastolic\ area - end\ systolic\ area)}{end\ diastolic\ area}\ X\ 100\%$$

Tricuspid annulus plane systolic excursion (TAPSE)

TAPSE was determined from an apical four-chamber view with a M-mode cursor through the lateral tricuspid annulus.

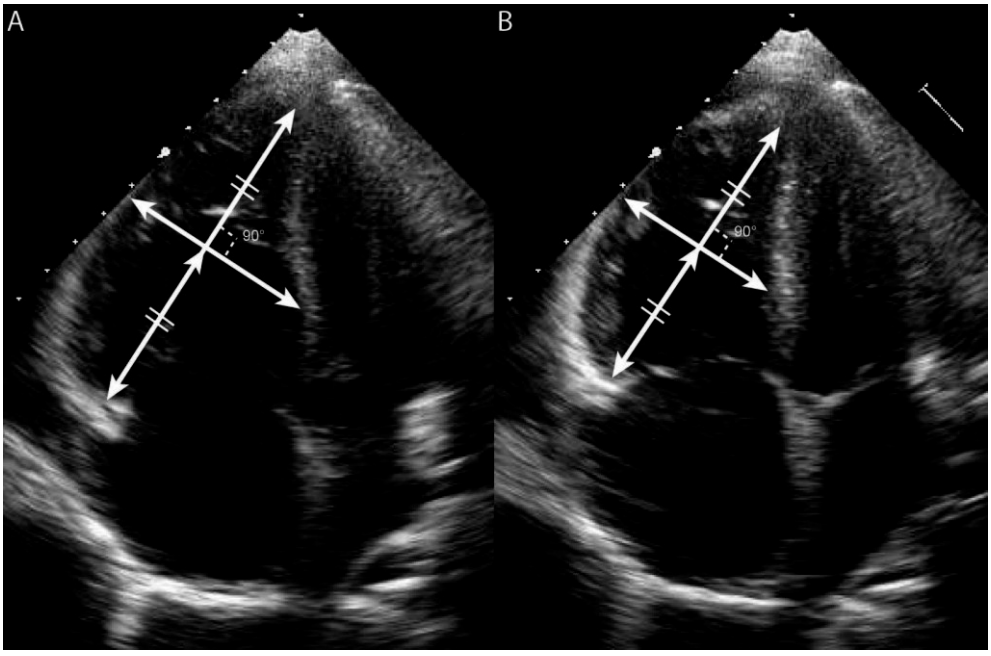

Figure 1: Assessment of the relative longitudinal and transverse wall motion. A = end-diastole; B = end-systole. The relative longitudinal wall motion was assessed by measuring the distance between the annulus of the tricuspid valve and the apex at end-diastole and end-systole. The relative transversal wall motion was assessed at 50% and perpendicular to the longitudinal distance at end-diastole and end-systole.

Fractional longitudinal wall motion (FLWM) and fractional transverse wall motion (FTWM)

FLWM and FTWM were not previously studied by echo, but showed reasonable correlations with RVEF in a recent CMRI study [15]. FLWM was determined from an apical four-chamber view by measuring the distance between the tricuspid annulus and apex at end-diastole and end-systole (figure 1). FLWM was than calculated as:

$$\text{FLWN} = \frac{(end\ diastolic\ longitudinal\ distance - end\ systolic\ longitudinal\ distance)}{end\ diastolic\ longitudinal\ distance}\ X\ 100\%$$

FTWM was determined from an apical four-chamber view. First a line was drawn from the tricuspid annulus to the apex. Halfway through and perpendicular to this line, the transverse distance between the RV endocardium and interventricular septum was drawn at end-diastole and end-systole (figure 1). Subsequently, FTWM was calculated as:

$$\text{FTWM} = \frac{end\ diastolic\ transverse\ distance - end\ systolic\ transverse\ distance}{end\ diastolic\ transverse\ distance}\ X\ 100\%$$

Cardiac magnetic resonance imaging (CMRI)

All CMRI scans were performed on a Siemens 1.5T Sonato or Avanto scanner (Siemens Medical Solutions, Erlangen, Germany). Image acquisition and post-processing was performed as described elsewhere [3]. Short-axis images were analyzed using the MASS software package (MEDIS Medical Imaging Systems, Leiden, the Netherlands). Endocardial borders of the RV were manually traced on end-diastolic images (defined as the first cine after the R-wave trigger) and on end-systolic images (defined as the cine with visually the smallest cavity). Trabeculae as well as papillary muscles were excluded from the cavity and RV end-diastolic and end-systolic volumes were assessed using the Simpson rule. RVEF was calculated as:

$$\text{RVEF} = \frac{(RV\ end\ diastolic\ volume - RV\ end\ systolic\ volume)}{RV\ end\ diastolic\ volume}\ X\ 100\%$$

Statistical analysis

Normal distribution of the data was checked and presented as mean ± SD, unless stated otherwise. Simple linear regression was performed to test the relation between CMRI-derived-RVEF and echo-derived parameters of RV systolic function. Receiver operating characteristic (ROC) analyses were used to test which echo parameter best predicted a RVEF<35% or ≥35% [3]. The areas under the curves (AUCs) of the different parameters were tested using the DeLong-method.

Intra-observer and inter-observer variability of all four echo parameters were assessed in 15 patients and tested using Bland and Altman analysis and intraclass correlation coefficients. Intra-observer and inter-observer variability was also assessed of CMRI-derived RVEF in 10 patients using Bland Altman analysis. For echo and CMRI intra- and interobserver variability measurements the moment of end-systole was independently chosen [16].

The comparison between the change in echo-derived parameters of RV systolic function and the change in CMRI-derived-RVEF during follow-up was firstly analysed by simple linear regression. Subsequently, sensitivity, specificity, negative predictive values (NPV) and positive predictive values (PPV) of the ability of the four echo-parameters to predict a deterioration in RV function were analysed. A decrease of >3% in CMRI-derived-RVEF was considered as deterioration in RV function

[16]. SDs of the bias of the interobserver variability of the different echo parameters were used as a cut-off value to define an echo-based deterioration in RV function. Statistical analyses were performed using SPSS version 20 for Windows (IBM Corp. Armonk, NY, USA), GraphPad Prism version 6.0 (Graphpad Software, Inc. San Diego, CA, USA) and Stata version 12 (Stata Corp. Stata Statistical Software: release 12. College Station, TX, USA). A p-value < 0.05 was considered statistically significant.

Results

Clinical, hemodynamic and cardiac characteristics are summarized in table 1 and 2.

Clinical characteristics	
Age (yr)	53 ± 16
Sex (M:F) (n)	27 : 69
BMI	25 ± 4.6
BSA	1.83 ± 0.2
NYHA functional class I/II/III/IV (n)	10/56/22/8
6MWD (m)	412 ± 147
Pro-BNP (ng/L)	1730 ± 2824
Diagnosis (n)	
Pulmonary arterial hypertension (PAH) (WHO group I)	75
Idiopathic/heritable PAH	54
Associated with connective tissue disease	13
Associated with congenital heart disease	7
Pulmonary veno-occlusive disease	1
CTEPH (WHO group IV)	17
PH with unclear and/or multifactorial mechanism (WHO group V)	4
Treatment (n)	
Treatment naive	31
Monotherapy (ERA or PDE5I)	18
Calcium channel blockers	2
Dual combination therapy	35
ERA+PDE5I	26
ERA + prostacyclin	3
PDE5I + prostacyclin	6

Triple combination therapy (ERA + PDE5I + prostacyclin)	8
Post-PTE	2
Hemodynamic characteristics	
Heart rate (beats/min)	78 ± 14
Mean pulmonary artery pressure (mmHg)	48 ± 15
Pulmonary arterial wedge pressure (mmHg)	10 ± 3
Mean right atrial pressure (mmHg)	9 ± 6
Pulmonary vascular resistance (dyn.s/cm5)	607 ± 398
Cardiac output (l/min)	5,6 ± 1,9
Mixed venous O2 saturation (%)	65 ± 11

Table 1: Clinical characteristics, treatment and hemodynamics. M = males; F = females; BMI = Body Mass Index; BSA = Body Surface Area; NYHA = New York Heart Association functional class; 6MWD = six minute walk distance; CTEPH = Chronic Thromboembolic Pulmonary Hypertension; ERA = Endothelin Receptor Antagonists; PDE5I = Phosphodiesterase-5 Inhibitors.

Parameters	**Mean ± SD**
CMRI-RVEF (%)	41.4 ± 15.2
Fractional area change (%)	35.8 ± 11.4
Tricuspid annular plane systolic excursion (mm)	18.8 ± 4
Longitudinal movements	
Tricuspid annulus-apex ED (mm)	92.4 ± 13.7
Tricuspid annulus-apex ES (mm)	75.8 ± 12.4
Tricuspid annulus-apex distance (mm)	11.8 ± 9.5
Fractional longitudinal wall motion (%)	17.6 ± 6.8
Transverse movements	
Septum to free wall ED (mm)	41.2 ± 11.1
Septum to free wall ES (mm)	30.9 ± 11
Septum to free wall distance (mm)	8.6 ± 6
Fractional transverse wall motion (%)	23.7 ± 11.1

Table 2: Right ventricular function. CMRI-RVEF = Right Ventricle Ejection Fraction derived from cardiac magnetic resonance imaging; RVFAC = right ventricular fractional area change; TAPSE = tricuspid annular plane systolic excursion; ED = end-diastole; ES = end-systole.

In the cohort of 96 patients, mean time between CMRI and echo was 2±2 days. CMRI-derived-RVEF correlated significantly to all echo parameters (figure 2). The strongest relation was seen between CMRI-derived-RVEF and RVFAC (r^2=0.567, P<0.001), while weaker correlations exist between RVEF

and fractional transverse wall motion (r^2=0.296), TAPSE (r^2=0.235) and fractional longitudinal wall motion (r^2=0.184) (figure 2).

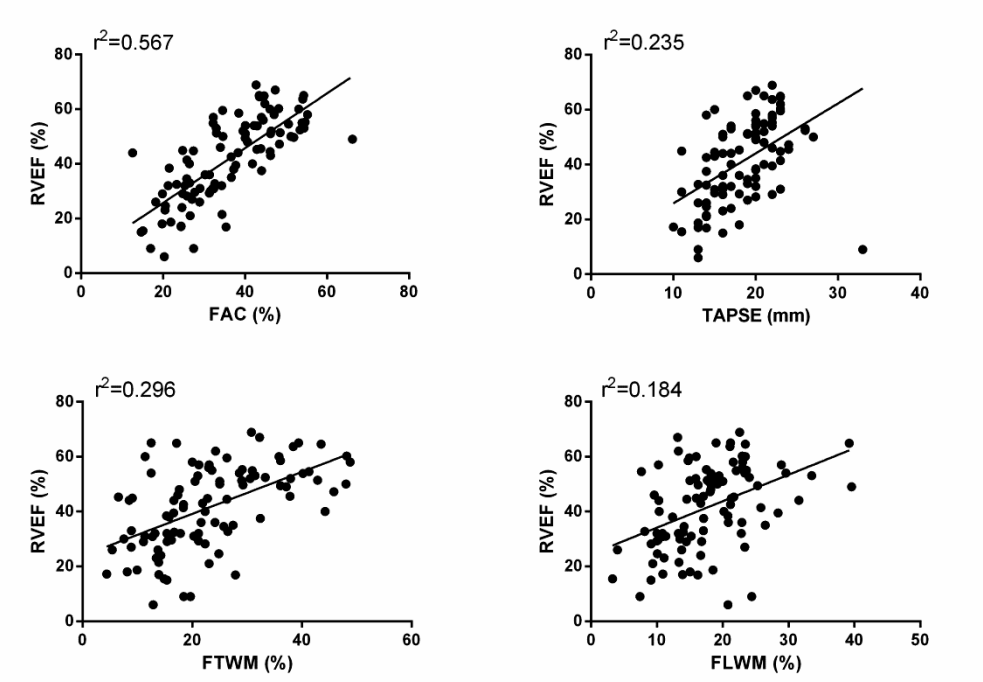

Figure 2: Relation between CMRI-derived-RVEF and echo parameters. RVEF = Right Ventricle Ejection Fraction; RVFAC = Right ventricular fractional area change; TAPSE = tricuspid annular plane systolic excursion; FLWM = fractional longitudinal wall motion. FTWM = fractional transverse wall motion.

As depicted in figure 3, RVFAC (AUC=0.90) was superior in detecting a RVEF<35% compared to TAPSE (AUC=0.80), FLWM (AUC=0.82) and FTWM (AUC=0.81). Comparison of AUCs of the different parameters showed a trend towards significance in favour of the AUC of RVFAC compared to the AUCs of TAPSE (p=0.069), FLMW (p=0.095) and FTWM (p=0.054).

Intra- and interobserver variability of all four echo-parameters are depicted in table 3 and figure A and B in the online supplement. Intraobserver variability and interobserver variability were best for TAPSE (ICC=0.97 and ICC=0.92).

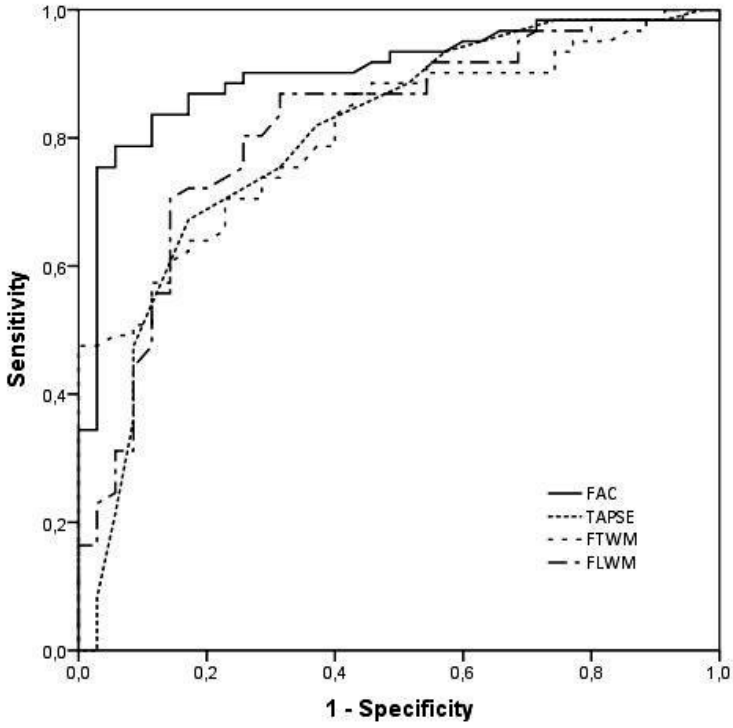

Figure 3: ROC analysis of echo parameters for predicting RVEF <35% or ≥35%. FAC = (right ventricular) fractional area change. TAPSE = tricuspid annulus plane systolic excursion. FLWM = fractional longitudinal wall motion. FTWM = fractional transverse wall motion.

Parameters	**Intraobserver**			**Interobserver**		
	ICC	**Bias**	**SD of bias**	**ICC**	**Bias**	**SD of bias**
RVFAC (%)	0.90	0.38	4.89	0.80	-1.08	5.39
TAPSE (mm)	0.97	-0.20	1.08	0.92	0.60	1.68
FLWN (%)	0.96	0.16	2.16	0.80	-0.93	4.59
FTWN (%)	0.78	-4.07	6.60	0.73	0.03	8.20

Table 3: Caption: Intra- and interobserver variability. ICC = intraclass correlation coefficient; SD = standard deviation; RVFAC = right ventricular fractional area change; TAPSE = tricuspid annulus plane systolic exercursion; FLWN: fractional longitudinal wall motion; FTWN = fractional transversal wall motion.

Characteristics of the 38 patients with a second set of a CMRI and echo are summarized in the online supplement (table A). The median (IQR) time between the first measurements and the second measurements was 192 (129-570) days. The time between the second CMRI and second echo was 2±6 days. The change in CMRI-derived-RVEF was significantly related to the change in all four echo parameters (figure 4), with the strongest relation found between the change in CMRI-derived-RVEF and the change in RVFAC (r^2=0.349 p<0.001).

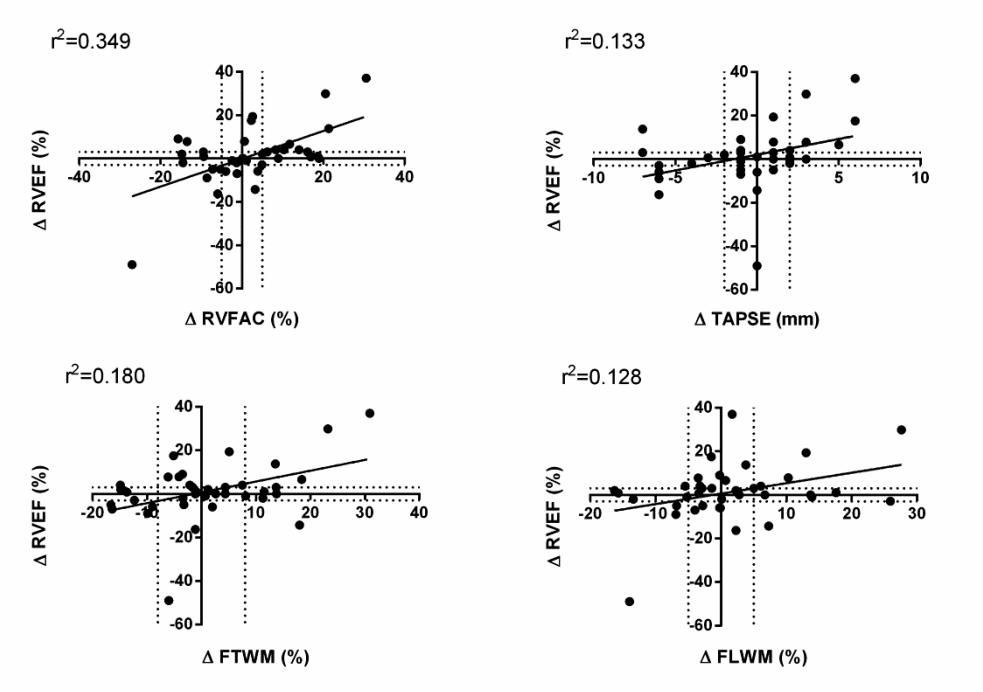

Figure 4: Relation between the change in CMRI-derived-RVEF and the change in echo parameters. The dotted lines represents the SD of the repeatability of CMRI-based-RVEF (ref: Bradlow) and the SD of interobserver variability of the four different echo-parameters. RVEF = right ventricular ejection fraction; RVFAC = right ventricular fractional area change. TAPSE = tricuspid annulus plane systolic excursion. FLWM = fractional longitudinal wall motion. FTWM = fractional transverse wall motion.

The sensitivity, specificity, NPV and PPV are summarized in table 4. Sensitivity of echo for predicting a deterioration in RV systolic function was poor for all four parameters, with the highest sensitivity for RVFAC (56%).

Parameters	Sensitivity (%)	Specificity (%)	NPV (%)	PPV (%)
ΔRVFAC (cut-off: <-5%)	56	79	85	55
ΔTAPSE (cut-off: <-2mm)	33	83	80	63
ΔFLWN (cut-off: <-5%)	33	83	80	63
ΔFTWN (cut-off: <-8%)	44	86	83	50

Table 4: Sensitivity, specificity, NPV and PPV for four echo-parameters for predicting a deterioration in RV function (defined as a decrease in RVEF >3% measured with CMRI (Ref: Bradlow et al.). Cut-off points of the four echo-parameters are based on the SD of the interobserver variability (table 3). RVFAC = right ventricular fractional area change; TAPSE = tricuspid annulus plane systolic excursion; FLWN: fractional longitudinal wall motion; FTWN = fractional transversal wall motion; NPV = negative predictive value; PPV = positive predictive value.

Discussion

We investigated in the largest cohort of patients with precapillary PH thus far, the relation between several simple echo-derived parameters of RV systolic function and CMRI-derived-RVEF (gold standard). Additionally, we studied whether echo-derived parameters of RV systolic function were able to detect a deterioration in RV systolic function during follow-up. We found that RVFAC best correlated with CMRI-derived-RVEF, however none of the four investigated echo-derived parameters were able to sensitively detect changes in CMRI-derived RVEF during follow-up.

Relation between echo parameters and CMRI-derived-RVEF

In two relatively small cohorts of PH patients, the relation was assessed between echo-derived parameters of RV systolic function and CMRI-derived-RVEF. These studies showed conflicting results. Sato et al. [11] compared CMRI-derived-RVEF with echo-derived RVFAC and TAPSE and found that RVEF was better related to TAPSE (r^2=0.71) than to RVFAC (r^2=0.23). Recently, Shiran and coworkers [12], found a stronger relation between RVEF and RVFAC (r^2=0.76) compared to TAPSE (r^2=0.64). These inconsistent findings prompted us to investigate the comparison between echo-derived parameters of RV systolic function and CMRI-derived RVEF in a large cohort of PH patients. Our results are in line with those of Shiran et al. [12] with a stronger relation between CMRI-derived-RVEF and echo-derived RVFAC (r^2=0.57) compared to TAPSE (r^2=0.24). Furthermore, RVFAC could best distinguish between a RVEF<35% and RVEF>35%. Kind et al. [15] compared 2D-CMRI-derived RV parameters with CMRI-derived-RVEF in a large cohort of PH patients and also found the best correlation between RVFAC and RVEF. Given the complex geometry of the RV cavity, it is not

unexpected that the more of the geometry of the RV is taken into account within a 2D measurement, the better it correlates to a 3D function parameter.

In addition, we assessed RV systolic function by the fractional transverse and longitudinal wall motion from the four-chamber view. The fractional transverse wall motion correlated better with CMRI-derived-RVEF compared to TAPSE and fractional longitudinal wall motion. This finding is in line with Kind et al. [15] comparing 2D-CMRI-derived parameters with CMRI-derived-RVEF. It has been shown that during deterioration of RV function in PH patients, the decrease in longitudinal wall motion is reaching a floor effect, while this does not apply to the decrease in transverse wall motion [6]. This could explain why fractional transverse wall motion better correlated to RVEF compared to fractional longitudinal wall motion.

Ability of echo to predict a deterioration in CMRI-derived-RVEF

Since monitoring RV function during follow-up of PH patients is of utmost importance, we assessed which echo-derived parameter of RV systolic function best followed the change in CMRI-derived-RVEF over time. The strongest correlation was found between the change in RVFAC and RVEF (r^2=0.349). Based on repeatability studies, a decrease in CMRI-derived-RVEF>3% is accepted as a real decrease in RV function [3, 16]. Since, as far as we know, no repeatability studies have been performed for TAPSE and RVFAC, echo-based cut-off values for a deterioration in RV function were based on the interobserver variability. All four echo parameters showed a poor sensitivity for detecting a deterioration in RV function. This suggests that echo-derived RVFAC, TAPSE, FTWM and FLWM may not be suitable parameters for the serial assessment of RV function in the follow-up of patients with precapillary PH.

We investigated four simple and rapidly assessable parameters of RV systolic function. Echo-derived parameters of RV systolic function, in particular RVFAC, could reasonably distinguish between a decreased or preserved CMRI-derived-RVEF. However, all four investigated echo-derived parameters of RV systolic function were insufficiently sensitive for detecting a deterioration in RV systolic function during follow-up. Therefore, CMRI remains the gold standard for the serial assessment of RV systolic function.

The number of patients that we used for measuring the ability of echo-derived parameters to follow the change in CMRI-derived RVEF is relatively low. This can have affected the positive and negative predictive values of the different echo-derived parameters.

Conclusions

Although RVFAC, TAPSE, FTWM and FLWM were significantly related to CMRI-derived-RVEF, all four echo-derived parameters of RV systolic function showed a low sensitivity for predicting a deterioration in CMRI-derived RVEF during follow-up. Therefore, RVFAC, TAPSE, FTWM and FLWN are not suitable for the serial assessment of RV systolic function in patients with precapillary PH.

References

[1] Benza RL, Miller DP, Gomberg-Maitland M, Frantz RP, Foreman AJ, Coffey CS, et al. Predicting survival in pulmonary arterial hypertension: insights from the Registry to Evaluate Early and Long-Term Pulmonary Arterial Hypertension Disease Management (REVEAL). Circulation. 2010; 122:164-72

[2] Humbert M, Sitbon O, Chaouat A, Bertocchi M, Habib G, Gressin V, et al. Survival in patients with idiopathic, familial, and anorexigen-associated pulmonary arterial hypertension in the modern management era. Circulation. 2010; 122:156-63

[3] van de Veerdonk MC, Kind T, Marcus JT, Mauritz GJ, Heymans MW, Bogaard HJ, et al. Progressive right ventricular dysfunction in patients with pulmonary arterial hypertension responding to therapy. Journal of the American College of Cardiology. 2011; 58:2511-9

[4] van de Veerdonk MC, Marcus JT, Westerhof N, de Man FS, Boonstra A, Heymans MW, et al. Signs of right ventricular deterioration in clinically stable patients with pulmonary arterial hypertension. Chest. 2015; 147:1063-71

[5] van Wolferen SA, Marcus JT, Boonstra A, Marques KM, Bronzwaer JG, Spreeuwenberg MD, et al. Prognostic value of right ventricular mass, volume, and function in idiopathic pulmonary arterial hypertension. European heart journal. 2007; 28:1250-7

[6] Mauritz GJ, Kind T, Marcus JT, Bogaard HJ, van de Veerdonk M, Postmus PE, et al. Progressive changes in right ventricular geometric shortening and long-term survival in pulmonary arterial hypertension. Chest. 2012; 141:935-43

[7] Vonk Noordegraaf A, Haddad F, Bogaard HJ, Hassoun PM. Noninvasive imaging in the assessment of the cardiopulmonary vascular unit. Circulation. 2015; 131:899-913

[8] Harrison A, Hatton N, Ryan JJ. The right ventricle under pressure: evaluating the adaptive and maladaptive changes in the right ventricle in pulmonary arterial hypertension using echocardiography (2013 Grover Conference series). Pulmonary circulation. 2013; 5:29-47

[9] Forfia PR, Fisher MR, Mathai SC, Housten-Harris T, Hemnes AR, Borlaug BA, et al. Tricuspid annular displacement predicts survival in pulmonary hypertension. American journal of respiratory and critical care medicine. 2006; 174:1034-41

[10] Raymond RJ, Hinderliter AL, Willis PW, Ralph D, Caldwell EJ, Williams W, et al. Echocardiographic predictors of adverse outcomes in primary pulmonary hypertension. Journal of the American College of Cardiology. 2002; 39:1214-9

[11] Sato T, Tsujino I, Ohira H, Oyama-Manabe N, Yamada A, Ito YM, et al. Validation study on the accuracy of echocardiographic measurements of right ventricular systolic function in pulmonary hypertension. J Am Soc Echocardiogr. 2012; 25:280-6

[12] Shiran H, Zamanian RT, McConnell MV, Liang DH, Dash R, Heidary S, et al. Relationship between echocardiographic and magnetic resonance derived measures of right ventricular size and function in patients with pulmonary hypertension. J Am Soc Echocardiogr. 2014; 27:405-12

[13] Galie N, Hoeper MM, Humbert M, Torbicki A, Vachiery JL, Barbera JA, et al. Guidelines for the diagnosis and treatment of pulmonary hypertension. The European respiratory journal. 2009; 34:1219-63

[14] Lang RM, Badano LP, Mor-Avi V, Afilalo J, Armstrong A, Ernande L, et al. Recommendations for cardiac chamber quantification by echocardiography in adults: an update from the American Society of Echocardiography and the European Association of Cardiovascular Imaging. J Am Soc Echocardiogr. 2015; 28:1-39 e14

[15] Kind T, Mauritz GJ, Marcus JT, van de Veerdonk M, Westerhof N, Vonk-Noordegraaf A. Right ventricular ejection fraction is better reflected by transverse rather than longitudinal wall motion in pulmonary hypertension. J Cardiovasc Magn Reson. 2010; 12:35

[16] Bradlow WM, Hughes ML, Keenan NG, Bucciarelli-Ducci C, Assomull R, Gibbs JS, et al. Measuring the heart in pulmonary arterial hypertension (PAH): implications for trial study size. J Magn Reson Imaging. 2010; 31:117-24

Supplementary material

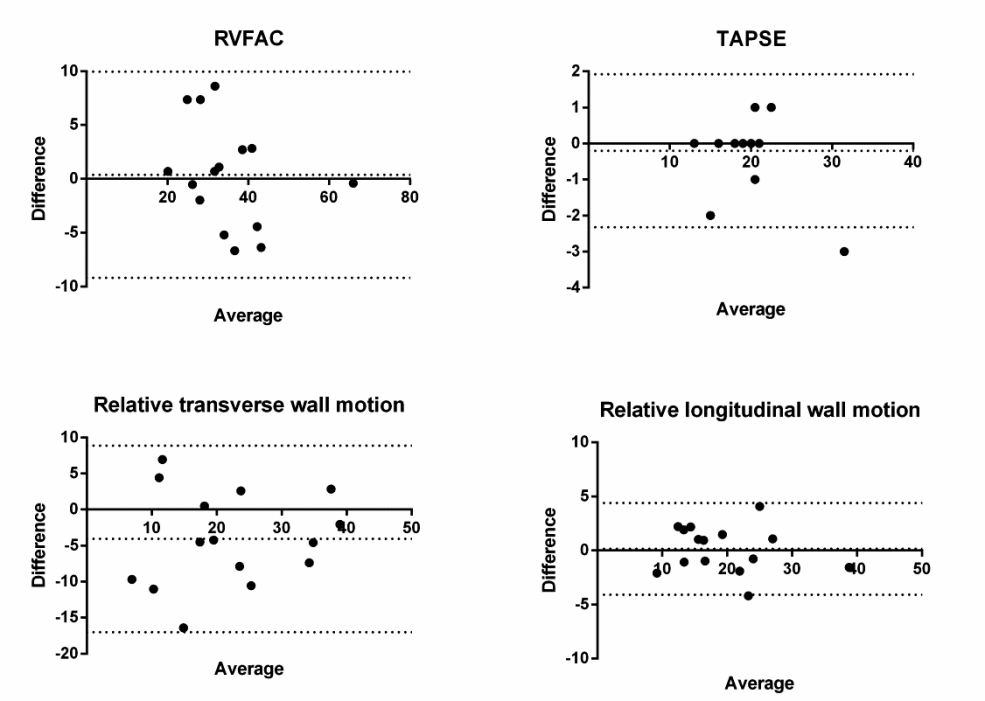

Figure A: Intra-observer analyses. Dotted lines represent the mean and 95%CI. A = intra-observer variability of RVFAC; B = intra-observer variability of TAPSE; C = intra-observer variability of FLWM; D= intra-observer variability of FTWM. RVFAC = right ventricular fractional area change. TAPSE = tricuspid annulus plane systolic excursion. FLWM = fractional longitudinal wall motion. FTWM = fractional transverse wall motion.

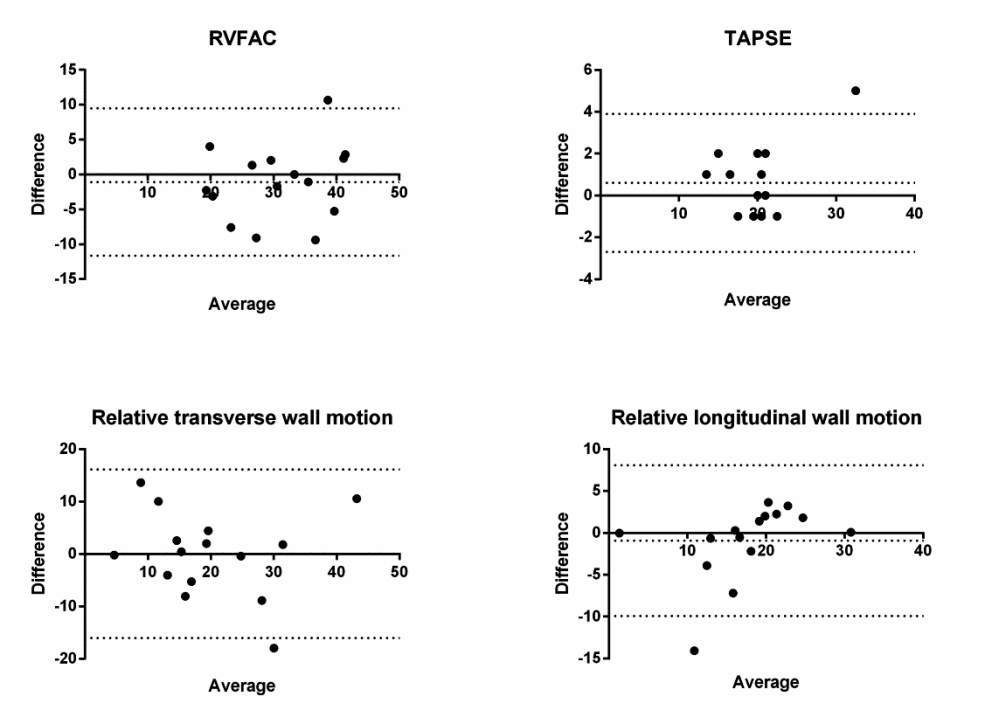

Figure B: Inter-observer analyses. Dotted lines represent the mean and 95%CI. A = inter-observer variability of RVFAC; B = inter-observer variability of TAPSE; C = inter-observer variability of FLWM; D= inter-observer variability of FTWM. RVFAC = right ventricular fractional area change. TAPSE = tricuspid annulus plane systolic excursion. FLWM = fractional longitudinal wall motion. FTWM = fractional transverse wall motion.

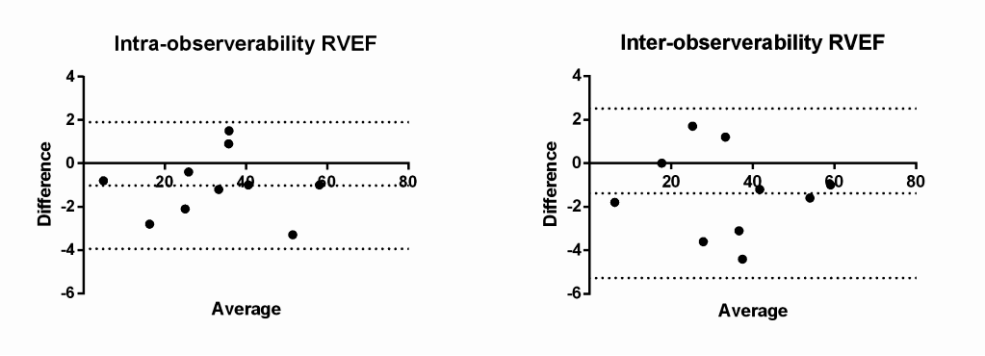

Figure C: Intra- and inter-observer analyses of RVEF. Dotted lines represent the mean and 95%CI. RVEF = right ventricular ejection fraction.

Clinical characteristics	
Age (yr)	46 ± 15
Sex (M:F) (n)	4 : 34
Diagnosis (n)	
Pulmonary arterial hypertension (PAH) (WHO group I)	36
Idiopathic/heritable PAH	24
Associated with connective tissue disease	6
Associated with congenital heart disease	5
Pulmonary veno-occlusive disease	1
CTEPH (WHO group IV)	2
Hemodynamic characteristics	
Heart rate (beats/min)	79 ± 18
Mean pulmonary artery pressure (mmHg)	50 ± 19
Pulmonary arterial wedge pressure (mmHg)	8 ± 3
Mean right atrial pressure (mmHg)	7 ± 4
Pulmonary vascular resistance (dyn.s/cm5)	714 ± 415
Cardiac output (l/min)	5.4 ± 1.7
Mixed venous O2 saturation (%)	65 ± 14

Table A: Characteristics of patients with two complete sets of a CMR and echo. Summarized characteristics are from the moment of the first measurement. M = males; F = females; WHO = World Health Organization clinical classification system; CTEPH = Chronic Thromboembolic Pulmonary Hypertension.

5

CHAPTER 6

Treatment response in patients with idiopathic pulmonary arterial hypertension and a severely reduced diffusion capacity

Pulmonary Circulation 2016

OA Spruijt[1], CEE van der Bruggen[1], Esther Nossent[1], P Trip[1], FS de Man[1,2], JT Marcus[3], HJ Bogaard[1], A Vonk Noordegraaf[1]

[1]Department of Pulmonary Medicine, VU University Medical Center, Amsterdam
[2]Department of Physiology, VU University Medical Center, Amsterdam
[3]Department of Physics and Medical Technology, VU University Medical Center, Amsterdam

Abstract

Introduction: Patients with idiopathic pulmonary arterial hypertension (IPAH) and a reduced diffusion capacity of the lung for carbon monoxide (DLCO) have a worse survival compared to IPAH patients with a preserved DLCO. Whether this poor survival can be explained by unresponsiveness to pulmonary hypertension (PH) specific vasodilatory therapy is unknown. Therefore, the aim of this study was to evaluate the hemodynamic and cardiac response to PH specific vasodilatory therapy in patients with IPAH and a reduced DLCO.

Methods: Retrospectively, we studied treatment naïve hereditary- and IPAH patients diagnosed between January 1990 and May 2015 at the VU University Medical Center. After exclusion of subjects without available baseline DLCO measurement or right heart catheterization data and subjects carrying a BMPR2 mutation, 166 subjects could be included in this study. Subsequently, hemodynamics, cardiac function, exercise capacity and oxygenation at baseline and after PH-specific vasodilatory therapy were compared between IPAH patients with a preserved DLCO (DLCO>62%), IPAH patients with an moderately reduced DLCO (DLCO 43-62%) and a severely reduced DLCO (DLCO<43%).

Results: Baseline hemodynamics and right ventricular function were not different between groups. Baseline oxygenation was worse in patients with IPAH and a severely reduced DLCO. Hemodynamics and cardiac function improved in all groups after PH specific vasodilatory therapy without worsening of oxygenation at rest or during exercise.

Conclusions: Patients with IPAH and a severely reduced DLCO show a similar response to PH-specific vasodilatory therapy in terms of hemodynamics, cardiac function and exercise capacity as patients with IPAH and an moderately reduced or preserved DLCO.

Introduction

Patients with pulmonary hypertension tend to have a mildly reduced pulmonary diffusion capacity for carbon monoxide (DLCO) compared to healthy subjects [1]. A severely reduced DLCO is most often seen in pulmonary hypertension related to connective tissue disease, lung parenchymal disease or in pulmonary veno-occlusive disease, but also in a subset of patients with idiopathic pulmonary arterial hypertension (IPAH) without signs of these underlying conditions [2-5]. Recent studies revealed that IPAH patients with a low DLCO have a worse survival [6]. Although it is yet unknown what causes this difference in survival, it has been argued that compared to other IPAH patients, IPAH patients with a severely reduced DLCO may have a distinct type of pulmonary vasculopathy that is less responsive to PAH-specific therapy [7,8]. Therefore, the aim of this study was to compare the response to pulmonary arterial hypertension specific vasodilatory therapy in terms of hemodynamics, cardiac function, exercise capacity and oxygenation between IPAH patients with different degrees of DLCO impairment.

Methods

We studied retrospectively treatment naïve hereditary- and IPAH patients who were diagnosed between January 1990 and May 2015 at the VU University Medical Center. Part of this cohort was described in the study of Trip et al. [5]. A diagnosis of hereditary- and IPAH was established by a multidisciplinary PH team, after rigorous clinical evaluation according to the ERS/ESC guideline [9]. Subjects without available baseline DLCO measurement, with severe emphysema or pulmonary fibrosis on HRCT [5] were excluded from this study. Furthermore, to avoid clouding of the results, patients carrying a BMPR2 mutation were excluded from this study as recent studies showed the reduced life-expectancy but preserved DLCO status in these subjects [4, 10]. In total 166 patients were included in this study (figure 1). The cohort was divided into three groups using tertiles, leading to one group with a severely reduced DLCO (<43%), one group with a moderately reduced DLCO (43%-62%) and one group with a preserved DLCO (>62%).

Right heart catheterization

Hemodynamics and RV pressure curve recordings were assessed with a balloon-tipped, flow directed 7.5F triple lumen Swan-Ganz catheter (Edwards Lifesciences LLC, Irvine, CA, USA). Cardiac output measurements were performed using thermodilution or the direct Fick method.

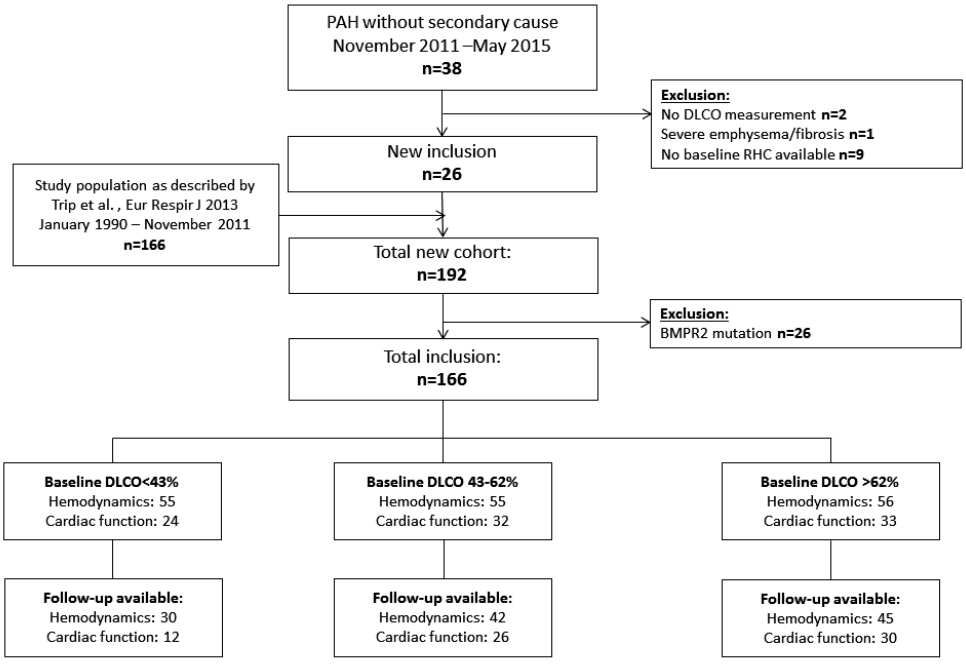

Figure 1: Flow chart. PAH = pulmonary arterial hypertension; RHC = right heart catheterization.

Cardiac function and volumes

RV function and volumes were assessed using cardiac magnetic resonance imaging (CMRI). All scans were performed on a Siemens 1.5T Sonata or Avanto scanner (Siemens Medical Solutions, Erlangen, Germany). Image acquisition and post-processing was done as described previously [11]. Left and RV volumes were indexed to body surface area (BSA). Stroke volume (SV) and ejection fraction (EF) were calculated according to the following formulas, in which EDV= end-diastolic volume and ESV = end-systolic volume: SV = EDV-ESV and EF = (EDV-ESV)/EDV.

Six-minute walking test (6 MWT)

6MWTs were performed according to the ATS guidelines [12, 13]. The distance walked (in meters) and the arterial oxygen saturation at rest and during exercise were measured at baseline and during follow-up.

Treatment response

Treatment responses were assessed by the baseline-to-follow-up responses in hemodynamics, cardiac function and 6MWD. Time between baseline and follow-up was 1.9 ± 1.6 years in the DLCO<43% group, 1.6 ± 1.2 years in the DLCO 43-62% group and 2.1 ± 2.2 years in the DLCO>62% group (p=0.860).

Statistical analysis

Data are presented as mean ± standard deviation (SD) unless stated otherwise. Comparisons of baseline hemodynamics, cardiac function and the change in hemodynamic and cardiac function after PAH-specific therapies between the DLCO<43%, DLCO 43-62% and the DLCO>62% group were performed using one-way ANOVA with Bonferroni post-hoc corrections and Kruskas-Wallis tests with Dunn's multiple comparisons post-hoc test as appropriate. Kaplan-Meier analyses were performed to test for survival differences between the DLCO<43%, DLCO 43-62% and the DLCO>62% groups in the entire cohort and the cohort in which a MRI at follow-up was present. Kaplan-meier analysis was also performed to test for survival differences between the subjects with and without a CMRI at follow-up in the DLCO<43% group. Subsequently, multivariable cox regression analyses were performed to correct the association between DLCO and survival for age differences. Statistical analyses were performed using SPSS for Windows version 20 (IBM Corp., Armonk, NY, USA) and GraphPad Prism for Windows version 6 (GraphPad Software, Inc., San Diego, CA, USA). P-values <0.05 were considered statistically significant.

Results

Characteristics of the DLCO<43%, DLCO 43-62% and DLCO>62% patients are summarized in table 1. A detailed characterization of the majority of patients was already given in our previous study [5].

Baseline measurements

SvO2, LVEDVI and LVESVI were significantly lower in the DLCO<42% group compared to the DLCO>62% group. Except from these, baseline hemodynamics and cardiac function were not different between groups. Exercise capacity, assessed by the 6MWT, was significantly lower in the DLCO<42% group compared to the moderately reduced and preserved DLCO group, as well as the arterial oxygen tension and saturation at rest. Furthermore, the DLCO<42% group showed a larger drop in arterial oxygen saturation during exercise (Table 1).

	DLCO<43%	DLCO 43-62%	DLCO>62%	p-value
Age at diagnosis (yrs)	65±13	53±18*	48±14#	<0.0001
Male (%)	58	18	27	<0.0001
6MWT				
6MWD (m)	286±136	366±119*	416±134#	<0.0001
6MWD (% predicted)	56±23	70±19*	71±23#	<0.01
SaO_2-rest (%)	91±4	94±3*	95±2#	<0.0001
SaO_2-exercise (%)	79±7	89±6*	89±6#	<0.0001
ΔSaO_2 (%)	-11 (-16—6)	-4 (-8 –2)*	-5 (-10—2)#	<0.0001
Laboratory tests				
NT-proBNP (ng·L)	1004 (304-2487)	802 (194-2888)	555 (156-1887)	0.45
PCO_2 (mmHg)	30±6	33±7	33±6	0.19
PO_2 (mmHg)	61±15	68±11	72±13#	<0.05
SaO_2 (%)	91±5	94±3*	94±3#	<0.01
Baseline hemodynamics				
HR (beats/min)	80±17	78±15	80±13	0.84
mPAP (mmHg)	48±12	51±14	52±15	0.33
mRAP (mmHg)	7 (4-9)	7 (4-11)	8 (5-11)	0.67
PAWP (mmHg)	10±3	9±4	8±4	0.27
PVR (dynes·s·cm^{-5})	706 (540-1000)	858 (476-1041)	569 (441-961)	0.56
CI (l/min/m²)	2.3±0.7	2.5±1.0	2.7±0.9	0.18
SvO_2 (%)	61±9	63±9	67±9#	<0.01
Baseline cardiac function				
LV EDVI (ml/m²)	40±10	41±11	48±13#	<0.05
LV ESVI (ml/m²)	15±6	14±6	18±7†	<0.05
LV EF (%)	63±10	66±10	62±10	0.21
RV EDVI (ml/m²)	76±27	76±17	88±21	0.06
RV ESVI (ml/m²)	54±26	50±18	59±23	0.31
RV EF (%)	33±12	36±12	35±12	0.67

Table 1: Baseline characteristics. 6MWD = six minute walking distance; SaO2 = arterial oxygen saturation; HR = heart rate; mPAP = mean pulmonary arterial pressure; mRAP = mean right atrial pressure; PAWP = pulmonary arterial wedge pressure; PVR = pulmonary vascular resistance; CI = cardiac index; SvO2 = mixed venous oxygen saturation; LVEDVI = left ventricular end-diastolic volume index; LVESVI = left ventricular end-systolic volume index; LVEF = left ventricular ejection fraction; RVEDVI = right ventricular end-diastolic volume index; RVESVI = right ventricular end-systolic volume index; RVEF = right ventricular ejection fraction. *DLCO<43% significantly different compared to DLCO 43-62%, #DLCO<43% significantly different compared to DLCO>62%, †DLCO 43-62% significantly different compared to DLCO>62%.

Treatment response

As can be appreciated from Table 2, the DLCO<42% group received more double-therapy, more prostacyclin monotherapy and less endothelin receptor antagonist or phosphodiesterase type 5 inhibitor mono therapy. Interestingly, a significantly higher percentage of patients switched from monotherapy to combination therapy in the severely reduced DLCO group (table 3).

	DLCO <43%	DLCO 43-62%	DLCO>62%	p-value
Mono ERA/PDE5i (%)	26.7	41.9	52.8	**<0.001**
Mono PGI_2 (%)	26.7	7.0	11.1	**<0.001**
Double: ERA+PDE5i (%)	40.0	37.2	22.2	**<0.05**
Double: PGI_2 +ERA/PDE5i (%)	5.7	2.3	0	**<0.05**
Triple (%)	0	2.3	8.3	**<0.01**
Calcium antagonist (%)	0	9.3	5.6	**<0.01**

Table 2: Pulmonary arterial hypertension specific medication during follow-up. ERA = endothelin receptor antagonist; PGI2 = prostacyclin; PDE5i = phosphodiesterase type 5 inhibitor.

	DLCO <43%	DLCO 43-62%	DLCO>62%	p-value
Mono to combi therapy (%)	32.0	20.0	11.1	**<0.01**
Mono to triple therapy (%)	0	0	2.8	0.05
Combi to triple therapy (%)	0	2.5	2.8	0.22

Table 3: Treatment changes during follow-up (changes after an unsatisfactory response to previous treatment, hemodynamic or clinical worsening).

All groups showed a decrease in mPAP and pulmonary vascular resistance (PVR), an increase in cardiac index (CI) and no change in pulmonary arterial wedge pressure (PAWP) and heart rate (HR) from baseline to follow-up (figure 2).

Cardiac responses are depicted in figure 3. Both groups showed no change in left ventricular end-systolic volume index (LVESVI). Delta left ventricular end-diastolic volume index (LVEDVI) and delta left ventricular ejection fraction (LVEF) did not differ between the three groups. Delta RVEDVI, RVESVI and RVEF were similar between severely reduced DLCO group, the moderately reduced group and the group with a preserved DLCO.

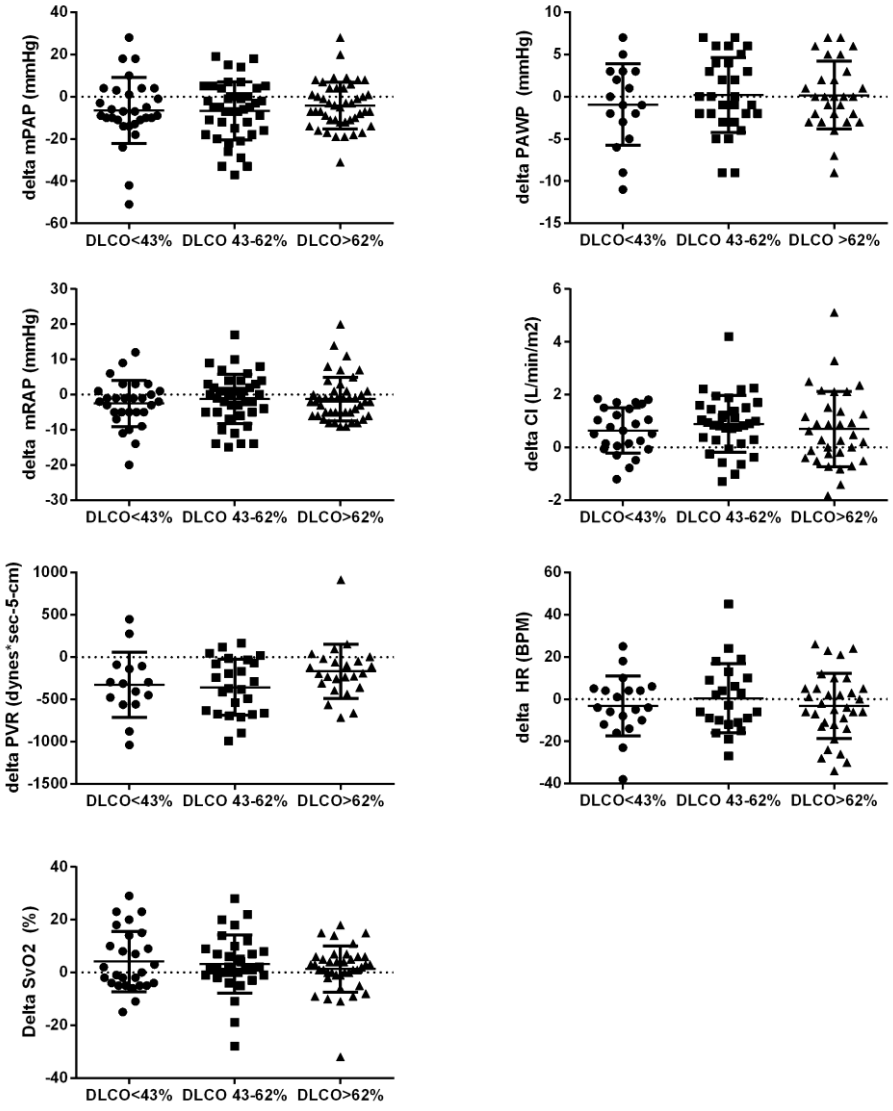

Figure 2: Hemodynamic treatment response. mPAP = mean pulmonary artery pressure; PAWP = pulmonary arterial wedge pressure; mRAP = mean right atrial pressure; PVR = pulmonary vascular resistance; CI = cardiac index; HR = heart rate. ns = non-significant. Data is presented as mean±SEM..

6MWD increased in all three groups after PH specific vasodilatory therapy. Arterial oxygen saturation did not change from baseline to follow-up, while the moderately reduced DLCO group had a lower arterial oxygen saturation after exercise compared to the severely reduced DLCO and preserved DLCO group (Figure 4).

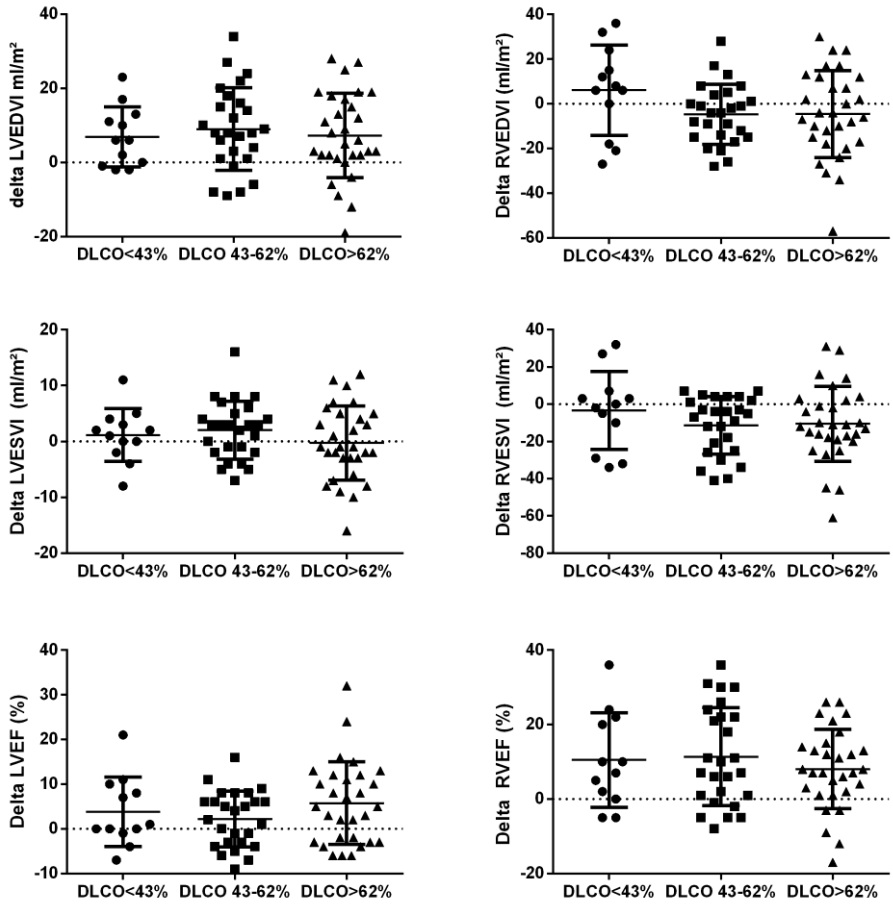

Figure 3: Cardiac response to treatment. LVEDV = left ventricular end-diastolic volume index; LVESVI = left ventricular end-systolic volume index; LVEF = left ventricular ejection fraction; RVEDVI = right ventricular end-diastolic volume index; RVESVI = right ventricular end-systolic volume index; RVEF = right ventricular ejection fraction. Data is presented as mean ± SEM.

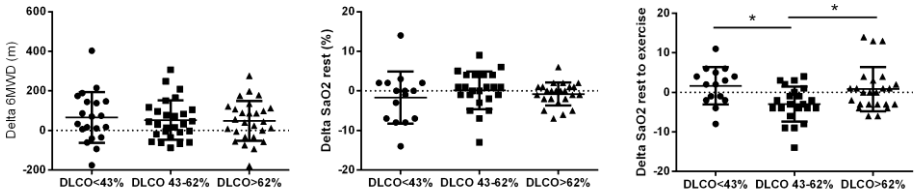

Figure 4: Treatment response in oxygenation and 6MWD. 6MWD = 6 minute walking distance; SaO2 rest = arterial oxygen saturation in rest; SaO2 rest-ex = change in arterial oxygen saturation during exercise. * = p<0.05. Data is presented as mean ± SEM.

Survival analyses

LVEDVI and LVESVI proved to be confounders to the survival analysis. LVEDVI and age-corrected survival was worse for patients with a DLCO<43% (figure 5A). These survival differences between DLCO<43% and DLCO 43-62% and DLCO>62% were also present in the selected cohort with a CMRI available at follow-up (figure 5B). No difference in survival was seen between patients with and without a CMRI at follow-up in the DLCO<43% group (figure 5C).

Discussion

In the present study we evaluated the effects of pulmonary hypertension specific vasodilatory therapy in IPAH patients with a severely reduced DLCO. It is known that IPAH patients with a low DLCO have a worse survival compared to IPAH patients with a preserved DLCO [6]. In addition, it has been shown that IPAH patients with a low DLCO have more coronary artery disease, a higher tobacco exposure, a higher body mass index, are older, have worse pulmonary function tests and show more mild abnormalities on HRCTs compared to IPAH patients with a preserved DLCO [5]. Although it seems that the IPAH patients with a low DLCO share some risk factors with group 2 and group 3 PH, normal PAWP pressures, spirometry and HRCT excluded left heart conditions and lung disease as a cause of PH. In addition, HRCTs of the IPAH patients with a low DLCO showed no signs of PVOD [14,15]. The question rises whether the low DLCO group has a different pulmonary vasculopathy compared to IPAH patients with a preserved DLCO [7,8]. The answer to this question remains elusive and requires further investigation. As a first step, we analyzed the treatment response in this patient cohort.

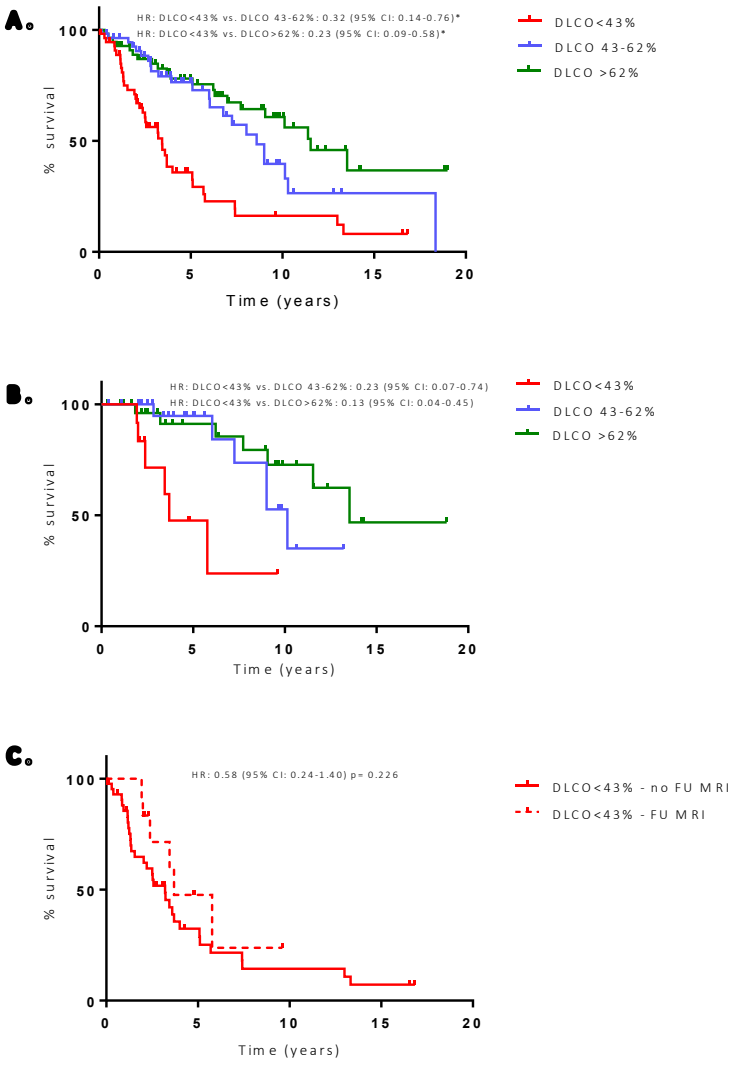

Figure 5: Survival analyses. A: Difference in survival between the DLCO<42%, DLCO 43-62% and DLCO≥63% groups in the total cohort (n=166). The DLCO<42% group showed a worse survival than the moderately reduced DLCO and preserved DLCO groups. B: Difference in survival between the severely reduced DLCO group, the moderately reduced DLCO and preserved DLCO group in the cohort in which a CMRI at follow-up was available (n=68). Also in this selected cohort the DLCO<42% group showed a worse survival compared to other two groups. C: Difference in survival between the group with and without a CMRI at follow up in the DLCO<42% group (n=42). No difference in survival was found between the group with and without a CMRI at follow-up in the DLCO<42% group. * adjusted for age and left ventricular end diastolic volume index.

Remarkably, we observed a significant improvement in hemodynamics, right ventricular function and exercise capacity upon pulmonary hypertension specific vasodilatory therapy without an impact on oxygen saturation in this cohort as in comparison to the IPAH patients with an moderately reduced or preserved DLCO.

Less follow-up data was available in the DLCO<43% group compared to the DLCO 43-62% and DLCO>62% group which could have led to a selection bias and subsequent overestimation of the treatment effect in the DLCO<43% group. However, no survival difference existed in the DLCO<43% group between the subjects with and without available follow-up data. This to some extent suggests that the subjects in the DLCO<43% group with follow-up data are representative for the total DLCO<43% group. Furthermore, survival differences between the DLCO<43% and the moderately reduced and preserved DLCO groups continued to exist when only the subjects with follow-up data were entered in the survival analysis further arguing against the presence of an important selection bias. At follow-up, the DLCO<43% group received more combination therapy compared to the DLCO≥43% groups. This may have confounded our results.

Based on the pulmonary vascular response on treatment there is no reason to withhold pulmonary arterial hypertension specific treatment from patients with IPAH and a severely reduced DLCO. The similarities in hemodynamic and cardiac treatment responses between IPAH patients with a severely reduced DLCO and IPAH patients with a preserved DLCO suggests that the poor survival in the low DLCO group is not explained by unresponsiveness of the pulmonary vasculature to current pulmonary arterial hypertension specific medications. Survival differences may be partially explained by the fact that the DLCO<42% group was older [16]. Cox proportional hazard analyses showed that age was a confounder for the differences in survival between groups, however, survival differences remained after adjusting for age. As such, the question remains why survival in this subgroup of patients with IPAH and a severely reduced DLCO is so poor [6].

Conclusions

Patients with IPAH and a severely reduced DLCO show a similar response to PH specific vasodilatory therapy as patients with IPAH and a moderately or preserved DLCO in terms of hemodynamics, right ventricular function, exercise capacity and oxygenation.

References

[1] Sun XG, Hansen JE, Oudiz RJ, Wasserman K. Pulmonary function in primary pulmonary hypertension. Journal of the American College of Cardiology. 2003; 41:1028-35
[2] Allanore Y, Borderie D, Avouac J, Zerkak D, Meune C, Hachulla E, et al. High N-terminal pro-brain natriuretic peptide levels and low diffusing capacity for carbon monoxide as independent predictors of the occurrence of precapillary pulmonary arterial hypertension in patients with systemic sclerosis. Arthritis and rheumatism. 2008; 58:284-91
[3] Montani D, Achouh L, Dorfmuller P, Le Pavec J, Sztrymf B, Tcherakian C, et al. Pulmonary veno-occlusive disease: clinical, functional, radiologic, and hemodynamic characteristics and outcome of 24 cases confirmed by histology. Medicine. 2008; 87:220-33
[4] Trip P, Girerd B, Bogaard HJ, de Man FS, Boonstra A, Garcia G, et al. Diffusion capacity and BMPR2 mutations in pulmonary arterial hypertension. The European respiratory journal. 2014; 43:1195-8
[5] Trip P, Nossent EJ, de Man FS, van den Berk IA, Boonstra A, Groepenhoff H, et al. Severely reduced diffusion capacity in idiopathic pulmonary arterial hypertension: patient characteristics and treatment responses. The European respiratory journal. 2013; 42:1575-85
[6] Chandra S, Shah SJ, Thenappan T, Archer SL, Rich S, Gomberg-Maitland M. Carbon monoxide diffusing capacity and mortality in pulmonary arterial hypertension. J Heart Lung Transplant. 2010; 29:181-7
[7] Hoeper MM, Simon RGJ. The changing landscape of pulmonary arterial hypertension and implications for patient care. Eur Respir Rev. 2014; 23:450-7
[8] Souza R, Fernandes CJ, Hoeper MM. Carbon monoxide diffusing capacity and the complexity of diagnosis in pulmonary arterial hypertension. The European respiratory journal. 2014; 43:963-5
[9] Galie N, Humbert M, Vachiery JL, Gibbs S, Lang I, Torbicki A, et al. 2015 ESC/ERS Guidelines for the diagnosis and treatment of pulmonary hypertension: The Joint Task Force for the Diagnosis and Treatment of Pulmonary Hypertension of the European Society of Cardiology (ESC) and the European Respiratory Society (ERS): Endorsed by: Association for European Paediatric and Congenital Cardiology (AEPC), International Society for Heart and Lung Transplantation (ISHLT). The European respiratory journal. 2015; 46:903-75
[10] Hoeper MM, Meyer K, Rademacher J, Fuge J, Welte T, Olsson KM. Diffusion Capacity and Mortality in Patients With Pulmonary Hypertension Due to Heart Failure With Preserved Ejection Fraction. Jacc. 2016; 4:441-9
[11] van de Veerdonk MC, Kind T, Marcus JT, Mauritz GJ, Heymans MW, Bogaard HJ, et al. Progressive right ventricular dysfunction in patients with pulmonary arterial hypertension responding to therapy. Journal of the American College of Cardiology. 2011; 58:2511-9
[12] ATS statement: guidelines for the six-minute walk test. American journal of respiratory and critical care medicine. 2002; 166:111-7
[13] Erratum: ATS Statement: Guidelines for the Six-Minute Walk Test. American journal of respiratory and critical care medicine. 2016; 193:1185
[14] Resten A, Maitre S, Capron F, Simonneau G, Musset D. [Pulmonary hypertension: CT findings in pulmonary veno-occlusive disease]. Journal de radiologie. 2003; 84:1739-45
[15] Resten A, Maitre S, Humbert M, Rabiller A, Sitbon O, Capron F, et al. Pulmonary hypertension: CT of the chest in pulmonary venoocclusive disease. Ajr. 2004; 183:65-70
[16] Hoeper MM, Huscher D, Ghofrani HA, Delcroix M, Distler O, Schweiger C, et al. Elderly patients diagnosed with idiopathic pulmonary arterial hypertension: results from the COMPERA registry. International journal of cardiology. 2013; 168:871-80

CHAPTER 7

Imaging: Emerging modalities (MR, PET and others)

Pulmonary Circulation: Diseases and Their Treatment, Fourth Edition, CRC Press 2016

A Vonk Noordegraaf[1], OA Spruijt[1]

[1]Department of Pulmonary Medicine, VU University Medical Center, Amsterdam

Introduction

Accurate assessment of right ventricular (RV) and arterial structure and function in pulmonary hypertension (PH) is essential for several reasons.

First, since direct visualization of the effects of the disease on the vessel wall is not possible, the assessment of disease severity and monitoring of therapeutic effects is only possible by studying the RV and pulmonary arterial function. Since the effects of treatment on RV and pulmonary arterial function are small, a prerequisite for such measurements is that they are accurate, reproducible, observer independent, and do not require geometric assumptions.

Second, the primary cause of death in most types of PH is RV failure. The diagnosis of early RV failure is thus of great clinical importance. In addition, the mechanisms of RV failure are currently poorly understood and can only be unraveled if the complex interaction between altered RV structure and function and the pivotal role of myocardial perfusion and metabolism on these parameters can be elucidated.

Thirdly, since it is known that most drugs used in the field of pulmonary arterial hypertension (PAH), not only act on the pulmonary vasculature, but also have an effect on the myocardium, discrimination of the effects of PH drugs on both the RV and the pulmonary vasculature are important.

Magnetic resonance imaging (MRI) and nuclear imaging techniques are both emerging techniques in the field of PH and offer novel possibilities to study the role of the RV in PH and the effects of treatment thereon. In addition, these techniques allow to determine the role of the different factors involved in RV failure, and subsequently to develop new therapeutic strategies. This chapter provides an overview of the application of MRI and nuclear imaging techniques in the field of PH and discusses future possibilities.

Magnetic Resonance Imaging

Quantification of Right Ventricular geometry and mass

In the early years of MRI, it was already recognized that this technique allows accurate measurement of the RV volumes [1-3]. Initially, the accuracy of global RV volume and function measurements was verified by using water-filled latex balloons and ventricular casts of excised bovine hearts [2].

In recent years, temporal and spatial resolution has been further improved, allowing more accurate quantification of global function of both the left and right ventricle and the complex interaction between both ventricles in PH [4, 5]. Short-axis images are used to reconstruct a 3D image of the right and left ventricle (LV), allowing the measurements of ventricular volumes and wall mass at all phases of the cardiac cycle.

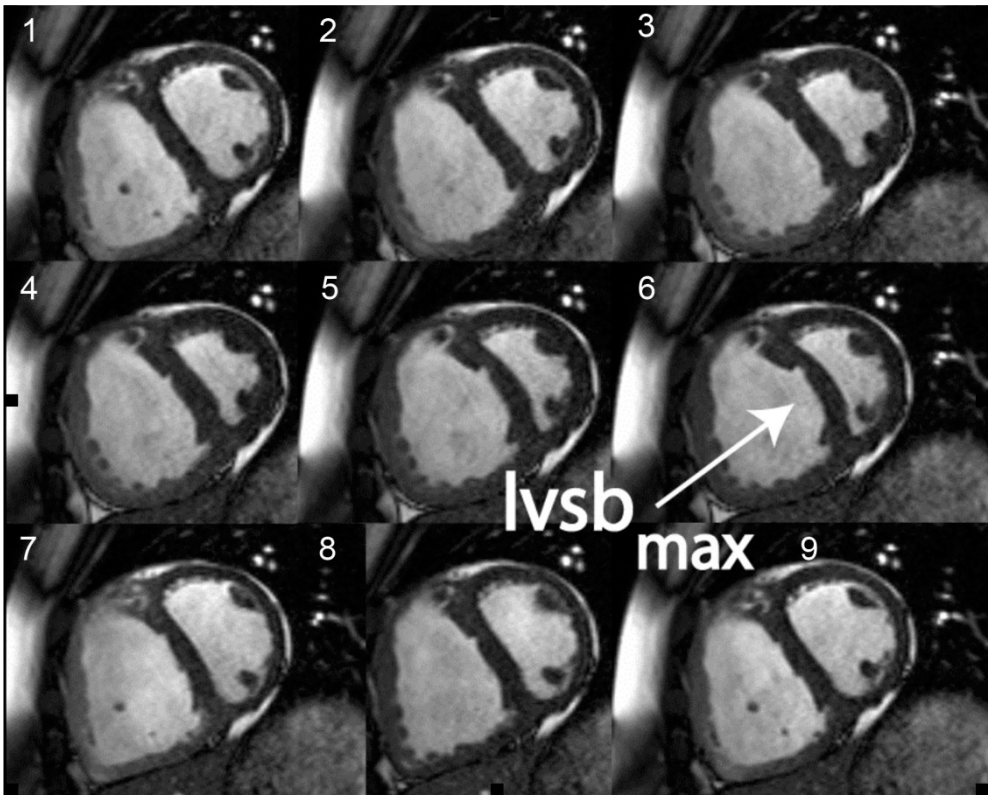

Figure 1: Short axis images covering the complete cardiac cycle made at the mid-ventricular level. The first image represents the end diastolic phase. Leftward ventricular septal bowing (LVSB) is observed in the early diastolic phase of the left ventricle, while the right ventricle is still contracting (left to right ventricular asynchrony).

Figure 1 shows short axis images covering the complete cardiac cycle made at the mid-ventricular level. Endocardial contours are drawn during post processing on end-diastolic and end-systolic frames, and total LV and RV volumes are calculated using the so called 'Simpson's rule', which takes into account the sum of individual slice volumes and the interslice gap. LV and RV end-systolic

volumes are subtracted from the end-diastolic volumes yielding stroke volumes. From the contours of epicardial and endocardial tracings, ventricular wall volume is derived and wall mass is the product of myocardial volume and muscle density (1.05 g/cm3). From the volume changes of the RV over time, parameters of systolic and diastolic function can be derived [4, 6, 7]. Previously, post processing was time consuming since all the contours were drawn manually, but new software solutions make a semiautomatic analysis possible.

The accuracy and inter-study reproducibility of volume measurements using semiautomatic analysis has been validated in several reports [5, 8-11] and appears to be superior to echocardiography [12]. Another advantage of MRI-based ventricular measurements is that this technique does not require geometric assumptions and can also be assessed in subset of patients difficult to study by means of echocardiography, such as is the case in COPD [13]. Bottini et al. showed that estimates of RV mass measured by MRI acquired pre-mortem in COPD patients corresponds closely with RV mass measured at autopsy [14].

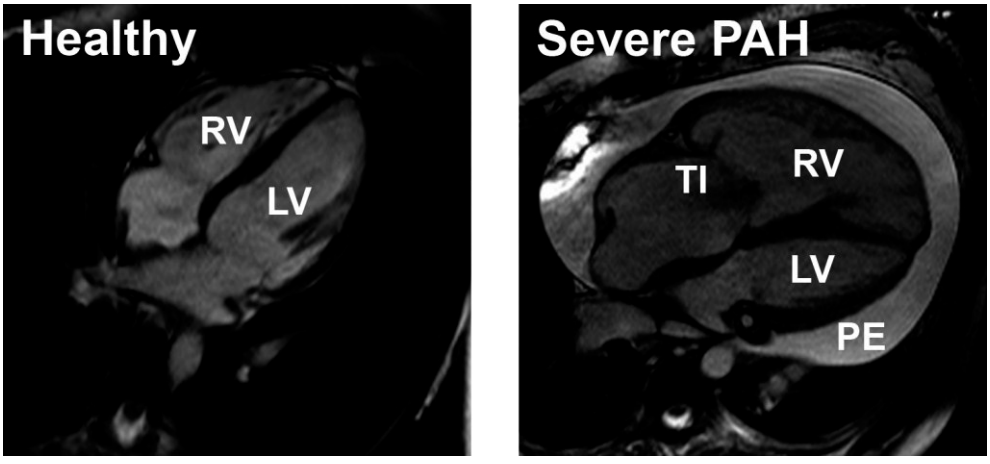

Figure 2: Long axis view of a healthy subject (A) and a patient with severe pulmonary arterial hypertension. RV = right ventricle, LV = left ventricle, PE= Pleural effusion, TI= tricuspid regurgitation.

The clinical value of the different MRI parameters in PH has been assessed in several studies. Earlier MRI studies revealed that in PH, RV volumes at end-diastole and end-systole are increased together with an increase in RV mass, whereas LV end-diastolic volume and stroke volume are decreased [2, 3, 15, 16]. As a consequence, RV ejection fraction is decreased, whereas LV ejection fraction is preserved or even increased [6, 7, 17]. Figure 2 shows a long axis image of a healthy control and a

patient with severe PH. Several studies showed that single MRI parameters of the RV are related to hemodynamic parameters and disease severity. For instance, two independent studies showed that MRI-measured RV ejection fraction is inversely related to NT-proBNP [6, 7] and that RV mass is related to pulmonary arterial pressure [18, 19]. In a group of 64 idiopathic PAH patients, van Wolferen et al. showed that RV end-diastolic volume, stroke volume and LV end-diastolic volume all measured at baseline conditions were strong predictors for first year mortality [20]. It has been shown that baseline RV ejection fraction and the change in RV ejection fraction after one year of PAH specific treatment are strong predictors of survival [21]. Furthermore, a recent study by Swift et al. found that, when corrected for age, sex and body surface area, RV end-systolic volume was an independent predictor of mortality [22].

Several studies have demonstrated the possibilities of MRI to monitor the effects of PAH therapy on the RV over time [16, 20, 23-25]. In these studies, an increased RV stroke volume and a decrease in RV wall mass was associated with improvement of symptoms and 6-minutes walking distance. In addition, it was shown that a progressive dilation of the RV during therapy accompanied with a decrease in stroke volume is associated with a poor outcome [20, 26].

The potential of MRI-derived parameters to be used as a primary end-point to compare different treatment strategies was demonstrated in the Seraph study; a randomized prospective study aimed to measure the different effects of bosentan and sildenafil on RV mass [27]. This study demonstrated that sildenafil, in contrast to bosentan, reduces RV mass. This finding is of interest; since it underlines that MRI provides additional insights in comparison to the functional parameters currently used to evaluate the efficacy of medication.

Finally, the volume of the RV might be considered as an additional treatment goal since a recent study showed that progressive dilatation of the RV in clinical stable PH patients predict worse outcome whereas a stable RV volume during the first year of treatment predicts a long term survival [28].

Advanced techniques to characterize the right ventricle

The MRI protocol can be extended with more advanced techniques that recently have been used in the study of the RV in PH. These techniques include delayed contrast enhancement to measure the presence of scar tissue in the RV wall, myocardial tagging to analyze regional myocardial shortening and measurement of coronary artery flow to the RV.

• Delayed Contrast Enhancement (DCE) can be used to visualize and quantify the deposition of collagen in the RV myocardium. DCE imaging is performed about ten minutes after injection of a MRI contrast agent. In healthy myocardium, the contrast agent then has been washed out, but in non-viable, damaged and fibrotic myocardium the contrast agent is still present. Thus, ''bright is dead'' with this technique. In two studies it was shown that abnormal DCE is present in the RV and confined to the insertion points of the RV and interventricular septum [29-31]. Interestingly, these findings may suggest that mechanical factors contribute to the occurrence of fibrosis. In both studies, the extent of contrast enhancement correlated positively with mean PAP, and pulmonary vascular resistance and was inversely related to RV ejection fraction. Figure 3 shows a typical example of DCE in PAH. T1 mapping might serve as a good alternative for DCE imaging [32].

Figure 3: Delayed contrast enhancement in a scleroderma patient with pulmonary hypertension. This figure shows extensive delayed contrast enhancement at the insertion points.

• A method to study regional myocardial contraction patterns is myocardial tagging, allowing for the measurement of segmental myocardial strain. This method labels the myocardial tissue with parallel lines or a grid (typical distance 7 mm) of magnetic pre-saturation at the beginning of the cardiac cycle (R-wave of ECG). These lines remain visible as 'dark' lines in MRI cine images, and thereby display the regional myocardial strains over the cardiac cycle by changes in the line- or grid-pattern. In PH, the RV myocardial wall is thick enough to explore RV contraction patterns by this technique, but in the non-hypertrophied RV wall spatial resolution of the technique

is insufficient. This technique has been successfully used in the study of the mechanisms of ventricular interdependency [33, 34]. These studies show that there is a left to right asynchrony in the peak of circumferential shortening, which is caused by RV overload and plays a role in the leftward septal bowing and thereby impairing LV filling (Figure 4). A relatively new technique to assess strain is feature tracking. The advantage of this technique is that there is no need to obtain additional sequences and strain analyses can be applied on standard short-axis images. Feature tracking has been validated for circumferential strain analyses [35].

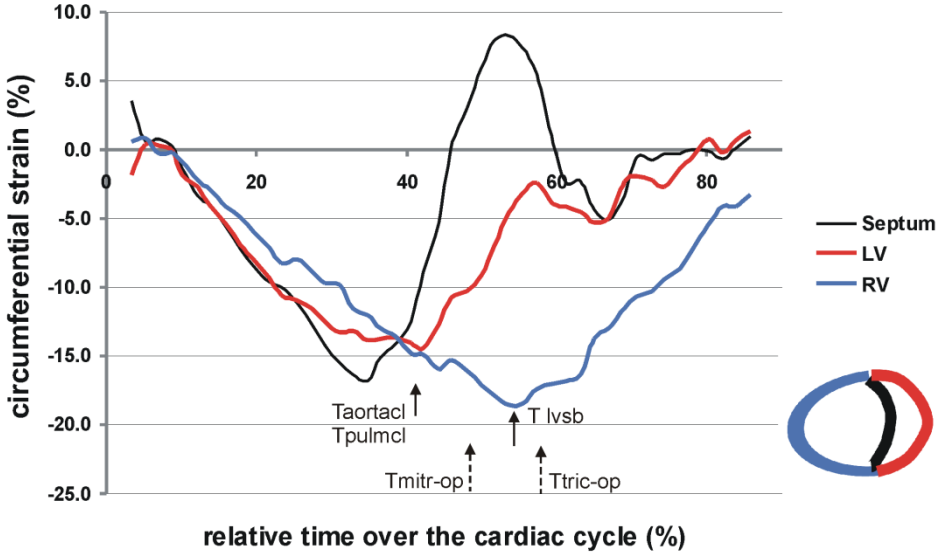

Figure 4: Circumferential strain curves after the electrocardiographic R-wave for the septum, right and left ventricle in a patient with severe pulmonary hypertension. MRI myocardial tagging is used to calculate the circumferential strain. From this image it is clear that time to right ventricular peak shortening is delayed in comparison to the left ventricle. As a consequense leftward septal bowing occurs. Note that right ventricular contraction continues after pulmonary valve closure leading to the so called end-systolic right ventricular isovolumetric shortening (adapted from: [33])

- Finally, advances in MRI make it possible to visualize and measure coronary artery flow and perfusion. From animal studies it is known that RV coronary perfusion is not or little impeded in systole. By using MR-based coronary flow assessment it was shown that in patients with RV hypertrophy coronary arterial flow in systole is impeded, and in severe RV hypertrophy even total mean flow to the RV is reduced [36]. Whether this reduction of coronary blood flow per gram RV

tissue might contribute to RV failure is unknown. In addition, using MRI perfusion techniques it was shown that pulmonary perfusion reserve is decreased in PAH [37].

Although the direct clinical value of these techniques is presently still uncertain, application of these techniques have advanced our understanding of RV function and failure and offers tools to increase our understanding in the near future.

Assessment of Pulmonary artery Flow and distensibility

Velocity encoded cine MRI provides an accurate and reproducible tool for quantification of pulmonary artery flow [38-40]. Kondo et al. described in 1992 for the first time the application of this technique in PAH patients [41]. It was found that in comparison to controls, flow acceleration time and distensibility of the pulmonary artery were decreased in patients with primary PAH; a finding similar to that observed in studies using Doppler echocardiography for measuring flow velocity. Several attempts have been made to estimate pulmonary artery pressure from the flow signal [42-44]. However, a validation study performed by Roeleveld et al. showed that all these approaches fail to estimate pulmonary arterial pressure accurately [18]. This can be explained by the fact that acceleration time is not only a parameter of the pulmonary vascular bed but is also influenced by the pump function characteristics of the RV.

The major advantage of flow measurements, however, is not the estimation of pulmonary artery pressure but the accurate assessment of effective stroke volume of the RV from MRI flow measurement in the pulmonary artery [38-41]. Stroke volume can be considered as one of the most important hemodynamic parameters in PAH, since it is a direct reflection of RV function in relation to its increased afterload. Earlier studies showed that stroke volume is decreased in PH and that exercise does not lead to an increase in stroke volume [45]. In addition, it was shown that baseline stroke volume accurately predicts 6-minutes walking distance in PAH and that improvements in stroke volume in patients under treatment are directly related to an improvement in the six minute walking distance [24, 46]. Furthermore, it was shown that stroke volume derived from the pulmonary artery flow measured by MRI is a strong predictor of mortality in PAH [18].

An additional feature of the abnormal flow in PH is the so called vortical flow which is flow rotating around an ax. It was found that vertical flow in the main pulmonary artery is a typical characteristic of the presence of PH [47] and that the duration of the vortex is related to the main pulmonary artery pressure [48].

Since the aorta flow can be measured in the same plane as the pulmonary artery flow, the ratio of right to left flow and vice versa can be used in the assessment of intra-cardiac shunts. Beerbaum et al. validated this MRI based shunt measurement approach, showing that right to left and left to right intra-cardiac shunts in children with congenital heart disease can be measured accurately in less than 60 seconds [38, 49]. A limitation of this technique is that in dilated pulmonary arteries turbulent flow can occur, causing an inaccuracy of the pulmonary blood flow estimates by MRI [49].

Another parameter that can be assessed from the flow measurements is the diameter and distensibility of the pulmonary artery. It is known that a progressive dilatation of the pulmonary artery harbours a poor prognosis [50]. In addition, from invasive studies it is known that compliance of the pulmonary vascular bed is decreased in advanced disease, and that this decrease is related to a poor outcome [51, 52]. Since compliance is quantitative measure of the elasticity of the large pulmonary vessels, this gives an important functional characterization of the vascular tree. Indeed, it was shown that loss of compliance of the large pulmonary vessels measured by MRI is related to a poor outcome [53].

Combining MRI flow measurements with invasive measurements

Measurement of the pulmonary vascular resistance requires an accurate assessment of pulmonary blood flow and pressure. Certain conditions, such as congenital heart disease might preclude a reliable invasive estimation of pulmonary blood flow. In these cases, combined MR measured flow with invasive measured pulmonary artery pressure, provides accurate estimations of pulmonary vascular resistance. In a group of 24 children with either suspected PAH or congenital heart disease it was shown that this approach provides more reliable data than invasive measurements [54].

Another application of the combined measurements of pressure and flow is the assessment of arterial input impedance [55, 56], as a comprehensive representation of RV load. Input impedance takes into account the pulsatile nature of blood flow and pressure and not only consists of pulmonary vascular resistance but also of compliance and characteristic impedance. The assessment of input impedance can only be obtained from spectral analysis of pressure and flow curves. Although the relevance of such measurements has been acknowledged for a long period of time, clinical application has been hampered by the requirement of simultaneous and instantaneous pulmonary pressure and flow, and sophisticated analysis techniques. With the advent of MRI scanners in the catheterization laboratory [57-60], pressure and flow can be measured

simultaneously; enabling advanced hemodynamic characterization of individual patients in clinical practice [61].

A limitation of the combined measurement of pressure and MRI derived flow is that a right sided heart catheterization is still required and that for simultaneous measurements an interventional (X-)MRI suite together with a special catheterization set must be used. Thus, although this approach can be of use in conditions that an accurate invasive stroke volume measurement is not possible, or in experimental settings, it is unlikely that this type of measurement will be performed routinely in the near future.

MRI pulmonary angiography and perfusion measurements

Although digital subtraction angiography of the pulmonary artery is still regarded as the reference technique for the diagnosis of chronic thromboembolic pulmonary hypertension, recent studies showed that MR angiography is a sensitive non-invasive alternative for the depiction of central thromboembolic material [62]. Typically, one static 3D image acquisition is performed, tailored for spatial resolution and signal to noise ratio during a breath-hold period of about 15 s. The advantage of MRI is not only that it provides high quality 3D images of the pulmonary vasculature, but also that these measurements can be combined with the assessment of RV function and perfusion measurements [63] (figure 5).

Figure 5: MR perfusion image of a patient with chronic thromboembolic pulmonary hypertension

MRI based dynamic pulmonary perfusion imaging is a technique visualizing the passage of an contrast bolus of an MRI-contrast agent through the lungs in a 3-dimensional way, enabling the visualization of sub-segmental perfusion defects in chronic thromboembolic PAH [63, 64]. In addition, post-processing of the perfusion images makes it possible to derive quantitative data from the dynamic perfusion scan such as pulmonary blood volume, flow and transit time defined as the time required for the contrast to transit through the lungs [65]. Although it has been shown that all of these MRI derived parameters are directly related to hemodynamic parameters such as pulmonary artery pressure and cardiac output, accurate calculation of the main determinant of the pulmonary vascular bed, the pulmonary vascular resistance, is not yet possible [66, 67].

Nuclear imaging techniques

Nuclear techniques can be used for imaging the lung and the heart. The application of lung perfusion scintigraphy in the diagnosis of chronic thromboembolic pulmonary hypertension is well established and its role is further discussed in chapter 13. A refinement of perfusion scintigraphy is single photon emission computed tomography (SPECT). This technique enables the reconstruction of perfusion images in a way similar to the reconstruction of CT images, further improving the diagnostic accuracy of perfusion scintigraphy [68].

The role of nuclear techniques in the diagnosis of RV failure is less well established despite the fact that these techniques play a pivotal role in the diagnosis of left heart disease. In the past, ventricular angiography was frequently used to assess RV volumes and function. Several approaches have been described to measure RV volumes, including SPECT equilibrium radionuclide angiography [69, 70]. Despite the fact that these approaches provide reliable data on RV volumes, its role is limited and has been replaced by echocardiography, magnetic resonance imaging and computed tomography. Recent insights obtained by nuclear imaging techniques are that the metabolic function of the RV is altered in PAH. Several studies showed that in PH the uptake of free fatty acids is decreased whereas the uptake of glucose is increased [71, 72]. In healthy subjects glucose uptake in the RV can barely be seen using fluoro-18-deoxyglucose ([18F]-FDG) positron emission tomography (PET). Figure 6 shows an example of glucose consumption measured by [18F]-FDG PET in the RV in a patient with severe PAH. This image shows that glucose uptake of the RV exceeds glucose uptake of the LV. Kluge et al. found that glucose uptake in the RV is closely related to RV function as measured by echocardiography indicating that a failing RV switches from free fatty acids metabolism to glucose metabolism [73]. In a study by Oikawa et al. it was shown that glucose uptake in the RV can

be reversed by epoprostenol therapy [74]. Although the mechanisms responsible for this metabolic switch remain to be elucidated, one possibility is that RV ischemia might induce such changes. Gomez et al. showed by using stress myocardial scintigraphy that nine of the 23 PAH patients examined had images consistent with RV ischemia [75]. In addition, they found a significant correlation between RV ischemia obtained through myocardial perfusion scintigraphy and hemodynamic measures of RV failure, underpinning the possible contribution of ischaemia to RV failure.

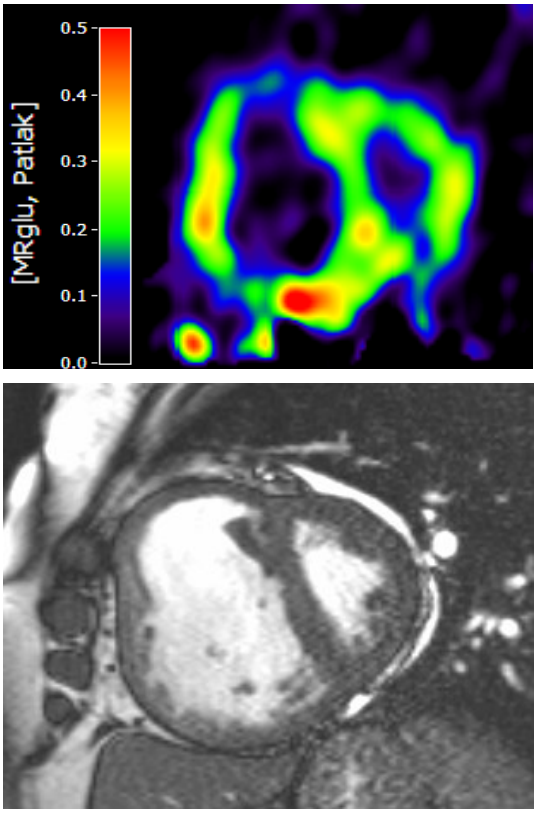

Figure 6: upper image: glucose consumption in the right and left ventricle as indicated as MRglu (metabolic rate of glucose (µmol/ml/min) measured by ^{18}FDG-PET. Lower image: corresponding short axis view measured by MRI

[11C]-Acetate and [15O]-oxygen tracers allow to study the oxidative metabolism of the pressure overloaded RV. In a study by Wong et al. it was shown by means of [11C]-acetate PET that heart rate and systolic pulmonary artery pressure are the main determinants of oxygen consumption in PAH patients [76]. In addition these tracers allow to obtain more insight in the pathophysiology of the

failing RV in relation to perfusion, metabolism and power output. For instance, in another study by Wong et al. it was shown that oxygen efficiency was reduced in more advanced right heart failure [77], indicating that mitochondrial dysfunction might play a role. Potential tracers of interest are [18F]-RGD to assess changes in angiogenesis [78] and [11C]-hydroxyephedrine [11C]-HED) and [11C]-CGP-12177 to assess changes in beta-adrenergic receptor density [79, 80] due to sympathetic nerve overactivity in PH.

A future application of nuclear imaging techniques in the field of PH is the use of tracers and radioligands to image the abnormal pulmonary vascular bed. Due to the large space of air and the double circulation of the lung (pulmonary and bronchial) methodological problems need to be solved before reliable answers can be provided and understand the current controversies in literature. For instance, Marsboom et al. found an increased [18F]-FDG uptake in the lungs of patients with PH, giving evidence for the so called glycolytic shift in the pulmonary vasculature [81]. However, Ruiter et al. corrected [18F]-FDG uptake for the decreased perfusion and could not observe this phenomenon [82]. The most interesting development is to image the pathobiology and site of action of drugs and by that guide treatment decisions and monitoring. An example of such a ligand is [11C]RAL-01PDE, a potential phosphodieseterase 5 (PDE5) ligand [83]. In a study by Jacobsen et al. it was shown that this ligand binds to the binding site of PDE5 on the myocardium and lung [83]. The results of this study showed that this ligand has the potential to quantify PDE5 expression in the lung of PAH patients and by that guide therapeutic decisions. A potential tracer to image the increased proliferation of endothelial cells and smooth muscle cells in the small pulmonary arteries is [18F]-fluorothymidine ([18F-FLT) [84], which has yet to be tested in PH.

Conclusions

Both MRI and nuclear imaging techniques are promising emerging techniques in the field of PH. MRI offers not only the possibility to measure accurately RV structure and function and its relation with changes in the pulmonary vasculature, but also provides information on morphological changes of the RV wall and coronary flow. In addition, although the role of MRI is not yet defined, the advantage of MRI to monitor PAH patients is presently well recognized by many clinicians [85]. Although nuclear imaging techniques have not been frequently applied to study RV failure, lessons learned from the LV, especially with respect to perfusion and metabolism, show that this modality can play an important role in the near future.

References

[1] Bouchard A, Higgins CB, Byrd BF, 3rd, Amparo EG, Osaki L, Axelrod R. Magnetic resonance imaging in pulmonary arterial hypertension. The American journal of cardiology. 1985; 56:938-42
[2] Boxt LM, Katz J, Kolb T, Czegledy FP, Barst RJ. Direct quantitation of right and left ventricular volumes with nuclear magnetic resonance imaging in patients with primary pulmonary hypertension. Journal of the American College of Cardiology. 1992; 19:1508-15
[3] Katz J, Whang J, Boxt LM, Barst RJ. Estimation of right ventricular mass in normal subjects and in patients with primary pulmonary hypertension by nuclear magnetic resonance imaging. Journal of the American College of Cardiology. 1993; 21:1475-81
[4] Gan C, Lankhaar JW, Marcus JT, Westerhof N, Marques KM, Bronzwaer JG, et al. Impaired left ventricular filling due to right-to-left ventricular interaction in patients with pulmonary arterial hypertension. American journal of physiology. 2006; 290:H1528-33
[5] Roeleveld RJ, Marcus JT, Faes TJ, Gan TJ, Boonstra A, Postmus PE, et al. Interventricular septal configuration at mr imaging and pulmonary arterial pressure in pulmonary hypertension. Radiology. 2005; 234:710-7
[6] Blyth KG, Groenning BA, Mark PB, Martin TN, Foster JE, Steedman T, et al. NT-proBNP can be used to detect right ventricular systolic dysfunction in pulmonary hypertension. The European respiratory journal. 2007; 29:737-44
[7] Gan CT, McCann GP, Marcus JT, van Wolferen SA, Twisk JW, Boonstra A, et al. NT-proBNP reflects right ventricular structure and function in pulmonary hypertension. The European respiratory journal. 2006; 28:1190-4
[8] Doherty NE, 3rd, Fujita N, Caputo GR, Higgins CB. Measurement of right ventricular mass in normal and dilated cardiomyopathic ventricles using cine magnetic resonance imaging. The American journal of cardiology. 1992; 69:1223-8
[9] Grothues F, Moon JC, Bellenger NG, Smith GS, Klein HU, Pennell DJ. Interstudy reproducibility of right ventricular volumes, function, and mass with cardiovascular magnetic resonance. American heart journal. 2004; 147:218-23
[10] Semelka RC, Tomei E, Wagner S, Mayo J, Kondo C, Suzuki J, et al. Normal left ventricular dimensions and function: interstudy reproducibility of measurements with cine MR imaging. Radiology. 1990; 174:763-8
[11] Suzuki J, Caputo GR, Masui T, Chang JM, O'Sullivan M, Higgins CB. Assessment of right ventricular diastolic and systolic function in patients with dilated cardiomyopathy using cine magnetic resonance imaging. American heart journal. 1991; 122:1035-40
[12] Grothues F, Smith GC, Moon JC, Bellenger NG, Collins P, Klein HU, et al. Comparison of interstudy reproducibility of cardiovascular magnetic resonance with two-dimensional echocardiography in normal subjects and in patients with heart failure or left ventricular hypertrophy. The American journal of cardiology. 2002; 90:29-34
[13] Vonk-Noordegraaf A, Marcus JT, Holverda S, Roseboom B, Postmus PE. Early changes of cardiac structure and function in COPD patients with mild hypoxemia. Chest. 2005; 127:1898-903
[14] Bottini PB, Car AA, Prisant, Calverley PM, Howatson R, Flenley DC, et al. Clinicopathological correlations in cor pulmonale. Thorax. 1992; 47:494-8
[15] Pattynama PM, Willems LN, Smit AH, van der Wall EE, de Roos A. Early diagnosis of cor pulmonale with MR imaging of the right ventricle. Radiology. 1992; 182:375-9
[16] Peacock AJ, Crawley S, McLure L, Blyth K, Vizza CD, Poscia R, et al. Changes in right ventricular function measured by cardiac magnetic resonance imaging in patients receiving pulmonary arterial hypertension-targeted therapy: the EURO-MR study. Circ Cardiovasc Imaging. 2014; 7:107-14
[17] Marcus JT, Vonk Noordegraaf A, Roeleveld RJ, Postmus PE, Heethaar RM, Van Rossum AC, et al. Impaired left ventricular filling due to right ventricular pressure overload in primary pulmonary hypertension: noninvasive monitoring using MRI. Chest. 2001; 119:1761-5
[18] Roeleveld RJ, Marcus JT, Boonstra A, Postmus PE, Marques KM, Bronzwaer JG, et al. A comparison of noninvasive MRI-based methods of estimating pulmonary artery pressure in pulmonary hypertension. J Magn Reson Imaging. 2005; 22:67-72
[19] Saba TS, Foster J, Cockburn M, Cowan M, Peacock AJ. Ventricular mass index using magnetic resonance imaging accurately estimates pulmonary artery pressure. The European respiratory journal. 2002; 20:1519-24
[20] van Wolferen SA, Marcus JT, Boonstra A, Marques KM, Bronzwaer JG, Spreeuwenberg MD, et al. Prognostic value of right ventricular mass, volume, and function in idiopathic pulmonary arterial hypertension. European heart journal. 2007; 28:1250-7
[21] van de Veerdonk MC, Kind T, Marcus JT, Mauritz GJ, Heymans MW, Bogaard HJ, et al. Progressive right ventricular dysfunction in patients with pulmonary arterial hypertension responding to therapy. Journal of the American College of Cardiology. 2011; 58:2511-9
[22] Swift AJ, Rajaram S, Campbell MJ, Hurdman J, Thomas S, Capener D, et al. Prognostic value of cardiovascular magnetic resonance imaging measurements corrected for age and sex in idiopathic pulmonary arterial hypertension. Circ Cardiovasc Imaging. 2014; 7:100-6
[23] Michelakis ED, Tymchak W, Noga M, Webster L, Wu XC, Lien D, et al. Long-term treatment with oral sildenafil is safe and improves functional capacity and hemodynamics in patients with pulmonary arterial hypertension. Circulation. 2003; 108:2066-9
[24] Roeleveld RJ, Vonk-Noordegraaf A, Marcus JT, Bronzwaer JG, Marques KM, Postmus PE, et al. Effects of epoprostenol on right ventricular hypertrophy and dilatation in pulmonary hypertension. Chest. 2004; 125:572-9

[25] van Wolferen SA, Boonstra A, Marcus JT, Marques KM, Bronzwaer JG, Postmus PE, et al. Right ventricular reverse remodelling after sildenafil in pulmonary arterial hypertension. Heart (British Cardiac Society). 2006; 92:1860-1
[26] Mauritz GJ, Kind T, Marcus JT, Bogaard HJ, van de Veerdonk M, Postmus PE, et al. Progressive changes in right ventricular geometric shortening and long-term survival in pulmonary arterial hypertension. Chest. 2012; 141:935-43
[27] Wilkins MR, Paul GA, Strange JW, Tunariu N, Gin-Sing W, Banya WA, et al. Sildenafil versus Endothelin Receptor Antagonist for Pulmonary Hypertension (SERAPH) study. American journal of respiratory and critical care medicine. 2005; 171:1292-7
[28] van de Veerdonk MC, Marcus JT, Westerhof N, de Man FS, Boonstra A, Heymans MW, et al. Signs of right ventricular deterioration in clinically stable patients with pulmonary arterial hypertension. Chest. 2014;
[29] Blyth KG, Groenning BA, Martin TN, Foster JE, Mark PB, Dargie HJ, et al. Contrast enhanced-cardiovascular magnetic resonance imaging in patients with pulmonary hypertension. European heart journal. 2005; 26:1993-9
[30] McCann GP, Beek AM, Vonk-Noordegraaf A, van Rossum AC. Delayed contrast-enhanced magnetic resonance imaging in pulmonary arterial hypertension. Circulation. 2005; 112:e268
[31] McCann GP, Gan CT, Beek AM, Niessen HW, Vonk Noordegraaf A, van Rossum AC. Extent of MRI delayed enhancement of myocardial mass is related to right ventricular dysfunction in pulmonary artery hypertension. Ajr. 2007; 188:349-55
[32] Bull S, White SK, Piechnik SK, Flett AS, Ferreira VM, Loudon M, et al. Human non-contrast T1 values and correlation with histology in diffuse fibrosis. Heart (British Cardiac Society). 2013; 99:932-7
[33] Marcus JT, Gan CT, Zwanenburg JJ, Boonstra A, Allaart CP, Gotte MJ, et al. Interventricular mechanical asynchrony in pulmonary arterial hypertension: left-to-right delay in peak shortening is related to right ventricular overload and left ventricular underfilling. Journal of the American College of Cardiology. 2008; 51:750-7
[34] Vonk-Noordegraaf A, Marcus JT, Gan CT, Boonstra A, Postmus PE. Interventricular mechanical asynchrony due to right ventricular pressure overload in pulmonary hypertension plays an important role in impaired left ventricular filling. Chest. 2005; 128:628S-30S
[35] Hor KN, Gottliebson WM, Carson C, Wash E, Cnota J, Fleck R, et al. Comparison of magnetic resonance feature tracking for strain calculation with harmonic phase imaging analysis. Jacc. 2010; 3:144-51
[36] van Wolferen SA, Marcus JT, Westerhof N, Spreeuwenberg MD, Marques KM, Bronzwaer JG, et al. Right coronary artery flow impairment in patients with pulmonary hypertension. European heart journal. 2008; 29:120-7
[37] Vogel-Claussen J, Skrok J, Shehata ML, Singh S, Sibley CT, Boyce DM, et al. Right and left ventricular myocardial perfusion reserves correlate with right ventricular function and pulmonary hemodynamics in patients with pulmonary arterial hypertension. Radiology. 2011; 258:119-27
[38] Beerbaum P, Korperich H, Barth P, Esdorn H, Gieseke J, Meyer H. Noninvasive quantification of left-to-right shunt in pediatric patients: phase-contrast cine magnetic resonance imaging compared with invasive oximetry. Circulation. 2001; 103:2476-82
[39] Fratz S, Hess J, Schwaiger M, Martinoff S, Stern HC. More accurate quantification of pulmonary blood flow by magnetic resonance imaging than by lung perfusion scintigraphy in patients with fontan circulation. Circulation. 2002; 106:1510-3
[40] Rebergen SA, van der Wall EE, Doornbos J, de Roos A. Magnetic resonance measurement of velocity and flow: technique, validation, and cardiovascular applications. American heart journal. 1993; 126:1439-56
[41] Kondo C, Caputo GR, Masui T, Foster E, O'Sullivan M, Stulbarg MS, et al. Pulmonary hypertension: pulmonary flow quantification and flow profile analysis with velocity-encoded cine MR imaging. Radiology. 1992; 183:751-8
[42] Bogren HG, Klipstein RH, Mohiaddin RH, Firmin DN, Underwood SR, Rees RS, et al. Pulmonary artery distensibility and blood flow patterns: a magnetic resonance study of normal subjects and of patients with pulmonary arterial hypertension. American heart journal. 1989; 118:990-9
[43] Laffon E, Vallet C, Bernard V, Montaudon M, Ducassou D, Laurent F, et al. A computed method for noninvasive MRI assessment of pulmonary arterial hypertension. J Appl Physiol (1985). 2004; 96:463-8
[44] Muthurangu V, Taylor A, Andriantsimiavona R, Hegde S, Miquel ME, Tulloh R, et al. Novel method of quantifying pulmonary vascular resistance by use of simultaneous invasive pressure monitoring and phase-contrast magnetic resonance flow. Circulation. 2004; 110:826-34
[45] Holverda S, Gan CT, Marcus JT, Postmus PE, Boonstra A, Vonk-Noordegraaf A. Impaired stroke volume response to exercise in pulmonary arterial hypertension. Journal of the American College of Cardiology. 2006; 47:1732-3
[46] Provencher S, Chemla D, Herve P, Sitbon O, Humbert M, Simonneau G. Heart rate responses during the 6-minute walk test in pulmonary arterial hypertension. The European respiratory journal. 2006; 27:114-20
[47] Reiter G, Reiter U, Kovacs G, Kainz B, Schmidt K, Maier R, et al. Magnetic resonance-derived 3-dimensional blood flow patterns in the main pulmonary artery as a marker of pulmonary hypertension and a measure of elevated mean pulmonary arterial pressure. Circ Cardiovasc Imaging. 2008; 1:23-30
[48] Reiter G, Reiter U, Kovacs G, Olschewski H, Fuchsjager M. Blood Flow Vortices along the Main Pulmonary Artery Measured with MR Imaging for Diagnosis of Pulmonary Hypertension. Radiology. 2014:140849
[49] Beerbaum P, Korperich H, Gieseke J, Barth P, Peuster M, Meyer H. Rapid left-to-right shunt quantification in children by phase-contrast magnetic resonance imaging combined with sensitivity encoding (SENSE). Circulation. 2003; 108:1355-61

[50] Boerrigter B, Mauritz GJ, Marcus JT, Helderman F, Postmus PE, Westerhof N, et al. Progressive dilatation of the main pulmonary artery is a characteristic of pulmonary arterial hypertension and is not related to changes in pressure. Chest. 2010; 138:1395-401
[51] Mahapatra S, Nishimura RA, Sorajja P, Cha S, McGoon MD. Relationship of pulmonary arterial capacitance and mortality in idiopathic pulmonary arterial hypertension. Journal of the American College of Cardiology. 2006; 47:799-803
[52] Mauritz GJ, Marcus JT, Boonstra A, Postmus PE, Westerhof N, Vonk-Noordegraaf A. Non-invasive stroke volume assessment in patients with pulmonary arterial hypertension: left-sided data mandatory. J Cardiovasc Magn Reson. 2008; 10:51
[53] Lankhaar JW, Westerhof N, Faes TJ, Gan CT, Marques KM, Boonstra A, et al. Pulmonary vascular resistance and compliance stay inversely related during treatment of pulmonary hypertension. European heart journal. 2008; 29:1688-95
[54] Razavi R, Hill DL, Keevil SF, Miquel ME, Muthurangu V, Hegde S, et al. Cardiac catheterisation guided by MRI in children and adults with congenital heart disease. Lancet. 2003; 362:1877-82
[55] Grant BJ, Paradowski LJ. Characterization of pulmonary arterial input impedance with lumped parameter models. The American journal of physiology. 1987; 252:H585-93
[56] Murgo JP, Westerhof N. Input impedance of the pulmonary arterial system in normal man. Effects of respiration and comparison to systemic impedance. Circulation research. 1984; 54:666-73
[57] Bock M, Muller S, Zuehlsdorff S, Speier P, Fink C, Hallscheidt P, et al. Active catheter tracking using parallel MRI and real-time image reconstruction. Magn Reson Med. 2006; 55:1454-9
[58] Gaynor SL, Maniar HS, Bloch JB, Steendijk P, Moon MR. Right atrial and ventricular adaptation to chronic right ventricular pressure overload. Circulation. 2005; 112:I212-8
[59] Kuehne T, Yilmaz S, Schulze-Neick I, Wellnhofer E, Ewert P, Nagel E, et al. Magnetic resonance imaging guided catheterisation for assessment of pulmonary vascular resistance: in vivo validation and clinical application in patients with pulmonary hypertension. Heart (British Cardiac Society). 2005; 91:1064-9
[60] Muthurangu V, Atkinson D, Sermesant M, Miquel ME, Hegde S, Johnson R, et al. Measurement of total pulmonary arterial compliance using invasive pressure monitoring and MR flow quantification during MR-guided cardiac catheterization. American journal of physiology. 2005; 289:H1301-6
[61] Lankhaar JW, Westerhof N, Faes TJ, Marques KM, Marcus JT, Postmus PE, et al. Quantification of right ventricular afterload in patients with and without pulmonary hypertension. American journal of physiology. 2006; 291:H1731-7
[62] Kreitner KF, Ley S, Kauczor HU, Mayer E, Kramm T, Pitton MB, et al. Chronic thromboembolic pulmonary hypertension: pre- and postoperative assessment with breath-hold MR imaging techniques. Radiology. 2004; 232:535-43
[63] Nikolaou K, Schoenberg SO, Attenberger U, Scheidler J, Dietrich O, Kuehn B, et al. Pulmonary arterial hypertension: diagnosis with fast perfusion MR imaging and high-spatial-resolution MR angiography--preliminary experience. Radiology. 2005; 236:694-703
[64] Ley S, Fink C, Zaporozhan J, Borst MM, Meyer FJ, Puderbach M, et al. Value of high spatial and high temporal resolution magnetic resonance angiography for differentiation between idiopathic and thromboembolic pulmonary hypertension: initial results. European radiology. 2005; 15:2256-63
[65] Ohno Y, Hatabu H, Murase K, Higashino T, Kawamitsu H, Watanabe H, et al. Quantitative assessment of regional pulmonary perfusion in the entire lung using three-dimensional ultrafast dynamic contrast-enhanced magnetic resonance imaging: Preliminary experience in 40 subjects. J Magn Reson Imaging. 2004; 20:353-65
[66] Ohno Y, Koyama H, Nogami M, Takenaka D, Matsumoto S, Onishi Y, et al. Dynamic perfusion MRI: capability for evaluation of disease severity and progression of pulmonary arterial hypertension in patients with connective tissue disease. J Magn Reson Imaging. 2008; 28:887-99
[67] Swift AJ, Telfer A, Rajaram S, Condliffe R, Marshall H, Capener D, et al. Dynamic contrast-enhanced magnetic resonance imaging in patients with pulmonary arterial hypertension. Pulmonary circulation. 2014; 4:61-70
[68] Harris B, Bailey D, Miles S, Bailey E, Rogers K, Roach P, et al. Objective analysis of tomographic ventilation-perfusion scintigraphy in pulmonary embolism. American journal of respiratory and critical care medicine. 2007; 175:1173-80
[69] Nichols K, Saouaf R, Ababneh AA, Barst RJ, Rosenbaum MS, Groch MW, et al. Validation of SPECT equilibrium radionuclide angiographic right ventricular parameters by cardiac magnetic resonance imaging. J Nucl Cardiol. 2002; 9:153-60
[70] Schulman DS. Assessment of the right ventricle with radionuclide techniques. J Nucl Cardiol. 1996; 3:253-64
[71] Matsushita T, Ikeda S, Miyahara Y, Yakabe K, Yamaguchi K, Furukawa K, et al. Use of [123I]-BMIPP myocardial scintigraphy for the clinical evaluation of a fatty-acid metabolism disorder of the right ventricle in chronic respiratory and pulmonary vascular disease. The Journal of international medical research. 2000; 28:111-23
[72] Nagaya N, Goto Y, Satoh T, Uematsu M, Hamada S, Kuribayashi S, et al. Impaired regional fatty acid uptake and systolic dysfunction in hypertrophied right ventricle. J Nucl Med. 1998; 39:1676-80
[73] Kluge R, Barthel H, Pankau H, Seese A, Schauer J, Wirtz H, et al. Different mechanisms for changes in glucose uptake of the right and left ventricular myocardium in pulmonary hypertension. J Nucl Med. 2005; 46:25-31
[74] Oikawa M, Kagaya Y, Otani H, Sakuma M, Demachi J, Suzuki J, et al. Increased [18F]fluorodeoxyglucose accumulation in right ventricular free wall in patients with pulmonary hypertension and the effect of epoprostenol. Journal of the American College of Cardiology. 2005; 45:1849-55
[75] Gomez A, Bialostozky D, Zajarias A, Santos E, Palomar A, Martinez ML, et al. Right ventricular ischemia in patients with primary pulmonary hypertension. Journal of the American College of Cardiology. 2001; 38:1137-42

[76] Wong YY, Westerhof N, Ruiter G, Lubberink M, Raijmakers P, Knaapen P, et al. Systolic pulmonary artery pressure and heart rate are main determinants of oxygen consumption in the right ventricular myocardium of patients with idiopathic pulmonary arterial hypertension. European journal of heart failure. 2011; 13:1290-5
[77] Wong YY, Ruiter G, Lubberink M, Raijmakers PG, Knaapen P, Marcus JT, et al. Right ventricular failure in idiopathic pulmonary arterial hypertension is associated with inefficient myocardial oxygen utilization. Circ Heart Fail. 2011; 4:700-6
[78] Higuchi T, Bengel FM, Seidl S, Watzlowik P, Kessler H, Hegenloh R, et al. Assessment of alphavbeta3 integrin expression after myocardial infarction by positron emission tomography. Cardiovascular research. 2008; 78:395-403
[79] Pietila M, Malminiemi K, Ukkonen H, Saraste M, Nagren K, Lehikoinen P, et al. Reduced myocardial carbon-11 hydroxyephedrine retention is associated with poor prognosis in chronic heart failure. European journal of nuclear medicine. 2001; 28:373-6
[80] Wichter T, Schafers M, Rhodes CG, Borggrefe M, Lerch H, Lammertsma AA, et al. Abnormalities of cardiac sympathetic innervation in arrhythmogenic right ventricular cardiomyopathy : quantitative assessment of presynaptic norepinephrine reuptake and postsynaptic beta-adrenergic receptor density with positron emission tomography. Circulation. 2000; 101:1552-8
[81] Marsboom G, Wietholt C, Haney CR, Toth PT, Ryan JJ, Morrow E, et al. Lung (1)(8)F-fluorodeoxyglucose positron emission tomography for diagnosis and monitoring of pulmonary arterial hypertension. American journal of respiratory and critical care medicine. 2012; 185:670-9
[82] Ruiter G, Wong YY, Raijmakers P, Huisman MC, Lammertsma AA, Knaapen P, et al. Pulmonary 2-deoxy-2-[(18)F]-fluoro-d-glucose uptake is low in treated patients with idiopathic pulmonary arterial hypertension. Pulmonary circulation. 2013; 3:647-53
[83] Jakobsen S, Kodahl GM, Olsen AK, Cumming P. Synthesis, radiolabeling and in vivo evaluation of [11C]RAL-01, a potential phosphodiesterase 5 radioligand. Nuclear medicine and biology. 2006; 33:593-7
[84] Direcks WG, Berndsen SC, Proost N, Peters GJ, Balzarini J, Spreeuwenberg MD, et al. [18F]FDG and [18F]FLT uptake in human breast cancer cells in relation to the effects of chemotherapy: an in vitro study. British journal of cancer. 2008; 99:481-7
[85] Benza R, Biederman R, Murali S, Gupta H. Role of cardiac magnetic resonance imaging in the management of patients with pulmonary arterial hypertension. Journal of the American College of Cardiology. 2008; 52:1683-92

7

CHAPTER 8

^{18}FLT PET depicts heterogeneous proliferation pathology in IPAH patient lung: a potential biomarker for PAH.

Submitted

A Ashek[1], OA Spruijt[2], HJ Harms[2], AA Lammertsma[3], J Cupitt[1], O Dubois[1], S Dabral[4], SS Pullamsetti[4], MC Huisman[3], V Frings[3], R Boellaard[3], FS de Man[2,3], A Vonk Noordegraaf[2], MR Wilkins[1], HJ Bogaard[2], L Zhao[1]

[1]Centre for Pharmacology and Therapeutics, Experimental Medicine, Imperial College London, Hammersmith Hospital, London
[2]Department of Pulmonary Medicine, VU University Medical Center, Amsterdam
[3]Department of Radiology and Nuclear Medicine, VU University Medical Center, Amsterdam
[4]Max-Planck Institute for Heart and Lung Research and University of Giessen and Marburg Lung Center, German Center for Lung Research, Bad Nauheim

Abstract

Introduction: Pulmonary vascular cell hyperproliferation is characteristic of pulmonary vascular remodelling in pulmonary arterial hypertension (PAH). A non-invasive imaging biomarker is needed to track the pathology and assess the response to treatments targeted at resolving the structural changes. Here we evaluate the application of radioligand 3'-deoxy-3'-[18F]-fluorothymidine (^{18}FLT) using positron emission tomography (PET).

Methods & results: We performed dynamic ^{18}FLT PET scanning in 8 idiopathic PAH patients (IPAH) and applied in-depth kinetic analysis with a reversible 2-compartment 4k model. Our results show significantly increased lung ^{18}FLT phosphorylation k3 in IPAH patients compared with non-PAH controls (0.086±0.034 min-1 vs 0.054±0.009 min-1; $P<0.05$). The lung ^{18}FLT signals are variable both between IPAH patients and within the lungs of each patient, compatible with histopathological reports of lungs from IPAH patients. Consistent with ^{18}FLT PET data, hyperproliferative pulmonary vascular fibroblasts isolated from IPAH patients exhibited upregulated expression of the key thymidine metabolism enzymes TK1 and thymidine transporter ENT1. In the monocrotaline rat PAH model, increased lung ^{18}FLT uptake was strongly associated with peripheral pulmonary vascular muscularization and the proliferation Ki-67 score, along with the prominent thymidine kinase TK1 and transporter ENT1 in the remodeled vessels. Importantly, lung ^{18}FLT measurements responded to two anti-proliferative treatments, dicholoroacetate and tyrosine kinase inhibitor imatinib.

Conclusions: Dynamic ^{18}FLT PET imaging can be used to report hyperproliferation in pulmonary hypertension and merits further study to evaluate response to treatment in IPAH patients.

Introduction

Pulmonary arterial hypertension (PAH) is characterized by structural remodeling of the pulmonary vasculature leading to increased pulmonary artery pressure and progressive right heart dysfunction [1-3]. Histopathology of lungs from PAH patients at the end stage of their disease show a complex pulmonary pathology including aberrant proliferation of pulmonary vascular cells, exuberant inflammatory cell infiltration and deposition of extra-cellular matrix, but with a patchy distribution [4-6]. The licensed treatments used in the clinic are based on restoration of an imbalance in vasoactive factors favoring vasoconstriction. While these drugs improve symptoms, they fail to halt the disease and have a limited effect on survival [7]. Innovative treatment strategies that inhibit the excessive proliferation of lung vascular cells, e.g. with the receptor tyrosine kinase inhibitor imatinib [8] and the metabolic modulator dichloroacetate (DCA) [9], show great promise in the preclinical setting. Disappointingly, imatinib was only partially efficacious in a larger PAH patient cohort [10]. A possible explanation for this failure to translate preclinical findings to patients may be the heterogeneity of pulmonary vascular remodeling in PAH, with some patients exhibiting profound active vascular proliferation but others a more quiescent state of end-stage fixed pulmonary vascular remodeling. A new tool for assessing PAH pathology in vivo would greatly improve the potential to translate therapeutic strategies targeted at resolving pulmonary vascular remodelling into the clinic. Ideally, such a tool would allow a strategy of precision medicine with therapies tailored to individual patients.

Positron emission tomography (PET) with appropriate ligands allows for spatial detection and localization of pathophysiological processes in vivo. It is used in oncology to stratify patients and assess disease progression and response to treatment, and predict clinical outcomes. The radioactive ligand 18F-3'-fluoro-3'-deoxythymidine (^{18}FLT) is a marker for cell proliferation [11,12] that correlates closely with histological markers, such as proliferating cell nuclear antigen (PCNA), Ki-67 and S phase fraction [13-16]. ^{18}FLT is a fluorine-modified thymidine analogue that is transported into the cell via passive diffusion and by nucleoside transporters, such as the equilibrative nucleoside transporter (ENT1), in a similar way as thymidine [17]. Thereafter, ^{18}FLT is phosphorylated by thymidine kinase 1 (TK1) and trapped intracellularly at a rate proportional to TK1 activity, which is elevated during the S phase of the cell proliferation cycle but decreased or absent in quiescent cells [18-21]. Importantly, ^{18}FLT PET is recognized for evaluating whole tumor proliferation heterogeneity [22].

Few studies have explored the application of PET imaging in PAH. Previously we have reported on ^{18}FDG-PET as a tool for following response to treatment in animal models and the signal from patients with PAH, but this ligand reports on both proliferation and inflammation. Here we evaluate the potential of ^{18}FLT PET as an imaging biomarker for assessing the distinctive hyper-proliferative pulmonary vascular pathology seen in PAH. First, we examined ^{18}FLT lung uptake in idiopathic PAH (IPAH) patients in comparison to control subjects. Second, we assessed whether ^{18}FLT PET could track pulmonary pathology in animal PAH models and their response to targeted therapies. Third, we examined ENT1 and TK1 expression in lung tissues and pulmonary vascular fibroblasts isolated from IPAH patients to understand the drivers of lung ^{18}FLT uptake in PAH.

Methods

Patient population

8 patients (Table 1) diagnosed with IPAH according to ERS guidelines [23] were recruited from the VU University Medical Center; both treatment naive and treated patients were included in this study. We made use of ^{18}FLT PET data sets from an oncology study of non-small cell lung cancer patients [24] from the VU University Medical Center as controls. We included 6 subjects who had confirmed one-sided lung tumor; ^{18}FLT PET data from the tumor-free side of the lung was used as control for comparison with IPAH patients. The study was approved by the Medical Ethical Review Committee of the VU University Medical Center (Toetsingonline: NL49166.029.14) and all IPAH patients gave written informed consent.

Right heart catheterizations and cardiac magnetic resonance imaging

All patients underwent right heart catheterization and cardiac magnetic resonance imaging (CMR) within one month of their PET/CT scan, and in this period all patients were stable on pulmonary hypertension targeted therapy. A balloon-tipped, flow-directed 7.5F, triple-lumen Swan-Ganz catheter (Edwards Lifesciences LLC, Irvine, CA) was inserted in the pulmonary artery via the jugular vein or femoral vein under local anesthesia and constant ECG monitoring, and measurements were performed according to guidelines [23]. Catheter ports were placed in the right atrium, right ventricle and pulmonary artery and the zero reference level for the pressure transducer was placed at mid-thoracic level in supine position.

CMR scans were performed on a Siemens 1.5T Sonato or Avanto scanner (Siemens Medical Solutions, Erlangen, Germany). Acquisition and post-processing were performed as described previously [25].

	IPAH (n=8)	**Controls (n=6)**
Age (yr)	46 ± 12	68 ± 9
Sex (M:F) (n)	4 : 4	3 : 3
NYHA functional class I/II/III/IV (n)		-
6MWD (m)	518 ± 125	-
NT-ProBNP	641 ± 992	-
Treatment		
Treatment naive	1	-
Monotherapy (ERA or PDE5I)	1	-
Dual combination therapy (ERA+PDE5I)	3	-
Triple combination therapy (ERA + PDE5I + prostacyclin)	3	-
Hemodynamic characteristics		
Heart rate (beats/min)	79 ± 8	-
Mean pulmonary artery pressure (mmHg)	52 ± 20	-
Pulmonary arterial wedge pressure (mmHg)	8 ± 3	-
Mean right atrial pressure (mmHg)	7 ± 4	-
Pulmonary vascular resistance (dyn.s/cm^5)	686 ± 482	-
Cardiac output (l/min)	5.6 ± 1.7	-
Mixed venous O2 saturation (%)	68 ± 10	-
Cardiac magnetic resonance imaging		
RVEDVI (ml/m^2)	93 ± 21	
RVESVI (ml/m^2)	59 ± 23	
RVEF (%)	39 ± 11	
LVEF (%)	63 ± 8	

Table 1: Clinical Characterization of Patients with Idiopathic Pulmonary Arterial Hypertension (IPAH) and 6 controls with unilateral lung cancer. M = males; F = females; NYHA = New York Heart Association functional class; 6MWD = six minute walk distance; ERA = Endothelin Receptor Antagonists; PDE5I = Phosphodiesterase-5 Inhibitors. RVEDI = right ventricular end diastolic volume index; RVESV = right ventricular end systolic volume index; RVEF = right ventricular ejection fraction; LVEF = left ventricular ejection fraction.

Summarized, short-axis images of the right and left ventricle were analyzed using MASS software (MEDIS Medical Imaging Systems, Leiden, The Netherlands). Endocardial borders of the right ventricle were manually traced on end-diastolic images and on end-systolic images. Right and left ventricular end-diastolic and end-systolic volumes were assessed using the Simpson rule.

IPAH Patients ^{18}FLT PET

^{18}FLT was synthesized as described previously [26]. Minimum 4 hours fasting was instructed prior to the PET scan, IPAH patients were scanned on a Philips Ingenuity PET/CT (Philips Healthcare, Best, The Netherlands), whilst control data sets were from a Philips Gemini TF-64 PET/CT (Philips Healthcare, Best, The Netherlands) using an identical scanning protocol. First, following a scout-CT scan, IPAH patients were positioned with lungs centered in the field of view of the PET scanner. Then, a dynamic 60-min emission scan was started simultaneously with automated bolus intravenous injection of 370 MBq of ^{18}FLT (0.8 mL/s). After completion of the emission scan, a low-dose CT scan was performed to correct for photon-attenuation and scatter. Finally, emission data were reconstructed in a 36 frame (1x10, 8x5, 4x10, 3x20, 5x30, 5x60, 4x150, 4x300 and 2x600 s) using the 3-Dimensional Row-Action Maximum Likelihood Algorithm (3D-RAMLA), applying all appropriate corrections for dead time, decay, scatter, attenuation and normalization. During the scan, venous blood samples were withdrawn at 5, 10, 20, 30, 40 and 60 minutes post injection and measured for the presence of radiolabeled metabolites (^{18}F-glucuronide) and the ratio of plasma and whole-blood activity concentrations as described by Hoekstra et al. [27].

Kinetic Model for Data Analysis

^{18}FLT PET data were analyzed using the plasma kinetic model as described previously [26]. The model consists of three or four rate constants, of which k3 represents phosphorylation of ^{18}FLT by thymidine kinase and this rate constant was assumed to most closely represent proliferation rate, thus used to represent the lung ^{18}FLT uptake. The model can be described using: $C_{PET}(t) = C_T(t) + V_A \cdot C_A(t) + V_V \cdot C_A(t)$ (1), in which $C_{PET}(t)$ represents the measured pulmonary activity concentrations, $C_T(t)$ the activity according to the plasma kinetic model, $C_A(t)$ and $C_V(t)$ are arterial and venous blood concentrations, respectively. To correct for contamination of the signal by blood-pool activity, V_A (arterial blood volume fraction) and V_V (venous blood volume fraction) were added to the model. For $C_T(t)$, both an irreversible 2-compartment 3k model (2T3k) and a reversible 2-compartment 4k model (2T4k) were tested and the best fit was obtained. The use of an

irreversible or reversible two-tissue model was evaluated using Akaike Information Criterion (AIC) [28]. For all patients and controls, AIC showed a significantly improved fit using a reversible 2T4k model and consequently, all results below are obtained using this model. In this model, k1 represents the rate constant for the transport of ^{18}FLT from blood into tissue, k2 represents the rate constant of the transport of ^{18}FLT from tissue back to blood, k3 reflects the rate constant of phosphorylation of ^{18}FLT and k4 describes the rate of ^{18}FLT dephosphorylation [29].

Input Functions

The lung has a dual circulation with perfusion coming from both the pulmonary and systemic (bronchial) circulation. Because systemic perfusion becomes quantitatively more important in PAH [30], we first determined model fits separately with pulmonary, systemic and combined input functions. Because the best model fit was obtained using a pulmonary input function, this was used for further calculations. Five 1cm diameter regions of interest (ROI) were drawn in the pulmonary artery at the level of the pulmonary trunk on early frames showing the first-pass of the bolus through the pulmonary circulation. Average activity through time $C_{PA}(t)$ was obtained from this region and assumed to represent the total supply of radioactivity to the lungs $C_A(t)$ in eq. (1). To obtain the arterial input function $C_{PL}(t)$, $C_{PA}(t)$ was multiplied with a sigmoid function fitted through the ratio of plasma and whole-blood activity concentrations and a second sigmoid function fitted through the fraction of non-metabolized tracer. This correction was performed as described previously [26]. A second set of ROIs was drawn in left atrial cavity in at least three slices. Average activity concentrations $C_{LA}(t)$ were obtained and used as correction factor for venous blood concentrations in the lungs $C_V(t)$ in eq. (1).

Lung Segmentation

Pulmonary activity concentrations were obtained using the low-dose CT scan. Using automated region-growing methods, a region of low tissue density between 0.05 and 0.6 g/mL was obtained for each lung. A layer of 2 voxels (8mm) was eroded from the borders of each lung region to reduce the effects of respiratory motion, spill-in of activity from the liver and other partial volume effects. To avoid any effects of a gradient signal in the lungs and of differences in the field of view of the scanner and patient positioning, data from a 2cm region at the level of the bifurcation of the pulmonary artery were used for analysis using the ROIs drawn in the pulmonary artery.

Parametric Mapping

To assess the spatial distribution of ^{18}FLT uptake within the lungs, volume of distribution was estimated from the slope of the linear regression on the Logan plot [31]. A parametric 3-dimentional map was generated by using volume of distribution values measured per voxel basis, typically 200000 voxels (2mm^2 per voxel) for a human subject.

Animals and Experimental Design

Adult male Sprague-Dawley (SD) rats (body weight 200-250g) (Charles River, UK) were used. All experiments were conducted in accordance with the UK Home Office Animals (Scientific Procedures) Act 1986 (London, UK). Pulmonary hypertension was induced by subcutaneous injection of monocrotaline (MCT, 60 mg/kg; Sigma-Aldrich).

In vivo experiments were designed as follows: a) *^{18}FLT PET – following MCT induced PH progression*; ^{18}FLT PET scans were performed in control and MCT PAH rats one week and four weeks after injection. b) *^{18}FLT PET – to assess the effects of treatments in MCT PH model*; rats were divided into 4 groups (n=6 per group) (i) control (C), (ii) MCT 4 weeks (4W) and MCT rats treated with (iii) Dichloroacetate acid 70mg/kg/day in drinking water (DCA, Sigma-Aldrich, UK), (iv) imatinib 100mg/kg/day (IMA, LC Laboratories, USA) by oral gavage. Each treatment was started 2 weeks post MCT injection and continued for the following 2 weeks. At the end of the treatment, ^{18}FLT PET scans were performed and tissues were collected for biochemical and histological examination.

In vivo ^{18}FLT PET

In vivo imaging was performed using a Siemens Inveon small-animal multimodality PET/CT system (Siemens Healthcare Molecular Imaging). Briefly, rats were anaesthetized with isoflurane (2-4%), ventilation was adjusted to maintain pO2, pCO2 and pH within normal range. After the completion of the CT scan, ^{18}FLT (approximately 35 MBq, <0.5ml) was injected through tail vein catheter. Dynamic emission scans were acquired in list-mode format for 60 minutes using conventional full-ring, whole-body PET. During PET scanning, serial blood samples were taken via a femoral artery line (20 µl each) 8 samples at 1st minute, and then at 2, 3, 5, 10, 15, 30, 45 and 60 minutes. At the end, animals were sacrificed and tissue samples (lung, RV, kidney, liver) were collected for gamma-counting, as well as snap frozen for biochemical measurement. The ratio of RV to left ventricle plus the septum mass (RV/ LV + septum) was used as an index of RV hypertrophy. Left lungs were inflated and fixed with 4% formalin for histology examination.

Data Analysis

PET image data were sorted into 0.5mm sinogram bins and 33 time frames and images were reconstructed using filtered back projection with CT-based attenuation correction. The frame durations used for the study were 12×5s, 4×15s, 6×30s, 11×300s. The reconstructed CT and PET images were analyzed using the 3-dimensional visualization toolbox in the Inveon Research Workplace software. (Siemens Healthcare Molecular Imaging).

The whole lung tissue time-activity curves (TACs) were calculated from lung PET images co-registered with ROI on CT lung images, covering the lung volume with clearly visible boundaries adjusted by CT density thresholding. Cumulative images over 0 to 60 min were used for kinetic analysis of tracer uptake. The image derived input functions (IDIFs) were determined individually by sampled arterial plasma time activity curves or the PET images derived activity curve from the LV blood pool.

Decay corrected whole lung TACs were normalized for injected activity (kBq) and body weight to obtain standardized uptake value (SUV). The dynamic image data was fitted to a 2-compartment 4k model using the Matlab-based in house kinetic analysis software package (CLICKFIT). In this model, K1 represents the rate constant for the transport of ^{18}FLT from blood into tissue, k2 represents the rate constant of the transport of ^{18}FLT from tissue back to blood, k3 reflects the rate constant of phosphorylation of ^{18}FLT, and k4 describes the rate of ^{18}FLT dephosphorylation [29].

Bio-distribution

The plasma and tissue samples (lung, RV, LV, septum, liver, and kidney) harvested following PET scanning were weighed and measured for radioactivity in a gamma counter. All data were corrected for radioactivity decay. The amount of radioactivity was expressed as percentage of injected dose per gram of tissue or blood (%ID/g).

Histology Examination

Transverse lung sections were processed for elastic Van Gieson (EVG) and hematoxylin and eosin (H&E) staining. Peripheral vessels less than 100 μm in lung were counted blindly under microscope (40X) and pulmonary vascular remodelling was expressed as the proportion of vessels with double elastic lamina to total vessels counted. Lung sections were also processed for Ki-67 (1:50, Thermo Scientific), CD68 (1:50; Serotec), TK1 (1:50; Abcam) and ENT1 (1:100; Abcam) immunostaining. Ki-67

score was calculated on a minimum of 20 randomly selected 40X high-power fields per slide and Ki-67 positive cells around the vessels (<100μm) were counted (approximately 40-50 vessels per slide). Number of Ki-67 positive cells per vessels was calculated for comparison between groups. CD68-positive cells were counted in whole-lung tissue sections and expressed as per mm^2.

Western Blotting

Rat lung samples were homogenized in RIPA buffer (150 mmol/L sodium chloride, 1.0% NP-40 or Triton X-100, 0.5% sodium deoxycholate, 0.1% SDS, 50 mmol/L Tris, pH 8.0, supplemented with protease inhibitor; Roche). Western blotting was performed according to the manufacturer's suggestions (rabbit polyclonal anti-TK1 and anti-ENT1 1:1000; Abcam). Proteins were detected by Novex ECL chemiluminescence (Invitrogen). Optical densities of individual bands were measured, and protein expression was standardized with GAPDH.

Cell Culture

Pulmonary artery adventitial fibroblasts isolated from the lungs of IPAH patients and healthy donors were obtained from the University of Giessen and Marburg Lung centre tissue bank. Our previous experiment have shown that the IPAH pulmonary arterial fibroblasts exhibited greater proliferation capacity 9. We extracted RNA by the Trizol method from pulmonary artery adventitial fibroblasts and donor cells cultured in 6-well plates. Total RNA was transcribed with a High Capacity cDNA Reverse Transcription Kit (Applied Biosystems), followed by real-time polymerase chain reaction analysis of ENT1 and thymidine metabolism enzyme genes (TK1 and thymidine phosphorylase TP) using primers described in Table 2.

Name	Forward Primer	Reverse Primer
TK 1	CCGTGGTTTAAAGCGGTCG	GGACGCGTCTCATCAACTCT
ENT1	ACTCCAAAGTCTCAGCAGCAGG	AGAGTTCCGCTCAGGCAAG
TP	AGGAGGCACCTTGGATAAGC	GCCCCTCCACGAGTTTCTTA

Table 2. Real-Time Polymerase Chain Reaction Primers for the Thymidine Kinase 1 (TK1), Equilibrative Nucleotide Transporter 1 (ENT1) and Thymidine Phosphorylase (TP).

Statistical Analysis

Data are presented as mean±SEM. Normal distribution was verified with the Kolmogorov-Smirnov test, and variance of homogeneity was tested by the Levene test. Differences between groups were

assessed by either the Student t test or an appropriate ANOVA followed by the Bonferroni post hoc test for multigroup comparisons. Correlations between ^{18}FLT uptake (k3) and clinical variables were determined by simple linear regression analyses. A P value <0.05 was considered statistically significant. All statistical analyses were performed with Statistical analyses were performed using SPSS for Windows version 20 (IBM Corp., Armonk, NY) and GraphPad Prism for Windows version 5 (GraphPad Software, La Jolla, CA).

Results

Increased Rate of ^{18}FLT Phosphorylation k3 in IPAH Patients

The clinical characteristics of the IPAH patients studied and details of the controls included in this study are summarized in Table 1. We calculated the rates of ^{18}FLT transportation by 2T4k modeling [29] based on the sixty-minute PET imaging dynamic acquisition. Compared with ^{18}FLT PET uptake in control subjects, ^{18}FLT phosphorylation k3 (Figure 1A) was increased significantly in IPAH patient lungs (0.086±0.034 vs 0.054±0.009; P<0.05). There was variation in k3 within the IPAH group, such that some patients exhibited uptake more than 2-fold above the control group whereas others were in the range of controls. Further analysis by 3-dimensional parametric mapping of computed per-voxel ^{18}FLT uptake from IPAH patients demonstrated that focal areas of relatively high uptake were distributed unevenly throughout the lung parenchyma (Figure 1B). Two representative IPAH patients with lowest and highest mPAP (Patient A 25mmHg vs Patient B 92mmHg) and PVR (Patient A 134 dyn.s/cm^5 vs Patient B 1005dyn.s/cm^5) demonstrated this variation (Table 1); computed per-voxel ^{18}FLT uptake from Patient B showed a distinctive uneven regional pattern of ^{18}FLT signal compared to Patient A.

We next looked at the relationship between lung ^{18}FLT uptake and cardiopulmonary hemodynamics in the IPAH group. There was no correlation between lung ^{18}FLT uptake (phosphorylation rates k3) and mean pulmonary artery pressure (mPAP, r^2=0.38, p=0.111) or pulmonary vascular resistance (PVR r^2=0.042, p=0.625) (Figure 1C). Interestingly, ^{18}FLT phosphorylation k3 levels were correlated significantly with right ventricular end-diastolic volume index (r^2=0.54, p=0.037), right ventricular end-systolic volume (r^2=0.65, p=0.015), right ventricular ejection fraction (r^2=0.51, p=0.048) and the load on the right ventricle (arterial elastance r^2=0.50, p=0.048). There was no correlation between k3 and cardiac index (r^2=0.05, p=0.604) (Supplement Figure I).

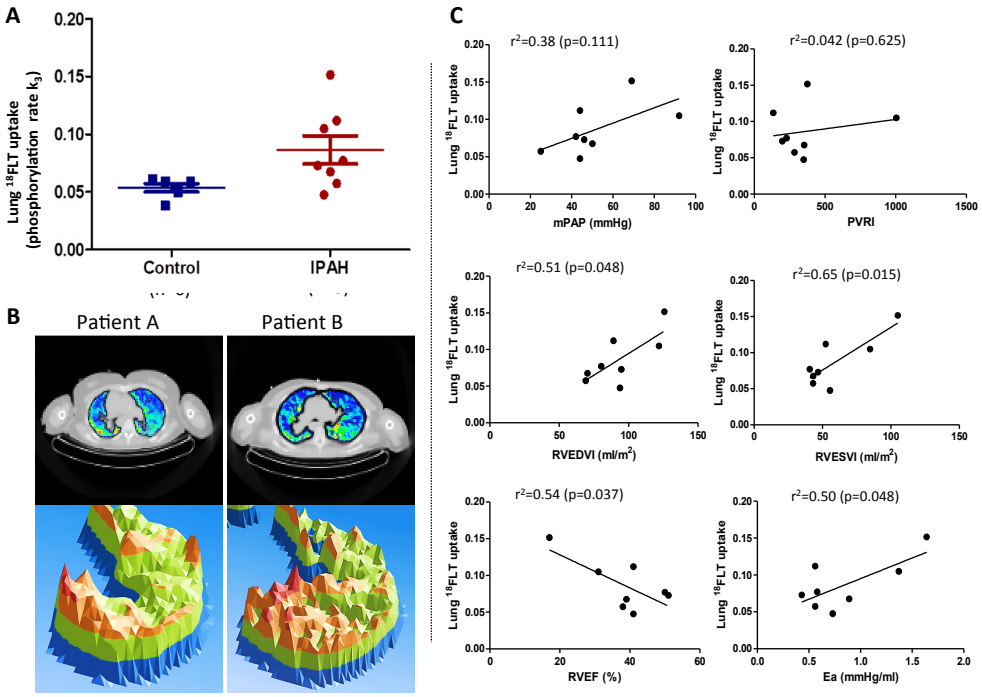

Figure 1. A. Lung ^{18}FLT uptake (rate of ^{18}FLT phosphorylation k3) was significantly increased in IPAH patient group (n=8, 0.086±0.012) compared with controls (n=6, 0.054±0.004; p<0.05). B. Upper panel: Parametric map of Lung ^{18}FLT uptake calculated from Logan analysis from two different IPAH patients having lowest (Patient A) and highest (Patient B) mPAP among the patient group (Table 1). Lower panel: 3D parametric map generated from computed per-voxel 18FLT uptake from IPAH Patients A and B, showing an uneven regional ^{18}FLT uptake which is considerably higher in Patient B. C. There was no significant correlation between lung ^{18}FLT uptake (k3) with mean pulmonary artery pressure (mPAP) or pulmonary vascular resistance (PVR). But lung ^{18}FLT uptake (k3) was closely correlated to right ventricular dimensions (RVEDVI and RVESVI) and right ventricular function (RVEF) as well as to the load on the right ventricle (Ea). (RVEDVI = right ventricular end-diastolic volume; RVESVI = right ventricular end-systolic volume; RVEF = right ventricular ejection fraction; Ea = arterial elastance).

Increased TK1, TP and ENT1 Expression in IPAH Fibroblast

The vascular remodeling in PAH involves all cellular elements of the vessel wall, including fibroblasts. We have shown previously that pulmonary fibroblasts from IPAH patients exhibit greater proliferation capacity in vitro [9]. Here, we examined the expression of the thymidine metabolism enzymes TK1 and TP, as well as the thymidine transporter ENT1, in pulmonary fibroblasts isolated

from 5 IPAH patients and 5 donor lungs in culture. IPAH pulmonary fibroblasts demonstrated increased expression of ENT1, TP and TK1 in comparison to control donor cells (Figure 2).

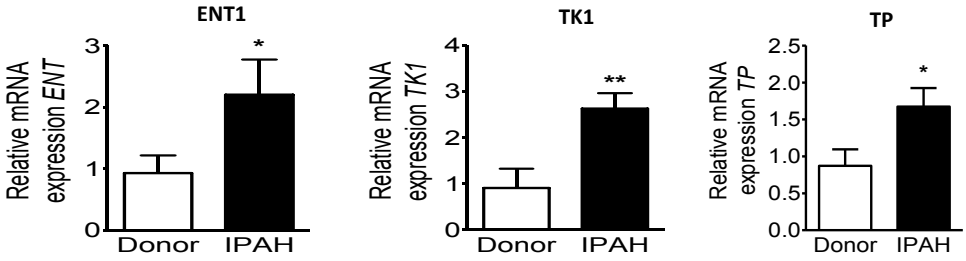

Figure 2. Pulmonary artery adventitial fibroblasts isolated from lungs of patients with idiopathic pulmonary arterial hypertension (IPAH) exhibited increased expressions of ENT1, TK1 and TP in transcription level compared with cells from donor lungs. Data are expressed as mean±SEM; n≥6 in each group. **P<0.01 , *P<0.05.

Increased Lung ^{18}FLT Uptake in a MCT PAH Model

To interpret the relationship between lung ^{18}FLT uptake and the underlying pulmonary vascular pathology, further studies were conducted in the MCT PAH rat. Static images obtained from 60 min dynamic PET acquisitions demonstrated significantly higher accumulation of ^{18}FLT in the MCT rat lung (Figure 3A); ^{18}FLT SUV in the 4 week MCT group was >50% greater than in the control group (Supplement Figure II). Dynamic 60 min PET data acquisition was used for kinetic modeling using a 2T4K compartmental model. There was a progressive increase in ^{18}FLT phosphorylation (k3) (Figure 3B) as well as overall ^{18}FLT influx rate (Ki) (Supplement Figure II) in MCT rat lungs, supported by direct tissue ^{18}FLT measurements (Figure 3C).

Histological examination of the MCT lung showed progressive vascular remodeling over 1 and 4 weeks post MCT injection as previously demonstrated [9].The remodeled vessels in the MCT rat lung demonstrated Ki67 expression (Figure 3D), as well as prominent ENT1 and TK1 expression (Figure 3F). The increased phosphorylation rate (k3) in MCT rats was in proportion to the vascular pathology and closely correlated (r^2=0.78, P> .0001) with the Ki-67 score (Figure 3E).

Attenuated Lung ^{18}FLT Uptake with Imatinib and DCA Treatment in the MCT Model

We investigated the response of ^{18}FLT PET measurements to treatments with proven anti-proliferative efficacy in the MCT rat model. Treatment with DCA or imatinib during weeks 2 to 4 post MCT attenuated pulmonary vascular remodelling, as demonstrated by significant reductions in the

proportion of remodelled vessels with double elastic lamina (Figure 4A), Ki67 score (Figure 4B), and right ventricular hypertrophy (RV/LV+sep ratio, DCA: 0.48±.03 imatinib: 0.32±.02; P<0.001 in comparison to placebo group: 0.61±.02, Figure 4C), consistent with previous data. This was accompanied by a marked reduction in the phosphorylation of ^{18}FLT k3 (Figure 4D). This was further supported by the direct measurement of lung tissue ^{18}FLT (Figure 4E).

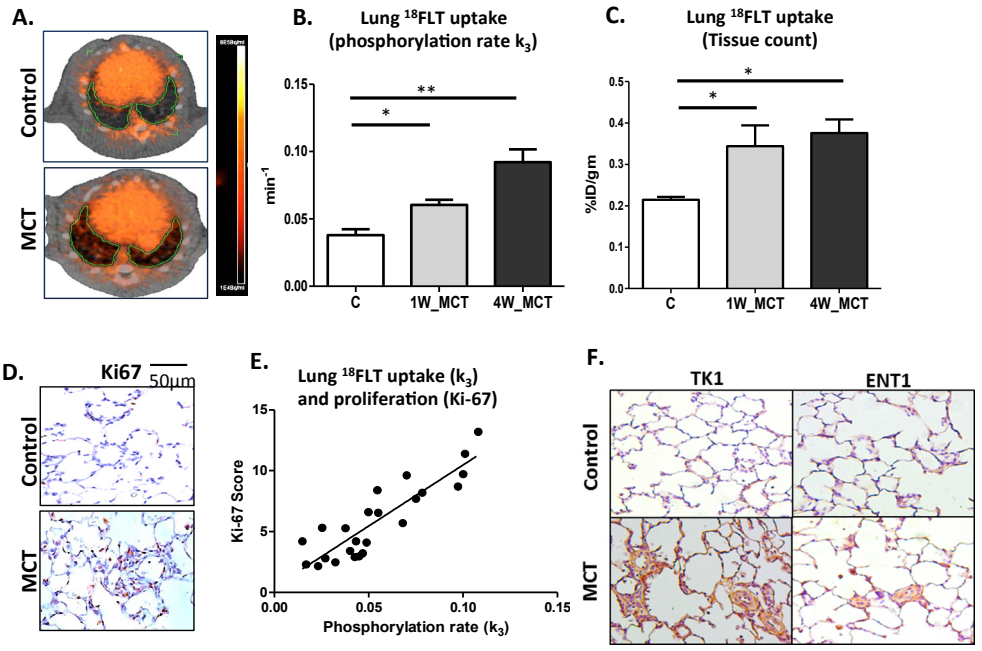

Figure 3. A. Representative static images from dynamically acquired positron emission tomography images over 60 minutes after ^{18}FLT injection. B. Compartmental analysis demonstrating a significantly increased lung ^{18}FLT uptake (phosphorylation rate k3) in rats after 1 week (1W) and 4 weeks (4W) of monocrotaline (MCT) injection. C. Measurement of ^{18}FLT uptake by gamma counter confirms significantly increased ^{18}FLT uptake in MCT rats. %ID/gm indicates percentage of injected dose per gram of tissue. Data are expressed as mean±SEM; n≥5 in each group. **P<0.01 , *P<0.05 vs control (C) group. D. Immunostaining with Ki67 in MCT lung sections demonstrated increased expression of Ki-67 positive nuclei around remodelled vessels. E. Relationship between ^{18}FLT phosphorylation rate and proliferation index Ki-67 score (r2=0.77, P<0.0001) in MCT rat lung. F. Prominent TK1 and ENT1 expression was observed around the remodelled peripheral pulmonary vessels.

Western blot analysis of lung homogenates demonstrated a significant increase in ENT1 and TK1 expression in the 4 week MCT rat lung, which was attenuated by imatinib and DCA treatments (Figure 4F).

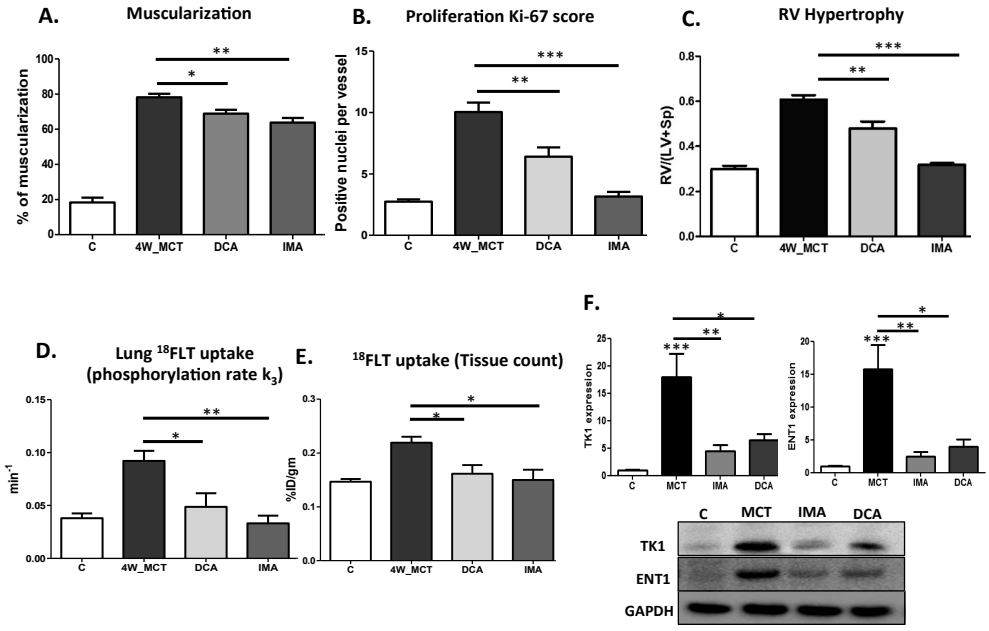

Figure 4. A. Treatment with dichloroacetate (DCA) and imatinib (IMA) attenuated pulmonary vascular muscularization. B. Effect of treatments on Ki-67–positive nuclei surrounding remodelled peripheral pulmonary vessels. C. Effect of treatments on attenuation of right ventricular hypertrophy in the monocrotaline (MCT) rat. D and E. Treatment with DCA and imatinib attenuated lung 18FLT uptake in MCT rats. %ID/gm indicates percentage of injected dose per gram of tissue. F. Summary data and representative western blot for TK1 and ENT1 expression in whole lung homogenate. Both TK1 and ENT1 expression, normalized to GAPDH, were increased in the MCT rat and attenuated by DCA and imatinib treatment. Data are expressed as mean±SEM; n≥5 in each group. ***P<0.001, **P<0.01, *P<0.05.

Discussion

This is the first study to explore dynamic ^{18}FLT PET imaging in PAH patients to track pulmonary vascular pathology. We found that lung ^{18}FLT uptake was increased in IPAH patients compared with control subjects, and that there is heterogeneity in the lung ^{18}FLT signal in IPAH, both between patients and within the lungs of each patient. The MCT rat model allowed us to investigate this signal in more depth. Increased lung ^{18}FLT uptake in this model responded to drugs that reduce pulmonary vascular remodeling in animal models. Further in depth kinetic 2T4k modelling of the lung ^{18}FLT signal showed an increased rate of ^{18}FLT phosphorylation k3. Together with gene expression studies in pulmonary arterial fibroblasts isolated from IPAH patients, our data support

the contention that the lung ^{18}FLT PET signal reflects pulmonary vasculature cellular proliferation in PAH.

We have previously shown that ^{18}FDG uptake is increased in the lungs of IPAH patients [9]. A limitation of this approach is the challenge of distinguishing inflammation from proliferation. In the field of oncology, the ^{18}FLT ligand has been used for imaging tumor cell proliferation [22], especially for improving the accuracy of anti-proliferative target delineation. ^{18}FLT has been shown to correlate better than ^{18}FDG with cell proliferation markers in excised tumors and has potential to better differentiate growing tumors from inflammation [32,33]. In addition, background activity of ^{18}FLT is low in the thorax as shown in studies of lung cancer [34-36]. In the current study, dynamic PET scanning data from IPAH patients allowed us to perform the in-depth kinetic analysis of the rates of ^{18}FLT transportation in the lung by 2T4k modeling [29]. We found a significantly higher rate of ^{18}FLT phosphorylation k3 in a proportion of IPAH patient lungs.

The ^{18}FLT phosphorylation reaction, denoted by k3, is the TK1 rate-limiting step during the cell cycle S-phase, determining the uptake and retention of ^{18}FLT in tissue. TK1 overexpression has been described in various tumour tissues including brain, breast and lung tumors and TK1 expression is correlated closely with Ki67 expression as well as ^{18}FLT uptake [18-21]. The measurement of intracellular levels of phosphorylated thymidine (as a surrogate of TK1 activation level) is regarded as an accurate method for estimating cellular growth [37]. Direct correlation of ^{18}FLT uptake with vascular remodeling in humans is not possible. We employed pulmonary fibroblasts, an active contributor to vascular remodeling in IPAH, that we isolated from IPAH patients to explore the biology in vitro. Consistent with increased lung uptake of ^{18}FLT PET and phosphorylation of ^{18}FLT in IPAH patients, we observed a significantly increased expression of thymidine metabolism enzymes TK1 and TP, as well as thymidine transporter ENT1,in these hyper-proliferative cells. These data are consistent with a lung ^{18}FLT signal that depicts the hyper-proliferative vascular pathology documented in the pulmonary hypertensive lung.

There was considerable variation in the distribution of lung ^{18}FLT uptake within the IPAH study group. Some patients exhibited a more than 2-fold increase in ^{18}FLT phosphorylation, k3, above the control group, whereas others were in the range of controls. This is not surprising as vascular proliferation is unlikely to be constant throughout the course of the disease. Little is known about

the natural history of the vascular pathology of IPAH; for example, it could be episodic with periods of vascular proliferation interspersed and with periods of relative quiescence, or vascular remodeling could be an early event with little cellular activity during the later stages of the disease. A cross sectional study of IPAH patients would be expected to reflect this variation. Furthermore, we analysed data by 3-dimensional parametric mapping of computed per-voxel ^{18}FLT uptake. There was an uneven pattern of ^{18}FLT signal distribution within the lungs of severe disease, which may report the patchy distribution of the vascular pathology within the lung, as seen on histological examination [4,6]. This variability is likely to explain the absence of an association between overall lung ^{18}FLT phosphorylation, k3, and mean pulmonary artery pressure or pulmonary vascular resistance in this small cohort of IPAH patients.

Results from pre-clinical animal studies and clinical oncology investigations indicate that ^{18}FLT PET could be a useful biomarker for measuring the difference in tumour growth rates in the course of therapy. Our data from the MCT rat model of PAH showed an association between increased lung ^{18}FLT uptake and the progression of pulmonary vascular remodelling. The remodelled vessels in the MCT rat lung demonstrated increased Ki-67 expression as well as prominent thymidine kinase TK1 and transporter ENT1 expression. ^{18}FLT phosphorylation, k3, levels were also increased in proportion to peripheral pulmonary vascular muscularization and the proliferation Ki-67 score. Treatment with DCA and imatinib in the MCT model attenuated pulmonary hypertension and vascular remodelling, reduced the disease-driven increase in lung TK1 and ENT1 expression, and the ^{18}FLT PET lung signal was reduced in line with decreased peripheral vascular muscularization. Our data suggests that ^{18}FLT PET may be a useful tool to assess response to treatment in patients with PAH.

Conclusions

The present study demonstrates the potential of dynamic ^{18}FLT PET imaging to report on the vascular pathology in IPAH. We suggest that, given the variability in uptake between patients, it might be a useful tool for identifying patients who might benefit most from anti-proliferative therapy and so support precision medicine. The value of ^{18}FLT PET as a tool in evaluating therapeutic strategies targeted at resolving pulmonary vascular remodelling in the clinic merits further study.

Sources of Funding

This research is supported by project grant from the British Heart Foundation (PG/14/88/31183), For the clinical studies in PAH patients, we received support from the Netherlands CardioVascular Research Initiative; the Dutch Heart Foundation, Dutch Federation of University Medical Centres, the Netherlands Organisation for Health Research and Development and the Royal Netherlands Academy of Sciences".

References

[1] Archer SL WE, Wilkins MR. Basic science of pulmonary arterial hypertension for clinicians: new concepts and experimental therapies. Circulation 2010; 121:2045–2066.
[2] Hassoun PM ML, Barberà JA, Eddahibi S, Flores SC, Grimminger F, Jones PL, Maitland ML, Michelakis ED, Morrell NW, Newman JH,Rabinovitch M, Schermuly R, Stenmark KR, Voelkel NF, Yuan JX, Humbert M. Inflammation, growth factors, and pulmonary vascular remodeling. J Am Coll Cardiol. 2009; 54:S10–S19.
[3] Schermuly RT GH, Wilkins MR, Grimminger F. Mechanisms of disease: pulmonary arterial hypertension. Nat Rev Cardiol. 2011; 8:443-455.
[4] Tuder RM. Pathology of pulmonary arterial hypertension. Semin Respir Crit Care Med 2009; 30:376-85.
[5] Price LC WS, Perros F, Dorfmüller P, Huertas A, Montani D, Cohen-Kaminsky S, Humbert M. Inflammation in pulmonary arterial hypertension. Chest. 2012; 141:210-221.
[6] Stacher E GB, Hunt JM, Gandjeva A, Groshong SD, McLaughlin VV, Jessup M, Grizzle WE, Aldred MA, Cool CD, Tuder RM. Modern age pathology of pulmonary arterial hypertension. Am J Respir Crit Care Med. 2012; 186:261-272.
[7] Farber HW, Miller DP, McGoon MD, Frost AE, Benton WW and Benza RL. Predicting outcomes in pulmonary arterial hypertension based on the 6-minute walk distance. J Heart Lung Transplant. 2015; 34:362-8.
[8] Schermuly RT, Dony E, Ghofrani HA, Pullamsetti S, Savai R, Roth M, Sydykov A, Lai YJ, Weissmann N, Seeger W and Grimminger F. Reversal of experimental pulmonary hypertension by PDGF inhibition. J Clin Invest. 2005; 115:2811-21.
[9] Zhao L AA, Wang L, Fang W, Dabral S, Dubois O, Cupitt J, Pullamsetti SS, Cotroneo E, Jones H, Tomasi G, Nguyen QD, Aboagye EO, El-Bahrawy MA, Barnes G, Howard LS, Gibbs JS, Gsell W, He JG, Wilkins MR. Heterogeneity in lung (18)FDG uptake in pulmonary arterial hypertension: potential of dynamic (18)FDG positron emission tomography with kinetic analysis as a bridging biomarker for pulmonary vascular remodeling targeted treatments. Circulation 2013; 128:1214-1224.
[10] Hoeper MM, Barst RJ, Bourge RC, Feldman J, Frost AE, Galie N, Gomez-Sanchez MA, Grimminger F, Grunig E, Hassoun PM, Morrell NW, Peacock AJ, Satoh T, Simonneau G, Tapson VF, Torres F, Lawrence D, Quinn DA and Ghofrani HA. Imatinib mesylate as add-on therapy for pulmonary arterial hypertension: results of the randomized IMPRES study. Circulation. 2013;127:1128-38.
[11] Salskov A TV, Grierson J, Vesselle H. . FLT: measuring tumor cell proliferation in vivo with positron emission tomography and 3'-deoxy-3'-[18F]fluorothymidine. Semin Nucl Med. 2007; 37:429-39.
[12] Shields AF GJ, Dohmen BM, Machulla HJ, Stayanoff JC, Lawhorn-Crews JM, Obradovich JE, Muzik O, Mangner TJ. Imaging proliferation in vivo with [F-18]FLT and positron emission tomography. Nat Med 1998; 4:1334-1336.
[13] Vesselle H GJ, Muzi M, Pugsley JM, Schmidt RA, Rabinowitz P, Peterson LM, Vallières E, Wood DE. In vivo validation of 3'deoxy-3'-[(18)F]fluorothymidine ([(18)F]FLT) as a proliferation imaging tracer in humans: correlation of [(18)F]FLT uptake by positron emission tomography with Ki-67 immunohistochemistry and flow cytometry in human lung tumors. . Clin Cancer Res. 2002; 8:3315-3323.
[14] Barthel H CM, Collingridge DR, Hutchinson OC, Osman S, He Q, Luthra SK, Brady F, Price PM, Aboagye EO. 3'-deoxy-3'-[18F]fluorothymidine as a new marker for monitoring tumor response to antiproliferative therapy in vivo with positron emission tomography. Cancer Res. 2003; 63:3791-3798.
[15] Rasey JS GJ, Wiens LW, Kolb PD, Schwartz JL. Validation of FLT uptake as a measure of thymidine kinase-1 activity in A549 carcinoma cells. J Nucl Med 2002; 43:1210-1217.
[16] Schwartz JL TY, Jordan R, Grierson JR, Krohn KA. Monitoring tumor cell proliferation by targeting DNA synthetic processes with thymidine and thymidine analogs. J Nucl Med. 2003; 44:2027-2032.
[17] Paproski RJ NA, Yao SY, Graham K, Young JD, Cass CE. The role of human nucleoside transporters in uptake of 3'-deoxy-3'-fluorothymidine. Mol Pharmacol 2008; 74:1372-1380.
[18] Barthel H PM, Latigo J, He Q, Brady F, Luthra SK, Price PM, Aboagye EO. The uptake of 3'-deoxy-3'-[18F]fluorothymidine into L5178Y tumours in vivo is dependent on thymidine kinase 1 protein levels. Eur J Nucl Med Mol Imaging. 2005; 32:257-263.
[19] Shields AF. Positron emission tomography measurement of tumor metabolism and growth: its expanding role in oncology. Mol Imaging Biol. 2006; 8:141-150.
[20] Grierson JR SJ, Muzi M, Jordan R, Krohn KA. Metabolism of 3'-deoxy-3'-[F-18]fluorothymidine in proliferating A549 cells: validations for positron emission tomography. Nucl Med Biol. 2004; 31:829-837.
[21] Arnér ES ES. Mammalian deoxyribonucleoside kinases. Pharmacol Ther. 1995; 67:155-186.
[22] Willaime JM TF, Kenny LM, Aboagye EO. Quantification of intra-tumour cell proliferation heterogeneity using imaging descriptors of 18F fluorothymidine-positron emission tomography. Phys Med Biol 2013; 58:187-203.
[23] Galiè N HM, Vachiery JL, Gibbs S, Lang I, Torbicki A, Simonneau G, Peacock A, Vonk Noordegraaf A, Beghetti M, Ghofrani A, Gomez Sanchez MA, Hansmann G, Klepetko W, Lancellotti P, Matucci M, McDonagh T, Pierard LA, Trindade PT, Zompatori M, Hoeper M. 2015 ESC/ERS Guidelines for the diagnosis and treatment of pulmonary hypertension: The Joint Task Force for the Diagnosis and Treatment of Pulmonary Hypertension of the European Society of Cardiology (ESC) and the European Respiratory Society (ERS): Endorsed by: Association for European Paediatric and Congenital Cardiology (AEPC), International Society for Heart and Lung Transplantation (ISHLT). Eur Respir J. 2015; 46:903-975.

[24] Frings V YM, Hoyng LL, Golla SS, Windhorst AD, Schuit RC, Lammertsma AA, Hoekstra OS, Smit EF, Boellaard R; for QuIC-ConCePT Consortium. Assessment of simplified methods to measure 18F-FLT uptake changes in EGFR-mutated non-small cell lung cancer patients undergoing EGFR tyrosine kinase inhibitor treatment. J Nucl Med. 2014; 55:1417-1423.
[25] van de Veerdonk MC KT, Marcus JT, Mauritz GJ, Heymans MW, Bogaard HJ, Boonstra A, Marques KM, Westerhof N, Vonk-Noordegraaf A. Progressive right ventricular dysfunction in patients with pulmonary arterial hypertension responding to therapy. J Am Coll Cardiol. 2011; 58:2511-2519.
[26] Frings V dLA, Yaqub M, Schuit RC, van der Veldt AA, Hoekstra OS, Smit EF, Boellaard R. Methodological Considerations in Quantification of 3'-Deoxy-3'-[18F]Fluorothymidine Uptake Measured with Positron Emission Tomography in Patients with Non-Small Cell Lung Cancer. Mol Imaging Biol. 2014; 16:136-145.
[27] Hoekstra CJ HO, Lammertsma AA. On the use of the injection catheter for venous blood sampling in quantitative FDG PET studies. Eur J Nucl Med. 2000; 27:1579.
[28] Akaike H. A new look at the statistical model identification. IEEE Transactions on automatic control. 1974; 19:716-723.
[29] Muzi MM, DA.; Grierson, JR.; Wells, JM.; Vesselle, H.; Krohn, KA. Kinetic modeling of 3'-deoxy-3'-fluorothymidine in somatic tumors: mathematical studies. J Nucl Med. 2005; 46:371-380.
[30] Ghigna MR, Guignabert C, Montani D, Girerd B, Jais X, Savale L, Herve P, Thomas de Montpreville V, Mercier O, Sitbon O, Soubrier F, Fadel E, Simonneau G, Humbert M and Dorfmuller P. BMPR2 mutation status influences bronchial vascular changes in pulmonary arterial hypertension. Eur Respir J. 2016.
[31] Munk OL. Model-independent plot of dynamic PET data facilitates data interpretation and model selection. J Theor Biol. 2012; 295:1-8.
[32] Buck AK, Halter G, Schirrmeister H, Kotzerke J, Wurziger I, Glatting G, Mattfeldt T, Neumaier B, Reske SN and Hetzel M. Imaging proliferation in lung tumors with PET: 18F-FLT versus 18F-FDG. J Nucl Med. 2003; 44:1426-31.
[33] van Waarde A, Cobben DC, Suurmeijer AJ, Maas B, Vaalburg W, de Vries EF, Jager PL, Hoekstra HJ and Elsinga PH. Selectivity of 18F-FLT and 18F-FDG for differentiating tumor from inflammation in a rodent model. J Nucl Med. 2004; 45:695-700.
[34] Yamamoto Y, Nishiyama Y, Ishikawa S, Nakano J, Chang SS, Bandoh S, Kanaji N, Haba R, Kushida Y and Ohkawa M. Correlation of 18F-FLT and 18F-FDG uptake on PET with Ki-67 immunohistochemistry in non-small cell lung cancer. Eur J Nucl Med Mol Imaging. 2007; 34:1610-6.
[35] Yamamoto Y, Nishiyama Y, Kimura N, Ishikawa S, Okuda M, Bandoh S, Kanaji N, Asakura M and Ohkawa M. Comparison of (18)F-FLT PET and (18)F-FDG PET for preoperative staging in non-small cell lung cancer. Eur J Nucl Med Mol Imaging. 2008; 35:236-45.
[36] Yap CS, Czernin J, Fishbein MC, Cameron RB, Schiepers C, Phelps ME and Weber WA. Evaluation of thoracic tumors with 18F-fluorothymidine and 18F-fluorodeoxyglucose-positron emission tomography. Chest. 2006; 129:393-401.
[37] Tehrani OS and Shields AF. PET imaging of proliferation with pyrimidines. J Nucl Med. 2013; 54:903-12.

Supplement Figures

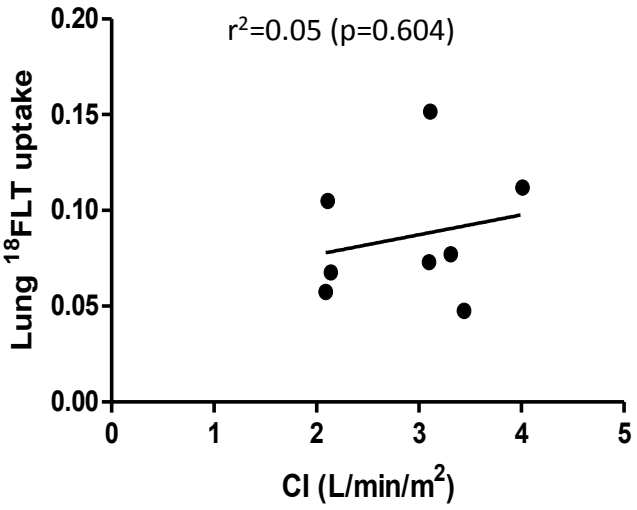

Figure I. There was no significant correlation between lung 18FLT uptake (k3) and cardiac index (CI).

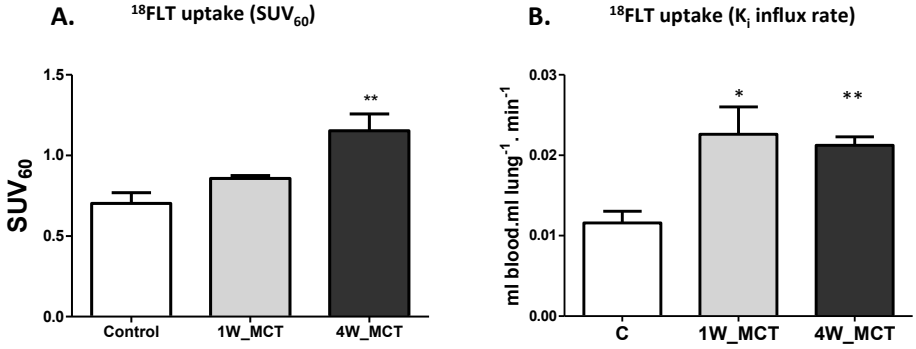

Figure II. A. Standard uptake value of Lung 18FLT uptake in monocrotaline (MCT) rat was increased after 4 weeks (4W_MCT) compare to controls. B. Two tissue 4K (2T4K) compartmental analysis demonstrated a significantly increased lung 18FLT influx Ki in rats after 1 week (1W_MCT) and 4 weeks (4W_MCT) of monocrotaline (MCT) injection.

CHAPTER 9

Increased native T1-values at the interventricular insertion regions in precapillary pulmonary hypertension

International Journal Cardiovascular Imaging 2016

OA Spruijt[1], L Vissers[1], HJ Bogaard[1], MBM Hofman[2], A Vonk Noordegraaf[1], JT Marcus[2]

[1]Department of Pulmonary Medicine, VU University Medical Center, Amsterdam
[2]Department of Physics and Medical Technology, VU University Medical Center, Amsterdam

Abstract

Introduction: Cardiac magnetic resonance imaging of the pressure overloaded right ventricle (RV) of precapillary pulmonary hypertension (PH) patients, exhibits Late Gadolinium Enhancement at the interventricular insertion regions, a phenomenon which has been linked to focal fibrosis. Native T1-mapping is an alternative technique to characterize myocardium and has the advantage of not requiring the use of contrast agents. The aim of this study was to characterize the myocardium of idiopathic pulmonary arterial hypertension (IPAH), systemic scleroderma related PH (PAH-Ssc) and chronic thromboembolic PH (CTEPH) patients using native T1-mapping and to see whether native T1-values were related to disease severity. Furthermore, we compared native T1-values between the different precapillary PH categories.

Methods: Native T1-mapping was performed in 46 IPAH, 14 PAH-SSc and 10 CTEPH patients and 10 control subjects. Native T1-values were assessed using regions of interest at the RV and LV free wall, interventricular septum and interventricular insertion regions.

Results: In PH patients, native T1-values of the interventricular insertion regions were significantly higher than the native T1-values of the RV free wall, LV free wall and interventricular septum. Native T1-values at the insertion regions were significantly related to disease severity. Native T1-values were not different between IPAH, PAH-Ssc and CTEPH patients.

Conclusions: Native T1-values of the interventricular insertion regions are significantly increased in precapillary PH and are related to disease severity. Native T1-mapping can be developed as an alternative technique for the characterization of the interventricular insertion regions and has the advantage of not requiring the use of contrast agents.

Introduction

Precapillary pulmonary hypertension (PH) is characterized by an increase in pulmonary vascular resistance (PVR) and right ventricular (RV) adaption to the increased load is one of the main determinants of patient outcome [1]. A well-established method to non-invasively characterize the myocardium is the assessment of late gadolinium enhancement (LGE) by cardiac magnetic resonance imaging (CMRI). Previous studies in PH patients showed delayed enhancement of the interventricular insertion regions [2-5] and linked this phenomenon to focal fibrosis [4, 6]. In addition, LGE was shown to correlate with disease severity [2, 4, 5]. A major drawback of the assessment of LGE is the need for the administration of the contrast agent gadolinium. Its toxicity due to depositions in other parts of the body, for example in the brain [7], is not completely understood, but gadolinium administration is contra-indicated in patients with renal insufficiency. Moreover, the LGE technique is not suitable to detect more diffuse myocardial pathologies since the calculation of the threshold of abnormal enhancement depends on a reference area of myocardium [8]. An alternative technique to characterize the myocardium is native T1-mapping. T1-mapping quantifies the T1 relaxation time per pixel tissue and different tissues show a characteristic range of T1-values [9-11]. Native T1-values increase when the heart is affected by edema and diffuse or focal fibrosis [12-20]. To quantify native T1-values, there is no need for a reference area of myocardium, making it possible to directly quantify the total myocardium. Moreover, native T1-values can be determined without the use of contrast agents [10]. Therefore, the aim of this study was to characterize the myocardium of idiopathic pulmonary arterial hypertension (IPAH), systemic scleroderma related PH (PAH-Ssc) and chronic thromboembolic PH (CTEPH) patients using native T1-mapping and to see whether native T1-values were related to disease severity. Furthermore, since the difference in presence of histologically confirmed myocardial fibrosis between these forms of precapillary PH vary between studies [21-23], we compared native T1-values between the different precapillary PH categories.

Methods

Subjects

We retrospectively analyzed all available native T1-mapping data of IPAH patients (n=46), PAH-SSc patients (n=14) and CTEPH patients (n=10) scanned between June 2011 and March 2014 in the VU University Medical Center. Data was acquired in the context of an ongoing prospective research

program to investigate the role of CMRI in the evaluation of PH patients. The study was approved by The Medical Ethics Review Committee of the VU University Medical Center. Since this study did not fall within the scope of the Medical Research Involving Human Subjects Act (WMO), the study was approved without requirement of an informed consent statement. IPAH, PAH-SSc and CTEPH were diagnosed according to ATS/ERS guidelines [24]. Both treatment naïve patients and patients under optimal PAH-therapies were included in the study. Patients with left sided heart failure and congenital heart disease were excluded from this study. Furthermore, native T1-mapping was performed in 10 healthy volunteers, who gave written informed consent for usage of the data for this study.

CMRI protocol

Native T1-mapping was acquired on a Siemens 1.5 T Avanto scanner. A single breath-hold Modified Look-Locker Inversion-recovery (MOLLI) pulse sequence was used on a mid-ventricular short axis imaging plane. Three, three, and five non-segmented images were acquired at end-diastole within 17 heart beats to sample the recovery of longitudinal magnetization after the inversion pulse. Minimal inversion time was 100 ms [25]. Inplane motion correction was applied. Motion correction was applied by exploiting the known exponential form of inversion recovery and treating the motion and inversion recovery as a joint estimation problem. This was performed with the generation of a series of motion free synthetic inversion recovery images which were used at each inversion time for registration with the measured MOLLI images [26].

CMRI analyses

Native T1-values were assessed using regions of interest (ROIs) at the interventricular insertion regions, the RV free wall, LV free wall, interventricular septum and interventricular insertion regions on mid-ventricular short axis T1-maps. ROIs were manually drawn as illustrated in figure 1. ROIs were carefully assessed and the borders of the myocardium were avoided to prevent partial volume effects due to surrounding tissue or the blood pool. ROIs in the RV free wall could be accurately positioned in all patients in the inferior part of the RV free wall (figure 1). We attempted to draw ROIs of the total RV free wall, but this was not feasible in the majority of patients because the RV free wall was too thin. Native T1-values of the RV wall could not be assessed in the control subjects because in all control subjects the RV wall was too thin. T1-values of the interventricular insertion

regions were averaged over the inferior and superior insertion regions. Ventricular volumes were assessed as described before [1].

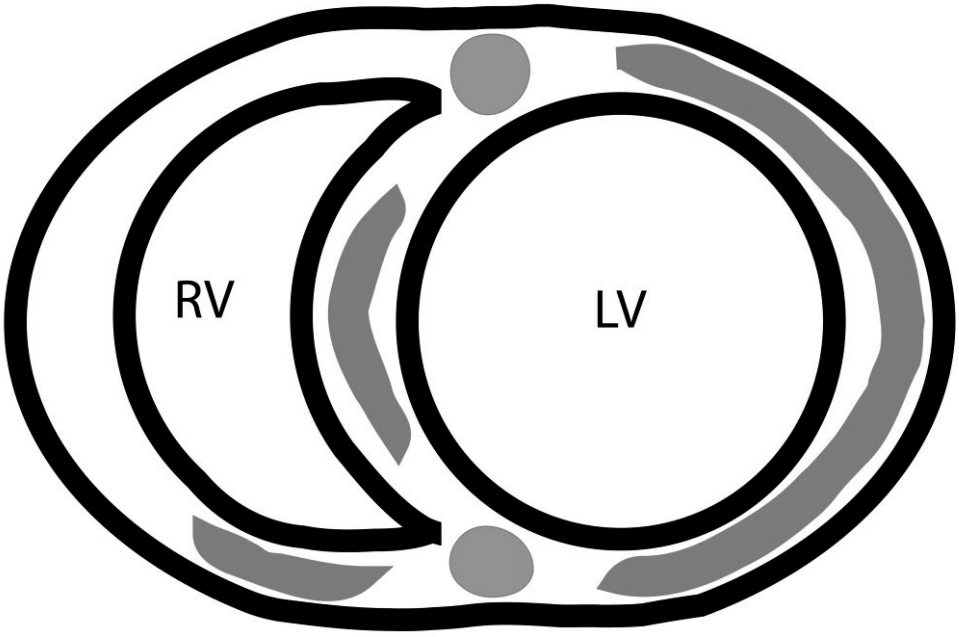

Figure 1: Schematic illustration of ROIs. Schematic illustration of a mid-ventricular short-axis image. ROIs of the different regions are marked. ROIs of the LV free wall covered the total LV free wall. ROIs of the RV free wall, were only analyzed in the inferior part of the RV free wall. Attempts to cover the total RV free wall failed because in a majority of the patients the free wall was too thin, resulting in unreliable native T1-values due to partial volume effects.

Statistical methods

Data are presented as mean ± standard deviation, unless stated differently. In PH patients, native T1-values between the RV free wall, LV free wall, interventricular septum and interventricular insertion regions were compared using repeated measures one-way ANOVA with Bonferroni post-hoc correction. In control subjects, native T1-values between the LV free wall, interventricular septum and interventricular insertion regions were compared using repeated measures one-way ANOVA with Bonferroni post-hoc correction. Native T1-values of the different regions of the myocardium between IPAH, PAH-SSc and CTEPH patients and healthy controls were compared using one-way ANOVA with Bonferroni post-hoc correction. In PH patients, pearson correlation analysis

were applied to assess the relation between native T1-values and hemodynamic and cardiac parameters of disease severity: right atrial pressure (RAP), mean pulmonary artery pressure (mPAP), pulmonary vascular resistance (PVR), cardiac index (CI), RV stroke volume index (SVI), RV end-diastolic volume index (RVEDVI), RV end-systolic volume index (RVESVI), RV ejection fraction (RVEF) and NT Pro-BNP. All analyses were performed using SPSS for Windows version 20.0 and Graphpad Prism for Windows version 5.0. P-values <0.05 were considered statistically significant.

Results

Patient characteristics, hemodynamics and standard CMRI measurements are summarized in table 1.

	N=70 (IPAH n=46; PAH-SSc n=14; CTEPH n=10)	**Control subjects (n=10)**	**P-value**
Female (%)	73	40	0.04
Age (years)	54 ± 16	20 ± 1	<0.001
Heart rate (bpm)	79 ± 14	74 ± 11	0.280
Hemodynamics:			
mPAP (mmHg)	47 ± 13	-	
PAWP (mmHg)	8 ± 3	-	
PVR (dyn*s/cm^5)	634 ± 342	-	
RAP (mmHg)	7 ± 4	-	
CI (L/min/m^2)	3 ± 1	-	
CMRI:			
RVEDVI (ml/m^2)	82 ± 38	-	
RVESVI (ml/m^2)	51 ± 37	-	
RVSVI (ml/m^2)	30 ± 12	-	
RVEF (%)	42 ± 16	-	
LVEF (%)	65 ± 11	-	
NT ProBNP (ng/L)	1393 ± 2283	-	

Table 1: Patient characteristics. mPAP = mean pulmonary artery pressure; PAWP = pulmonary arterial wedge pressure; PVR = pulmonary vascular resistance, RAP = right atrial pressure; CI = cardiac index; CMRI = cardiac magnetic resonance imaging; RVEDVI = indexed right ventricular end-diastolic volume; RVESVI = indexed right ventricular end-systolic volume; RVSVI = right ventricular stroke volume index; RVEF = right ventricular ejection fraction; LVEF = left ventricular ejection fraction.

Control subjects were significantly younger than PH patients (20 ± 1 and 54 ± 16 p<0.001). 40% of the control subjects were female. Heart rate (HR) was not significantly different between control subjects (74 ± 11bpm) and PH patients (79 ± 14bpm).

Native T1-values in PH patients and control subjects

In PH patients, native T1-values of the interventricular insertion regions (1060 ± 70ms) were significantly higher than the native T1-values of the RV free wall, LV free wall and interventricular septum (figure 2 and 3).

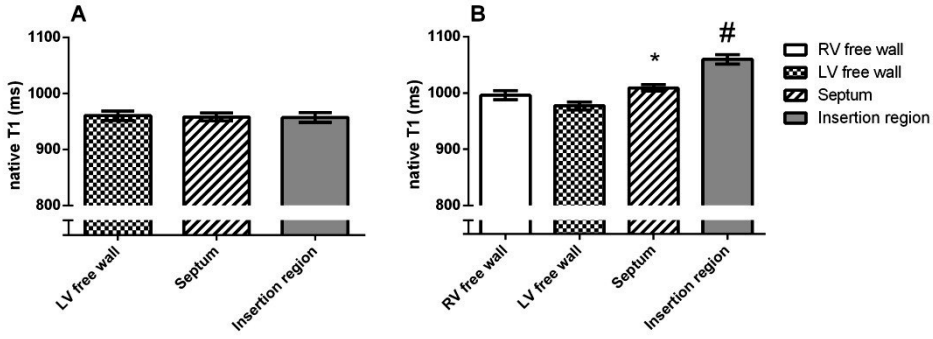

Figure 2: Native T1-values(ms) of the RV free wall, LV free wall, interventricular septum and the interventricular insertion regions. Data is presented as mean and standard error of the mean. A: Regional differences in the myocardium of control subjects. No regional differences were found in control subjects. B: Regional differences in the myocardium of PH patients. T1-values of the RV free wall of PH patients were not different from T1-values of the LV free wall and interventricular septum. * = T1-values of the interventricular septum of PH patients were significantly higher compared to native T1-values of the LV free wall. # = Native T1-values of the interventricular insertion regions of PH patients were significantly higher compared to native T1-values of the RV free wall, LV free wall and interventricular septum.

Native T1-values of the RV free wall (996 ± 69ms) were not significantly different from the native T1-values of the LV free wall (977 ± 60ms) and interventricular septum (1009 ± 48ms). Native T1-values of the LV free wall were significantly lower than the native T1-values of the interventricular septum.

In control subjects, no differences were found between native T1-values of the LV free wall (961 ± 26ms), interventricular septum (958 ± 23ms) and interventricular insertion regions (957 ± 27ms) (figure 2).

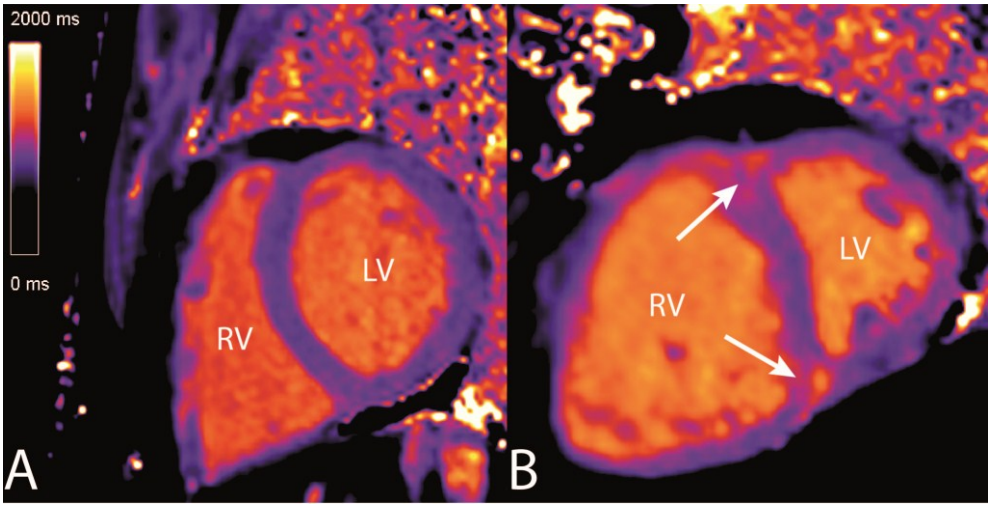

Figure 3: Native T1-maps showing increased native T1-values at the interventricular insertion regions. Two examples of native T1-maps of a control subject (A) and an IPAH (B) patient. The white arrows indicate the increased native T1-values at the interventricular insertion regions.

Relation between native T1-values of the interventricular insertion regions and disease severity in PH patients

In PH patients, native T1-values of the interventricular insertion regions were significantly related to RAP (pearson r=0.310; p=0.01), RVEDVI (pearson r=0.376; p=0.001), RVESVI (pearson r = 0.358 p=0.002), RVEF (pearson r=-0.282; p=0.018) and NT pro-BNP (pearson r=0.392; p=0.001), but not to CI, PVR, RVSVI and mPAP (figure 4).

Comparison of native T1-values between IPAH, CTEPH and PAH-Ssc patients and control subjects

Native T1-values of the RV free wall, LV free wall, interventricular septum and the interventricular insertion regions were not significantly different between IPAH, CTEPH and PAH-SSc patients.

Native T1-values of the LV free wall were not significantly different between control subjects and PH patients. Native T1-values of the interventricular septum was significantly higher in IPAH and CTEPH patients compared to control subjects.

Native T1-values of the interventricular insertion regions were significantly higher in all PH categories compared to control subjects (figure 5).

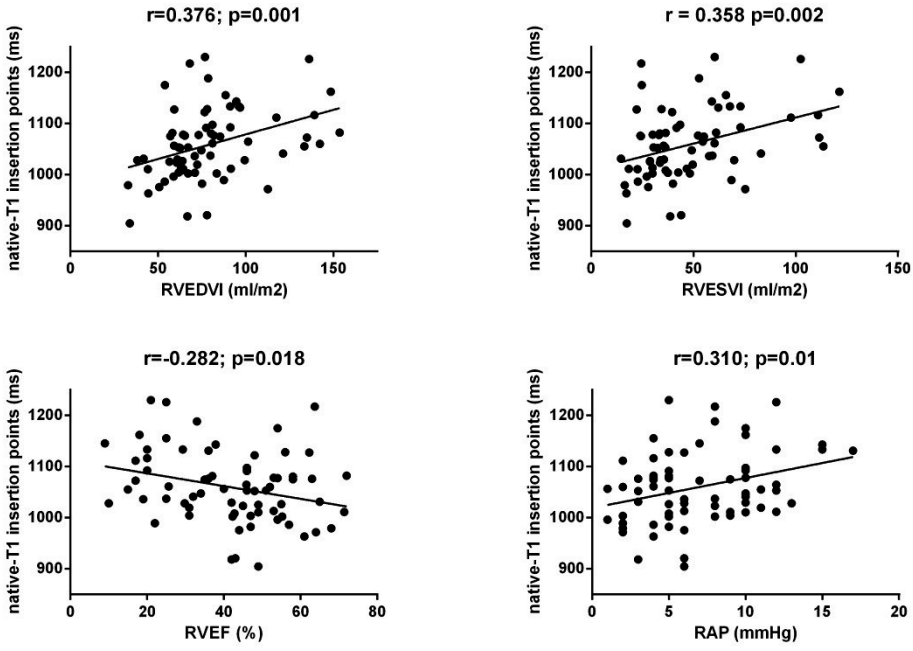

Figure 4: Correlations between native T1-values of the interventricular insertion regions and RVEDVI, RVESVI, RVEF and RAP in PH patients. Native T1-values of the interventricular insertion regions of PH patients were significantly related to RVEDVI, RVESVI, RVEF and RAP. RVEDVI = right ventricular end-diastolic volume index; RVESVI = right ventricular end-systolic volume index; RVEF = right ventricular ejection fraction; RAP = right atrial pressure.

Discussion

This is the first study using the native T1-mapping technique to characterize the myocardium in precapillary PH patients. In PH patients, native T1-values of the interventricular insertion regions were significantly increased compared to the native T1-values of the RV free wall, LV free wall and interventricular septum. Furthermore, native T1-values of the interventricular insertion regions were related to disease severity.

Increased Native T1-values of the interventricular insertion regions

LGE studies in PH showed the late enhancement of the interventricular insertion regions and it has been suggested that this phenomenon most likely reflect locally increased focal fibrosis [2-5].

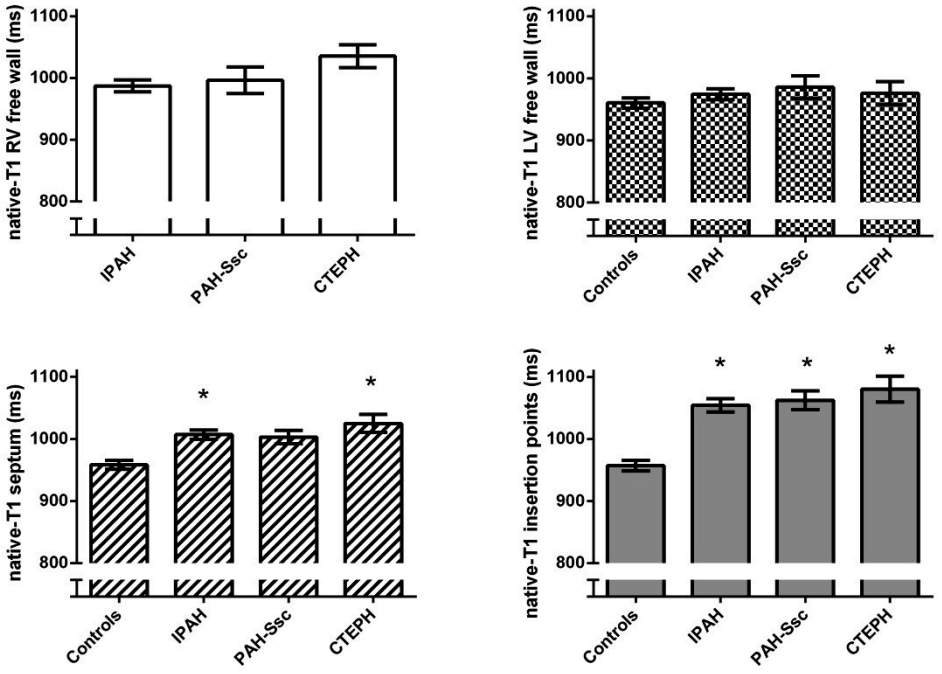

Figure 5: Comparison of native T1-values between IPAH, PAH-SSc and CTEPH patients and control subjects. Data is presented as mean and standard error of the mean. The Y-axis Native T1-values of the RV free wall (blue), LV free wall (red), interventricular septum (yellow) and interventricular insertion regions (green) were not significantly different between IPAH, PAH-SSc and CTEPH patients. Native T1-values of the LV free wall was not significantly different between control subjects and PH patients. Native T1-values of the interventricular septum was significantly higher in IPAH and CTEPH patients compared to control subjects. Native T1-values of the interventricular insertion regions were significantly increased in all PH categories compared to control subjects.

This suggestion was strengthened by McCann et al. by finding increased focal fibrosis at the interventricular insertion regions in the histology of the myocardium of two PH patients [4]. Bull et al. linked the native T1-values to histological findings in patients with severe aortic stenosis and found a good correlation between native T1-values and the collagen volume fraction [12]. Furthermore, a recent study investigating native T1-values in a chronic PH animal model also found increased native T1-values at the interventricular insertion regions. In this study, the PH group showed increased interstitial collagen at the interventricular insertion regions compared to the sham group [27]. Therefore, the increased native T1-values of the interventricular insertion regions

most likely reflect locally increased focal fibrosis. However, McCann et al. [4] also described edema at the interventricular insertion regions, which also can contribute to an increase in native T1-values [17]. It is suggested that predilection for fibrosis to develop at the interventricular insertion regions is caused by mechanical stress due to the bowing of the interventricular septum into the LV [2] which is often seen in precapillary PH patients. However, late enhancement at the interventricular insertion regions is also described in patients with hypertrophic cardiomyopathy [3, 28] indicating that this phenomenon is not specific for a pressure overloaded RV.

Increased native T1-values of the interventricular insertion regions were moderately, but significantly related to disease severity. This is in line with previous LGE studies showing comparable correlations between the late enhancement of the interventricular insertion regions and RVEF, RV volumes and mPAP [2, 4, 5]. Furthermore, similar correlations were found between native T1-values of the interventricular insertion regions and measures of disease severity [27]. The correlations between native T1-values of the interventricular insertion regions and RV functional measures and NT-proBNP is probably related to the associated increase in RV wall tension. It has been shown that RV wall tension is associated with the delay in time to peak shortening of the RV, causing the leftward shift of the interventricular septum during late RV systole [29]. The right-to-leftward shifting of the interventricular septum probably increases the mechanical shear stress on the interventricular insertion regions.

In a recent study, native T1-values were assessed in the RV of healthy subjects and the authors found increased native T1-values in the RV free wall compared to the LV free wall and suggested that this finding could be due to a higher collagen content of the RV free wall [30]. In the PH patients in our study, native T1-values of the RV free wall were not significantly higher than those of the LV free wall and were in the same range as the native T1-values of the RV free wall in healthy subjects [30]. We could not assess the native T1-values of the RV wall in our control subjects because the wall was too thin. Kawel-Boehm et al. [30] could assess native T1-values of the RV free wall of healthy subjects because they performed native T1-mapping at the end-systolic phase.

Native T1-values of the LV free wall were not significantly different between PH patients and control subjects and were in the same range as native T1-values of the LV free wall conducted in a large cohort of healthy subjects of the same age [11]. This is in line with LGE studies showing no late enhancement in the myocardium of precapillary PH patients apart from the interventricular insertion regions [2-5].

Native T1-values between IPAH, PAH-SSc and CTEPH patients

A recent study of Ntusi et al [18] found increased native T1-values of the total myocardium in no-PH systemic sclerosis patients compared to controls. We found no differences in native T1-values between IPAH, PAH-SSc and CTEPH patients. The presence of myocardial fibrosis found in these different forms of precapillary PH differ between studies. No differences in myocardial fibrosis of RV free wall tissue were found between controls, IPAH and PAH-SSc patients [21], while others found an increased amount of myocardial fibrosis in PAH patients compared to no-PH controls [22]. Ntusi et al. [18] included both limited cutaneous (lcSSc) and diffuse cutaneous systemic sclerosis (dcSSc) patients, while in our study we only included patients with lcSSc. It is known that cardiac involvement of systemic sclerosis is much higher in dcSSc patients compared to lcSSc patients [31], which can explain the differences in results.

Limitations

We could not assess native T1-values of the total RV free wall, since in most patients the RV free wall was too thin to avoid partial volume effects. Only the inferior part of the RV free wall could be accurately assessed in all patients. Although we did not assess the total RV free wall, large variances in native T1-values between different regions of the RV free wall are not expected in a pressure overloaded RV.

Our study is a retrospective analysis and we included both treatment naïve and treated PH patients. From our data we cannot rule out any treatment effects on the measured native T1-values.

The control subjects were significantly younger compared to PH patients. It is known that age can influence native T1-values of the myocardium, with higher native T1-values found at a younger age [11]. Since native T1-values of the interventricular insertion regions were significantly increased in PH patients compared to control subjects, this only strengthens our findings.

The MOLLI technique as we applied is known to slightly underestimate native T1 values at higher heart rates [32]. The main conclusions in this study rely on regional differences, and are therefore not affected. Moreover, heart rates were not different between patients and controls. Another potential confounder is the effect of the T2 relaxation time: the absolute T1 values obtained with the MOLLI technique defer from their actual values in tissues with short T2 [33]. Whether or not T2-changes play a role in our study, is still to be explored. A technique such as SASHA [34] is more accurate, however, the values obtained with this SACHA technique show a larger variability and the MOLLI method performs more precisely [35].

Conclusions

Native T1-values of the interventricular insertion regions are increased compared to native T1-values of the LV free wall, RV free wall and interventricular septum in patients with precapillary PH and are related to disease severity. Native-T1 values are not different between IPAH, PAH-SSc and CTEPH patients. Native T1-mapping can be an alternative for the characterization of the interventricular insertion regions without the use of contrast agents.

References

[1] van de Veerdonk MC, Kind T, Marcus JT, Mauritz GJ, Heymans MW, Bogaard HJ, et al. Progressive right ventricular dysfunction in patients with pulmonary arterial hypertension responding to therapy. Journal of the American College of Cardiology. 2011; 58:2511-9

[2] Blyth KG, Groenning BA, Martin TN, Foster JE, Mark PB, Dargie HJ, et al. Contrast enhanced-cardiovascular magnetic resonance imaging in patients with pulmonary hypertension. European heart journal. 2005; 26:1993-9

[3] McCann GP, Beek AM, Vonk-Noordegraaf A, van Rossum AC. Delayed contrast-enhanced magnetic resonance imaging in pulmonary arterial hypertension. Circulation. 2005; 112:e268

[4] McCann GP, Gan CT, Beek AM, Niessen HW, Vonk Noordegraaf A, van Rossum AC. Extent of MRI delayed enhancement of myocardial mass is related to right ventricular dysfunction in pulmonary artery hypertension. Ajr. 2007; 188:349-55

[5] Sanz J, Dellegrottaglie S, Kariisa M, Sulica R, Poon M, O'Donnell TP, et al. Prevalence and correlates of septal delayed contrast enhancement in patients with pulmonary hypertension. The American journal of cardiology. 2007; 100:731-5

[6] Moon JC, Reed E, Sheppard MN, Elkington AG, Ho SY, Burke M, et al. The histologic basis of late gadolinium enhancement cardiovascular magnetic resonance in hypertrophic cardiomyopathy. Journal of the American College of Cardiology. 2004; 43:2260-4

[7] McDonald RJ, McDonald JS, Kallmes DF, Jentoft ME, Murray DL, Thielen KR, et al. Intracranial Gadolinium Deposition after Contrast-enhanced MR Imaging. Radiology. 2015; 275:772-82

[8] Kwong RY, Farzaneh-Far A. Measuring myocardial scar by CMR. J Am Coll Cardiol Img. 2011; 4:157-60

[9] Burt JR, Zimmerman SL, Kamel IR, Halushka M, Bluemke DA. Myocardial t1 mapping: techniques and potential applications. Radiographics. 2014; 34:377-95

[10] Moon JC, Messroghli DR, Kellman P, Piechnik SK, Robson MD, Ugander M, et al. Myocardial T1 mapping and extracellular volume quantification: a Society for Cardiovascular Magnetic Resonance (SCMR) and CMR Working Group of the European Society of Cardiology consensus statement. J Cardiovasc Magn Reson. 2013; 15:92

[11] Piechnik SK, Ferreira VM, Lewandowski AJ, Ntusi NA, Banerjee R, Holloway C, et al. Normal variation of magnetic resonance T1 relaxation times in the human population at 1.5 T using ShMOLLI. J Cardiovasc Magn Reson. 2013; 15:13

[12] Bull S, White SK, Piechnik SK, Flett AS, Ferreira VM, Loudon M, et al. Human non-contrast T1 values and correlation with histology in diffuse fibrosis. Heart (British Cardiac Society). 2013; 99:932-7

[13] Dall'Armellina E, Piechnik SK, Ferreira VM, Si QL, Robson MD, Francis JM, et al. Cardiovascular magnetic resonance by non contrast T1-mapping allows assessment of severity of injury in acute myocardial infarction. J Cardiovasc Magn Reson. 2012; 14:15

[14] Ferreira VM, Piechnik SK, Dall'Armellina E, Karamitsos TD, Francis JM, Choudhury RP, et al. Non-contrast T1-mapping detects acute myocardial edema with high diagnostic accuracy: a comparison to T2-weighted cardiovascular magnetic resonance. J Cardiovasc Magn Reson. 2012; 14:42

[15] Ferreira VM, Piechnik SK, Dall'Armellina E, Karamitsos TD, Francis JM, Ntusi N, et al. T(1) mapping for the diagnosis of acute myocarditis using CMR: comparison to T2-weighted and late gadolinium enhanced imaging. J Am Coll Cardiol Img. 2013; 6:1048-58

[16] Ferreira VM, Piechnik SK, Dall'Armellina E, Karamitsos TD, Francis JM, Ntusi N, et al. Native T1-mapping detects the location, extent and patterns of acute myocarditis without the need for gadolinium contrast agents. J Cardiovasc Magn Reson. 2014; 16:36

[17] Maestrini V, Treibel TA, White SK, Fontana M, Moon JC. T1 Mapping for Characterization of Intracellular and Extracellular Myocardial Diseases in Heart Failure. Current cardiovascular imaging reports. 2014; 7:9287

[18] Ntusi NA, Piechnik SK, Francis JM, Ferreira VM, Rai AB, Matthews PM, et al. Subclinical myocardial inflammation and diffuse fibrosis are common in systemic sclerosis--a clinical study using myocardial T1-mapping and extracellular volume quantification. J Cardiovasc Magn Reson. 2014; 16:21

[19] Puntmann VO, D'Cruz D, Smith Z, Pastor A, Choong P, Voigt T, et al. Native myocardial T1 mapping by cardiovascular magnetic resonance imaging in subclinical cardiomyopathy in patients with systemic lupus erythematosus. Circ Cardiovasc Imaging. 2013; 6:295-301

[20] Puntmann VO, Voigt T, Chen Z, Mayr M, Karim R, Rhode K, et al. Native T1 mapping in differentiation of normal myocardium from diffuse disease in hypertrophic and dilated cardiomyopathy. J Am Coll Cardiol Img. 2013; 6:475-84

[21] Overbeek MJ, Mouchaers KT, Niessen HM, Hadi AM, Kupreishvili K, Boonstra A, et al. Characteristics of interstitial fibrosis and inflammatory cell infiltration in right ventricles of systemic sclerosis-associated pulmonary arterial hypertension. International journal of rheumatology. 2010; 2010

[22] Rain S, Handoko ML, Trip P, Gan CT, Westerhof N, Stienen GJ, et al. Right ventricular diastolic impairment in patients with pulmonary arterial hypertension. Circulation. 2013; 128:2016-25, 1-10

[23] Ruiter G, van de Veerdonk MC, Bogaard HJ, Wong YY, Marcus JT, Lammertsma AA, et al. The interventricular septum in pulmonary hypertension does not show features of right ventricular failure. International journal of cardiology. 2014; 173:509-12

[24] Galie N, Hoeper MM, Humbert M, Torbicki A, Vachiery JL, Barbera JA, et al. Guidelines for the diagnosis and treatment of pulmonary hypertension. The European respiratory journal. 2009; 34:1219-63

[25] Messroghli DR, Greiser A, Frohlich M, Dietz R, Schulz-Menger J. Optimization and validation of a fully-integrated pulse sequence for modified look-locker inversion-recovery (MOLLI) T1 mapping of the heart. J Magn Reson Imaging. 2007; 26:1081-6
[26] Xue H, Shah S, Greiser A, Guetter C, Littmann A, Jolly MP, et al. Motion correction for myocardial T1 mapping using image registration with synthetic image estimation. Magn Reson Med. 2012; 67:1644-55
[27] Garcia-Alvarez A, Garcia-Lunar I, Pereda D, Fernandez-Jimenez R, Sanchez-Gonzalez J, Mirelis JG, et al. Association of myocardial T1-mapping CMR with hemodynamics and RV performance in pulmonary hypertension. J Am Coll Cardiol Img. 2015; 8:76-82
[28] Choudhury L, Mahrholdt H, Wagner A, Choi KM, Elliott MD, Klocke FJ, et al. Myocardial scarring in asymptomatic or mildly symptomatic patients with hypertrophic cardiomyopathy. Journal of the American College of Cardiology. 2002; 40:2156-64
[29] Marcus JT, Gan CT, Zwanenburg JJ, Boonstra A, Allaart CP, Gotte MJ, et al. Interventricular mechanical asynchrony in pulmonary arterial hypertension: left-to-right delay in peak shortening is related to right ventricular overload and left ventricular underfilling. Journal of the American College of Cardiology. 2008; 51:750-7
[30] Kawel-Boehm N, Dellas Buser T, Greiser A, Bieri O, Bremerich J, Santini F. In-vivo assessment of normal T1 values of the right-ventricular myocardium by cardiac MRI. The international journal of cardiovascular imaging. 2013; 30:323-8
[31] Hunzelmann N, Genth E, Krieg T, Lehmacher W, Melchers I, Meurer M, et al. The registry of the German Network for Systemic Scleroderma: frequency of disease subsets and patterns of organ involvement. Rheumatology (Oxford, England). 2008; 47:1185-92
[32] Piechnik SK, Ferreira VM, Dall'Armellina E, Cochlin LE, Greiser A, Neubauer S, et al. Shortened Modified Look-Locker Inversion recovery (ShMOLLI) for clinical myocardial T1-mapping at 1.5 and 3 T within a 9 heartbeat breathhold. J Cardiovasc Magn Reson. 2010; 12:69
[33] Chow K, Flewitt JA, Pagano JJ, Green JD, Friedrich MG, Thompson RB. T2-dependent errors in MOLLI T1 values: simulations, phantoms, and in-vivo studies. J Cardiovasc Magn Reson. 2012; 14(Suppl 1):281
[34] Chow K, Flewitt JA, Green JD, Pagano JJ, Friedrich MG, Thompson RB. Saturation recovery single-shot acquisition (SASHA) for myocardial T(1) mapping. Magn Reson Med. 2013; 71:2082-95
[35] Roujol S, Weingartner S, Foppa M, Chow K, Kawaji K, Ngo LH, et al. Accuracy, precision, and reproducibility of four T1 mapping sequences: a head-to-head comparison of MOLLI, ShMOLLI, SASHA, and SAPPHIRE. Radiology. 2014; 272:683-9

CHAPTER 10

The effects of exercise on right ventricular contractility and right ventricular - arterial coupling in pulmonary hypertension

American Journal of Respiratory Critical Care Medicine 2015

OA Spruijt[1], FS de Man[1,2], H Groepenhoff[1], F Oosterveer[1], N Westerhof[1,2], A Vonk Noordegraaf[1], HJ Bogaard[1]

[1]Department of Pulmonary Medicine, VU University Medical Center, Amsterdam
[2]Department of Physiology, VU University Medical Center, Amsterdam

Abstract

Introduction: Exercise tolerance is decreased in patients with pulmonary hypertension (PH). It is unknown whether exercise intolerance in PH coincides with an impaired rest-to-exercise response in right ventricular (RV) contractility. Therefore, the aim of this study was to investigate in PH patients the RV exertional contractile reserve, defined as the rest-to-exercise response in end-systolic elastance (ΔEes), and the effects of exercise on the matching of Ees and RV afterload (Ea), i.e. RV-arterial coupling (Ees/Ea). In addition, we compared ΔEes with a recently proposed surrogate, the rest-to-exercise change in pulmonary artery pressure (ΔPAP).

Methods: We prospectively included 17 patients with precapillary PH and 7 no-PH control subjects who performed an submaximal invasive cardiopulmonary exercise test between January 2013 and July 2014. Ees and Ees/Ea were assessed using single beat pressure-volume loop analysis.

Results: Exercise data in 16 PH patients and 5 no-PH control subjects were of sufficient quality for analysis. Ees significantly increased from rest-to-exercise in control subjects, but not in PH patients. Ea significantly increased in both groups. As a result, exercise led to a decrease in Ees/Ea in PH patients while Ees/Ea was unaffected in control subjects (p-interaction=0.009). In PH patients, ΔPAP was not related to ΔEes, but significantly correlated to the rest-to-exercise change in heart rate (ΔHR).

Conclusions: In contrast to controls, PH patients were unable to increase Ees during submaximal exercise. Failure to compensate for the further increase in Ea during exercise led to a deterioration in Ees/Ea. Furthermore, ΔPAP did not reflect ΔEes, but rather ΔHR.

Introduction

Precapillary pulmonary hypertension (PH) is characterized by an increase in pulmonary vascular resistance (PVR), increasing the load on the right ventricle (RV). The RV's ability to cope with the increased load is the most important determinant of survival in PH patients [1]. RV dysfunction tends to be more visible during exercise [2-5] and most PH patients experience exercise intolerance due to an inadequate increase in pulmonary blood flow during physical activity [2, 4]. In healthy individuals, increased demand of oxygen is met by a proportional increase in cardiac output (CO) caused by an increase in stroke volume (SV) and heart rate. In PH patients CO response is truncated during exercise due to a blunted maximal heart rate response together with an inability to increase stroke volume (SV) [3, 5-10]. It is unclear whether exercise intolerance and the impaired CO response to exercise in PH, coincide with a failure to increase RV contractility during exercise, i.e. an impaired exertional contractile reserve.

The only way to assess the exertional contractile reserve is by determining end-systolic elastance (Ees): a load-independent measure of contractility which can be derived either from a family of pressure volume loops or from the so called single beat method [11, 12]. As such, the exertional contractile reserve can be described as the rest-to-exercise response in Ees (ΔEes). Pressure-volume loop analysis also provides the opportunity to determine arterial elastance (Ea), a measure of RV afterload. The matching of Ees to Ea is known as RV-arterial coupling and its preservation is important in terms of ventricular efficiency [13, 14]. Since in PH, Ees is already considerably increased at rest [15], we hypothesized that PH patients are unable to further increase Ees during exercise. Therefore, the increase in Ea will lead to a deterioration of RV-arterial coupling during exercise.

The aim of this study was to investigate in PH patients and no PH controls, the effects of exercise on RV contractility (Ees), arterial elastance (Ea) and RV-A coupling (Ees/Ea). Additionally, the exertional contractile reserve was compared with a recently proposed surrogate measure, the rest-to-exercise change in pulmonary artery pressure (ΔPAP) [16]. The findings of this paper contribute to a better understanding of exercise intolerance and right heart failure in PH. Some of the results of this study has been previously reported in the form of an abstract [17].

Methods

Subjects

We prospectively included precapillary PH patients (idiopathic pulmonary arterial hypertension (IPAH), hereditary pulmonary arterial hypertension (HPAH) and chronic thromboembolic pulmonary hypertension (CTEPH)) and no-PH controls who performed an invasive cardiopulmonary exercise test (iCPET) in the VU University Medical Center from January 2013 until July 2014. Subjects with a history of left sided heart failure, valvular heart disease, arrhythmias or neuromuscular disease preventing the subject to exercise, were excluded.

In total, 24 subjects performed an iCPET test, including 17 PH patients (13 IPAH, 1 HPAH and 3 CTEPH patients) and 7 no-PH control subjects. The control group consisted of subjects in whom the iCPET did not confirm a previous suspicion of PH. In 9 IPAH patients, the iCPET was part of an ongoing clinical trial that was approved by the Medical Ethical Review Committee of the VU University Medical Center (Registration number: NL41878.029.13). In the remaining 15 subjects, the iCPET was part of their clinical evaluation. All subjects gave written informed consent for usage of the data for research purposes.

Maximal cardiopulmonary exercise test (CPET)

The day prior to the invasive exercise test, a maximal CPET was performed in the upright position using an electromagnetically braked cycle-ergometer (Ergoline GmbH, Bitz, Germany) according to the ATS guidelines [18]. Breath-by-breath measurements were made of oxygen consumption (VO2), carbon dioxide output (VCO2) and ventilation (VE) (Vmax229, Sensormedica, Yorba Linda, CA, USA).

Invasive cardiopulmonary exercise test (iCPET)

A balloon-tipped, flow directed 7,5 Fr, triple-lumen Swan-Ganz catheter (Edwards Lifesciences LLC, Irvine, CA) was inserted in the pulmonary artery via the jugular vein under local anesthesia and constant ECG monitoring. The ports of the catheter were placed in the right atrium, right ventricle and pulmonary artery. The zero reference level for the pressure transducer was placed at mid-thoracic level in supine position. Subsequently, a second catheter was placed in the radial artery under local anesthesia. After placement of the pulmonary artery and radial artery catheters, patients were positioned on a recumbent bicycle (Lode, Groningen, The Netherlands) in supine position. After calibration of the equipment, resting hemodynamics (right atrial pressure, right ventricular pressure, pulmonary artery pressure and systemic blood pressure) were continuously

recorded using a Powerlab data acquisition system (Chart 5 for Windows, AD Instruments, Sydney, Australia), resting mixed venous oxygen and arterial oxygen blood samples were drawn from the pulmonary artery and radial artery catheters and breath-by-breath measurements were made of VO2, VCO2 and VE (Vmax229, Sensormedica, Yorba Linda, CA, USA).

The exercise protocol consisted of one minute of unloaded cycling followed by two minutes of submaximal exercise (40% of maximal workload (Wmax) during maximal CPET) with continuous recording of hemodynamics. Near the end of exercise, mixed venous and arterial blood samples were again drawn from the pulmonary artery and radial artery catheters.

For subjects whose Wmax was <150W, submaximal workloads were immediately increased to 40% of Wmax after one minute of unloaded exercise. For subjects with a Wmax >150W, a direct increase to 40% of Wmax was too large and therefore these subjects were exercised at one additional intermediate step of one minute of exercise at 35W in PH patients and 45W in control subjects. This intermediate step allowed data comparison at approximately similar absolute work rates in all subjects.

Measurements

CO at rest and during exercise were measured using the direct Fick method. SV was calculated as CO divided by heart rate (HR). Cardiac output and SV were indexed for body surface area (BSA). Pulmonary artery pressures (PAP) were averaged over a period of 15 seconds to be sure that the PAP was measured over multiple respiratory cycles.

The end-systolic elastance (Ees), a load-independent measure of RV contractility, was calculated at rest and during submaximal exercise as:

$$\text{Ees} = \frac{maximal\ isovolumic\ pressure - mean\ pulmonary\ artery\ pressure}{stroke\ volume\ index}$$

The maximal isovolumic pressure (Pmax) was determined using the single beat method [11, 12]. Pressure data were averaged over several beats to reduce respiratory variations. The load on the RV was calculated as arterial elastance (Ea):

$$\text{Ea} = \frac{mean\ pulmonary\ artery\ pressure}{stroke\ volume\ index}$$

Subsequently, RV–arterial coupling was calculated as [11, 13-15, 19-21]:

$$\text{RV} - \text{arterial coupling} = \frac{Ees}{Ea}$$

Statistical methods

Data are presented as mean ± standard deviation, unless stated differently. Comparisons of characteristics, CPET parameters and resting hemodynamics between PH patients and control subjects were performed using independent t tests for normally distributed data and Mann-Whitney U tests for not normally distributed data. Chi square tests were used to analyze dichotomous variables. Comparison of rest-to-exercise responses between PH patients and control subjects were performed using 2- way- repeated measures ANOVA with Bonferroni post-hoc correction. The p-interaction represents the p-value for the effect of exercise in PAH-patients in comparison to control subjects. Since PH patients were significantly older than control subjects, the differences between PH patients and control subjects in rest-to-exercise responses of heart rate, Ees, Ea and RV-arterial coupling were adjusted for age using MANCOVA. Simple linear regression was performed to describe the relationship between rest-to-exercise responses of different parameters in the PH group. Statistical analyses were performed using Graphpad Prism for Windows version 5 and SPSS for Windows version 20. A p-value < 0.05 was considered statistically significant.

Results

Of the 24 subjects that performed an iCPET, in 16 PH patients and 5 control subjects, hemodynamic data at 40% of Wmax was of sufficient quality to analyze. In 1 IPAH patient and in 2 control subjects the pressure signal was lost during exercise due to displacement of the pulmonary artery catheter. 10 of the 16 PH patients used PH specific treatment at the moment of the iCPET.

PH patients were significantly older than the control subjects (table 1). As expected, PH patients showed, during maximal CPET, significantly lower maximal oxygen consumption, workload and HR compared to control subjects (table 1). Resting hemodynamics showed significantly higher mPAP, pulmonary vascular resistance (PVR) and right atrial pressure (RAP) and significantly lower cardiac index (CI), arterial and mixed venous oxygen levels in PH patients compared to the control subjects (table 1). Between groups there was no difference in heart rate (HR) at rest. RV contractility (Ees) and RV afterload (Ea) at rest were significantly increased in PH patients compared to control

subjects, while no difference was seen in RV-A coupling (table 1). Final diagnosis and medication of control subjects are summarized in table 2.

	Control subjects (n=5)	PH (n=16)	P-value
Characteristics			
Age (years)	38 (12)	57 (14)	0.015
Sex (n female)	3	11	0.717
BSA (m2)	1.853 (0.327)	1.883 (0.181)	0.850
Diagnosis		12 IPAH; 1 HPAH	
		3 CTEPH	
NYHA (II/III, n)		9 / 7	
Treatment (n)			
None		5	
ERA		2	
PDE5I		1	
Prostanoids		0	
ERA + PDE5I		8	
Ca antagonists		1	
B-blockers		2	
CPET max			
VO2/kg (ml/kg/min)	31 (8)	16 (5)	<0.001
Work (Watt)	187 (87)	90 (44)	0.005
HR (BPM)	174 (5)	139 (15)	<0.001
RHC rest			
HR (BPM)	75 (14)	77 (15)	0.785
CI (L/min)	4.7 (0.8)	3.1 (0.6)	<0.001
mPAP (mmHg)	18 (2)	53 (8)	<0.001
PAWP (mmHg)	11 (2)	12 (2)	0.475
PVR (dyne/s/cm5)	69 (14)	582 (168)	<0.001
mRAP (mmHg)	4 (1)	7 (4)	0.015
SaO2 (%)	99 (0.5)	95 (2)	<0.001
SvO2 (%)	82 (2)	70 (4)	<0.001
CMRI			
RVEDV (ml)	-	151 (52)	
RVESV (ml)	-	88 (53)	

RVEF (%)	-	47 (13)	
LVEF (%)	-	61 (15)	
Load independent RV function rest			
Ees (mmHg/ml/m2)	0.47 (0.20)	2.00 (0.50)	<0.001
Ea (mmHg/ml/m2)	0.29 (0.05)	1.36 (0.45)	<0.001
Ees/Ea	1.63 (0.74)	1.61 (0.54)	0.963

Table 1: Characteristics, maximal CPET and resting hemodynamics. Data is presented as mean ± standard deviation. BSA = body surface area. ERA = endothelin receptor antagonist. PDE5I = phosphodiesterase inhibitors. VO2/kg = oxygen consumption per kilogram. HR = heart rate. CI = cardiac index. mPAP = mean pulmonary artery pressure. PAWP = pulmonary artery wedge pressure. PVR = pulmonary vascular resistance. mRAP = mean right atrial pressure. SaO2 = arterial oxygen saturation. SvO2 = mixed venous oxygen saturation. RVEDV = right ventricular end-diastolic volume. RVESV = right ventricular end-systolic volume. RVEF = right ventricular ejection fraction. LVEF = left ventricular ejection fraction. Ees = end-systolic elastance (RV contractility). Ea = aterial elastance (RV afterload). Ees/Ea = right ventricular-arterial coupling.

Control subject	Final diagnosis	Medication
1	High frequency ventilation and scoliosis	Long-acting beta agonist; Inhalation glucocorticoid
2	Physical deconditioning after PE	Vitamin K antagonist
3	No cause found	None
4	No cause found	None
5	Physical deconditioning after PE	Vitamin K antagonist

Table 2: Final diagnosis and medication of control subjects. PE = pulmonary embolism.

Exercise hemodynamics

In control subjects 40% of Wmax was 70±34W and in PH patients this was 39±14W (p=0.009). From rest-to-exercise, both groups showed a significant increase in CI (figure 1A), with a larger increase in CI in control subjects (p-interaction=0.003). During exercise, both groups showed a significant increase in HR, but no change in SVI (figure 1B). The increase in HR was larger in control subjects in comparison to PH patients (p-interaction=0.039), but not after correction for age (p=0.300) (figure 1C). The mPAP and RV systolic pressures (RV Psys) increased significantly during exercise in control subjects and PH patients (figure 1D+E), with larger increases seen in the PH group (mPAP p-interaction=0.005; RV Psys p-interaction=0.019). Maximum isovolumic pressure (Pmax), derived from the single beat method, was significantly higher than resting values in both groups (figure 1F). Total pulmonary vascular resistance (TPVR) significantly decreased in PH patients from rest to exercise (figure 1G).

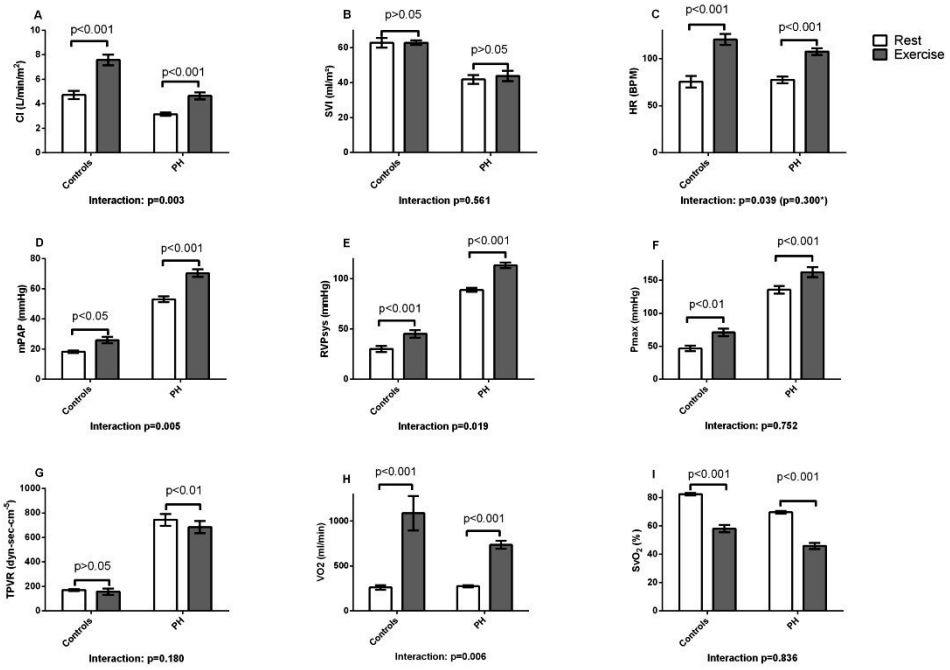

Figure 1: Rest-to-exercise responses at 40% of Wmax. Data is presented as mean and standard error. Blue bars represents the data at rest, red bars represents the data during exercise at 40% of Wmax. A: CI = cardiac index. CI significantly increased in both groups during exercise, with a larger increase in CI in the control subjects (p-interaction: 0.003). B: SVI = stroke volume index. SVI did not increase in both groups. C: HR = heart rate. * = p-interaction adjusted for age. HR significantly increased during exercise in both groups during exercise, with a larger increase in HR in the control subjects (p-interaction: 0.039). After correction for age, the rest-to-exercise response in HR between groups was not different (p=0.300*). D: mPAP = mean pulmonary artery pressure. mPAP significantly increased in both groups during exercise, with a larger increase in mPAP in PH patients (p-interaction: 0.005). E: RVPsys = right ventricular systolic pressure. RVPsys significantly increased in both groups during exercise, with a larger increase in RVPsys in PH patients (p-interaction: 0.019). F: Pmax = maximal isovolumic pressure. Pmax significantly increased in both groups during exercise. G: TPVR = total pulmonary vascular resistance. TPVR significantly decreased in PH patients during exercise. H: VO2 = oxygen consumption. VO2 significantly increased in both groups during exercise, with a larger increase in VO2 in control subjects (p-interaction: 0.006). I: SvO2 = mixed venous oxygen saturation. SvO2 significantly decreased in both groups during exercise.

The exertional contractile reserve (ΔEes)

From rest-to-exercise, RV contractility (Ees) increased significantly in control subjects, but not in PH patients (p-interaction=<0.001), implying an impaired exertional contractile reserve (figure 2).

Effects of exercise on RV-arterial coupling

RV afterload (Ea) increased significantly during exercise in both groups (figure 2). As a result, RV-arterial coupling during exercise decreased in PH patients, but remained stable in control subjects (p-interaction=0.013) (figure 2).

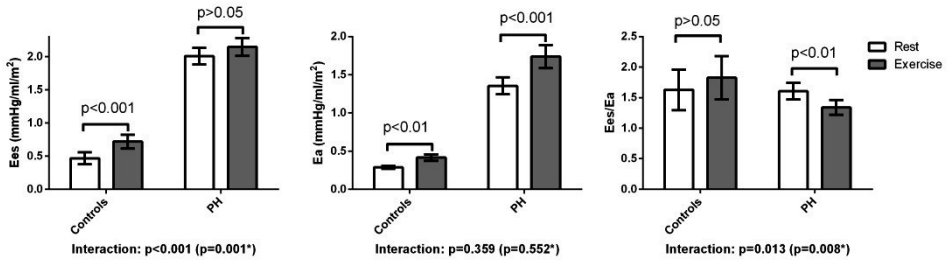

Figure 2: Rest-to-exercise responses of Ees, Ea, Ees/Ea at 40% of Wmax. Data is presented as mean and standard error. The blue bars represents the data at rest, the red bars represents the data during exercise at 40% of Wmax. * = p-interaction adjusted for age. A: Ees = end-systolic elastance (RV contractility). Ees significantly increased during exercise in control subjects during exercise, but not in PH patients (p-interaction: p<0.001). B: Ea = arterial elastance (RV afterload). Ea significantly increased in both groups during exercise. C: Ees/Ea = right ventricular-arterial coupling. Ees/Ea significantly decreased in PH patients during exercise, but not in control subjects (p-interaction: 0.013).

Comparison between ΔEes and ΔPAP

There was no relation between the rest-to-exercise response in Ees (ΔEes) and pulmonary artery pressures (ΔEes and ΔsPAP r=0.350 R2=0.123 p=0.184; ΔEes and ΔmPAP r=0.182 R2=0.033; p=0.500), neither was ΔEes related to ΔHR (r=0.055 R2=0.003; p=0.838) or ΔSVI (r=0.373 R2=-0.139; p=0.155).

ΔsPAP and ΔmPAP were both related to ΔHR (ΔsPAP and ΔHR r=0.579 R2=0.335 p=0.019; ΔmPAP and ΔHR r=0.788 R2=0.621 p<0.001) (figure 3), but not to SVI.

Discussion

This is the first study to describe the RV exertional contractile reserve in PH patients and the effects of exercise on RV-arterial coupling. We showed that PH patients have an impaired exertional contractile reserve and that the failure to increase contractility during exercise in response to the increased RV afterload, led to a deterioration of RV-arterial coupling.

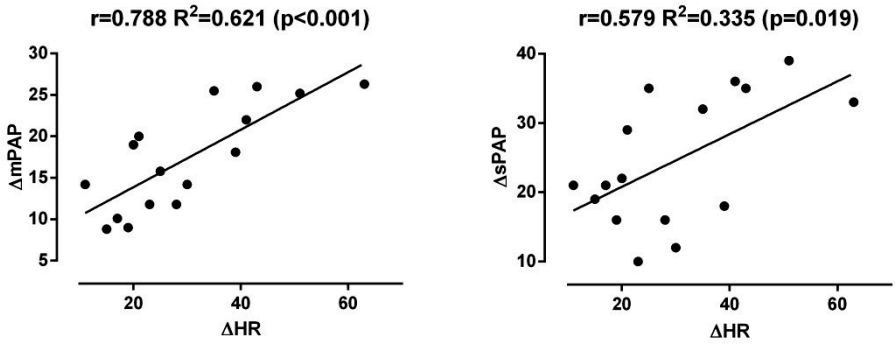

Figure 3: Relation between the change in pulmonary artery pressure and the change in heart rate (Δ HR) from rest-to-exercise. There was a significant relation between the change in pulmonary artery pressure and the change in heart rate from rest-to-exercise (ΔsPAP and ΔHR r=0.579 R2=0.335 p=0.019; ΔmPAP and ΔHR r=0.788 R2=0.621 p<0.001).

The RV exertional contractile reserve (ΔEes)

In line with previous studies, RV contractility (Ees) measured at rest was larger in PH patients than in control subjects [15, 22]. Here we show that PH patients are unable to increase RV contractility during exercise and this suggests that RV contractility is already maximally increased at rest.

As far as we know, the rest-to-exercise response in a load-independent measure of RV contractility has never been studied in healthy subjects. In the left ventricle of healthy humans, the increase in load-independent measures of contractility during exercise [23-25] is largely due to an increase in beta-adrenergic stimulation [26]. The impaired rest-to-exercise response in RV contractility in PH patients could relate to the downregulation and desensitization of beta-adrenergic receptors which has been shown in PH rat models [27] and PH patients [28]. It has been suggested that the increased catecholamine levels at rest in PAH [29], may lead to an inability to increase catecholamine levels during exercise [30]. Interestingly, an impaired inotropic RV response was also observed in a recent study using different PH rat models treated with several inotropic agents [27]. The impaired exertional contractile reserve found in our study, add to the debate whether it is useful to treat PH patients with RV failure with inotropic agents [30]. While a degree of caution has to be taken into account regarding the extrapolation of our findings during submaximal exercise to a situation of RV failure, the usefulness of inotropic agents in PH patients with RV failure should be studied in a randomized controlled trial. Absence of a contractile reserve suggests that it may be more useful to treat RV failure with agents that reverse maladaptive RV remodeling.

The rest-to-exercise response in RV-arterial coupling

We found a significant increase in load (Ea) on the RV in PH patients and control subjects during exercise, while TPVR (= Ea · HR), significantly decreased in PH patients and remained stable in control subjects. Most hemodynamic exercise studies measured load as PVR and showed a decrease or stable PVR during exercise in both PH patients and healthy controls [2, 31-34]. The difference between both measures of load is explained by the way in which they are calculated: PVR as pressure divided by CO, and Ea as pressure divided by SV. Despite the larger RV afterload in PH patients at rest, no differences in RV-arterial coupling between PH patients and control subjects were found, implying that RV-arterial coupling at rest was well maintained. It was shown in a large cohort of IPAH patients, that RV-arterial coupling at rest was maintained in stable PH patients and decreased in PH patients with a more progressive disease [15]. Another study showed a decrease in RV-arterial coupling at rest in PH patients compared to control subjects [35]. In this study, the calculation of Ees was simplified as end-systolic pressure divided by end-systolic volume (measured by MRI), assuming the volume at zero pressure (V0) is zero. However, it has been shown that V0 depends on RV dilatation and therefore that the assumption of V0=0 leads to an underestimation of Ees and RV-arterial coupling [21].

The insufficient response in RV contractility to the increase in load, resulted in a deterioration in RV-arterial coupling during exercise in PH patients, while in control subjects the exertional contractile reserve was sufficient to maintain RV-arterial coupling. Studies of the LV showed that at an Ees/Ea ratio of 1, ventricular stroke work is optimal [14], although maximal ventricular efficiency, defined as ventricular stroke work divided by myocardial oxygen consumption, is reached at an Ees/Ea ratio of 2 [13]. Theoretically, the decrease in RV-arterial coupling in PH patients suggests that the coupling is shifted to an optimal ventricular stroke work at the cost of ventricular efficiency, although this cannot be determined from the current data.

Comparison of ΔEes with the rest-to-exercise change in pulmonary artery pressures

A recent study in PH patients defined the contractile reserve as the increase in systolic pulmonary artery pressure (PAP) during exercise [16]. In this study, a larger increase in sPAP was associated with a better survival. The rationale for using ΔsPAP as a measure of contractile reserve was derived from the pressure-flow relation. The authors stated that a greater increase in pressure allows the ejection of a higher SV and that therefore, the contractile reserve can be described by the increase

in pressures. In our study ΔPAP did not correlate with ΔEes or with ΔSVI. Since it is known that the increase in SV in PH patients during exercise is only minor [3, 5-9], the increase in CI during exercise is highly HR dependent. Our data showed significant relations between the increases in pulmonary artery pressures and ΔHR. This is in line with a recent study showing a strong relation between ΔmPAP and ΔHR during exercise in PAH patients [7]. Therefore, a large increase in pulmonary artery pressures during exercise seems not to indicate an intact contractile reserve, but rather a more preserved HR response. The ability to increase HR is a well-known predictor of survival [36, 37] and the better survival found by Grunig et al [16] in PH patients with a larger increase in pulmonary artery pressures during exercise could reflect a relatively intact HR response.

Clinical implications

Although a direct link between exercise capacity and RV contractile reserve was not investigated in this study, our findings suggest that a decreased exercise capacity in PH is not only the direct result of an increased pressure in the lung circulation, but also caused by intrinsic changes in RV contractility. Moreover, our study results imply that inotropic drugs may have little value in improving RV dysfunction in PH. Studies are warranted to identify interventions which could restore RV contractile reserve by reversing maladaptive remodeling.

Because the rest-to-exercise response in pulmonary artery pressures was not related to the rest-to-exercise response in Ees, but rather reflected an intact HR response, the rest-to-exercise response in pulmonary artery pressures should not be used as a surrogate measure of the exertional contractile reserve.

Limitations

For safety reasons, we exercised subjects only at submaximal workloads (40% of Wmax). In a sub-analysis hemodynamic data were compared at comparable submaximal workloads of 37W±12 in PH patients and 46W±5 in control subjects (p=0.096). Differences between PH patients and control subjects in rest-to-exercise responses of hemodynamics and load-independent measures of RV function were similar in direction and magnitude as in the data at 40% of Wmax (results not shown). From our results, we cannot determine whether the observed differences at submaximal exercise can be extrapolated to maximal exercise testing.

In the calculation of Ees, we used mPAP as a surrogate for RV end-systolic pressure (RVESP) based on a study of Chemla et al [38] who found that in normal subjects mPAP was closely related to

RVESP. It is possible that in a pressure overloaded RV, RVESP is more closely related to the systolic RV pressure (RVSP) [39] which would have led to an overestimation of Ees. However, mPAP and RVSP were strongly related both at rest and during exercise, implying that the choice of pressure will not influence the direction of the rest-to-exercise response.

Although the single beat method has been developed and validated for the left ventricle [12], validation of the method in PH has been restricted to animals [11]. The results of that study showed, in a wide range of Pmax values, that an excellent relation exist between Pmax determined by the single beat method and the Pmax values determined after clamping of the pulmonary artery.

We used relatively deconditioned control subjects, as the primary indication to perform iCPET in these subjects was unexplained dyspnea. Based on the literature [3, 40-42], including a previous study from our institute [3], we did not expect to find an unchanged SV in healthy subjects during submaximal exercise. The difference in SV response in control subjects between the current study and our previous study [3] can probably be explained by the fact that the control subjects in our previous study were healthy volunteers in good condition. Several previous studies showed physiological explanations for an unchanged SV from rest-to-exercise. A reduced filling time due to an increase in HR can result in an inability to increase SV in healthy subjects. Furthermore, in the upright position, the venous return is increased from rest-to-exercise via the muscle pump. When exercise is performed in the supine position, the venous return is already increased at rest due to the return of pooled blood due to gravity, resulting in an inability to increase SV during exercise [6, 43-49]. Since we already found large differences in the hemodynamic rest-to-exercise responses between PH patients and relatively deconditioned control subject, the inclusion of relatively deconditioned control subjects only strengthens our findings.

Conclusions

PH patients had no RV exertional contractile reserve, which resulted in RV-arterial uncoupling during submaximal exercise. Rest-to-exercise responses in pulmonary artery pressures rather reflected the rest-to-exercise response in heart rate, than an exertional contractile reserve and should therefore not be used as a surrogate measure of exertional contractile reserve.

References

[1] van de Veerdonk MC, Kind T, Marcus JT, Mauritz GJ, Heymans MW, Bogaard HJ, et al. Progressive right ventricular dysfunction in patients with pulmonary arterial hypertension responding to therapy. Journal of the American College of Cardiology. 2011; 58:2511-9
[2] Chaouat A, Sitbon O, Mercy M, Poncot-Mongars R, Provencher S, Guillaumot A, et al. Prognostic value of exercise pulmonary haemodynamics in pulmonary arterial hypertension. The European respiratory journal. 2014; 44:704-13
[3] Holverda S, Gan CT, Marcus JT, Postmus PE, Boonstra A, Vonk-Noordegraaf A. Impaired stroke volume response to exercise in pulmonary arterial hypertension. Journal of the American College of Cardiology. 2006; 47:1732-3
[4] Lewis GD, Bossone E, Naeije R, Grunig E, Saggar R, Lancellotti P, et al. Pulmonary vascular hemodynamic response to exercise in cardiopulmonary diseases. Circulation. 2013; 128:1470-9
[5] Nootens M, Wolfkiel CJ, Chomka EV, Rich S. Understanding right and left ventricular systolic function and interactions at rest and with exercise in primary pulmonary hypertension. The American journal of cardiology. 1995; 75:374-7
[6] Almeida AR, Loureiro MJ, Lopes L, Cotrim C, Lopes L, Repolho D, et al. Echocardiographic assessment of right ventricular contractile reserve in patients with pulmonary hypertension. Rev Port Cardiol. 2014; 33:155-63
[7] Chemla D, Castelain V, Hoette S, Creuze N, Provencher S, Zhu K, et al. Strong linear relationship between heart rate and mean pulmonary artery pressure in exercising patients with severe precapillary pulmonary hypertension. American journal of physiology. 2013; 305:H769-77
[8] Deboeck G, Taboada D, Hagan G, Treacy C, Page K, Sheares K, et al. Maximal cardiac output determines 6 minutes walking distance in pulmonary hypertension. PloS one. 2014; 9:e92324
[9] Groepenhoff H, Westerhof N, Jacobs W, Boonstra A, Postmus PE, Vonk-Noordegraaf A. Exercise stroke volume and heart rate response differ in right and left heart failure. European journal of heart failure. 2010; 12:716-20
[10] Provencher S, Chemla D, Herve P, Sitbon O, Humbert M, Simonneau G. Heart rate responses during the 6-minute walk test in pulmonary arterial hypertension. The European respiratory journal. 2006; 27:114-20
[11] Brimioulle S, Wauthy P, Ewalenko P, Rondelet B, Vermeulen F, Kerbaul F, et al. Single-beat estimation of right ventricular end-systolic pressure-volume relationship. American journal of physiology. 2003; 284:H1625-30
[12] Sunagawa K, Yamada A, Senda Y, Kikuchi Y, Nakamura M, Shibahara T, et al. Estimation of the hydromotive source pressure from ejecting beats of the left ventricle. IEEE transactions on bio-medical engineering. 1980; 27:299-305
[13] Burkhoff D, Sagawa K. Ventricular efficiency predicted by an analytical model. The American journal of physiology. 1986; 250:R1021-7
[14] Sunagawa K, Maughan WL, Sagawa K. Optimal arterial resistance for the maximal stroke work studied in isolated canine left ventricle. Circulation research. 1985; 56:586-95
[15] Trip P, De Man FS, Raamsteeboers AJ, Westerhof N, vonk-Noordegraaf A. Right Ventriculo-Arterial Coupling In Long-Term, Mid-Term and Short-Term Surviving Patients With Pulmonary Arterial Hypertension. Am J Respir Crit Care Med. 2013; Abstract: American Thoracic Society International Conference 2013, Philadelphia:187;A2550
[16] Grunig E, Tiede H, Enyimayew EO, Ehlken N, Seyfarth HJ, Bossone E, et al. Assessment and prognostic relevance of right ventricular contractile reserve in patients with severe pulmonary hypertension. Circulation. 2013; 128:2005-15
[17] Spruijt OA, Bogaard HJ, De Man FS, Oosterveer F, Groepenhoff H, Westerhof N, et al. The coupling of the right ventricle to its load during exercise in pulmonary hypertension. Am J Respir Crit Care Med. 2014; Abstract: American Thoracic Society International Conference 2014, San Diego:189;A4720
[18] Ross RM. ATS/ACCP statement on cardiopulmonary exercise testing. Am J Respir Crit Care Med. 2003; 167:1451; author reply
[19] Vonk-Noordegraaf A, Westerhof N. Describing right ventricular function. The European respiratory journal. 2013; 41:1419-23
[20] Spruijt OA, Bogaard HJ, Vonk-Noordegraaf A. Assessment of right ventricular responses to therapy in pulmonary hypertension. Drug discovery today. 2014; 19:1246-50
[21] Trip P, Kind T, van de Veerdonk MC, Marcus JT, de Man FS, Westerhof N, et al. Accurate assessment of load-independent right ventricular systolic function in patients with pulmonary hypertension. J Heart Lung Transplant. 2013; 32:50-5
[22] Kuehne T, Yilmaz S, Steendijk P, Moore P, Groenink M, Saaed M, et al. Magnetic resonance imaging analysis of right ventricular pressure-volume loops: in vivo validation and clinical application in patients with pulmonary hypertension. Circulation. 2004; 110:2010-6
[23] Chantler PD, Lakatta EG, Najjar SS. Arterial-ventricular coupling: mechanistic insights into cardiovascular performance at rest and during exercise. J Appl Physiol (1985). 2008; 105:1342-51
[24] Chantler PD, Melenovsky V, Schulman SP, Gerstenblith G, Becker LC, Ferrucci L, et al. The sex-specific impact of systolic hypertension and systolic blood pressure on arterial-ventricular coupling at rest and during exercise. American journal of physiology. 2008; 295:H145-53
[25] Najjar SS, Schulman SP, Gerstenblith G, Fleg JL, Kass DA, O'Connor F, et al. Age and gender affect ventricular-vascular coupling during aerobic exercise. Journal of the American College of Cardiology. 2004; 44:611-7
[26] Little WC, Cheng CP. Effect of exercise on left ventricular-arterial coupling assessed in the pressure-volume plane. The American journal of physiology. 1993; 264:H1629-33

[27] Piao L, Fang YH, Parikh KS, Ryan JJ, D'Souza KM, Theccanat T, et al. GRK2-mediated inhibition of adrenergic and dopaminergic signaling in right ventricular hypertrophy: therapeutic implications in pulmonary hypertension. Circulation. 2012; 126:2859-69
[28] Bristow MR, Minobe W, Rasmussen R, Larrabee P, Skerl L, Klein JW, et al. Beta-adrenergic neuroeffector abnormalities in the failing human heart are produced by local rather than systemic mechanisms. The Journal of clinical investigation. 1992; 89:803-15
[29] Nootens M, Kaufmann E, Rector T, Toher C, Judd D, Francis GS, et al. Neurohormonal activation in patients with right ventricular failure from pulmonary hypertension: relation to hemodynamic variables and endothelin levels. Journal of the American College of Cardiology. 1995; 26:1581-5
[30] Ryan JJ, Archer SL. The right ventricle in pulmonary arterial hypertension: disorders of metabolism, angiogenesis and adrenergic signaling in right ventricular failure. Circulation research. 2014; 115:176-88
[31] Blumberg FC, Arzt M, Lange T, Schroll S, Pfeifer M, Wensel R. Impact of right ventricular reserve on exercise capacity and survival in patients with pulmonary hypertension. European journal of heart failure. 2013; 15:771-5
[32] Kovacs G, Olschewski A, Berghold A, Olschewski H. Pulmonary vascular resistances during exercise in normal subjects: a systematic review. The European respiratory journal. 2012; 39:319-28
[33] Tolle JJ, Waxman AB, Van Horn TL, Pappagianopoulos PP, Systrom DM. Exercise-induced pulmonary arterial hypertension. Circulation. 2008; 118:2183-9
[34] Waxman AB. Exercise physiology and pulmonary arterial hypertension. Progress in cardiovascular diseases. 2012; 55:172-9
[35] Sanz J, Garcia-Alvarez A, Fernandez-Friera L, Nair A, Mirelis JG, Sawit ST, et al. Right ventriculo-arterial coupling in pulmonary hypertension: a magnetic resonance study. Heart (British Cardiac Society). 2011; 98:238-43
[36] Groepenhoff H, Vonk-Noordegraaf A, van de Veerdonk MC, Boonstra A, Westerhof N, Bogaard HJ. Prognostic relevance of changes in exercise test variables in pulmonary arterial hypertension. PloS one. 2013; 8:e72013
[37] Henkens IR, Van Wolferen SA, Gan CT, Boonstra A, Swenne CA, Twisk JW, et al. Relation of resting heart rate to prognosis in patients with idiopathic pulmonary arterial hypertension. The American journal of cardiology. 2009; 103:1451-6
[38] Chemla D, Hebert JL, Coirault C, Salmeron S, Zamani K, Lecarpentier Y. Matching dicrotic notch and mean pulmonary artery pressures: implications for effective arterial elastance. The American journal of physiology. 1996; 271:H1287-95
[39] Redington AN, Rigby ML, Shinebourne EA, Oldershaw PJ. Changes in the pressure-volume relation of the right ventricle when its loading conditions are modified. British heart journal. 1990; 63:45-9
[40] Rigaud M, Boschat J, Rocha P, Ferreira A, Bardet J, Bourdarias JP. Comparative haemodynamic effects of dobutamine and isoproterenol in man. Intensive care medicine. 1977; 3:57-62
[41] Roest AA, Kunz P, Lamb HJ, Helbing WA, van der Wall EE, de Roos A. Biventricular response to supine physical exercise in young adults assessed with ultrafast magnetic resonance imaging. The American journal of cardiology. 2001; 87:601-5
[42] Surie S, van der Plas MN, Marcus JT, Kind T, Kloek JJ, Vonk-Noordegraaf A, et al. Effect of pulmonary endarterectomy for chronic thromboembolic pulmonary hypertension on stroke volume response to exercise. The American journal of cardiology. 2014; 114:136-40
[43] Daley PJ, Sagar KB, Wann LS. Doppler echocardiographic measurement of flow velocity in the ascending aorta during supine and upright exercise. British heart journal. 1985; 54:562-7
[44] Elstad M, Nadland IH, Toska K, Walloe L. Stroke volume decreases during mild dynamic and static exercise in supine humans. Acta physiologica (Oxford, England). 2009; 195:289-300
[45] Elstad M, Toska K, Chon KH, Raeder EA, Cohen RJ. Respiratory sinus arrhythmia: opposite effects on systolic and mean arterial pressure in supine humans. The Journal of physiology. 2001; 536:251-9
[46] Loeppky JA, Greene ER, Hoekenga DE, Caprihan A, Luft UC. Beat-by-beat stroke volume assessment by pulsed Doppler in upright and supine exercise. Journal of applied physiology: respiratory, environmental and exercise physiology. 1981; 50:1173-82
[47] Puchalska L, Belkania GS. Haemodynamic responses to the dynamic exercise in subjects exposed to different gravitational conditions. J Physiol Pharmacol. 2006; 57 Suppl 11:103-13
[48] Steding-Ehrenborg K, Jablonowski R, Arvidsson PM, Carlsson M, Saltin B, Arheden H. Moderate intensity supine exercise causes decreased cardiac volumes and increased outer volume variations: a cardiovascular magnetic resonance study. J Cardiovasc Magn Reson. 2013; 15:96
[49] Toska K, Eriksen M. Respiration-synchronous fluctuations in stroke volume, heart rate and arterial pressure in humans. The Journal of physiology. 1993; 472:501-12

10

CHAPTER 11

Summary and Future Perspective

OA Spruijt[1]

[1]Department of Pulmonary Medicine, VU University Medical Center, Amsterdam

Summary

Pulmonary arterial hypertension is characterized by remodeling of the small pulmonary arteries leading to an increase in resistance of the pulmonary vascular bed and an increase in pulmonary artery pressures. The vascular remodeling comprises several features. The lumen of the vessels is narrowed because of vasoconstriction, hyperproliferation of smooth muscle cells and endothelial cells, inflammation and several other aspects. The increase in resistance increases the load on the right ventricle.

Initially, the right ventricle will try to adapt to the increase in pressures and subsequent rise in wall stress through a complex interplay of ventricular remodeling, neuro-hormonal activation and changes in myocardial metabolism. Simplified, the first step in the process of remodeling is right ventricular hypertrophy and an increase in contractility. If, despite these adaptive changes, cardiac output cannot be maintained, the right ventricle will dilate further increasing wall stress. Finally, right ventricular failure will occur, which is the main cause of death in pulmonary arterial hypertension. In this thesis, a number of techniques and methods were evaluated that may contribute to earlier recognition of PAH and improved monitoring and prognostication.

Early recognition and prognostication in pulmonary hypertension

Due to the non-specific nature of symptoms at presentation, most patients with pulmonary arterial hypertension are diagnosed by the time their disease is in an advanced stage. It has been shown that early detection of PH and a timely initiation of treatment can significantly improve the clinical outcome. Computed tomography pulmonary angiography (CTPA) is a diagnostic tool often used in the diagnostic process of patients that present with unexplained dyspnea, for example to exclude pulmonary emboli. Such scans can already reveal clues for the presence of pulmonary hypertension. A well-known clue for the presence of pulmonary hypertension is an increased ratio between the diameter of the pulmonary artery and the diameter of the ascending aorta. In **chapter 2**, we investigated whether the predictive value of CTPA for the presence of pulmonary hypertension could be improved by combining this measurement with the diameter ratio of the right ventricle and left ventricle. We found that the predictive value of CTPA for precapillary pulmonary hypertension improved when ventricular and pulmonary artery measurements were combined.

The prognostic value of right ventricular parameters in pulmonary hypertension is well-established. Whether a combination of parameters of the right heart merged into a risk score predict outcome in

precapillary pulmonary hypertension was investigated in **chapter 3**. We found a good prognostic value of a simple right heart score and this score showed a good correlation with more established complex risk scores (REVEAL score and NIH score).

Treatment response in pulmonary hypertension

Since the prognosis of patients with pulmonary hypertension is determined by right ventricular function, monitoring of right ventricular function is of utmost importance. In **chapter 4** we summarized available methods for measuring the right ventricular response to therapy. Cardiac magnetic resonance imaging (CMRI) is the gold standard for monitoring right ventricular function. Since CMRI scans are expensive, not widely available and analyses are time-consuming, monitoring right ventricular function using simple echocardiographic measurements would be ideal in daily practice. Therefore, in **chapter 5**, we investigated the usage of simple echocardiographic parameters for the serial assessment of right ventricular function by comparing four different echo-derived parameters with CMRI-derived right ventricular ejection fraction. The strongest relationship was found between CMRI-derived right ventricular ejection fraction and echo-derived right ventricular fractional area change. However, the sensitivity of echocardiography to predict a deterioration in CMRI-derived right ventricular ejection fraction was poor for all four echo-derived parameters (ranging from 33-56%). Echo-derived parameters of right ventricular systolic function, in particular right ventricular area change, can reasonably distinguish between a decreased or preserved CMRI-derived right ventricular ejection fraction. However, echo-derived parameters are not suitable for the serial assessment of right ventricular systolic function.

Patients with idiopathic pulmonary arterial hypertension and a reduced diffusion capacity of the lung for carbon monoxide (DLCO) have a worse survival compared to idiopathic pulmonary arterial hypertension patients with a preserved DLCO. Whether this poor survival can be explained by unresponsiveness to pulmonary hypertension specific vasodilatory therapy is unknown. Therefore, in **chapter 6** we investigated the hemodynamic and cardiac response to PH specific vasodilatory therapy in patients with IPAH and a reduced DLCO. Baseline hemodynamics and cardiac function were not different in the two groups and hemodynamics and cardiac function improved in both groups after PH specific vasodilatory therapy without a worsening of oxygenation at rest or during exercise. Therefore, we concluded that patients with idiopathic pulmonary arterial hypertension and a severely reduced DLCO show a similar response to pulmonary hypertension - specific vasodilatory

therapy in terms of hemodynamics, cardiac function and exercise capacity as patients with idiopathic pulmonary arterial hypertension and a preserved DLCO.

Emerging modalities in pulmonary hypertension

Chapter 7 summarizes emerging imaging techniques in the setting of pulmonary hypertension. A well-known technique to characterize the myocardium with CMRI is the assessment of late gadolinium enhancement.

Currently, there is no possibility to clinically assess the primary disease process in the pulmonary arteries of patients with pulmonary arterial hypertension. Therefore, in **chapter 8**, we investigated whether 3'-[18F]fluoro-3'-deoxythymidine ([18F]-FLT) positron emission tomography (PET/CT) could be used to quantitatively assess proliferation in the pulmonary vasculature of patients with idiopathic pulmonary arterial hypertension. Subsequently, we assessed whether [18F]-FLT could track the pulmonary vascular remodeling in a monocrotaline ratmodel (animal model of pulmonary hypertension) and the reverse remodeling after treating the animals with targeted therapies. We found that the uptake of [18F]-FLT in the lungs of patients with idiopathic pulmonary arterial hypertension was significantly increased compared to control subjects and was related to markers of disease severity. The uptake of [18F]-FLT was heterogeneous among IPAH patients. Furthermore, [18F]-FLT was able to track the pulmonary vascular remodeling in the monocrotaline ratmodel and the reverse remodeling after treating the animals with dichloroacetate and imatinib. Our results suggest that [18F]-FLT PET/CT can be developed as a tool to select IPAH patients with a hyperproliferative stat that may benefit from anti-proliferative therapy. In addition, [18F]-FLT PET/CT might be used to assess treatment response.

An emerging technique to characterize the myocardium by CMRI is native T1-mapping. To quantify native T1-values, there is no need for a reference area of myocardium, making it possible to directly quantify the total myocardium. Furthermore, native T1-mapping has the advantage of not requiring the usage of contrast agents. In **chapter 9** we investigated this technique in precapillary pulmonary hypertension patients. Native T1-values were increased at the interventricular insertion regions compared to the RV free wall, LV free wall and interventricular septum. Native T1-values at the interventricular insertion regions were significantly related to markers of disease severity. No differences in native T1-values were found between patients with idiopathic pulmonary arterial hypertension, systemic scleroderma related pulmonary arterial hypertension and chronic thromboembolic pulmonary hypertension. Our results suggests that native T1-mapping can be

developed as an alternative technique for the characterization of the interventricular insertion regions with the advantage of not requiring the use of contrast agents.

Patients with pulmonary hypertension have a decreased exercise tolerance. This exercise intolerance in mainly determined by circulatory limitations. Whether this exercise intolerance coincided with an inability to increase right ventricular contractility was investigated in **chapter 10** using an invasive cardiopulmonary exercise test. We prospectively included patients with precapillary PH and control subjects. The rest-to-exercise change in load-independent measures of right ventricular contractility, the contractile reserve, as well as the rest-to-exercise change in the coupling between the right ventricle and its load (right ventricular arterial coupling) were assessed using single beat pressure-volume loop analysis. We found that, in contrast to controls, pulmonary hypertension patients have no contractile reserve. Failure to compensate for the rest-to-exercise increase in load on the right ventricle led to a deterioration in right ventricular arterial coupling during exercise. Furthermore, we found that the contractile reserve was not related to a recently proposed surrogate, the rest-to-exercise change in pulmonary artery pressure.

Future perspectives

Non-invasive quantification of pulmonary vascular remodeling

In chapter 2 we investigated the usage of 3'-[18F]fluoro-3'-deoxythymidine ([18F]-FLT) positron emission tomography (PET/CT) for quantitative assessment of proliferation in the pulmonary vasculature of patients with idiopathic pulmonary arterial hypertension (IPAH). In this study we found an increased uptake of [18]-FLT in the lungs of patients with IPAH compared to control subjects. Furthermore, [18F]-FLT was able to track the pulmonary vascular remodeling in a monocrotaline ratmodel and the reverse remodeling after treating the animals with targeted therapies.

An important next study would be a test-retest study to assess repeatability of the uptake of [18F]-FLT in IPAH patients. Good repeatability is essential to be able to use [18F]-FLT PET/CT in the future to select patients with a hyperproliferative state that may benefit from anti-proliferative agents and to assess treatment responses. Current pulmonary hypertension therapies mainly have vasodilatory effects and thus may not influence proliferation rate. Therefore, application of [18F]-FLT should be assessed with future anti-proliferative compounds that directly target the pulmonary vascular remodeling.

In addition to the further development of [18F]-FLT, alternative tracers to quantify pulmonary vascular remodeling should be investigated. The increased expression of growth factor receptors may be reflected by enhanced uptake of radio-labeled tyrosine kinase inhibitors. It has been shown that there is an increased expression of the epidermal growth factor receptor (EGF-R) in the intima and media of pulmonary arteries of patients with pulmonary arterial hypertension [1]. In a pilot study we tested the tracer [11C]-Erlotinib (unpublished data), which binds to the EGF-R. We found that the uptake of [11C]-Erlotinib was not increased in patients with idiopathic pulmonary arterial hypertension compared to control subjects.

Other growth factors are upregulated as well in pulmonary arterial hypertension (platelet derived growth factor receptor (PDGF-R), vascular endothelial growth factor receptor (VEGF-R) and fibroblast growth factor receptor (FGF-R)) [2] and can potentially be used to quantify the pulmonary vascular remodeling using PET/CT. Nintedanib is a tyrosine kinase inhibitor targeting the PDGF-R, VEGF-R and FGF-R. Moreover, in preclinical studies Nintedanib showed potential to reverse pulmonary vascular remodeling [3]. Therefore, development of a Nintedanib tracer would be of interest to quantify pulmonary vascular remodeling in patients with pulmonary hypertension.

Characterization of myocardium using native T1-mapping

As described in chapter 7, native-T1 values of the right ventricular free wall could only be accurately assessed in small parts of the myocardium [4]. Presence of pericardial fat at the border of the frequently irregularly shaped right ventricular free wall can make it difficult to quantify native T1-values of the total right ventricular free wall. A voxel at the border of the right ventricular free wall can contain a partial volume of pericardial fat. Due to the fact that fat has a high signal intensity and very short T1-value, such a partial volume effect can already dominate the T1-value of the total voxel. This phenomenon can bias the quantification of native T1-values of the right ventricular free wall. By inserting a fat saturation pulse in the T1 mapping pulse sequence the effects of fat can be eliminated [5]. Future studies should test whether insertion of the fat saturation pulse can improve the quantification of the right ventricular free wall using T1-mapping.

Effect of exercise training on the right ventricle in patients with pulmonary hypertension

Several studies showed that exercise training progams can improve exercise capacity and quality of life in patients with pulmonary hypertension [6-11]. The mechanisms for the improvement in exercise capacity are yet incompletely understood. It has been shown that exercise training programs can increase capillarization of muscles [9] and can improve hemodynamics at rest and during exercise [6].

Handoko et al. evaluated the effects of exercise training on right ventricular function in a pulmonary hypertension rat model and showed that TAPSE decreased in rats with progressive pulmonary hypertension while an increased TAPSE was seen in rats with stable pulmonary hypertension [12]. In the same study exercise training did not affect right ventricular contractility at rest.

Currently, studies on the effects of exercise training on the right ventricle in patients with pulmonary hypertension are lacking. Randomized controlled trails are needed that investigate the effects of exercise training on the function of the right ventricle, not only at rest but also on the right ventricular contractile reserve. Ideally, assessment of right ventricular contractile reserve in such studies should combine pressure-volume loop analysis to assess the effects of exercise training on the load-independent contractile reserve (Chapter 10) and cardiac magnetic resonance imaging to assess the effects on the load-dependent contractile reserve [13-18], both measured during maximal incremental exercise protocols.

Contractile reserve of patients with scleroderma related pulmonary hypertension and patients with scleroderma and borderline pulmonary hypertension

In chapter 10 we compared the contractile reserve between control subjects and precapillary pulmonary hypertension patients. Whether differences exist between different precapillary pulmonary hypertension subtypes is unknown. In systemic scleroderma related pulmonary hypertension right ventricular contractility and right ventricular – arterial coupling at rest are more severely compromised compared to idiopathic pulmonary hypertension patients [19, 20]. Whether or not differences are even more pronounced during exercise is unknown. As such, it would be interesting to study the contractile reserve in systemic scleroderma patients with borderline pulmonary hypertension.

Effectiveness of inotropic drugs in patients with pulmonary hypertension

Contractility can increase due to ß-adrenergic stimulation. Inotropic drugs increase catecholamine release which binds to ß-adrenergic receptors subsequently activating sarcomeres, the contractile elements of cardiomyocytes.

The European pulmonary hypertension guideline recommends to treat patients with pulmonary arterial hypertension admitted to the hospital because of right ventricular failure with inotropes, with a preference for dobutamine [21]. However, this recommendation is mostly based on expert opinions rather than clear scientific evidence [22-24].

In the right ventricle of patients with pulmonary hypertension there is a downregulation and desensitization of ß-adrenergic receptors [25, 26] and patients with pulmonary hypertension have an impaired exertional contractile reserve [13, 14, 16, 18]. Therefore, it can be questioned whether patients with pulmonary hypertension benefit from inotropic drugs. Decreased contractile reserve measured by TAPSE upon dobutamine infusion has been shown in patients with pulmonary hypertension compared to control subjects [27] as well as in a pulmonary hypertension piglet model [28].

Acosta et al. studied the effects of dobutamine in patients with liver cirrhosis and pulmonary hypertension and showed that load-independent right ventricular contractility could increase upon administration of dobutamine [29]. However, pulmonary hypertension in these patients was relatively mild and therefore we do not know whether these results can be extrapolated to pulmonary hypertension patients with more severely compromised hemodynamics.

Whether or not patients with pulmonary arterial hypertension admitted to the hospital because of right ventricular failure benefit from inotropic drugs is still unclear. Therefore, there is an urgent need for studies to unravel the effects of inotropics in patients with pulmonary arterial hypertension and right ventricular failure.

References:

[1] Overbeek MJ, Boonstra A, Voskuyl AE, Vonk MC, Vonk-Noordegraaf A, van Berkel MP, et al. Platelet-derived growth factor receptor-beta and epidermal growth factor receptor in pulmonary vasculature of systemic sclerosis-associated pulmonary arterial hypertension versus idiopathic pulmonary arterial hypertension and pulmonary veno-occlusive disease: a case-control study. Arthritis research & therapy. 2011; 13:R61

[2] Voelkel NF, Gomez-Arroyo J, Abbate A, Bogaard HJ, Nicolls MR. Pathobiology of pulmonary arterial hypertension and right ventricular failure. The European respiratory journal. 2012; 40:1555-65

[3] Awad KS, Elinoff JM, Wang S, Gairhe S, Ferreyra GA, Cai R, et al. Raf/ERK drives the proliferative and invasive phenotype of BMPR2-silenced pulmonary artery endothelial cells. American journal of physiology. 2016; 310:L187-201

[4] Spruijt OA, Vissers L, Bogaard HJ, Hofman MB, Vonk-Noordegraaf A, Marcus JT. Increased native T1-values at the interventricular insertion regions in precapillary pulmonary hypertension. The international journal of cardiovascular imaging. 2016; 32:451-9

[5] Kellman P, Bandettini WP, Mancini C, Hammer-Hansen S, Hansen MS, Arai AE. Characterization of myocardial T1-mapping bias caused by intramyocardial fat in inversion recovery and saturation recovery techniques. J Cardiovasc Magn Reson. 2015; 17:33

[6] Ehlken N, Lichtblau M, Klose H, Weidenhammer J, Fischer C, Nechwatal R, et al. Exercise training improves peak oxygen consumption and haemodynamics in patients with severe pulmonary arterial hypertension and inoperable chronic thrombo-embolic pulmonary hypertension: a prospective, randomized, controlled trial. European heart journal. 2015; 37:35-44

[7] Babu AS, Padmakumar R, Maiya AG, Mohapatra AK, Kamath RL. Effects of Exercise Training on Exercise Capacity in Pulmonary Arterial Hypertension: A Systematic Review of Clinical Trials. Heart, lung & circulation. 2015; 25:333-41

[8] Chan L, Chin LM, Kennedy M, Woolstenhulme JG, Nathan SD, Weinstein AA, et al. Benefits of intensive treadmill exercise training on cardiorespiratory function and quality of life in patients with pulmonary hypertension. Chest. 2013; 143:333-43

[9] de Man FS, Handoko ML, Groepenhoff H, van 't Hul AJ, Abbink J, Koppers RJ, et al. Effects of exercise training in patients with idiopathic pulmonary arterial hypertension. The European respiratory journal. 2009; 34:669-75

[10] Grunig E, Lichtblau M, Ehlken N, Ghofrani HA, Reichenberger F, Staehler G, et al. Safety and efficacy of exercise training in various forms of pulmonary hypertension. The European respiratory journal. 2012; 40:84-92

[11] Mereles D, Ehlken N, Kreuscher S, Ghofrani S, Hoeper MM, Halank M, et al. Exercise and respiratory training improve exercise capacity and quality of life in patients with severe chronic pulmonary hypertension. Circulation. 2006; 114:1482-9

[12] Handoko ML, de Man FS, Happe CM, Schalij I, Musters RJ, Westerhof N, et al. Opposite effects of training in rats with stable and progressive pulmonary hypertension. Circulation. 2009; 120:42-9

[13] Claessen G, La Gerche A, Dymarkowski S, Claus P, Delcroix M, Heidbuchel H. Pulmonary vascular and right ventricular reserve in patients with normalized resting hemodynamics after pulmonary endarterectomy. Journal of the American Heart Association. 2015; 4:e001602

[14] Claessen G, La Gerche A, Wielandts JY, Bogaert J, Van Cleemput J, Wuyts W, et al. Exercise pathophysiology and sildenafil effects in chronic thromboembolic pulmonary hypertension. Heart (British Cardiac Society). 2015; 101:637-44

[15] Holverda S, Gan CT, Marcus JT, Postmus PE, Boonstra A, Vonk-Noordegraaf A. Impaired stroke volume response to exercise in pulmonary arterial hypertension. Journal of the American College of Cardiology. 2006; 47:1732-3

[16] Houston BA, Tedford RJ. Putting "at-rest" evaluations of the right ventricle to rest: insights gained from evaluation of the right ventricle during exercise in CTEPH patients with and without pulmonary endarterectomy. Journal of the American Heart Association. 2015; 4:e001895

[17] La Gerche A, Claessen G, Van de Bruaene A, Pattyn N, Van Cleemput J, Gewillig M, et al. Cardiac MRI: a new gold standard for ventricular volume quantification during high-intensity exercise. Circ Cardiovasc Imaging. 2012; 6:329-38

[18] Spruijt OA, de Man FS, Groepenhoff H, Oosterveer F, Westerhof N, Vonk-Noordegraaf A, et al. The effects of exercise on right ventricular contractility and right ventricular-arterial coupling in pulmonary hypertension. American journal of respiratory and critical care medicine. 2015; 191:1050-7

[19] Overbeek MJ, Lankhaar JW, Westerhof N, Voskuyl AE, Boonstra A, Bronzwaer JG, et al. Right ventricular contractility in systemic sclerosis-associated and idiopathic pulmonary arterial hypertension. The European respiratory journal. 2008; 31:1160-6

[20] Tedford RJ, Mudd JO, Girgis RE, Mathai SC, Zaiman AL, Housten-Harris T, et al. Right ventricular dysfunction in systemic sclerosis-associated pulmonary arterial hypertension. Circ Heart Fail. 2013; 6:953-63

[21] Galie N, Humbert M, Vachiery JL, Gibbs S, Lang I, Torbicki A, et al. 2015 ESC/ERS Guidelines for the diagnosis and treatment of pulmonary hypertension: The Joint Task Force for the Diagnosis and Treatment of Pulmonary Hypertension of the European Society of Cardiology (ESC) and the European Respiratory Society (ERS): Endorsed by: Association for European Paediatric and Congenital Cardiology (AEPC), International Society for Heart and Lung Transplantation (ISHLT). The European respiratory journal. 2015; 46:903-75

[22] Hoeper MM, Granton J. Intensive care unit management of patients with severe pulmonary hypertension and right heart failure. American journal of respiratory and critical care medicine. 2011; 184:1114-24

[23] Price LC, Wort SJ, Finney SJ, Marino PS, Brett SJ. Pulmonary vascular and right ventricular dysfunction in adult critical care: current and emerging options for management: a systematic literature review. Critical care (London, England). 2010; 14:R169
[24] Zamanian RT, Haddad F, Doyle RL, Weinacker AB. Management strategies for patients with pulmonary hypertension in the intensive care unit. Critical care medicine. 2007; 35:2037-50
[25] Bristow MR, Minobe W, Rasmussen R, Larrabee P, Skerl L, Klein JW, et al. Beta-adrenergic neuroeffector abnormalities in the failing human heart are produced by local rather than systemic mechanisms. The Journal of clinical investigation. 1992; 89:803-15
[26] Piao L, Fang YH, Parikh KS, Ryan JJ, D'Souza KM, Theccanat T, et al. GRK2-mediated inhibition of adrenergic and dopaminergic signaling in right ventricular hypertrophy: therapeutic implications in pulmonary hypertension. Circulation. 2012; 126:2859-69
[27] Sharma T, Lau EM, Choudhary P, Torzillo PJ, Munoz PA, Simmons LR, et al. Dobutamine stress for evaluation of right ventricular reserve in pulmonary arterial hypertension. The European respiratory journal. 2015; 45:700-8
[28] Guihaire J, Haddad F, Noly PE, Boulate D, Decante B, Dartevelle P, et al. Right ventricular reserve in a piglet model of chronic pulmonary hypertension. The European respiratory journal. 2015; 45:709-17
[29] Acosta F, Sansano T, Palenciano CG, Falcon L, Domenech P, Robles R, et al. Effects of dobutamine on right ventricular function and pulmonary circulation in pulmonary hypertension during liver transplantation. Transplantation proceedings. 2005; 37:3869-70

11

CHAPTER 12

Nederlandse samenvatting

OA Spruijt[1]

[1]Afdeling Longziekten, VU Medisch Centrum, Amsterdam

Nederlandse samenvatting:

Bij de ziekte pulmonale arteriële hypertensie vindt er remodulering plaats in de kleine pulmonaal arteriën hetgeen leidt tot een vernauwing van het lumen. De remodulering van het arteriële longvaatbed is een complex proces en wordt onder andere gekenmerkt door vasoconstrictie, hyperproliferatie van endotheelcellen en gladde spiercellen alsmede inflammatie. Door de vernauwing van het lumen neemt de weerstand van het longvaatbed toe hetgeen resulteert in een verhoogde druk in de pulmonaal arteriën. De toegenomen weerstand leidt tot een toename van de load op de rechter ventrikel en een toename van de wandspanning. Via een complex adaptatieproces zal de rechter ventrikel zoveel mogelijk zijn functie proberen te behouden. Globaal gesteld zal er in eerste instantie hypertrofie optreden en de contractiliteit van de rechter ventrikel toenemen om het hartminuutvolume zoveel mogelijk te behouden. Wanneer dit onvoldoende gelukt zal er dilatatie optreden ter compensatie hetgeen echter tevens leidt tot een toename van de wandspanning. Uiteindelijk treedt er rechter hartfalen op hetgeen de belangrijkste doodsoorzaak is van patiënten met pulmonale arteriële hypertensie.

Vroege herkenning en prognose bij patiënten met pulmonale hypertensie

De diagnose pulmonale arteriële hypertensie wordt vaak gesteld in een laat stadium van de ziekte. Dit komt omdat de klachten waarmee patiënten zich in eerste instantie presenteren niet specifiek zijn. In de diagnostische fase van patiënten die zich presenteren met onbegrepen dyspneu wordt vaak een CT met contrast vervaardigd van het longvaatbed, bijvoorbeeld ten behoeve van het uitsluiten van longembolieën als mogelijke oorzaak. Het was reeds bekend dat op een dergelijke CT scan ook aanwijzingen kunnen worden gevonden voor de aanwezigheid van pulmonale hypertensie, waarbij de meest onderzochte aanwijzing die is van een vergrootte diameter van de pulmonaal arterie ten opzichte van de diameter van de aorta ascendens. In **hoofdstuk 2** hebben we onderzocht of de voorspellende waarde van een CT met contrast van het longvaatbed kan worden vergroot door de diameter ratio tussen de pulmonaal arterie en de aorta ascendens te combineren met de diameter ratio tussen de rechter ventrikel en linker ventrikel. Het predictiemodel, waarbij de diameter ratio tussen de pulmonaal arterie en de aorta ascendens werd gecombineerd met de diameter ratio tussen de linker en rechter ventrikel had een betere voorspellende waarde voor de aanwezigheid van pulmonale hypertensie dan het predictiemodel met alleen de diameter ratio tussen de pulmonaal arterie en de aorta ascendens.

Uit veel studies is gebleken dat bij de ziekte pulmonale arteriële hypertensie verschillende rechter ventrikel parameters een belangrijke prognostische waarde hebben. In **hoofdstuk 3** hebben we een eenvoudige toepasbare risico score ontwikkeld gebaseerd op een combinatie van metingen van het rechter hart en deze vergeleken met reeds bestaande risico scores. De rechter hart score toonde een goede prognostische waarde en correleerde met algemeen bekende, complexere risicoscores (REVEAL en NIH score).

Het meten van de behandel respons bij patiënten met pulmonale hypertensie

De remodulering van het vaatbed in patiënten met pulmonale arteriële hypertensie leidt tot een toename van de load op de rechter ventrikel. Zoals reeds eerder vermeld is rechter hartfalen de belangrijkste doodsoorzaak van patiënten met pulmonale arteriële hypertensie hetgeen het belang onderstreept van monitoring van de functie van de rechter ventrikel tijdens de follow-up van patiënten. In **hoofdstuk 4** gaven wij een overzicht van de beschikbare methoden en parameters waarmee de respons van de functie van de rechter ventrikel op therapie het best kan worden gemeten.

Tegenwoordig wordt MRI gezien als de beste beeldvormende techniek voor het meten van de functie van de rechter ventrikel. Deze techniek relatief duur, niet in alle ziekenhuizen beschikbaar en het analyseren van de volumina en de functie van de rechter ventrikel kost relatief veel tijd. Echocardiografie is een goedkopere techniek en is in vrijwel alle ziekenhuizen voor handen. De tweedimensionale functiematen van de rechter ventrikel die met echocardiografie verkregen kunnen worden, kunnen ook relatief sneller worden geanalyseerd. Daarom onderzochten wij in **hoofdstuk 5** of eenvoudige tweedimensionale functiematen van de rechter ventrikel kunnen worden gebruikt voor de monitoring van patiënten met pulmonale hypertensie. Hiertoe vergeleken wij de verandering van tweedimensionale functie maten in de tijd verkregen met echocardiografie met de verandering van de rechter ventrikel ejectie fractie berekend met MRI. Wij vonden een goede relatie tussen tweedimensionale functiematen verkregen met echo en de rechter ventrikel ejectie fractie berekend met MRI. Echter, de verandering van de rechter ventrikel ejectie fractie in de tijd gemeten met MRI kon niet goed worden gevolgd door de tweedimensionale functie maten verkregen met echocardiografie. Onze resultaten suggereren dat echocardiografie onvoldoende sensitief is voor het monitoren van de rechter ventrikelfunctie.

Patiënten met idiopathische pulmonale arteriële hypertensie en een lage diffusie capaciteit van de longen voor koolstofmonoxide (DLCO) hebben een slechtere overleving dan patiënten met

idiopathische pulmonale arteriële hypertensie en een behouden DLCO. Of dit deels wordt verklaart door een slechtere response op pulmonale hypertensie specifieke vasodilatoire therapie was niet bekend. Daarom onderzochten wij in **hoofdstuk 6** de cardiale en hemodynamische response op therapie bij patiënten met idiopathische pulmonale arteriële hypertensie en een verlaagde DLCO. De hemodynamica en functie van het hart van patiënten met idiopathische pulmonale arteriële hypertensie en een lage DLCO was op moment van diagnose niet verschillend van patiënten met idiopathische pulmonale arteriële hypertensie en een behouden DLCO. Beide groepen toonden een verbetering in hemodynamica en functie van het hart met pulmonale hypertensie specifieke vasodilatoire therapie zonder een verslechtering van de oxygenatie in rust en tijdens inspanning. Kortom, patiënten met idiopathische pulmonale arteriële hypertensie en een lage DLCO reageren hetzelfde op pulmonale hypertensie specifieke vasodilatoire therapie in termen van hemodynamica en cardiale functie als patiënten met idiopathische pulmonale arteriële hypertensie en een behouden DLCO.

De toepassing van nieuwe technieken binnen pulmonale hypertensie

Hoofdstuk 7 geeft een overzicht van nieuwe beeldvormende technieken en nieuwe toepassingen van bestaande technieken binnen de ziekte pulmonale hypertensie.

Bij patiënten met pulmonale arteriële hypertensie wordt de druk in het longvaatbed gemeten tijdens een rechter hartkatheterisatie. De gevolgen van de toegenomen load op de rechter ventrikel kunnen in beeld worden gebracht met een MRI of een echo van het hart. Echter is het op dit moment niet mogelijk het primaire ziekteproces, de remodulering van het longvaatbed, in beeld te brengen. In **hoofdstuk 8** onderzochten wij of middels 3'-[18F]fluoro-3'-deoxythymidine ([18F]-FLT) positron emissie tomografie (PET/CT) het proces van hyperproliferatie als onderdeel van de remodulering van het longvaatbed kon worden gekwantificeerd in patiënten met idiopathische pulmonale arteriële hypertensie. Vervolgens onderzochten wij met behulp van het monocrotaline ratmodel of [18F]-FLT PET/CT in staat was de remodulering van het vaatbed in de long te volgen, alsmede de effecten van gerichte therapie. De opname van [18F]-FLT in de longen van patiënten met idiopathische pulmonale arteriële hypertensie was significant hoger dan de opname in de longen van controle patiënten en was gerelateerd aan bekende parameters van ziekte-ernst. De opname van [18F]-FLT in de long toonde heterogeniteit tussen patiënten met idiopathische pulmonale arteriële hypertensie. In het monocrotaline ratmodel van pulmonale hypertensie vonden

wij tevens dat een afname van proliferatie geïnduceerd door specifieke therapie (dichloroacetaat en imatinib) leidde tot een proportionele afname in de opname van [18F]-FLT in de long.

Een bekende techniek waarmee het myocard kan worden gekwantificeerd met MRI is Late Gadolinium Enhancement. Een nieuwe techniek om het myocard te kwantificeren in native T1-mapping. Native T1-mapping heeft een aantal voordelen ten opzichte van Late Gadolinium Enhancement. Een van de voordelen is dat voor het maken van de native T1-maps geen contrast hoeft te worden toegediend aan de patiënt tijdens de MRI scan. In **hoofdstuk 9** hebben wij deze techniek toegepast bij patiënten met pre-capillaire pulmonale hypertensie ter karakterisering van het myocard. Native T1-waarden waren verhoogd ter plaatse van de interventriculaire insertiepunten ten opzichte van het septum, de rechter ventrikel vrije wand en linker ventrikel vrije wand. Er werd geen verschil gevonden in native T1-waarden tussen patiënten met idiopathische pulmonale arteriële hypertensie, patiënten met pulmonale arteriële hypertensie geassocieerd met systemische sclerose en patiënten met chronische tromboembolische pulmonale hypertensie. De native T1-waarden ter plaatse van de insertiepunten waren significant gerelateerd aan bekende parameters van ziekte-ernst.

Patiënten met pulmonale arteriële hypertensie kunnen zich vaak minder goed inspannen. Uit onderzoek is gebleken dat de inspanningsintolerantie voornamelijk het gevolg is van circulatoire limitaties. In **hoofdstuk 10** hebben we tijdens een invasieve inspanningstest met behulp van het meten van druk-volume relaties met de zogeheten 'Single Beat methode' onderzocht of er verschillen zijn tussen patiënten met pulmonale hypertensie en controles in de contractiele reserve, oftewel de reserve in contractiliteit van rust naar inspanning. Tevens hebben we de effecten van inspanning op de koppeling tussen de rechter ventrikel en de load tussen beide groepen vergeleken. In tegenstelling tot controles, bleken de patiënten met pulmonale hypertensie geen contractiele reserve te hebben hetgeen leidde tot een verslechtering van de koppeling tussen de rechter ventrikel en de load tijdens inspanning. De contractiele reserve bleek niet te correleren met een recent voorgestelde surrogaat meting van de contractiele reserve, de verandering van de pulmonaal druk tijdens inspanning.

12

List of Publications

Full papers

Spruijt OA, Ashek A, Harms HJ, Lammertsma AA, Cupitt J, Dubois O, Dabral S, Pullamsetti SS, Huisman MC, Frings V, Boellaard R, de Man FS, Vonk Noordegraaf A, Wilkins MR, Bogaard HJ, Zhao L ^{18}FLT PET depicts heterogeneous proliferation pathology in IPAH patient lung: a potential biomarker for PAH. Submitted

Spruijt OA, van der Bruggen CEE, Nossent EJ, Trip P, de Man FS, Marcus JT, Bogaard HJ, Vonk Noordegraaf A. Treatment response in patients with idiopathic pulmonary arterial hypertension and a severely reduced diffusion capacity. Pulm Circ 2017

Huis In 't Veld AE, Van Vliet AG, **Spruijt OA**, Handoko ML, Marcus JT, Vonk Noordegraaf A, Bogaard HJ. CTA-derived left to right atrial size ratio distinguishes between pulmonary hypertension due to heart failure and idiopathic pulmonary arterial hypertension. Int J Cardiol 2016

Vonk-Noordegraaf A, **Spruijt OA**. Book chapter: Emerging modalities (MR, PET and others). Book Pulmonary Circulation, Fourth Edition. Taylor & Francis Group 2016

Spruijt OA, Di Pasqua MC, Bogaard HJ, Oosterveer F, Marcus JT, Vonk-Noordegraaf A, Handoko ML. Serial assessment of right ventricular systolic function in patients with precapillary pulmonary hypertension using simple echocardiographic parameters: a comparison with cardiac magnetic resonance imaging. J Cardiol 2016

Van der Bruggen CEE, Happe CM, Dorfmuller P, Trip P, **Spruijt OA**, Rol N, Hoevenaars FP, Houweling AC, Girerd B, Mercier O, Humbert M, Handoko ML, Van Der Velden J, Vonk Noordegraaf A, Bogaard HJ, Goumans MJ, de Man FS. Bone Morphogenetic Protein Receptor Type 2 Mutation in Pulmonary Arterial Hypertension, A view on the Right Ventricle. Circulation 2016

Spruijt OA, Vissers L, Bogaard HJ, Hofman MBM, Vonk-Noordegraaf A, Marcus JT. Increased native T1-values at the interventricular insertion regions in precapillary pulmonary hypertension. Int J Cardiovasc Imaging 2016

Van der Bruggen CEE, **Spruijt OA**, Meijboom LJ, Vonk Noordegraaf A. Book chapter: Pulmonary hypertension. Book: ERS monograph: Imaging 2015

Haddad F, **Spruijt OA**, Denault AY, Finocchiaro G, Brunner N, Mercier O, Fadel E, Schnittger I, Vrtovec B, Wu J, Perez V, Vonk-Noordegraaf A, Zamanian R. A simple score for predicting outcome in patients with idiopathic and drug and toxin pulmonary arterial hypertension. JACC Cardiovasc Imaging 2015

Spruijt OA, de Man FS, Groepenhoff H, Oosterveer F, Westerhof N, Bogaard HJ, Vonk-Noordegraaf A. The effects of exercise on right ventricular contractility and ventriculo-arterial coupling in pulmonary hypertension, Am J Respir Crit Care Med 2015

Spruijt OA, Vonk-Noordegraaf A, Bogaard HJ. Book chapter: Hemodynamic evaluation and exercise testing in chronic RV failure. Book: The right Ventricle in health and disease, Springer 2015

Spruijt OA, HJ Bogaard, Heijmans MW, Lelij RJ, van de Veerdonk MC, de Man FS, Westerhof N, Vonk-Noordegraaf A. Predicting pulmonary hypertension using standard computed tomography angiography, Int J Cardiovasc Imaging 2015

Spruijt OA, Bogaard HJ, Vonk-Noordegraaf A. Assessment of right ventricular responses to therapy in pulmonary hypertension. Drug Disc Today 2014

van de Veerdonk MC, Dusoswa SA, Tim Marcus J, Bogaard HJ, **Spruijt OA**, Kind T, Westerhof N, Vonk-Noordegraaf A. The Importance of trabecular hypertrophy in right ventricular adaptation to chronic pressure overload. Int J Cardiovasc Imaging 2014

Spruijt OA, Bogaard HJ, Vonk-Noordegraaf. Pulmonary arterial hypertension combined with a high cardiac output state: Three remarkable cases. Pulm Circ 2013

de Graaf W, Heger M, **Spruijt OA**, Maas A, de Bruin K, Hoekstra R, Bennink RJ, van Gulik TM. Quantitative Assessment of Liver Function after Ischemia-Reperfusion Injury and Partial Hepatectomy in Rats. J Surg Res. 2010

Oral and poster presentations

2007: SEOHS (Symposium Experimenteel Onderzoek Heelkundige Specialismen), Leiden, The Netherlands. Oral presentation. Title: Quantitative Assessment of Liver Function after Ischemia-Reperfusion Injury and Partial Hepatectomy in Rats.

2013: ATS (American Thoracic Society), Philadephia, United States of America. Poster presentation. Title: Uni-dimensional ventricular measurements on standard computed tomography angiography for predicting pulmonary hypertension.

2013: Institute for Cardiovascular Research VU, Amsterdam. Poster presentation. Title: Uni-dimensional ventricular measurements on standard computed tomography angiography for predicting pulmonary hypertension.

2013: ERS (European Respiratory Society), Barcelona, Spain. Poster presentation. Title: Predicting pulmonary hypertension with standard computed tomography angiography.

2014: Thalys-meeting, Paris, France. Oral presentation. Title: Right Ventricular Response to therapy in scleroderma-related pulmonary arterial hypertension; in comparison to idiopathic pulmonary arterial hypertension.

2014: ATS (American Thoracic Society), San Diego, United States of America. Poster presentation. Title: The coupling of the right ventricle to its load during exercise in pulmonary hypertension.

2014: GSK 2nd Scientific seminar on pulmonary hypertension, Amsterdam, The Netherlands. Oral presentation. Title: The right ventricular

exertional contractile reserve and the effects of exercise on right ventricular – arterial coupling in pulmonary hypertension.

2015: ATS (American Thoracic Society), Denver, United States of America. Poster discussion. Title: The Right Ventricular Contractile Reserve In Pulmonary Hypertension.

2015: VU University Medical Center Amsterdam 9th Science Exchange Day. Poster presentation. Title: Increased native T1-values at the interventricular insertion regions of precapillary pulmonary hypertension patients.

2015: ERS (European Respiratory Society), Amsterdam, The Netherlands. Poster presentation. Title: Increased native T1-values at the interventricular insertion regions of precapillary pulmonary hypertension patients.

2015: Pulmonary hypertension: Next Generation symposium, London, UK. Oral presentation. Title: Native T1 values in Pulmonary Hypertension.

2015: GSK 3rd Scientific seminar on pulmonary hypertension, Lund, Sweden. Oral presentation. Title: Molecular imaging of the lung in pulmonary hypertension.

2016: PVRI 10th Annual World Congress, Rome, Italy. Oral presentation. Title: Repeated measurements of right ventricular function and structure with cardiac magnetic resonance imaging in pulmonary hypertension.

2016: ATS (American Thoracic Society), San Francisco, United States of America. Poster presentation. Title: Serial assessment of right ventricular systolic function in patients with precapillary pulmonary hypertension.

Curriculum Vitae

Curriculum Vitae

Onno Anthonius Spruijt was born in Amsterdam, The Netherlands on May 4, 1985. In 2003 he completed secondary school (VWO) at the Keizer Karel College in Amstelveen. He graduated from Medical School in 2011 at the University of Amsterdam (AMC). After working as a resident at the department of Internal Medicine at the St. Antonius Hospital in Utrecht, he started in 2012 to work as an investigator in the field of pulmonary hypertension at the department of Pulmonary Medicine, VU University Medical Center in Amsterdam under the supervision of Harm-Jan Bogaard and Anton Vonk Noordegraaf. August 1, 2016 he started working as a resident at the department of Internal Medicine at OLVG west as part of his specialization in Pulmonary Medicine at the VU University Medical Center.

Onno Anthonius Spruijt is geboren in Amsterdam, Nederland op 4 mei 1985. Hij volgde het VWO aan het Keizer Karel College te Amstelveen alwaar hij in 2003 zijn diploma behaalde. Vervolgens studeerde hij af aan de faculteit Geneeskunde van de Universiteit van Amsterdam in 2011. Na een jaar te hebben gewerkt als arts-assistent niet in opleiding tot specialist (ANIOS) op de afdeling Interne Geneeskunde van het St Antonius Ziekenhuis te Utrecht, startte hij als arts-onderzoeker op de afdeling Longziekten van het VU Medisch Centrum onder leiding van Harm-Jan Bogaard en Anton Vonk Noordegraaf. Op 1 augustus 2016 startte hij als arts-assistent op de afdeling Interne Geneeskunde van het OLVG-west als onderdeel van zijn specialisatie tot longarts.

Dankwoord

Al speelde mijn promotie zich af binnen de muren van een ziekenhuis, mijn werkomgeving had soms meer weg van dat van een kantoor.

The Office – Aflevering 1 – Een dubbele rij knopen

Als geïndoctrineerde AMC geneeskunde student voelde het toch als vreemdgaan toen ik voor het eerst een witte jas omsloeg met daarop het logo van het VU Medisch Centrum. Dit was direct tijdens mijn sollicitatie. Prof. dr. Vonk Noordegraaf (promotor) gaf aan eerst nog even een paar patiënten te moeten spreken op zaal alvorens het over onderzoek te hebben, of ik gelijk even meeliep. Beste Anton, de ideeënbus van de PH wereld, dank dat jij mij de mogelijkheid hebt gegeven om onderzoek te doen onder jouw vleugels. Jouw gedrevenheid en liefde voor het onderzoek is zeer aanstekelijk. Een onderzoek bespreking met jou was altijd behoorlijk intensief, maar meestal resulteerde dit in een A4tje vol nieuwe ideeën en inzichten. Regelmatig ook onnavolgbaar als ik met het A4tje vol aantekeningen terugkwam op mijn kamer en de tekst overdacht. Dank voor alle hulp. Ik kijk ernaar uit ook in de kliniek veel van je te leren.

Na het gesprek werd ik doorgestuurd naar een uithoek van de kelder van het polikliniekgebouw om kennis te maken met dr. Marcus (co-promotor). Hij sloeg direct het boekje van een van de voorgaande onderzoekers (Taco Kind) open met twee pagina's vol onmogelijke formules, waarna hij kalm zei: 'hier zal je dus verder op moeten bouwen'. Enigszins terneergeslagen verliet ik het pand. Beste Tim, heel wat dinsdag- en woensdagavonden heb ik met jou gespendeerd in jouw natuurlijke habitat, bij jouw grote liefde, de Avanto magneet. Dankzij de liefde voor het MRI onderzoek en daarmee de schat aan data die beschikbaar is op de afdeling, hebben meerdere hoofdstukken uit dit boekje tot stand kunnen komen. Dank voor alle hulp met een engelen geduld.

The Office – Aflevering 2 – Team PH

Dr. Bogaard (co-promotor). Harm-Jan alias HJ. De man met de eeuwig jeugdige looks (door mijn beperkte haardos ziet hij er misschien wel jonger uit dan ik). Gezien jouw vrolijkheid, enthousiasme in het algemeen en voor het onderzoek en goede ideeën is samenwerken met jou een feest. De deur stond altijd open voor een snelle vraag tussendoor of een wat langere discussie bij een ingewikkelder probleem. Dank voor alle hulp en vele wijze lessen. Mooi dat jij mijn co-promotor bent. Hopelijk zit er in de toekomst nog meer onderzoeksamenwerking in.

Dr. de Man - Handoko. Frances, moeke der PH onderzoekers, statistisch wonderkind, streng als nodig maar vooral heel lief, dank voor alle hulp in eerste instantie als collega en daarna als supervisor. Ook bij jou kon ik altijd terecht voor hulp of een (statistische) vraag. Veel dank voor alle wijze lessen en de gezelligheid. Ps. Wanneer ga jij je eens opgeven voor 'Heel Holland bakt'?
Prof. dr. Westerhof. Beste Nico, dank voor alle hulp met het onderzoek. Ik heb genoten van uw gedrevenheid en de mooie fysiologie presentaties tijdens de PH-werkgroep. Het is een voorrecht met u te hebben mogen samenwerken. Ik hoop dat nog vele onderzoekers na mij dit mogen meemaken.

Dr. Boonstra. Beste Anco, vader der PH in het VUmc, dank voor het enthousiasmeren van patiënten voor deelname aan het onderzoek. Dank voor de inspirerende en vaak ook grappige onderwijs momenten tijdens het ochtendonderwijs. Daarnaast veel dank dat jij mij de mogelijkheid hebt gegeven de opleiding tot longarts te kunnen volgen.

Frank Oosterveer, een goedzak pur sang. Een middag doorbrengen bij Frank tijdens de rechter hartcatheterisaties is eigenlijk een feest. Dank voor alle hulp en het geduld tijdens het uitvoeren van de inspanningscatheterisaties. Dank voor de vaste Eredivisie-discussies op de maandag samen met die PSV-er van de afdeling en dank voor de hulp met die eeuwige MRI-planning. Jouw vrolijkheid, positiviteit en betrokkenheid bij de patiënten vind ik zeer bewonderenswaardig.
Martha, Iris en Gwen, dank voor alle hulp, jullie zijn onmisbaar voor het team PH.

The Office – Aflevering 3 – The Office
Zoals waarschijnlijk bij elke grote organisatie het geval is, begint een nieuwe medewerker met een algemene introductie, een soort propaganda tour van de instelling. Aldaar leerde ik mijn eerste collega kennen. Chris alias Happe, de rattenvanger van de VU. De man met yellow fever tijdens het Edelweiss festival. Happe, in menig hotelkamer in de wereld tijdens congressen heb jij mijn gesnurk moeten aanhoren. Dank voor de vele mooie momenten binnen en buiten de VU. Succes met het afronden van het boekje en de opleiding geneeskunde. Ben benieuwd wat het gaat worden! Wanneer pakken we weer een kippetje bij van t Spit?

Mijn kamer bevond zich op afdeling 6D, een stuk niemandsland dat men vergeten was bij het OK-complex te trekken met een panorama view over het Nieuwe Meer. 6D-118, schaar, perforator en nietmachine deelde ik met Mariëlle, Romane en Wouter.
Mariëlle, koningin van de magneet. Dank voor de vele (domme) vragen die ik heb mogen afvuren aan het begin van mijn promotie aangaande het MRI-onderzoek, het intekenen van de MRI's en de statistiek. Ik heb echt super veel van je geleerd. Succes met de cardiologie.
Romane en Wouter, het oncologische gedeelte van de kamer. Wouter had naast zijn onderzoek misschien wel de belangrijkste taak van het kantoor, het bijhouden en bestellen van de cupjes voorraad bij Nespresso. Wouter, dank voor de mooie tijd, succes met de opleiding tot longarts. Romane, dank voor de gezelligheid en succes met de opleiding tot huisarts.

The Office – aflevering 4 – De buren
Een deur verder, iets verder van de lift, maar dichterbij de pantry, dus kantoor technisch een prima locatie, was een kantoor volledig ingenomen door PH volk. De raamkant werd bezet door Frances en Bart met in de vensterbank een soort lego dorp (emoticon-icon: vreemd). Bart, mede liefhebber van het Amsterdamse amateurvoetbal in de kelderklasse, expert in het uitputten van COPD patiënten op een fietsje. Dank voor de hulp met het opzetten van de inspanningsstudie. Mooi dat je nu als opponent aanwezig bent bij mijn verdediging. Waarschijnlijk hebben we nog wat overlap op de afdeling en leer ik van jou nog graag de wondere wereld van de Wasserman plotjes.
Strategisch achter de deur zat Pia alias de Tripmeister alias Pmax. De vrouw die het een dag vol hield in een huwelijk met Johannesma op het Edelweiss-festival en vooral de vrouw bekend van de karaoke hit: 'Teenage dirtbag'. Trip, dank voor alle single beat hulp, de introductie in de load-onafhankelijke wereld en alle gemütlichkeit. Ik kijk ernaar uit weer samen te werken op de VU tijdens de opleiding.
In de deuropening, toch niet de beste plek op een kantoor, wel het dichts bij de pantry, Gerrina, groot afnemer van tonijn pizza en zoals bleek in Gent, de kipcorn. Dank voor de mooie momenten vooral out-of-office en tijdens congressen. Succes met de opleiding tot longarts, mooi dat wij straks ook weer samenwerken.

The Office – Aflevering 5 – Het geluid
Halverwege mijn eerste jaar waren er enkele transfers op kantoor 6D-120. Another-day-at-the-office werd abrupt verstoord. Het Nespresso apparaat op 6D-118 resoneerde een nog niet eerder gehoord

geluid. Het bleek het geluid van een lach. Een meisje, ik schatte haar 16, had de plaats ingenomen van Bart aan het raam. Al snel verplaatste de lach zich via een rolstoel na een knie incident tijdens een potje zaalvoetbal. Gelukkig werd een longembolie uitgesloten middels een CT scan. Cathelijne alias panda, dank voor alle vrolijkheid, jouw eeuwige optimisme en jouw relativerend vermogen als het onderzoek weer eens tegen zat. Dank voor de mooie tijd. Succes met de laatste loodjes van jouw proefschrift. Dat PSV maar nooit meer kampioen mag worden.
Bij de buren op 6D-120 kon je niet ongestraft terugkomen van vakantie. Meestal betekende dit na terugkomst dat je eerst je gehele werkplek grondig moest schoonmaken. Bij de buren had men bedacht het bureau vol te zetten met bekertjes water (emoticon-icon: flauw). Terwijl Justine op haar knieën onder het bureau van Pia bekertjes aan het vullen was, liep daar net prof. Postmus de kamer binnen. Een hoogtepunt (was dit het moment dat je besloot radiotherapeut te worden in plaats van longarts?). Justine alias Jus, dank voor alle gezelligheid en de mooie racefietstocht langs het Markermeer. Met wind tegen denk ik vaak terug aan de Houtribdijk. Succes met de opleiding radiotherapie. Moeten snel maar weer eens een nieuw tochtje gaan maken.

The Office – Aflevering 6 – Middagje vrij

Paul alias Johannesma, een jaar na je start maakte je je debuut op 6D. Dat is niet onopgemerkt gebleven. Dit debuut zal hebben plaatsgevonden rond de klok van 11, eerder was Paul niet te vinden in het VUmc. Mensen die het kantoor om 17h verlieten kregen voortaan steevast te horen of zij een ‘middagje vrij?’ waren. Dit was eigenlijk wel fijn daar een kantoortijger meestal een middagdip kent rond 16h en na 17h de motor weer een beetje op gang kwam. Daar heb ik dus regelmatig nog een aantal productieve uurtjes kunnen pakken. Een maand later zaten we met een full-gear racefiets (Paul zelfs met zijn initialen op helm en fiets) en al na een week verloren we de Dam-tot-Dam-fietsclassic-‘die-fietsen-we-zeker-30km/u-gemiddeld’-weddenschap die we op 6D afsloten (die twee lekke banden hielpen natuurlijk ook niet). Sindsdien volgden er nog vele ritjes en vooral ook vele biertjes buiten kantoortijd. Paul, een zeer harde werker, een man met het hart op de tong, de man met de bulderstem. Jouw vrolijkheid, energie en humor kan ik zeer waarderen en hoop ik nog lang mee te maken. Dank voor de mooie tijd in-and-out-of-office.

The Office – Aflevering 7 – 3F

Halverwege mijn promotie werd uiteindelijk opgemerkt dat ze bij de bouw van het OK-complex een stukje waren vergeten, 6D was niet meer. 6D118 werd 3F-11. Een nette vleugel die werd gedeeld

met de orthopedie. De pantry alhier was verboden terrein en werd bewaakt door de secretaresse van de orthopedie. Mijn bureau keek voortaan uit op een roze muur van ordners, met daar achter posters van mannen aan de muur. Het leek een zware tijd te worden daar ik werd geplaatst tegenover het meisje met de lach.
Nadat er langzaam een leegloop was ontstaan op 3F (Wouter, Justine en Paul gone) was daar plotseling een nieuw gezicht. Anna, een pittige doch lieve tante, kwam met gestrekt been in. Een zeer harde werkster en nog eens geordend ook. De GOSPEL-studie was bij jou dan ook in perfecte handen. Dank voor de samenwerking en alle gezelligheid. Succes met het afronden van je proefschrift. De volgende keer als we een cabrio huren richting Yosemite park moet je ook maar eens voorin gaan zitten.

The Office – Aflevering 8 – Het tooltje
Door menig onderzoeker was ik gewaarschuwd mij niet te wagen aan PET-onderzoek, maar tijdens een onderzoeksmeeting in mijn 2e jaar werd mij een PET-onderdeel van het PHEADRA project in de schoenen geschoven. Anton benoemde dit project tijdens deze meeting met de geruststellende woorden: 'jouw Waterloo'. Gelukkig was daar plotseling Hans alias professor Harms. De uitvinder van 'het tooltje'. Een wetenschapper avant la lettre. Hans, zonder jou was er nooit een PET-hoofdstuk verschenen in dit boekje. Dank voor de samenwerking, al je geduld met het beantwoorden van de vele (domme) vragen en de stink-kaas marathon op het Bachus wijnfestival.

The Office – Aflevering 9 – Komkommer water
Het laatste jaar van mijn promotie was daar. Verdere uitbreiding van 3F liet niet lang op zich wachten. Joanne, een semi-professionele wielrenster, en Anna-Larissa, een niet-professioneel tennisster, kwamen het team versterken. Joanne, dank voor alle hulp met het invullen van de tourpoultjes. Je weet dat ik voortaan in juli weer even pols wie ik wel en niet in mijn team moet opnemen. Dank voor de gezelligheid op 3F en succes met het PET onderzoek. Anna-Larissa, aandeelhoudster van Nivolumab, de vrouw met de droge humor. Altijd te porren voor een vrijmibo. Dank voor de gezellige tijd en veel succes met het afmaken van je promotie. Niet veel later werd Adinda 'ik kan wel janken' Mieras van Marktplaats geplukt inclusief een kan komkommer water en een pak rijstwafels. Dank voor de gezellige tijd, de flauwe grappen en succes met het afmaken van je onderzoek!

The Office – Aflevering 10 – Einde

Tsja en dan zijn er opeens 4 jaar om. Achteraf toch wel omgevlogen. Inmiddels heb ik het kantoor verlaten voor de kliniek. Ook heel leuk, maar af en toe kijk ik toch met weemoed terug naar mijn kantoorplek. Het was een mooie tijd. Dank allen!

The Office – Losse fragmenten

Beste Ella, Ellen en Anny, dank voor alle administratieve hulp tijdens mijn promotie. Ella, ik zal de Flamenco voorstelling op het bureau niet snel vergeten. Anny, veel dank voor alle hulp met de rompslomp die komt kijken bij het afronden van een promotie.

Nina, tijdens de PH meeting had jij voor mij toch vaak de meest lastige materie. Dank voor alle gezelligheid en succes met het afronden van je proefschrift en de co-schappen!

Beste Jurjan, de man die ik in Denver heb leren kennen als iemand die wél het juiste biertje wist te bestellen. Dank voor de gemütlichkeit tijdens de congressen.

Beste Louis, dank voor de hulp en samenwerking met ons echo stuk. Succes met de cardiologie.

Robert, Michiel, Sun, Pepe, Deni, Josien, Jasmijn en Esther dank voor alle samenwerking en de gezelligheid.

Said, Luuk, Tijmen en Judith, dank voor alle hulp met de vaak taaie MRI uitwerkingen en succes met jullie verdere carrière!

Alle stafleden en arts-assistenten van de afdeling Longziekten, veel dank voor de vele onderwijsmomenten en de input tijdens onderzoekpresentaties. Tot snel in de kliniek.

Het PHAEDRA-consortium, dank voor het onderzoek dat ik onder jullie vleugels heb kunnen doen. Dank voor alle wijze lessen en mooie symposia. Hopelijk leidt deze samenwerking nog tot veel moois in de toekomst.

Tot slot wil ik alle patiënten bedanken die hebben meegewerkt met het onderzoek. De betrokkenheid van veel PH patiënten bij het onderzoek naar pulmonale hypertensie vind ik heel bijzonder. Het kabaal van de MRI scanner, het eeuwig stil liggen in de PET scanner of horizontaal moeten fietsen, geen gemakkelijke opgave. Veel dank!

Out of office
Lieve vrienden en familie, ik ga jullie hier niet allemaal apart bedanken maar veel dank voor jullie aanwezigheid en steun! Geel-zwarte leeuwen van het 14e, collegae van het OLVG-westside dank voor alle mooie momenten.

Paranimfen, Jacob Bosma en Bas Nijmeijer. Cobus, bekend als schrijver van de hit 'lijn 170: geen dienst' en de Jambers aflevering 'nooit voelt men zich eenzamer dan in een groot gezelschap'. Een man met een zwak voor kersen tatoeages. Een hechte vriendschap ontstaan tijdens het 1e jaar van Demeter. Dank voor de vele mooie momenten, mooi dat je nu mijn paranimf bent. Nijmeijer, een paaldanser pur sang, een man met een voorliefde voor auto's met een hoge instap, aanhanger van hetzelfde gladde kapsel. De man die de gendarmerie van Nice in het Spaans door een wijk commandeert. We go way back. Mooi dat ook jij mijn paranimf bent.

Lieve padre y madre, Matthijs en Joeri: het fundament. Dank voor alle steun, liefde en kansen die jullie mij altijd hebben gegeven. Zonder jullie was dit natuurlijk allemaal niet gelukt. Liefde.

Maurien Arkema alias Arkemeister. Lieve Mau, al 9 jaar mijn grootste avontuur. Jouw energie, positiviteit en ondernemendheid zijn prachtig. Jouw liefde onvoorwaardelijk. Met Mau aan de zij is zo'n promotie zo gepiept. Ik kijk uit naar onze nieuwe avonturen. Love you long time.